Hydrology of the Chalk Aquifer in East Yorkshire from Spring Recession Analysis

Nozad Hasan Azeez

Submitted in accordance with the requirements for the degree of

Doctor of Philosophy

University Of Leeds

School Of Earth and Environment

2017

The work in Chapter 6 and 8 of the thesis has appeared in publication as follows:

Azeez, N., West, LJ and Bottrell, SH (2015) Numerical simulation of spring hydrograph recession curves for evaluating behavior of the East Yorkshire chalk aquifer.

In: Doctor DH; Land L; Stephenson JB (Ed) Proceedings of the 14th Sinkhole Conference pp.521-530. October, 7th. 2015

I was responsible for analyzing information, constructing numerical models, interpretation the results and writing the paper. The contribution of the other authors was reviewing the results and writing.

Acknowledgements

I would like to thank Dr Jared West and Prof Simon Bottrell for their time, support, guidance and supervisor through the duration of this project. I also wish to thank and appreciate Dr Noelle Odling for her supervision during the first and second year of this study.

My special thanks to Dr Raul Perulero Serrano for his help with using Groundwater Vistas 4 modelling software. Many thanks to Rolf Farrell from Environment Agency for provision of the flow rate data. My thanks to Kirk Handley for his assistance in the field.

I would also like to say thanks to Chartell Bateman and Dominic Emery of the Field and lab facilities, School of Geography/ University of Leeds for providing the stream flow meter.

I would like to extend my thanks to my family for their encouragement, my wife for her supports throughout my study and for my lovely son Nali.

The Human Capacity Development Programme (HCDP) Ministry of Planning /Kurdistan Region-Iraq are gratefully acknowledged for funding this project.

Abstract:

This thesis presents a study of the flow system in the unconfined Chalk aquifer in East Yorkshire, based on the behaviour of spring discharge during the recession period.

Groundwater is an important natural water resource in the UK, nearly one-third of England's water supplies are provided by groundwater (almost 60% of the total by the Cretaceous Chalk aquifer). Springs drain water from large areas of the Chalk aquifer in East Yorkshire, so the discharge is governed by cumulative effects from flow systems and recharge. This study investigates whether the recession curve of spring hydrographs can be used to identify the characteristics of aquifer flow system, e.g. the extent of fracture and conduit flows. For this purpose analytical, hydrochemical and numerical modelling approaches been used. Due to the complexity of the hydrogeological system in the study area, various data sets have been used to conceptualize two gauged catchments within the Chalk aquifer outcrop area. Therefore climatic, hydrological, geological information has been collated and field monitoring of groundwater level, groundwater temperature, stream water temperature, stream water electrical conductivity, spring water CFCs concentration and stream water discharge undertaken. Annual recharge and water balances were calculated and interpreted for the two catchments (Kirby Grindalythe and Driffield).

Geological information has been used to construct geological models of the two gauged catchments; hydrological conceptual models have been developed through combining hydrogeological information with the geological models. Actual evapotranspiration and rainfall data have been used for calculating annual recharge and estimating the timing of the start of the spring recession period for each hydrological year (i.e. the cessation of groundwater recharge). A tabulation method technique was used for constructing a Master Recession Curve (MRC) for selected gauged springs over 15 hydrological year recession periods. The MRC approach averages out the variation in between recession curves from different hydrological

years, thus removing the effects of recharge variations between years, to produce a recession curve reflecting mainly topographical and hydrogeological factors.

The MRC were analysed using the Maillet method; the Kirby Grindalythe MRC can be represented by a single recession coefficient, whereas that for the Driffield catchment was better represented by a two-segment curve (i.e. two recession coefficients). This result showed that the springs in the Kirby Grindalythe catchment drain from an aquifer consisting of a single reservoir, whereas that in the larger Driffield catchment may indicate a dual-reservoir aquifer (probably a network of smaller fractures in the interfluves, with a network of larger fractures or conduits in the valley).

In order to investigate whether the topographic divide represents the groundwater divide, and also to investigate whether the gauged springs were responsible for draining all recharge water from the catchments, water balance has been calculated for each catchment. The result revealed that in both study catchments the net rainfall recharge is always greater than outflow (spring discharge plus abstraction). This result showed that either there is uncertainty in the catchment size (ie the topographic divides are not the groundwater divides) or there is groundwater discharge from the study catchments. The ratio of net rainfall recharge/spring outflow from water balance was compared to the maximum flow rate during the recession for water years 2010-2014. The ratio was fairly constant for Driffield catchment with average value 3.5, but in Kirby Grindalythe catchment the ratio was about 5.6. The most probable reason for this difference is that a considerable portion of the groundwater is flowing out from both catchments in the form of subsurface flow.

The concentration of CFC11 and CFC12 in the water samples during the recession period of the springs were monitored in order to estimate the residence time of the groundwater in the aquifer. The result showed that the groundwater is contaminated with CFCs; therefore, the concentration of CFCs in the water samples was not able to be used in the Groundwater age estimation. It was noticed that the concentration

of the contaminated CFCs has a pattern; therefore its pattern was compared with the pattern of the stream flow rate. A correlation has been noticed between CFCs concentration and flow rate. Through the analysis of this correlation it has been found that this correlation can be used for estimating flow system in the aquifer. In addition, the mixing CFC-11 and CFC-12 model has been used for estimating the flow system in the studied catchments. The results showed that Driffield catchment includes two flow systems. It is also showed that Kirby Grindalythe catchment consists of two sub-catchments; one of the sub-catchments feeds Duggleby-1 spring and the second one feeds Duggleby-2 spring. The sub-catchment which feeds the Duggleby-1 contain two flow systems and the sub-catchment which feeds Duggleby-2 contain single flow system.

Transient three-dimensional numerical models were developed to simulate both Kirby Grindalythe and Driffield catchments. The aquifers in each catchment were simulated with the finite difference block centred groundwater model MODFLOW2000 using Groundwater Vistas version 6 (GV 6). The recession curves from the models were calibrated to the observed MRC in each case. The outcome confirmed that in Kirby Grindalythe catchment the chalk aquifer consists of a single reservoir flow system, whereas in the Driffield catchment the aquifer consists of a double reservoir flow system.

Contents

List of Figures

List of Tables

Chapter 1. Introduction

1.1. General background:

Groundwater is considered the most important source of clean and potable water in the world. Generally, groundwater has adequate microbiological and chemical quality. (Okafor and Mamah, 2012). Groundwater is an important natural water resource in the UK. Nearly one-third of the UK's public water demand, which includes water used by domestic, agriculture and industry, is provided by groundwater. About 85% of the total groundwater abstraction in the UK, which is about 2400 million m^3/day, is from two main aquifer types: Cretaceous Chalk and Permo-Triassic Sandstone. The Chalk aquifer provides almost 60% of the total abstraction groundwater. This illustrates the importance of Chalk aquifers in the UK.

Chalk underlies much of the eastern and southern UK (Figure 1.1).

1.2. Lithology of the UK Chalk:

The Chalk is a fine grained porous marine limestone; calcium carbonate formed nearly 98% of its composition (mainly consisting of coccolithophores skeletal components) (Allen et al., 1997). It was deposited over much of Northern Europe during the Upper Cretaceous period when the area was submerged under the shallow to moderately deep warm sea (Downing et al., 1993).

Layers of marl can be found in the Chalk with a thickness ranging between millimeters and several centimeters and lateral continuity can consist of several hundreds of kilometers. The marl consists of inorganic material, mainly composed of clay and a lesser amount of silt or sand (Allen et al., 1997). The Chalk also contains flints which appear either in the form of thin (less than 1 cm) continuous sheets or discrete irregular nodules layers (of thickness between 1 to 30 cm). The flint was formed from diagenesis of biogenic silica (Maurice, 2009).

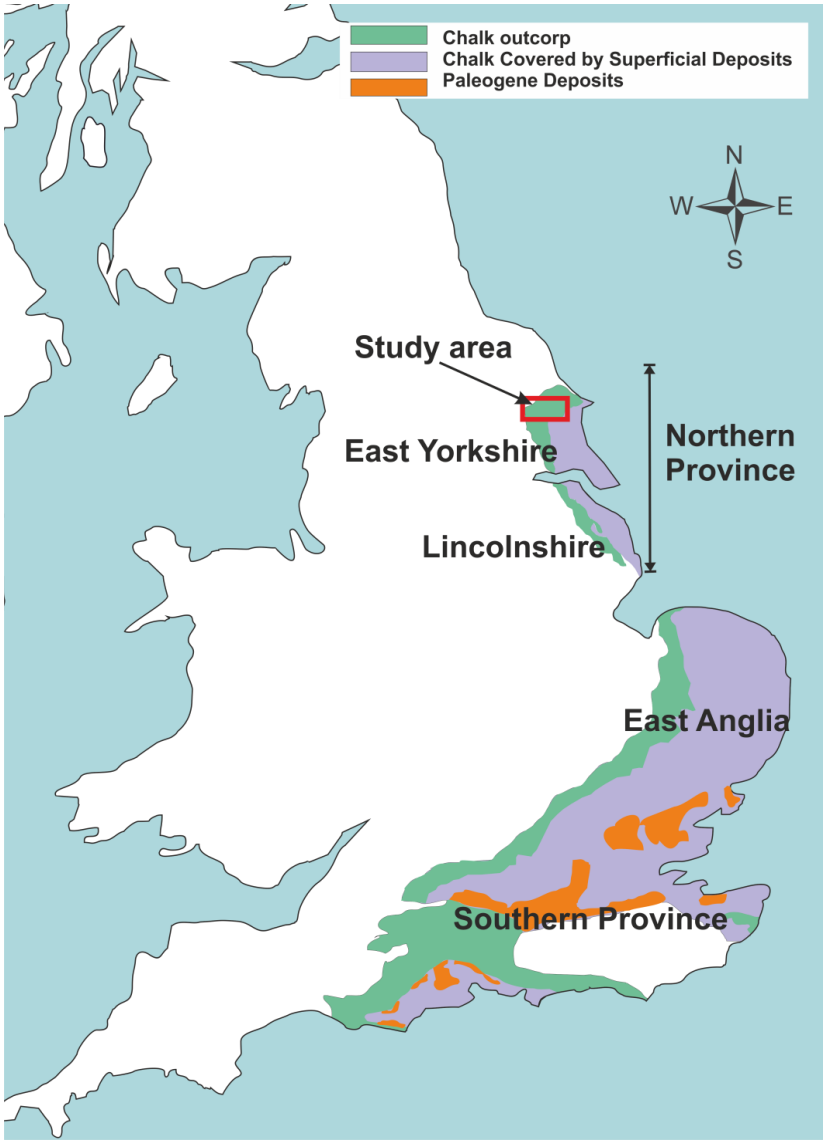

Figure 1-1Chalk distribution in the UK and geographical location of the study area (Allen et al., 1997).

1.2.1. The Chalk distribution and stratigraphy in the UK

Chalk covers large areas of southern and eastern England. It has been divided into two main areas: the Southern Province comprising the South and North Downs and the confined chalk areas of the Hampshire and London Basins and the Northern Province that includes Yorkshire and Lincolnshire (Lloyd, 1993). Meanwhile, the Chalk of East Anglia is considered a transitional area between the Northern and Southern Provinces.

The North Province Chalk differs from the South Province Chalk in that the North Province Chalk is harder and the flint nodules and flint horizons are mostly weakly developed. The greater hardness of the Northern Chalk is related to the diagenesis processes. Burial of the Chalk at great depth caused pressure solution of carbonates that were then re- deposited and recrystallized in the pores (Allen et al., 1997). The weak development of the nodular and flint beds has been related to the depositional environment of the Chalk; accordingly it has been interpreted that the Northern Province Chalk was deposited in a deeper water environment than the Southern Province Chalk (Mortimore et al., 2001). The diagenesis that causes hardening of the Northern Province Chalk affected the hydraulic properties of the rock, with porosity decreasing and transmissivity increasing. Precipitation of carbonate in the pores reduced matrix porosity while the greater hardness caused a higher degree of fracturing and increased the total transmissivity.

The traditional classification of English Chalk, which was proposed during the nineteenth century, divided Chalk into three Formations: lower, middle and upper chalk (Jukes-Browne, 1880; Penning and Jukes-Browne, 1881; Jukes-Browne and Hill, 1903, 1904). Recognition boundaries between these formations are based on remarkable hard rocks including the Melbourn Rock at the Lower - Middle boundary and the Chalk Rock at the Middle-Upper boundary (Woods et al., 2012). Studies revealed that this classification is more applicable for the Southern Province Chalk (Southern England). In the Southern Province Chalk, these boundary markers are

clear, whereas they have not been recognised in the Northern Province Chalk. Also, lithological and paleontological differences have been recognised between the Chalk in Northern and Southern England. Therefore, another division for Chalk rock has been proposed which classifies the Chalk succession into three main parts depending on the presence or otherwise of flints.

Further classification of the Chalk group was introduced by Wood and Smith (1978), who divided Northern Province Chalk into four formations ranging from older to younger, namely, the Ferriby, Welton, Burnham and Flamborough Chalk Formations, typically some 25m, 50m, 150m, and 260 m respectively in thickness (Sumbler, 1999; Wood and Smith, 1978; Mortimore et al., 2001).

In November 1999 the UK Stratigraphic Commission of the Geological Society of London and the British Geological Survey suggested a new classification for the Upper Cretaceous Chalk in England, the Grey Chalk and White Chalk subgroups (Rawson et al., 2001). The Grey Chalk Subgroup in the Northern Province contains one formation only (Ferriby Chalk Formation). In the Southern and Transitional provinces, the Grey Chalk Subgroup includes two formations (the West Melbury Marly Chalk Formation at the base and the overlying Zig Zag Chalk Formation) (Mortimore et al., 2001).

1.3. Hydrology of the Chalk

Hydrogeologically the Chalk is a rock most commonly described as having dual porosity and a dual permeability medium (Price, 1987; Barker, 1991; Price et al., 1993; Parker, 2009). Two types of porosity systems have been recognised in the chalk rocks: primary and secondary porosity. Primary porosity refers to pore spaces formed between rock grains during rock formation processes, simply termed “matrix porosity”. Secondary porosity exists in the form of fractures which were produced by dissolution and tectonic activity (Singhal & Gupta 2010). This characteristic of dual porosity in the Chalk aquifer was confirmed by many studies (Foster and Crease,

1974; Wellings & Bell 1980; Price 1987; Price et al., 1993; Downing et al., 2005; Mathias et al., 2005).

In general, the assumption regarding the dual porosity rock system is that the matrix pores provide a storage medium while the fractures act as pathways for groundwater flow. However, this assumption does not completely apply to the chalk aquifer as the flow within the chalk is more complex: in the Chalk the pore throats are very small, and therefore do not readily drain; while the fracture system consists of a complex network of different sizes ranging from very fine fractures to fissures. Therefore fractures work mainly as the effective storage and primary flow path of the groundwater (Price et al. 1976).

1.3.1. Chalk Porosity:

Matrix porosity:

East Yorkshire Chalk has an average porosity of 35% (Allen et al., 1997). According to the saturation method, the effective porosity of the Upper Chalk of Yorkshire ranges between 17.7 and 36.4 % (Bell et al., 1999). Bloomfield et al. (1995), throughtesting 191 samples of Upper Chalk in Northern England, found that the average porosity was 35.4 ± 8.3%. In general, the porosity in the British Chalk ranges between 3.3 and 55.5%, with an average value of 34% (Bloomfield, 1996). Matrix porosity reduces with burial depth of the Chalk due to the overlying load.

Fracture porosity:

Fractures have a significant role in developing chalk aquifer properties, as without fractures the permeability and specific yield of the Chalk would be negligible. The term fracture will be used to describe discontinuities in rock. In the chalk three types of fractures have been identified: bedding plane fractures, joints, and faults (Bloomfield, 1996). The origin of fractures is related to tectonic activity, they commonly exist in three closely developed orthogonal sets: a bedding parallel set,

and two roughly perpendicular sets, which are less continuous, predominantly orientated in NW-SE and NE-SW directions (Downing et al., 1993; Price, 1987). Some fractures have been widened by solution; these may be termed fissures or conduits (or generally 'solutionally enlarged fractures') (Maurice et al., 2006). Conduits are distinguished from fissures by the aspect ratio they present in the rock cross section, which is around 1 for conduits; in contrast, fissures have a trace length to maximum aperture ratio greatly in excess of 10 (Maurice et al.,2006).

The porosity in the Chalk of East Yorkshire due to fractures and fissures is typically less than 2% (Gale and Rutter, 2004). The fracture system in the Chalk can be classified into two components: primary fractures and secondary fissures (Price, 1987). Primary fractures arise due to tectonic activity, while secondary fissures are related to weathering and dissolution activity, which causes enlargement of fractures.

1.3.2. Chalk hydraulic conductivity and transmissivity:

Hydraulic conductivity of the matrix in the Chalk is approximately linearly proportional to the matrix porosity. The Chalk contains high matrix porosity, but due to the small size of the pores and pore throats its hydraulic conductivity is very small (Allen et al., 1997). Scanning electron microscopy for East Yorkshire Chalk revealed a pore size range of between 0.3 and 10 μm with an average of 5.9 μm (Patsoules and Cripps, 1982). The hydraulic conductivity of the English Chalk matrix is extremely small, based on 977 gas permeability measurements the average conductivity of the matrix is about 6.3×10^{-4} m/d (Allen et al., 1997). Because the hydraulic conductivity of the matrix is very small with respect to the hydraulic conductivity of the fracture system, the bulk hydraulic conductivity of the Chalk can be considered to be dominated by fractures.

The transmissivity of the Chalk in Yorkshire Chalk varies between 1 m^2/d and over 10000 m^2/d (Allen, D. J., et al., 1997; Gale and Rutter, 2006). The variation of the transmissivity has been related to the maturation degree of the fracture system and

distribution of the fissures and joints (Foster and Milton,1976; Smedley et al., 2004). This very high transmissivity can be a result of solution-enlarged fractures (i.e. fissures and conduits). Tracer tests around Kilham pumping station found velocities of around 130–475 m day^{-1}, suggesting that the fractures are highly enlarged and the aquifer is more likely to become karstic in some places (Smedley et al., 2004).

1.3.3. Chalk hydraulic storage coefficient:

Although the East Yorkshire Chalk contains high porosity (about 35% on average), the specific yield in the unconfined chalk is very small. The pores and pore throats are very small, so about 90% of the total water in the matrix pores is retained by capillary force (Price et al.,1993). The specific yield in the East Yorkshire Chalk ranges from (0.001-0.02) (Allen et al., 1997; Gale and Rutter, 2006; Parker, 2009).

1.3.4. Vertical variation of the permeability in the Chalk:

Vertical variation of the permeability is one of the important features in the Chalk. Generally, the permeability is better developed towards the top of the aquifer (the water table). The porosity of the Chalk is variable, and is influenced by lithology but more effectively by the degree of diagenesis. The effect of diagenesis increases with burial depth due to overburden loads causing two types of diagenesis, mechanical compaction, which reduces the size of the pore size, and chemical compaction, which causes the dissolution and precipitation of minerals (Bloomfield et al., 1995; Bloomfield, 1997). Furthermore, the overburden load also causes fracture frequency and aperture size to reduce with depth below ground surface (Allen et al., 1997).

In relation to the topography, transmissivity within the Chalk has long been discovered to be related to the topography as it is greater in valleys than on the interfluves (Woodland, 1946; Ineson, 1962). However, a clear understanding of this variation remains elusive because of lack of data across interfluves (Allen et al., 1997).

1.4. The karstic behaviour of the Chalk:

In hydrogeological terms, karst is a geological medium which comprises of an extensive network of dissolutionally enlarged fractures, conduits, and caves through which groundwater flows rapidly.

Various features and behaviours indicate the karstic nature of the English Chalk, for example, small scale karst geomorphological features such as dolines, stream sinks, caves and dry valleys are widely observed (Fagg, 1958; Docherty, 1971; Sperling et al., 1977; Edmonds, 1983). In many regions such as Sussex, Devon and Kent, explorable caves, which originated due to paleo- solution by freshwater, have been reported in the Chalk (Reeve 1981, 1982; Fogg, 1984; Lowe, 1992). Furthermore, a large stream sink complex was identified in the Chalk at North Mimms, Hertfordshire (Walsh and Ockenden, 1982), while subsurface sediment-filled dissolution pipes have been observed in quarries, with densities of up to 265 per hectare (Lamont-Black, 1995). In addition, other phenomena in the English Chalk that have been related to the karstic nature of the Chalk include such as: rapid groundwater flow recorded by tracer tests within the Chalk aquifers in different locations (Atkinson and Smith, 1974; Ward, 1989; Price et al., 1992; Banks et al., 1995; Ward and Williams, 1995; Harold, 1937); pumping sand in the boreholes within the Chalk of the South Downs, which is expected to be located within the enlarged solution fractures (Southern Science, 1992); and quick response of the water level in boreholes and springs relatively far from the pumping borehole, for example, at Swanbourne Lake, South Downs (Southern Science, 1994).

Evidence of the Karstic behaviour of the East Yorkshire Chalk has been presented by several studies. Tracer tests near to Kilham pumping station observed velocities of around 130– 475 m day^{-1}, suggesting that the aquifer is karstic in some places (Smedley et al., 2004).

Evidence from surface investigations showed that karstic features are less common in the Northern Chalk Province than in the Southern Province (Maurice et al., 2012). However, the difference in the karstification degree between the Chalk of the North and South Provinces has not been precisely assessed because fewer studies have been carried out regarding the karst behaviour in the Chalk aquifers of the Northern Province.

Although some small scale karst geomorphological features have been observed in the English Chalk, the greatest subsurface dissolution appears to result in fissures and small conduits (Maurice, 2009). In hydrogeological studies, boreholes are the significant and important means of aquifer exploration, and the commonest karstic features investigated in the boreholes in the Chalk are fissures (Maurice et al., 2006). Atkinson and Smart (1981) suggested it is possible to consider the Chalk as a Karst aquifer but at the lower end of the karstification scale.

Based on the above discussion regarding karstic behaviour of the Chalk, and its hydraulic properties, it can be concluded that the Chalk (neglecting the effect of the matrix permeability) contains two main flow systems: a relatively slow flow system through the fractures and small fissures, and very fast flow system through the enlarged fissures and conduits.

1.5. Groundwater regime and surface water courses in East Yorkshire:

Several rivers exist in East Yorkshire on the superficial deposits, but the Gypsey Race is the only significant watercourse on the Yorkshire Wolds outcrop, see figure (1.2). The upper reaches of the Gypsey Race rise at Duggleby and extend to the east along the Great Wold Valley towards Bridlington. The Great Wold Valley was formed by the River Ure during the Tertiary period, with additional erosion occurring during periglacial conditions in the Quaternary (ESI, 2010). Flow in the existing stream is controlled by seasonal variation of the groundwater table

elevation; during times of lower groundwater level the flow becomes intermittent, and during the late summer and extended periods of drought, the Gypsey Race becomes dry. The Gypsey Race rises from groundwater discharge at 4 springs around Duggleby. Because of its ephemeral behaviour at its upper reaches, Gypsey Race is considered as a typical Chalk stream, which does not discharge during dry periods.

During its journey, the Gypsey Race changes from a losing to a gaining stream; it becomes a losing stream when the water table is below the stream bed and becomes gaining when the water table is above the stream bed. In the uppermost reach of the Gypsey Race (1 to 2 km from its sources), typically the stream starts feeding the Chalk aquifer because the stream bed is above the water table elevation, and becomes dry between West Lutton(grid reference: SE930691) and Rudston (grid reference: TA096672). East of Rudson the stream bed falls below the groundwater level again, so the Gypsey Race becomes a gaining stream (Gale and Rutter, 2006). Figure (1.2) shows the Gypsey Race and springs around Duggleby and Driffield which were the subject of this investigation.

Unconfined Chalk represents the catchment area for groundwater recharge, with the recharge water flowing through the unsaturated zone as a combination of matrix and by-pass flow. The majority of the recharge happens via fissures, especially solution enhanced bedding planes and joints (Ward et al., 1997).

The predominant groundwater flow direction in the East Yorkshire Chalk is eastwards along the dip slope, with westward flow direction along the escarpment (Gale and Rutter, 2006; ESI report 2010 and 2015). However, there is a local variable flow direction due to the local topographic variation and groundwater abstraction. Groundwater flow is largely restricted to the upper 50–100 m of the Chalk where significant fracture permeability is available, within the zones of present and past water table fluctuation. In the unconfined aquifer, the seasonal

average head (water table) variation is about 30m, while it is smaller in confined Chalk aquifers (Berridge and Pattison, 1994).

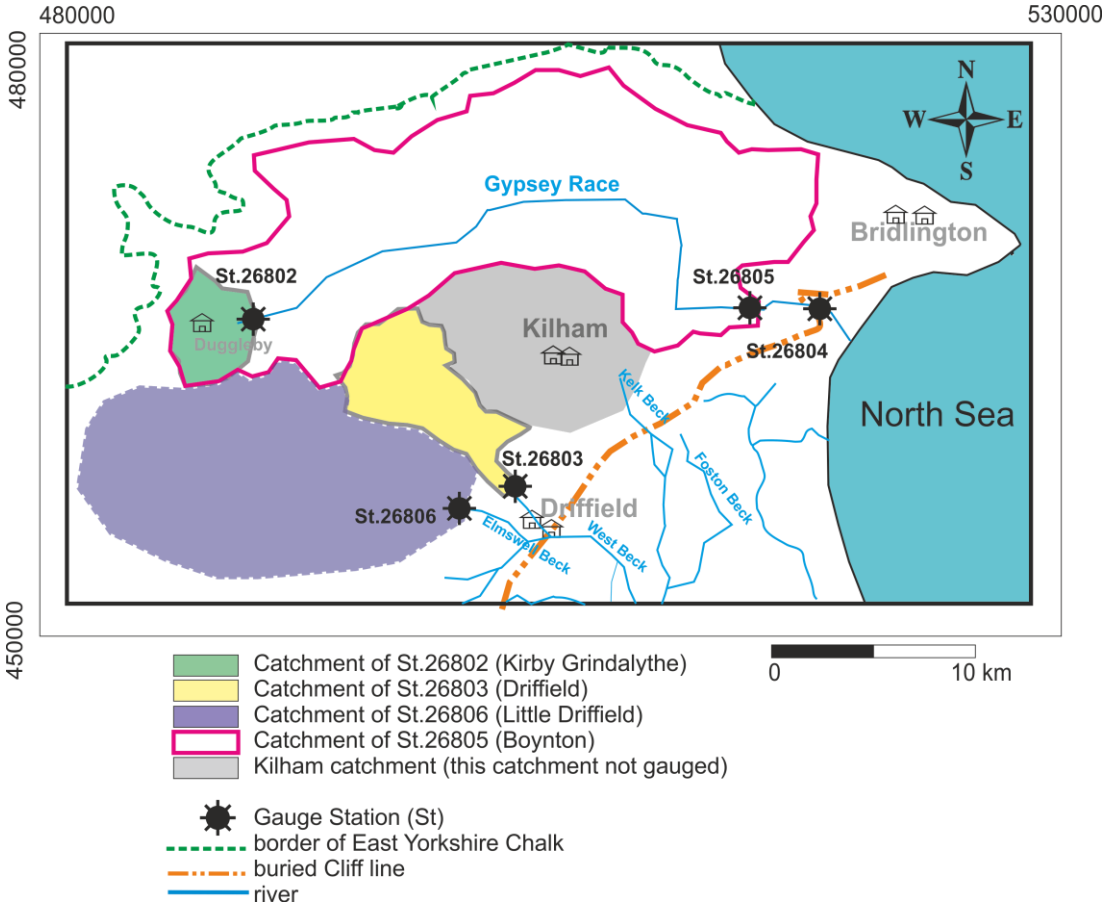

Figure 1-2Map showing the distribution of the main rivers in East Yorkshire and the main gauged catchments and the location of the gauging stations in the Yorkshire Wolds. This map developed according to the information from National River Flow Archive website at http://nrfa.ceh.ac.uk/data/search.

1.6. Springs

Springs are spots on the surface of the earth where the groundwater emerges naturally; spring water is a natural source of groundwater. Unlike water wells, water from a spring discharges naturally under the effect of gravity (in the unconfined aquifer) and hydrostatic pressure (in the confined aquifer) (Kresic and Stevanovic, 2009).

Several factors influence the discharge rate from springs, the most important being rainfall, shape and size of catchment area, the geology of the aquifer and hydraulic characteristics of the aquifer.

1.6.1. Type of springs

Springs are classified into different types based on the factors which lead to the formation of the spring. They are commonly divided into two groups depending on the energy driving the groundwater in the aquifer system (Kresic and Stevanovic, 2009).

- Gravity or Descending springs: this type of spring emerges under the influence of the gravitational force in an unconfined condition where the ground surface is intersected by the water table.
- Artesian or Ascending springs: this type of spring discharges under the influence of the pressure due to the condition where the aquifer is confined by impermeable layers. The spring arises where discontinuities such as faults or joints intersect the aquifer and the land surface.

Depending on the appearance of the spring and reason for its existence, springs have been classified into depression, contact, fracture, karst, lava and fault springs (Kreye et al., 1996).

Two set of springs arise in the East Yorkshire Wolds; the first set arises at the western border of the Wolds along the escarpment, whereas the second group arises along the contact line between unconfined and confined chalk of the Wold. All these springs are gravity springs, in fact, those along the escarpment are gravity springs arising from the scarp rather than the dip slope of the aquifer, and those along the unconfined/confined contact are gravity springs arising from the dip slope of the aquifer.

In the catchments selected for examination in this study, several springs of these two types exist. The springs at Kirby Grindalythe are of dip slope and scarp slope gravity type and the Driffield spring is of the depression gravity type. The hydrogeology situation and the reason for these springs will be examined in detail in the geological and hydrogeological section of this thesis.

1.6.2. The importance of springs as a hydrologic tool:

Groundwater from the Cretaceous Chalk is important to the natural landscape of East Yorkshire. A number of the rivers and tributaries in East Yorkshire are fed by the groundwater that depletes naturally through a number of springs. Consequently, the springs have a significant role in Yorkshire's natural surface water hydrology. Understanding the hydrogeology of these springs and interrelation with the aquifer helps in understanding the behaviour of the aquifer, and also helps in management and protection of the spring water.

Several approaches have been developed for studying the aquifer, including near-surface geophysical techniques, surface geological investigations and hydrogeological data analysis (Milsom, 1996; Ward, 1990; Fetter, 2000; Cunningham and Schalk, 2011; Bourke et al., 2014 ; Cozma et al., 2016). However, the majority of these methods are not very precise in the case of the dual porosity aquifer because of the complexity of the fractured system. Studying the recession limb of spring hydrographs is one method that could offer information for examining hydraulic properties of the aquifer. Studying hydrograph recession curves of springs

may provide hydrogeological information, especially where fracture or conduit flows are significant. This approach is preferred over other geological and geophysical methods (Dreiss,1982; Bakalowicz, 2005; Goldscheider and Drew 2007) because the spring drains water from large areas of the aquifer, so the discharge is governed by a cumulative effect from the flow systems that exist in the aquifer. This contrasts with other geological and geophysical methods that only represent the aquifer locally at the investigation points.

1.7. Study area:

The study area is located in the Wolds of East Yorkshire, northeast England. The area is part of the Northern Province of the English Chalk, with the Chalk being the predominant rock in the area. In the eastern part of Yorkshire the Chalk crops out on the surface to form the Yorkshire Wolds; these are bordered to the east by the buried paleo cliff line beyond which the Chalk is confined by superficial deposits forming the region called the Holderness Plain.

In the Yorkshire Wolds, 5 flow rate gauging stations are available. These stations monitor the flow rate of three streams. Three of these stations are located on the Gypsey Race stream, the first station (26802 - Gypsey Race at Kirby Grindalythe) being at Kirby Grindalythe village at the very beginning reach of the Gypsey Race stream. Another two stations are located near the end of the Gypsey Race stream: station 26004 - Gypsey Race at Bridlington (2.3km from the North Sea) and station 26005 - Gypsey Race at Boynton. The other two stations – 26803 and 26006 – are located on the Water Forlorns stream in Driffield town, and Elmswell Beck stream at Little Driffield village respectively. More information about these gauging stations can be found in the table (1.1); in addition the locations of each gauging station and the catchment boundaries can be seen in Figure (1.2). These stations are managed by the Environment Agency-Yorkshire, and information about the locations, including the type of weir and catchment boundaries, is available on the National River Flow Archive (NRFA) website (http://nrfa.ceh.ac.uk/data/search).

This study used the flow rates from two of these gauging stations: Kirby Grindalythe gauging station and Driffield gauging station. The data, obtained in the form of average daily discharge for the water years 1998 to 2015, were provided by the Environment Agency.

Table 1-1 Gauging stations at the East Yorkshire Wolds, from the National River Flow Data (NRFD) (http://nrfa.ceh.ac.uk/data/search).

name	NGR	Catchment area (km2)	gauge type	Operating period
26802 - Gypsey Race at Kirby Grindalythe	SE904675	15.9	Small, rectangular thin-plate, sharp-edged weir	1998-now
26803 - Water Forlornes at Driffield	TA023583	32.4	Thin-plate sharp edged weir, inside a broad-crested	1970-now
26806 - Elmswell Beck at Little Driffield	TA009575	136	Thin-plate weir	1980-2015
26005 - Gypsey Race at Boynton	TA136677	240	Flat-V weir	1981-now
26004 - Gypsey Race at Bridlington	TA165675	253.8	Crump weir	1971-1981
Note: station 26005 (Boynton) replaced the downstream gauge 26004 (Bridlington).				

1.7.1. Description of the catchments used in this study

In this study two catchments, Kirby Grindalythe and Driffield, were selected for studying the flow behaviour of the spring and its relation to the aquifer structure. These catchments were chosen because of their different hydrogeological configurations. They were regarded as providing particularly valuable examples to represent the spring system in the East Yorkshire hydrogeological system because:

- Kirby Grindalythe is located at the Wolds escarpment border, where the springs are of the scarp slope and dip slope types. Driffield catchment is located near the boundary of confined and unconfined Chalk, where the springs are of the depression type. As the springs in these two catchments reflect different hydrogeological situations and hydrogeological factors, it was considered that they could offer good representation of the range of springs in the Yorkshire Wolds.
- These two catchments are relatively small compared to the catchments gauged by the Boynton and Little Driffield gauging stations. The larger catchments are geologically more complex than the smaller catchments, therefore the possibility of uncertainty due to hydraulic characteristics is much bigger in the larger catchment.
- Kirby Grindalythe and Driffield catchments have a different shape, which gives the opportunity to test spring recession curves under different catchment shape conditions.

For more detailed information about the geographical locations of these two catchments (according to topographic divide), the monitored springs and gauge stations along with some other places of interest, see the OS map in appendix 1.

Kirby Grindalythe:

The Kirby Grindalythe catchment is located near the west border of the East Yorkshire Wolds near the Chalk escarpment (Fig. 1.2). The location is 10.5 km southeast of Malton and 33 km north-east of York, between the grid lines East 486039 and 488595, North 464071 and 470358 [grid reference SE860640 and SE885703]. The catchment is bounded by hills on the north, west, and south sides and drains into the headwaters of the Gypsey Race to the east. Kirby Grindalythe catchment, according to the topographic water divide, occupies 15.9 km^2 and is approximately fan-shaped with transverse and longitudinal dimensions of 3.5 km and 4.8 km respectively.

The groundwater is depleted through several springs; during the field observation four such springs were identified around Duggleby village, and the water from these springs aggregates to form the Gypsey Race stream. The discharge from the Gypsey Race is recorded by gauging station 26802-Gypsey Race at Kirby Grindalythe village. This gauging station consists of a rectangular thin-plate sharp edged weir (76.5cm wide and 21.7 cm depth), see Figure 1.3. Originally, this station was built to monitor water discharge for the purpose of prediction of flooding in the stream. The station was built in the 1970s, and over time fell into disrepair before being renovated and re-commissioned in 1998.

This station is managed by the UK Environment Agency (EA) under the code 26802-Gypsey Race at Kirby Grindalythe. Information regarding this station can be found on the National River Flow Data (NRFD) website http://nrfa.ceh.ac.uk/data/station/info/26802.

Driffield:

The Driffield catchment, according to the topographic water divide, occupies an area of 32.4 km^2 and is located northwest of Great Driffield town between grid lines Easting 494000 and 502000, Northing 458000 and 468000 [grid reference SE940580 and TA020680]. The catchment is bounded by topographic highs with reducing elevations toward the SE and forms an elongated leaf-like valley. The catchment has approximate transverse and longitudinal dimensions of 3.51 km 9.2 km respectively. It extends northwest-southeast. Water discharges in a large spring in Great Driffield village at the narrow end of the catchment (Easting 501944, Northing 458672). The discharge from this spring is recorded by a gauging station coded as 26803 - Water Forlorns by the EA, located just a short distance downstream from the pond created by the emergence of the spring.

Station 26803 - Water Forlorns at Driffield consists of a thin-plate sharp edged weir (64cm wide and 22 cm depth), inside a broad-crested, vertical sided masonry weir around 4.79 m wide. This station was constructed in the early 1970s but fell into disrepair in the 1980s, and was renovated in 1998. It is located in Northend Park-Driffield town, around 0.19 km downstream of the source at Grid Reference TA023583. Figure (1.3) shows the geographical location of the station and a photo of the station respectively.

Information about this station can be found on the National River Flow Data (NRFD) website http://nrfa.ceh.ac.uk/data/station/info/26803.

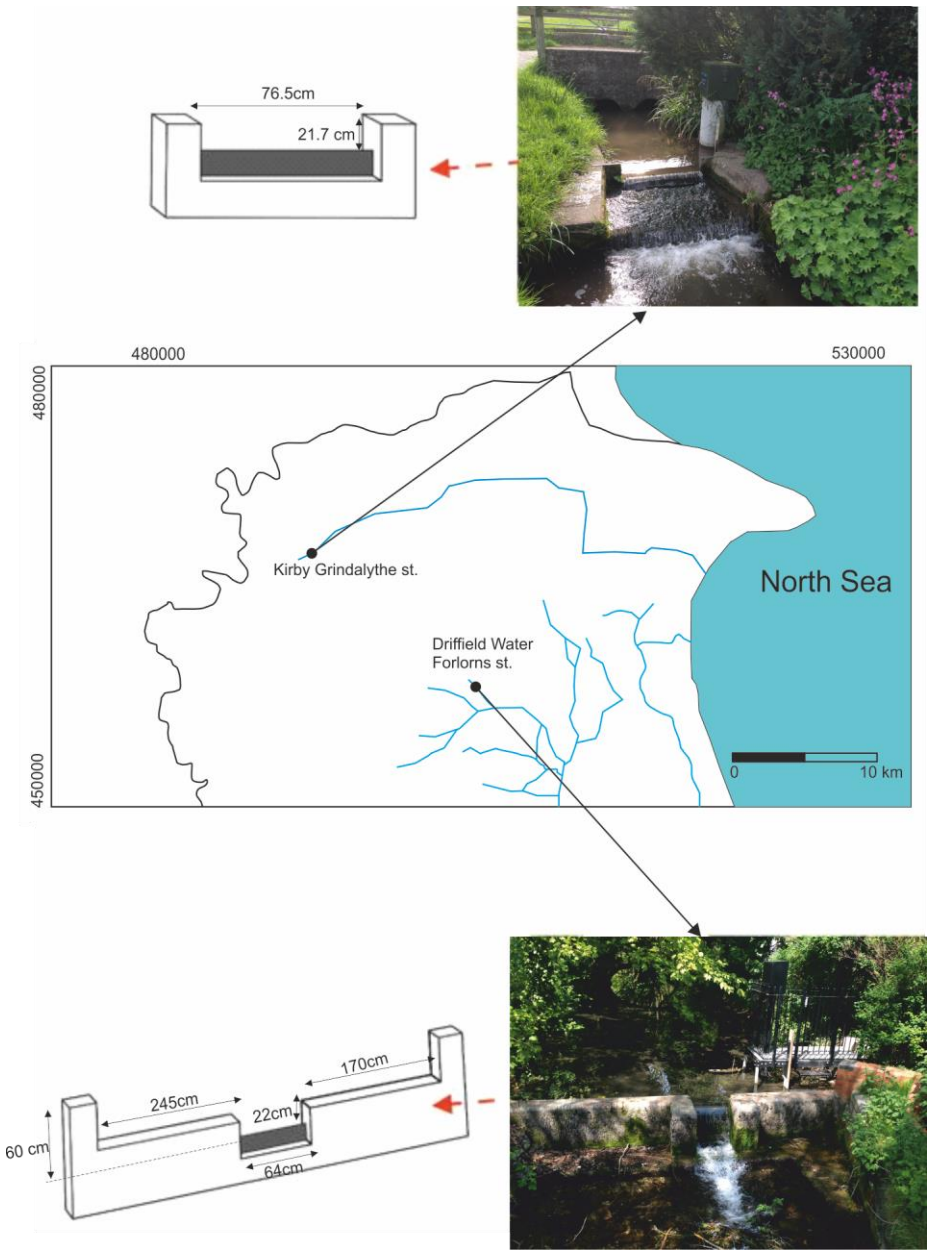

Figure 1-3Geographical location and structure of the Kirby Grindalythe and Driffield – Water Forlorns gauging station.

1.8. Aims:

The overall aim of this project is to investigate the chalk aquifer system of East Yorkshire from the variations in flow rate, temperature and electrical conductivity of the spring discharge during the recession period.

Many springs rise from the Cretaceous Chalk aquifer in the East Yorkshire area; hence, the project was designed in order to take advantage of existing flow-rate data for these springs as a source for investigating the hydraulic structure of the aquifer. The study aimed to use both analytical and numerical approaches to better understand the factors that influence the shape spring recession curve, as well as to characterise the relationships between spring location/discharge and electrical conductivity/temperature and CFC composition of spring water.

To meet the aim of the project, an intensive field-based campaign was undertaken. The campaign comprised of borehole and stream water temperature and electrical conductivity monitoring, stream flow measurement and measurement of groundwater elevation and temperature in a limited number of monitoring wells. Interpretational approaches included water balance calculation, analytical interpretation of the recession curves, CFC analysis and numerical simulation of the recession behaviour.

1.9. Specific Objectives:

To address the above aim, the following objectives were identified:

- Construct geological and hydrogeological conceptual catchment models to facilitate interpretation of recession, water balance and water compositional data.
- Apply analytical methods to the recession curves to yield recession coefficients, and critically analyse the results to determine the most appropriate approach for analysing chalk aquifer recession curves.

- Monitor temperature and conductivity of stream water in the study area by installing hydrogeological loggers in the spring-fed streams. This is aimed at assessing the use of stream water electrical conductivity and temperature as a natural tracer for identification of the source of water in the stream, i.e. groundwater versus quick flow.
- Monitor groundwater levels and groundwater temperature in boreholes through installing hydrogeological loggers. The main purpose of monitoring groundwater fluctuation is to estimate the regional groundwater flow direction and seasonal variation. Meanwhile, the temperature of the groundwater in boreholes would be monitored in order to interpret the relationship between the spring fed stream water temperature and ground water temperature. [In addition, monitoring of water temperature is required to calibrate chlorofluorocarbons (CFCs) analysis results to the in-situ temperature.]
- Undertake water discharge and water stage measurement. This work is needed to evaluate whether the stage of zero flow assumed by the EA rating curves is still valid, which can be done using only low flow rate data.
- Calculate water balance for Kirby Grindalythe and Driffield catchments, using gauging station data and available data on effective rainfall. Water balance calculation facilitates validation of the estimated size of the catchment area based on topography, and the extent of any subsurface flows.
- Numerically simulate groundwater flow within catchments, calibrated to spring recession curves, to identify hydraulic characteristics and the nature of flow systems. This approach investigates links between parameters such as hydraulic conductivity, hydraulic conductivity structure, and recession behaviour.
- Sample spring water for chlorofluorocarbons (CFCs), in an attempt to estimate the water residence time in the groundwater flow system.

1.10. Thesis layout:

Chapter 1 Provides a brief summary of the background, aim, specific objectives, and thesis layout.

Chapter 2 Provides a geological model of the study catchments constructed based on the geological characteristics obtained from the British Geological Survey reports and map and local boreholes information.

Chapter 3 Provides a summary of the hydraulic properties of the Chalk aquifer in the study area. It also, presents hydrogeological conceptual models of the studied catchment constructed through combining the aquifer hydraulic properties with the geological models outlined in Ch.2. The constructed conceptual models illustrate the interrelation between the geological framework, topography and hydrogeological characteristics to show the boundary conditions that govern the aquifer system.

Chapter 4 reports the methodology and results for the borehole and stream water monitoring including electrical conductivity and groundwater temperature, hydraulic head from boreholes, and the interpretation of these results.

Chapter 5 Reports the methodology for calculation of water balance for the study catchments and shows the findings from the water balance calculation, and their interpretation in terms of flow pathways.

Chapter 6 Reports the results of the validation of the stage of zero flow of the gauging station data via field flow and stage. This chapter also reports uncertainty analysis on the discharge data. In addition, the methods and results for constructing the master recession curve for the gauging stations, and the analytical interpretation of the recession data in terms of recession coefficient are presented.

Chapter 7 Reports the methods and the results of CFCs analysis, the methodology of CFC sampling and CFCs analysis. It also presents the findings from the CFC-11 and CFC-12 interpretation.

Chapter 8 Reports the methods and the findings from the numerical simulation of the two study catchments during the recession period, an interpretation of the simulations in terms of the aquifer characteristic and the distribution of permeability

within the chalk. The descriptions of the numerical simulation parameters and those from hydraulic testing are discussed and interpreted.

Chapter 9 Reports the conclusions and recommendations for further work.

Chapter 2. Geology of the East Yorkshire Wolds: development of geological models for the study catchments

2.1. Introduction:

The geological characteristics of the strata have a significant control on groundwater flow. Consequently, knowledge of the geological and hydrogeological properties of a catchment will be essential in understanding the groundwater system.

2.2. Geology of the Yorkshire Wolds:

Regional structure and morphology of sea floor during Jurassic and early Cretaceous produced a significant impact on the sedimentation pattern and thickness of rocks that were deposited during the Cretaceous (Gale and Rutter, 2006). during the late Jurassic – early Cretaceous, shallowing sea has led to the deposition of claystone and mudstones, later during the Cretaceous period due to the further depositions these Claystones covered unconformably by a group of the Chalk rocks. (Gale and Rutter, 2006).

Chalk rocks of the Cretaceous period formed the predominant bedrock in East Yorkshire. In the western part of the area, the Chalk crops out forming Yorkshire Wolds. Toward the eastern part it is buried beneath superficial deposits (drift sediments) forming the Yorkshire Holderness Plain. The superficial deposits mainly consist of the glacial deposits of Late Pleistocene age represented by till, and fluvioglacial sand and gravel. Uplift of the Jurassic and Cretaceous depositional basin caused a variation in the Chalk thickness; the thickness of Chalk increases toward the North Sea. The Chalk strata are in general dipping gently toward the southeast with an average dip angle of 3 to 5 degrees (Sumbler, 1999).

The geology of East Yorkshire is expressed in Figure (2.1), this map is obtained from BGS geological map of the United Kingdom (http://mapapps.bgs.ac.uk).

The East Yorkshire Chalk is bounded to the north by Flamborough Head, at the West by the escarpment of the East Yorkshire Wolds, at the south by River Humber and to the east by the North Sea. The area enclosed by the Chalk escarpment in the west and the North Sea at the east is determined approximately by the GR [SE 800 250] at the south and [TA 153 755] at the north. The Chalk outcrops in Yorkshire extend from Flamborough Head at the North and arcs round southward to the west of Kingston-upon-Hull. Chalk outcrops formed the Yorkshire Wolds dipping gently south and eastward buried under superficial deposits of the Quaternary. The thickness of the Quaternary deposits increases toward the southeast.

A network of dry valleys is distributed in the Wolds, the base of these valleys area covered by a shallow lime-rich sandy soil and by lime-rich loamy deposits. These type of deposits are known as the head and contain very high permeability allowing the water to drain freely.

The boundary between the Chalk outcrop (Yorkshire Wolds) and superficial deposits dominated region (Holderness Plain) extends along the western side of the belt which represents the paleo cliff line. The paleo cliff line formed due to the erosion activity along the coastline during the Ipswichian interglacial of the Pleistocene age. It extends from Bridlington in the north, to the southwest through Great Driffield and then toward the south reaching the Humber Estuary, see Figure (2.2).

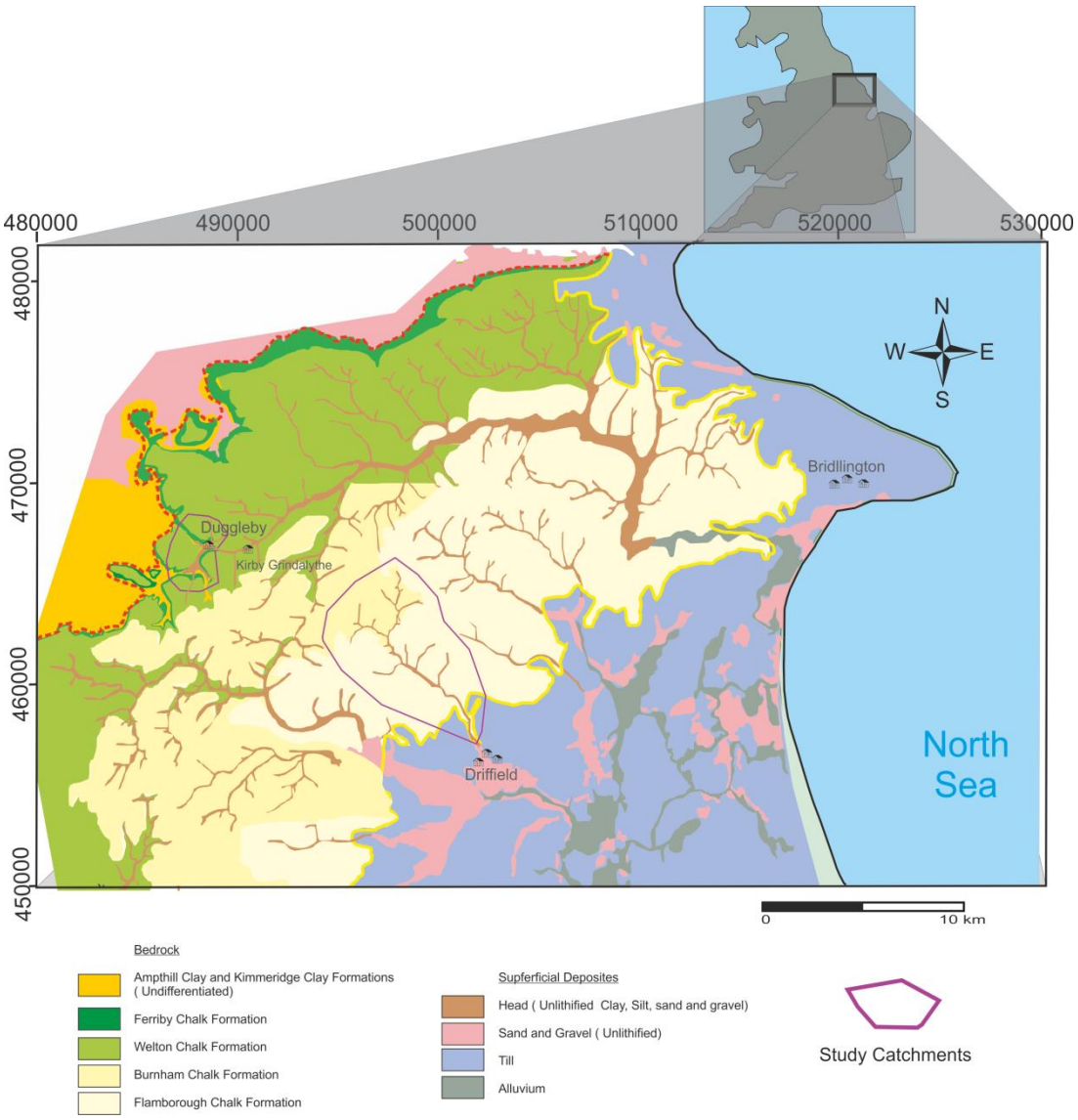

Figure 2-1 Geological map of the East Yorkshire, UK (from British Geological Survey geological map of UK) .

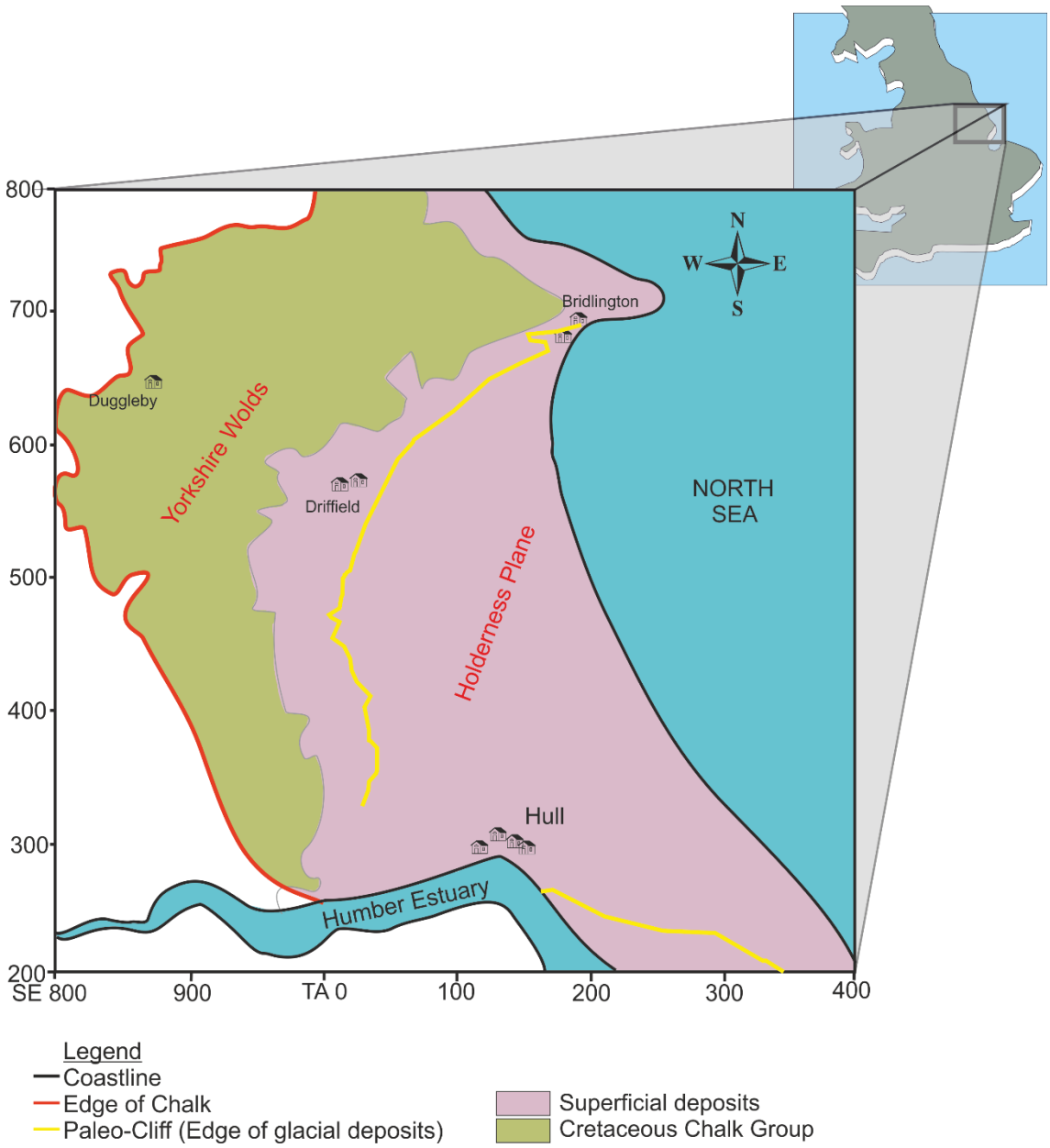

Figure 2-2 Map show the Chalk regions in East Yorkshire, Yorkshire Wolds, the region where the Chalk crops out, and Holderness Plain, the region where the Chalk is covered by superficial deposits.

Physiographically, the upland areas are in the northwest where elevation reaches about 180 m above sea level; elevation reduces toward the North Sea in the east. At the east where the Chalk is covered by thick Quaternary deposits, the ground becomes a relativity flat, low-lying coastal plain (usually about 1-2 m asl). A network of valleys is distributed across the Yorkshire Wolds (Chalk outcrop region). Mostly these valleys are dry. The most probable reason of the dryness these valleys is the depth to groundwater, where the valleys are not deep enough to intersect the water table. Also the high infiltration capacity of the near surface Chalk and chalk-bearing deposits allows water filter into the ground easily (ESI , 2010).

2.2.1. Geological sequence and lithology:

A group of the Chalk rocks of the Cretaceous period is the predominant bedrock in the area. In the majority of the area, the Chalk rock outcrops to the surface except for the valleys where it covered by the sediments of the Quaternary period. Claystone beds of Jurassic age underlay these Chalks. These claystone beds crop out to the west and as inliers in the base of valleys that cut into the escarpment of the Yorkshire Wolds.

Limestone and calcareous clay (Jurassic – Early Cretaceous):

In the late Jurassic and early Cretaceous the area was part of a shallow sea which led to deposition limestone and calcareous clay. During the late Jurassic, the Ancholme Group were deposited which consist of gray, marine mudstone, and silty mudstone; beds of argillaceous limestone nodules; and units of siltstone and sandstone at some levels. The Speeton Clay Formation of Cretaceous age overlies this Group unconformably. This Early Cretaceous deposit mainly comprises mudstones, cement-stones, and sporadic bentonites. The Hunstanton Formation or Red Chalk is part of the succession which includes Speeton Clay. Red Chalk consists of marl and red, iron-stained Chalk beds, it is used as a key marker bed for identification base of the Chalk group (Allen et al., 1997). These rocks are overlaid by the Chalk group and they only crop out at some locations to the west of the Yorkshire Wolds (near

the Western side of the escarpment). Figure (2.3) shows the stratigraphic cross section of the East Yorkshire (ESI, 2010).

period	group	subgroup	Formation	Lithological Discription	Thickness (m)
Quaternary				Till	1 - 5
~~ ~~~~~~~~~~~~ Unconformity ~~~~~~~~~~~~~~~~~~~~~~					
Cretaceous	Chalk	White Chalk	Rowe Chalk	Chalk with flints	70
			Flamborough Chalk	Chalk with marl bands, no flints	240 - 260
			Burnham Chalk	Chalk with flints	130 - 150
			Welton Chalk	Chalk with Flints, Marl member at the base of the Formation	44 - 53
			Ferriby Chalk	Marly Chalk, no flints	20 - 30
		Red Chalk	Hustanton	Marly Chalk,	1 - 30
			Carston	Gritty sanndstone	
	Speeton Clay			Marine clays	~ 60
~~ ~~~~~~~~~~~~ Unconformity ~~~~~~~~~~~~~~~~~~~~~~					
Jurassic	Ancholme Clay		Ancholme clays		
			Brantingham		
			Kellaways Beds		

Figure 2-3. Stratigraphic column for East Yorkshire (ESI, 2010).

Chalk Formations (Cretaceous):

Calcium carbonate sediments are the primary component of the chalk group; the chalk sediments were deposited 65 million years ago during the late Cretaceous period in a shelf sea that covered much of northwest Europe. Very fine calcareous particles of the biogenic debris are the raw material of chalk group. The majority of

the chalk succession is very pure, except the lower part, which includes marl (clay minerals). Pure chalks are occasionally associated with flint, which is a form of cryptocrystalline quartz (silica) formed due to the diagenesis. The origin of silica that produced flint was the skeletons of marine organisms (such as sponges and diatoms).

Four Chalk Formations cover the study area, they cropped out from the northwest to the southeast in succession from the oldest to newest. At the western side, the Ferriby Formation and Welton Formation are exposed at the surface successively. The outcrop of the Burnham Formation covers the middle and southwest of the study area. The Flamborough Formation comprised the majority part of the East Yorkshire region extending from the middle to the east and southeast, in the central part of the area, the Flamborough Formation is exposed to the surface, while the east and southeast of the area it covered by superficial deposits.

- Ferriby Chalk Formation: This Formation is equivalent to the Lower Chalk of the southern province; it consists of flintless chalk with variable clay content. The base of the Ferriby Chalk Formation is marked by a succession of Red Chalk, soft nodular chalk with marly and hard shelly limestone.
- Welton Chalk Formation: this formation is nearly equivalent to the Middle Chalk of the Southern province. It consists mainly of thick and fairly hard Chalk strata. Black bands of marl occur but are more dominant at the base of the Formation. The formation includes discontinuous bands of flint.
- Burnham Chalk Formation: This formation corresponds to the lower part of the Upper Chalk of the southern province. It consists mainly of the white chalk of medium hardness, interbedded by thin marl bands and tabular flint beds.
- Flamborough Chalk Formation: this Formation is approximate to the upper part of the Upper Chalk of the southern province. The Formation composed of the soft white chalk and thin marl beds with no flint (or flint is so rare that its existence is often neglected).

Superficial deposits:

Superficial deposits (or drift as it known by the British Geological Survey BGS) are non-stratified unconsolidated sediments which rest on the bedrock. These sediments are youngest geological deposits in the area formed at less than 2.5 Ma during the Quaternary period. They formed and were deposited primarily due to glacial activity. Its thickness is variable spatially over the region, typically up to 10 m, but thickness may reach up to 40 m in the east of the Holderness Plain area (ESI, 2010).

Superficial deposits are classified into several subgroups; head, alluvium, and till deposits. Head; unconsolidated superficial deposits formed by hill wash and soil creep; mainly consisting of sand and gravel, locally with lenses of silt and clay. This kind of recent deposit is thin and more prevalent in the dry valleys on the Chalk, from weathering of interfluves and hillsides. Till: unsorted and non-stratified sediments deposited directly by glacial ice. It is complex lithologically, mainly consists of silt or clay with some gravel (and is sometimes misleadingly called Boulder Clay). Till may also comprise silt, sand and occasionally boulders (Carlisle, 2005).

Putty Chalk or Marl is another type of the superficial deposits that form due to the weathering of the upper surface of the Chalks, its thickness is variable up to 5 m. Distribution of this type of deposits has a vital hydrogeological role as it confined the Chalk over the Holderness plain (ESI, 2010).

Alluvium: loose or slightly consolidated recent sediments deposited by rivers; for example in the East Yorkshire the River Hull and its tributaries. Mostly consisting of silty clay but can contain layers of silt, sand, peat and fluvioglacial gravels. Fluvioglacial gravels are important sediments hydrogeologically because of their capability for storing and transporting water and play a significant role in the hydrological situation of the area. Locally they form windows through impermeable superficial deposits, which becomes discharge and recharge areas for the confined

Chalk, for instance, the Blue Keld spring at the southeast Hutton village (TA022523) .

The paleo cliff line at the East Yorkshire area has a significant impact on the thickness and distribution of the superficial deposits as it nearly represent the border between Wolds and Holderness Plane. At the eastern of the cliff line, the area is flat and dominated by superficial deposits, mostly of glacial till deposits. The thickness of these deposits increases eastward from paleo cliff toward the North Sea. The cliff lines itself is buried below thin glacial deposits (sands and gravels). Westward from the paleo cliff line the thickness of superficial decrease until the Chalk outcrop is reached.

2.2.2. Regional Structure of East Yorkshire

The Cretaceous Chalk overly the older rocks unconformably. In general, the chalk beds dip east and east-southeast gently with a dip angle of 3 to 5 degrees. The contour map on the base of the Chalk for the East Yorkshire (Versey, 1947; Foster and Milton, 1976; Baker et al., 1984; Gale and Rutter, 2006), see Figure (2.4), shows that the base of the Chalk rises above sea level toward the western boundary of the Yorkshire Wolds. The contour pattern indicates that the general direction of dip is East-Southeast (ESE). Toward the coast, beneath the superficial deposits of the Holderness Plain, the elevation of the base of the Chalk falls more gradually toward the Southeast. The Hunmanby Fault with an axis NNE-SSE at the north of the area significantly affects the dip direction of the base of the Chalk, as a result the contours become East- West beneath Flamborough Head with the dip direction toward the South (Versey, 1947).

In East Yorkshire, several normal and reverse faults in the basement rocks have been discovered, with the general strike East - West. These faults produced bending in the overlying Chalk beds formed a sequence of wide and gently sloping syncline and anticlines with axis east – west and northwest - southeast. From the structural maps Figure (2.4) and Figure (2.5), which respectively shows fold and fault distribution in

East Yorkshire, a strong relation between these two types of structure can be noticed. The development history of the Bempton Fault (near the Bridlington) and folds could be a good example revealing this relationship. The Bempton Fault network developed before deposition of the Chalk (Kirby and Swallow, 1987), these faults re-activated later and propagated into the overlying Chalk in the form of a thrust fault producing folding in the Chalk (Starmer, 2008).

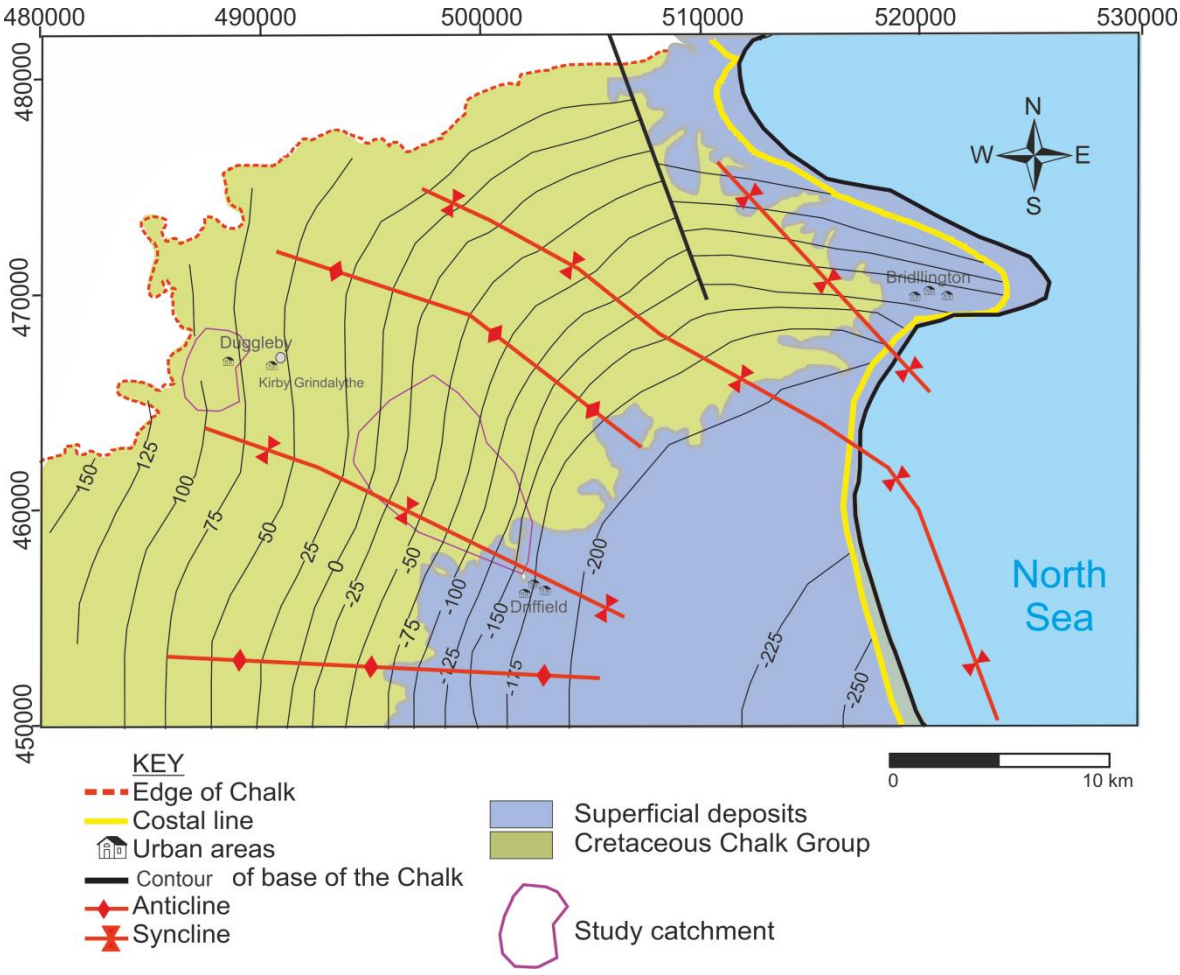

Figure 2-4. The map shows the structure contours on the base of the Chalk group and display the main anticline and syncline in the area (from Allen et al, 1997, Gale and Rutter, 2006).

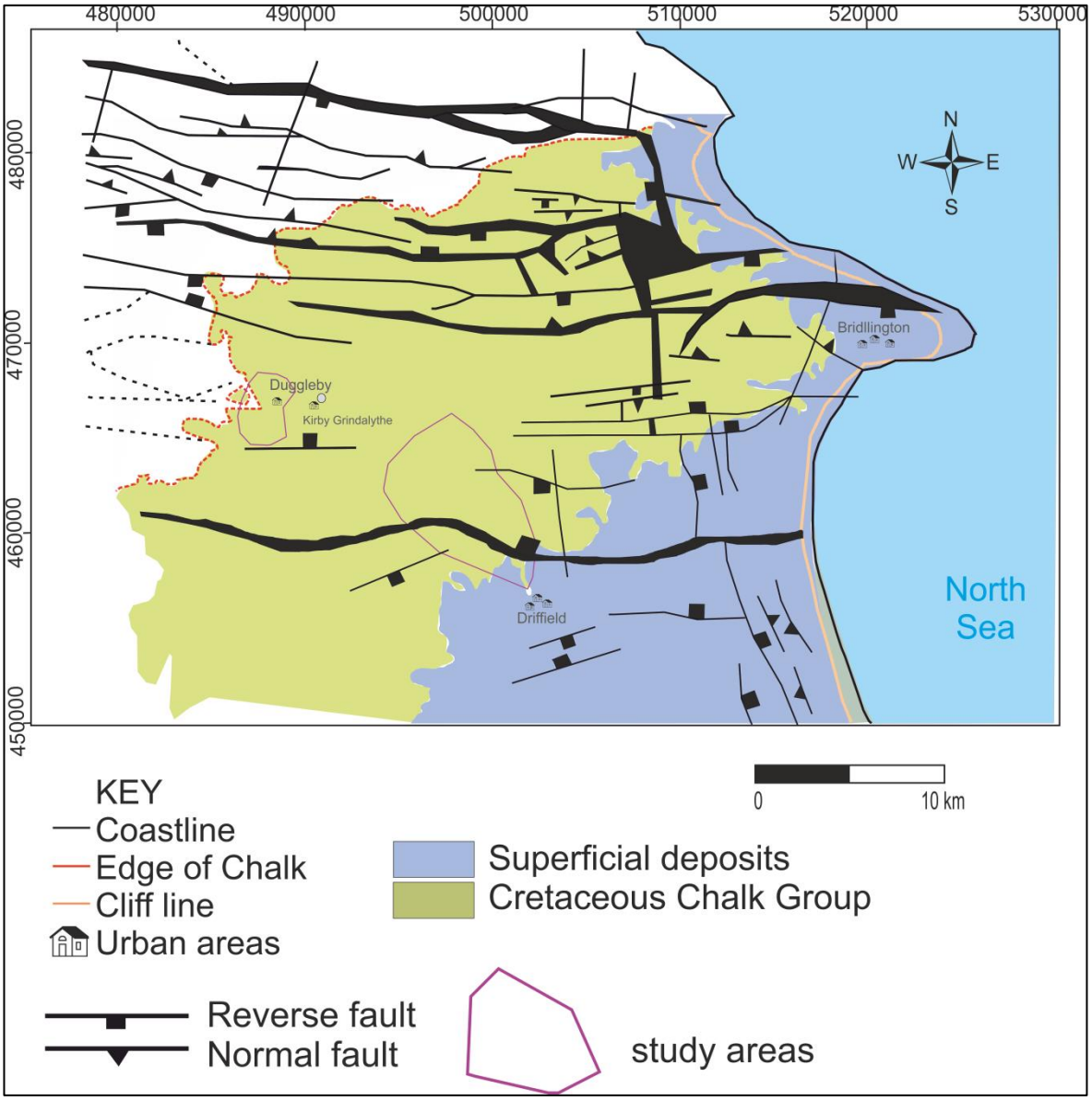

Figure 2-5. Structure map of East Yorkshire shows the main Fault system in the area (from Gale and Rutter, 2006).

2.3. Developing a geological model for the study catchments:

2.3.1. The geological cross section in the Wolds from Kirby Grindalythe to Driffield catchments:

For the purpose of understanding the geological setting of the area and to investigate how geology affects the groundwater, flow direction and the springs that emergence at Duggleby and Driffield a geological cross section has been constructed during this study. The cross-section is in the NW-SE direction from grid references [SE 85127 68152] at Duggleby to [TA 02990 57302[at Driffield. This section is almost parallel to the general strike of the Chalk beds.

Constructing the cross-section have been accomplished depending on the topographic map, geological map and contour map of the base of Chalk (the topographic and geological map were from BGS and base of the Chalk from Gale and Rutt, 2006). At the first stage, the dip of the Chalk strata were estimated from the map of the base of the chalk. The trigonometric method has been used for calculating dip angle. Along the selected profile the value of the minimum contour line subtracted from the value of the maximum, the result is the difference in the elevation of the Chalk along the profile (the result was 80m). Then, the horizontal distance along the profile was measured, which was 1788m. The dip angle is $\tan^{-1}$ of the ratio:

$$\tan_{dip\ angle} = \frac{elevation}{horizontal\ distance} = \frac{80}{1788} = 0.0448$$

$$Dip\ angle = \tan^{-1} 0.0448 = 2.56 \text{ degrees}$$

From overlapping topographic map and map of the base of the Chalk the surface topography and contact surface between the Chalk and underlying Formation has been drawn on the cross section. Then, from the geological map, the contact of the Chalk Formations was transferred to the geological cross section and the dip angle

for the contact surface between the Chalk Formations drawn using the dip angle above (Figure 2.6). The contouring and 3D surface mapping software 'Surfer' has been used for constructing this cross section.

A similar section has been drawn by Smedley et al. (2004) at the East Yorkshire. The section was at the southern of Driffield extended from Market Weighton [GR: SE877417] to the west to the Hornsea [GR: TA200475]at the east.

2.3.2. Geological model of the study catchments:

A 3D-geological model is a three-dimensional diagram that indicates the spatial and vertical distribution of the rocks and structure (Artimo et al. 2003, Kassenaar et al. 2003, Hinsby & Abatzis 2004). It shows the stratigraphy and structural condition of the area and allows easy understanding the relation and interconnection between them. This model will be a strong foundation for building an appropriate hydrogeological conceptual model.

Geological model of Kirby Grindalythe:

Two borehole logs, Low and High Mowthorope, located east of the study area at the grid reference SE 89325 67007 and SE 89700 67400 respectively (Figure 2.7), geological map (BGS geological map) (Figure 2.8) and topographic map (OS) are the main information which have been used for constructing the geological model for the Kirby Grindalythe catchment. 3D-topographic map of the catchment was drawn after digitizing the original topographic map using Surfer software. The digitized data then put in the Surfer for drawing the coloured-relief topographic map,(Figure 2.9).

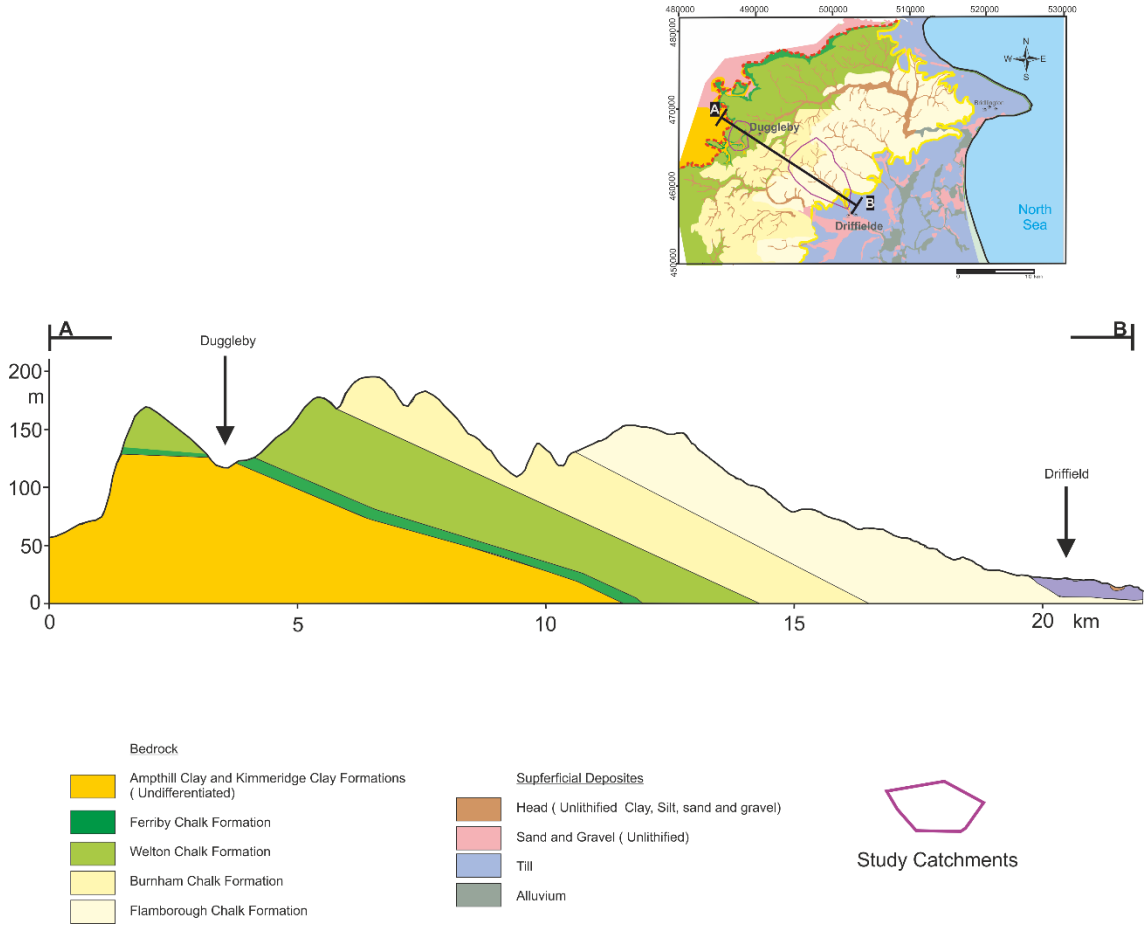

Figure 2-6 Geological cross section, extend NW-SE direction from the Duggleby to the Driffield. Note vertical scale exaggeration to show the detail of the topography. Note:vertical scale exaggerated to show the topography variation.

The outcome 3D-geological model and a geological cross section for Kirby Grindalythe catchment is demonstrated in Figure (2.10). In the model, the dip angle of the contact surface between the Formations appears greater than the real dip-angle, the reason is that the vertical scale exaggerated order to shows the variation of the topography.

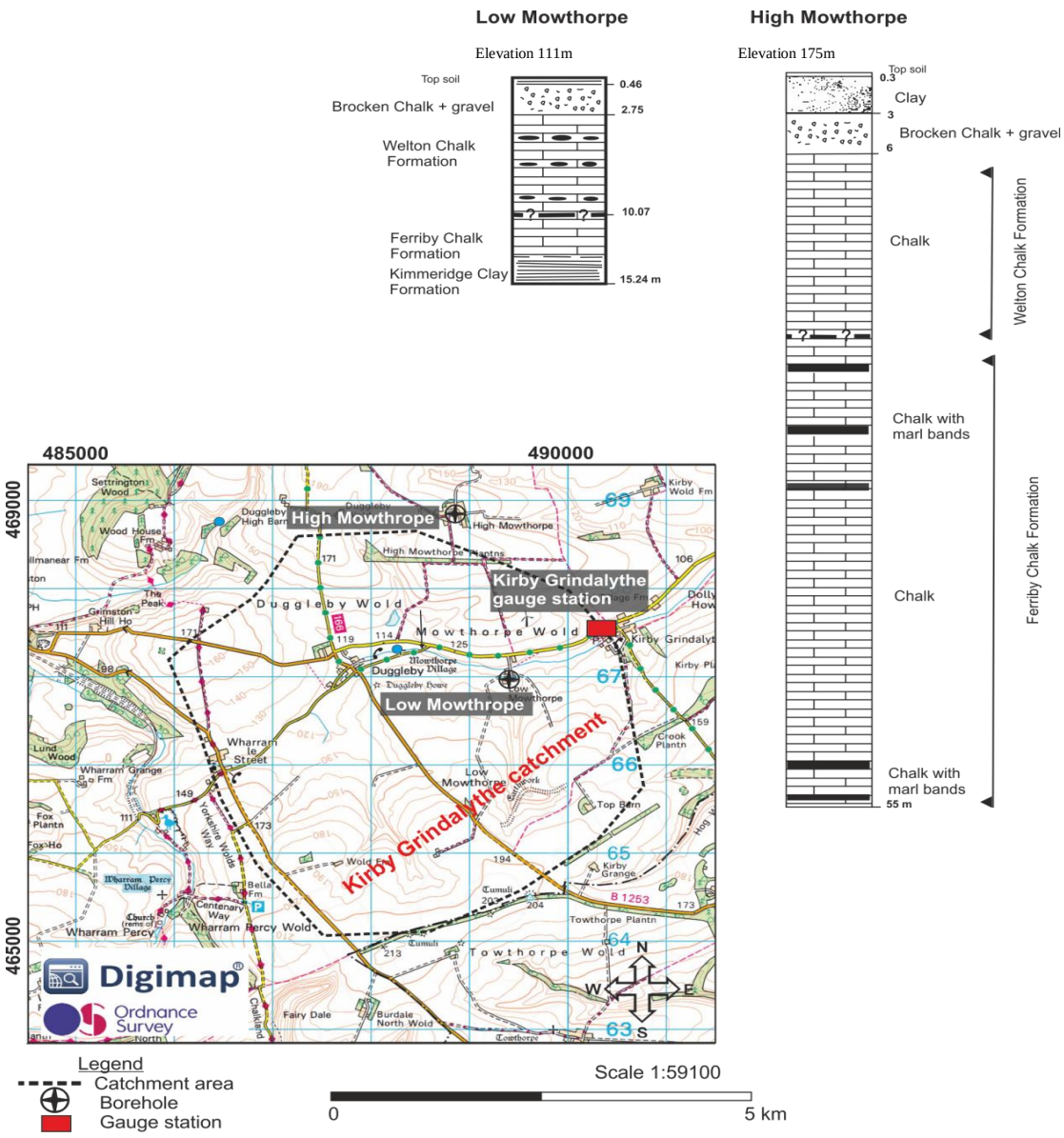

Figure 2-7 Stratigraphic logs from boreholes at Low Mowthrope and High Mowthorpe. From the borehole reports of British Geological Survey BGS. the national grid reference (NGR)of Low Mowthorope is SE 89325 67007 and High Mowthorpe is SE 88744 68846.

Figure 2-8. Geological map of Kirby Grindalythe catchment (from BGS geological map of the UK on http://mapapps.bgs.ac.uk/geologyofbritain/home.html).

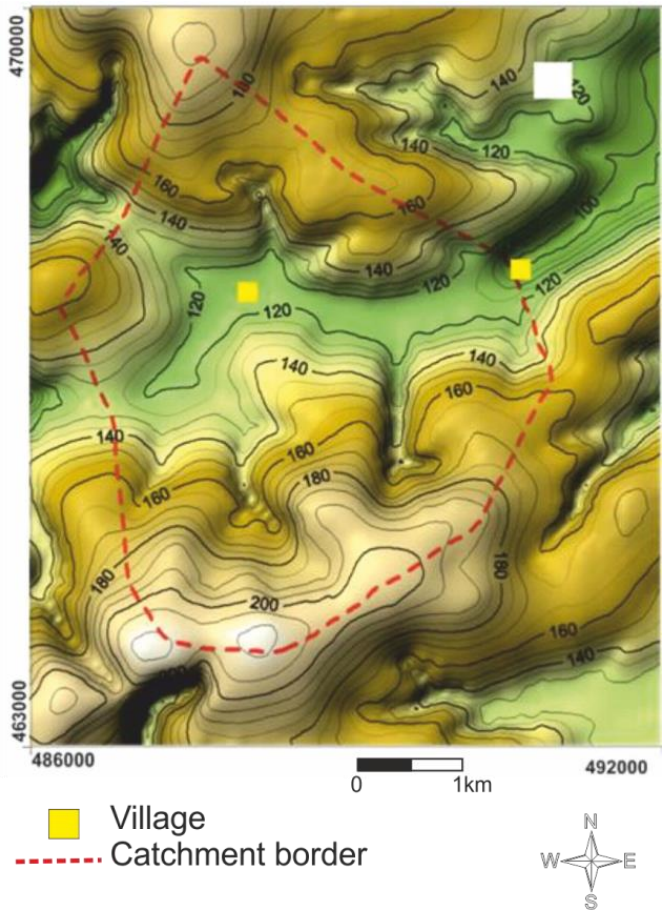

Figure 2-9 Shows the topography and catchment boundary of the Kirby Grindalythe aquifer. Topographic map formed by Surfer (Golden Software), the catchment boundary from National River Flow Data on http://nrfa.ceh.ac.uk/data/station.

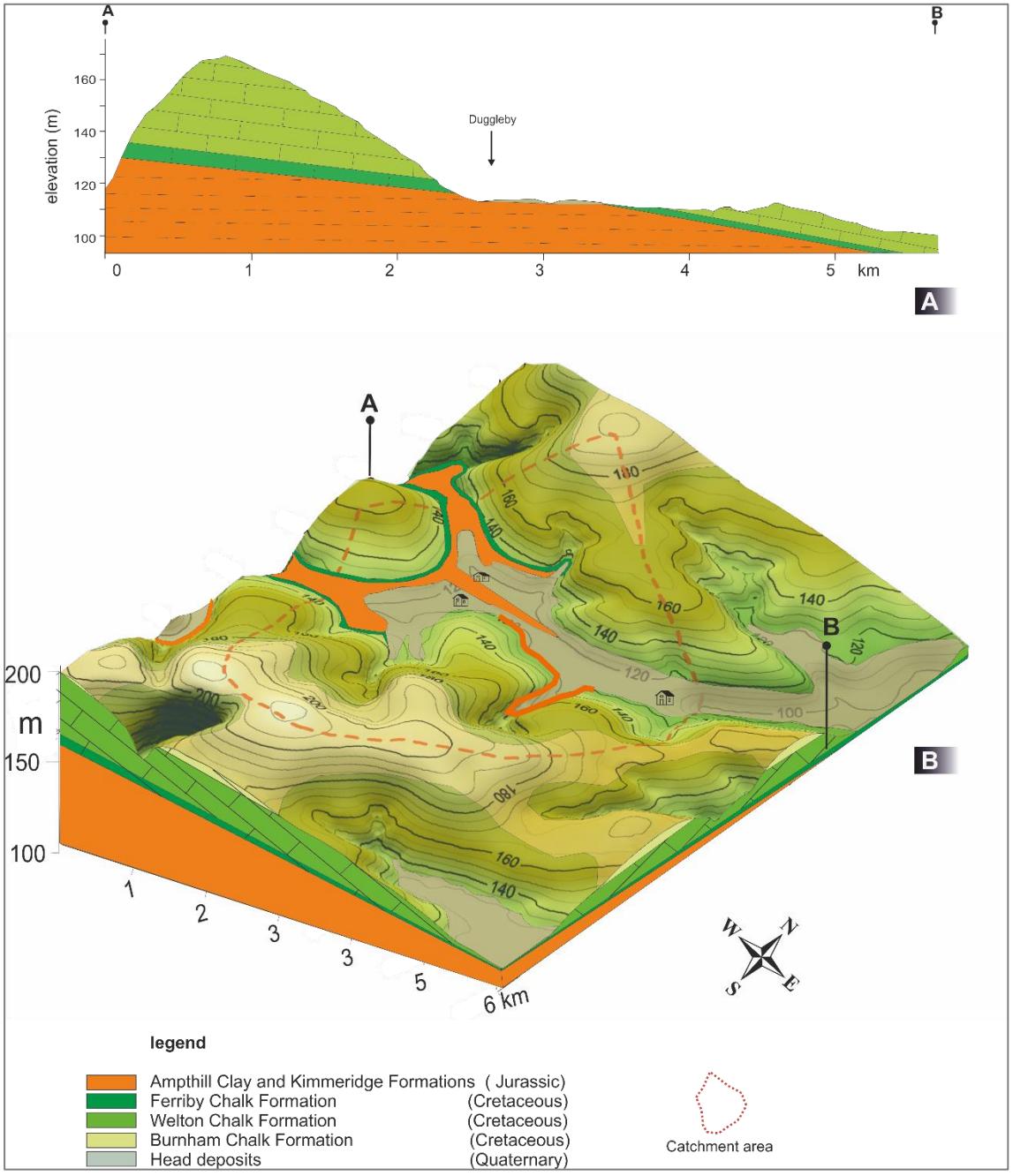

Figure 2-10. Geology of the Duggleby- Kirby Grindalythe area. (A) The geological cross section from the West to the East of the Kirby Grindalythe catchment showing the relation between the Chalk Formations and underlying Clay Formations. (B) Three-dimensional geological model of the area. (Surface geology from the BGS UK geological map). Note: vertical scale exaggeration to show the detail of the topography. [Grid reference of point A: SE85517 67693, B:SE91536 67970].

Morphological map of the unconformity surface between the Chalk and underlying Clay formations:

In the Kirby Grindalythe catchment the contact surface between the Chalk and underlay Clay Formation, which is an impermeable contact surface, crops out in the valleys. Consequently, it acts as a boundary condition for groundwater flow and distribution of the springs in the area. Furthermore, it can be used for estimating the thickness of the Chalk in the area. Because of its importance, this study constructed a contour map for this contact surface, Figure (2.11).

Often the contact surface between different stratigraphic units is determined depending on the boreholes, geophysical profiles, and outcrops. Unfortunately, no geophysical investigations have been done at the Kirby Grindalythe Catchment. In addition, not enough boreholes are availability inside the catchment, only the Low Mowthorpe and High Mowthorpe boreholes exist in the area, and only Low Mowthorpe penetrates the Chalk/ Clay Formations contact surface (Figure 2.7). therefor as an alternative in the catchment the map of the contact surface was constructed depending on the outcrop of the contact surface between Chalk Group and underline Clay Formation (in the area most probably is Kimmeridge Clay Formation) and the borehole at Low Mowthorpe village. Surfer software was used in constructing the contact surface contour map. The geological map (BGS map) and topographic map (OS map) have been overlaid then along the contact surface, a number of the locations with a different elevation have been selected. At each location, the elevation of the contact surface and coordinates of the locations have been read. All recorded data was then imported to Surfer.

The contour map showed that at the north and south of the mapped area the contour lines are closer than the contours in the middle area. This indicates that the contact surface has a steeper slope angle in the north and south of the maped area , which represent the area outside the northern and southern border of the Kirby Grindalythe catchment.

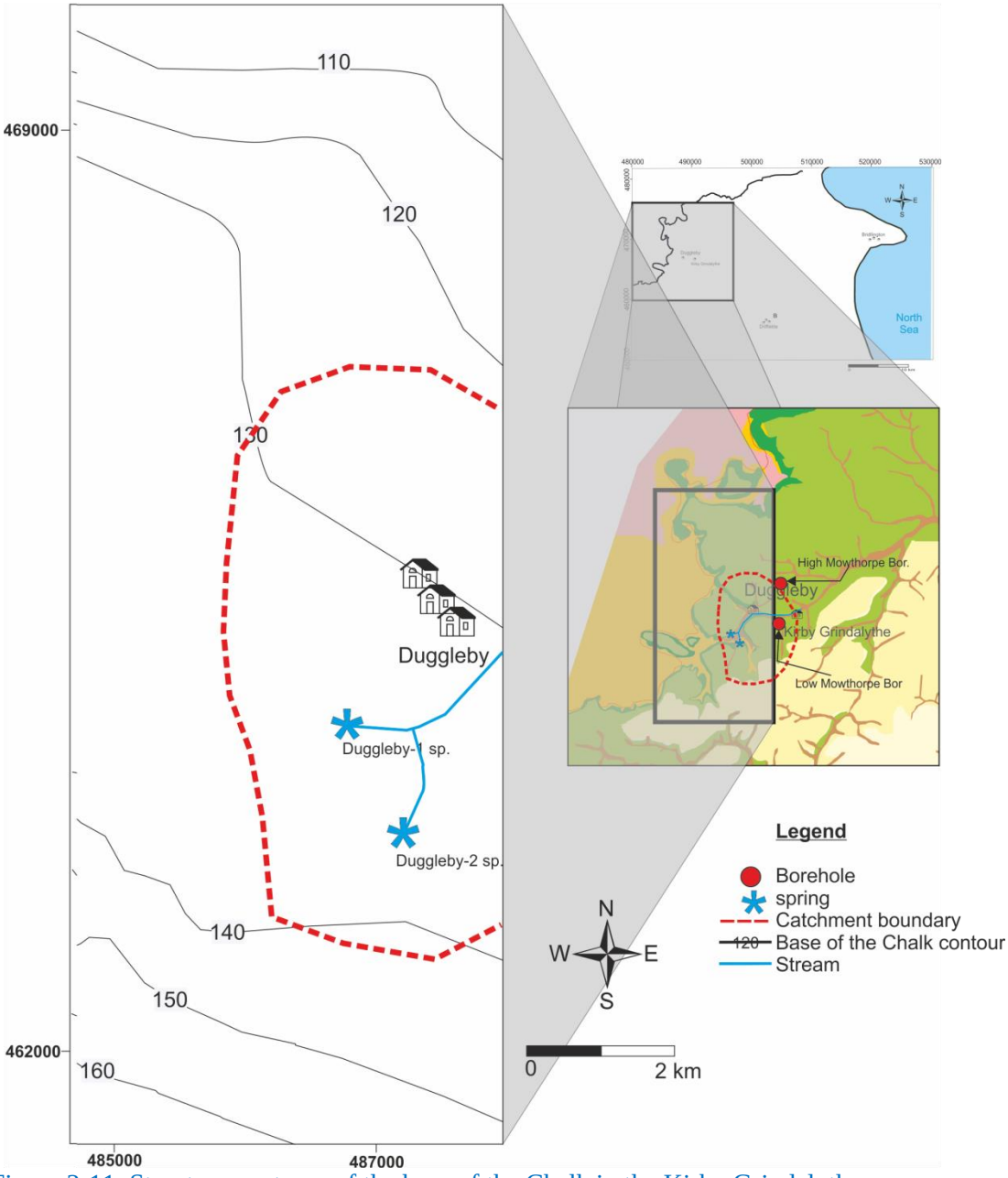

Figure 2-11. Structure contours of the base of the Chalk in the Kirby Grindalythe catchment.

The map shows that the slope direction of the contact surface is North-Northeast (or 017 degrees) with an average slope angle about 0.4 degree (calculated as an average angle over the entire map in the direction of the slope). Nevertheless, the study catchment located in the middle of the area, at this area the slope of the contact surface was samller, around 0.1 degree. The slope direction of the contact surface is similar to the Jurassic Clay Formation bedding, as (because of pre-Cretaceous movements) these rock beds dip North-Northeast (Versey, 1947).

The same technique has been used for estimating the dip angle and dip direction of the Chalk beds depending on the altitude of the outcropped contact surface between Ferriby Chalk and Welton Chalk Formation); this dips toward the east with the dip angle of 0.5 degree

Superficial deposits of the catchment:

The Chalk in the area is covered by a soft loamy soil at the interfluvial area, and by a highly permeable Head deposits along the valleys and river beds. The thickness distribution of the cover deposits was controlled by the factor of physiography.it is thin to intermediate (BGS UKSO soil thickness terms) over the interfluve and hill slopes i.e. few centimeters to one meter. In contrast, it is thick in the valleys and riverbeds, i.e. exceeds one meter. The obove information about the type and thickness of the soil cover were obtained from British Geological Survey-UK soil (BGS-UKSO) and Centre for Ecology and Hydrology (CEH).

The thickness of the aquifer and the Chalk Formations:

The thickness will be a vertical thickness between the ground surface and the contact between the Chalk Formations and underlying Clay Formations. According the surface topographic map (Fig 2.9) and contour map of the base of the Chalk (Fig 2.11), these two maps showed that the thickness of the Chalk in Kirby Grindalythe is between 0m below the valleys up to 70m below the interfluve. the High Mowthorpe

borehole, which located on the interfluve at High Mowthorpe farm ,showed that the thickness of the Chalk is more than 55m (see Figure 2.7).

In the Figure (2.7) big contrast in the overall thickness of the Chalk from the profile of the boreholes Low and High Mowtorpe can be noticed. The thickness of the Chalk in the Low Mowthorope about 10 m, while in the High Mowthorpe is > 55 m. Taking in the consideration the Chalk hill to the west of the Duggleby (see Figure 2.10), it can be noticed that thickness of the Chalk toward the flank of the hill. So similarly the difference in the Chalk thickness between Low and High Mowthorpe boreholes arises because of the topographical location of each borehole. Low Mowthorope located in the valley with the elevation 111m while High Mowthorope located in the interfluve side with an elevation 175m.

However if the stratigraphic section of the borehole Low and High Mowthorpe correct this difference most probably due to the sudden change in the dip angle of the strata. According to the profile of these boreholes, the thickness of Ferriby Chalk is only 5m at Low Mowthorpe, while it is about 30 m at High Mowthorpe. In addition, the base of Welton Chalk is about 100m a.s.l. at Low Mowthorpe and about 155m a.s.l. at High Mowthorpe. the difference in the Chalk thickness and difference in the elevation of the base the contact of the Chalk Formation imply a steep dip of the Chalk beds. For producing this difference in the Chalk thickness the dip angle of the Chalk at High Lowmothrope expecting to be about 60 and at Low Mowthorpe close to zero. However, the attitude of the outcrop contact surface between the Chalk Formation in the area did not support the statement of the steep dip.

Geological Model of Driffield

Superficial deposits of the catchment:

The Chalk is covered by shallow to intermediate highly permeable soil and recent deposits. Loamy soil covers more than 85% of the area including northwestern side and middle part of the area. Riverbeds are filled with soft to firmly consolidated

deposits, known as Head. The cover deposits changes toward the southeast, consisting mainly of sand and gravel around the stream, which rises at Driffield spring, close to the feather edge of the glacial till deposits. Figure (2.12) is a geological map of the Driffield catchment, which shows the rock and superficial deposit distribution (solid geology map from Digimap, and soil texture from UKSO).

Thiscatchment located in an area not subjected to complex faulting or folding. A reverse traversal fault (with E-W direction) passes through the southern part of the area. This fault produced a wide syncline with an NW-SE trend and gentle sloping limbs.

Geological cross section of the catchment:

The geological cross section of the catchment derived from the geological map of the area and boreholes profiles. the geographical location and information about the boreholes which used for study this catchment are illustrated in the Figure (2.13) and table (2.1).

From five boreholes a panel diagram for the catchment has been constructed in an attempt to express the stratigraphical cross section of the Chalk over the catchment area , see Figure (2.14). however the borehole profiels show the lithological information but unfortunately, the contact between Chalk formations is mostly not determined; only one borehole identifies the contact between Ferriby and Burnham Chalk (borehole no.1 in Figure 2.13). Therefore, the information from the boreholes was not valuable for determining dip angle or dip direction of the Chalk beds. Alternatively, for the purpose of estimating dip angle and dip direction the information from the outcrop pattern and regional structure have been employed. From the geological map and topography map of the Driffield catchment, the contour lines of the contact between the Burnham and Flamborough Chalk formations have been constructed, see Figure (2.12). This contour constructed based on the same methodology used for constructing contour map of the contact surface between the Chalk and underlay Clay Formation in the Kirby Grindalythe catchment.

The contour lines reveal that the Chalk beds are dipping toward the southeast with the dip angle about 2.2 degrees. This result indicates that the folding (syncline) which passes through the southern part of the Driffield catchment may not significantly affect the general bedding direction SE, as suggested by the BGS reports (Gale and Rutter, 2006; Allen et al., 1997).

The southeastern border of the catchment at and around the location where spring arise covered by the superficial deposits. A geological panel diagram for this part of the catchment has been constructed depending on the lithological profile of the shallow boreholes (labelled 6-10) that located near the top reach of the stream that feeds by the Driffield spring, Figure (2.15). This diagram was constructed to express the lithology and thickness distribution of the superficial deposits around the stream.

The panel diagram showed a lithological information up to 10 m depth as the maximum depth of the shallow boreholes in the area is 10 m. The area covered by about 0.3m top soil, followed by 4 m thick of firm silty-sand with chalk fragments, with the pockets of sand and chalk gravel. Then, from the depth 4 m to 10m depth the composition of the deposits changed and become a mixture of clay bound chalk, flint gravel, and brown silty clay. The diagram shows that the thickness of these deposits reduces in the direction away from the stream channel. The thickness of the superficial deposits is more than 10 m along this section of the stream channel, i.e. this reveals that base of the Northend stream does not cut into the chalk formations here.

The thickness of the aquifer and the Chalk Formations:

The morphology of the base surface of the Chalk does not show a significant variation, the average slope of this surface (contact surface between Chalk and underlying Clay Formations) in the Yorkshire Wolds is about 0.8 degrees toward southeast (according to the contour map of the base of the Chalk in East Yorkshire , see Figure 2.4). A number of the dry valleys crossed the area, OS topographic map of the area showing that the depth of the valleys in general ranges between 60- 100

m. Hence, in the area because the Chalk cropped out its thickness controlled by the surface topography. The thickness is greater below the interfluves than the valleys. From the contour map of the base of the Chalk and surface topographic map of the area, the thickness of the Chalk has been estimated which is about 160 m in the highest area, and about 100 m in the valleys. The borehole number one in the panel diagram, located near the NW edge of the catchment area, confirmed that the thickness of the Chalk is more than 148m here.

From the above information and topographic map of the area (Figure 2.16), a 3D geological model for Driffield catchment has been constructed, see Figure (2.17). The topographic map and 3D geological map have been constructed using the Surfer software.

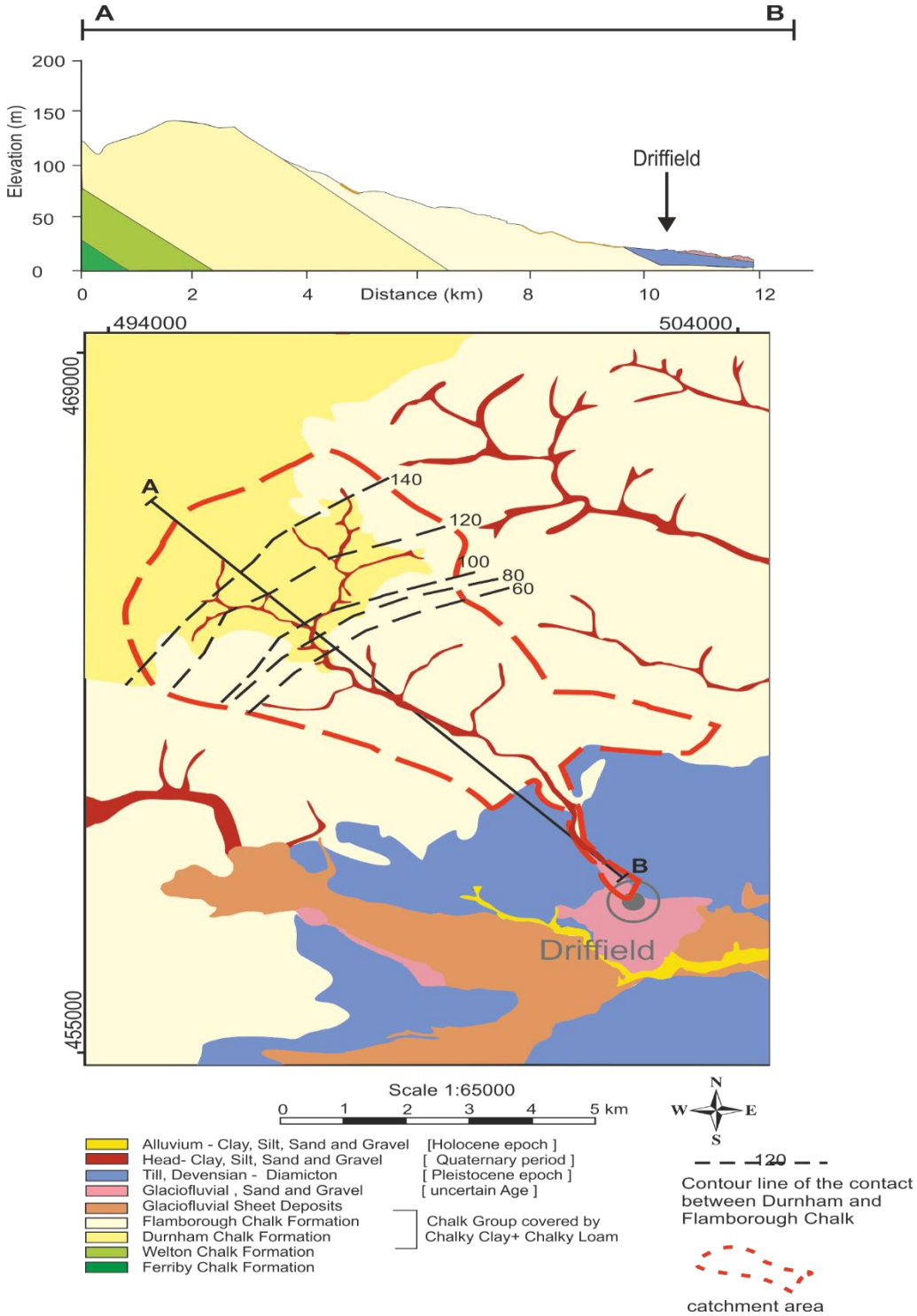

Figure 2-12 Geological map and cross section of the Driffield catchment. This map is from the BGS geological map. The cross section was drawn using the geological map and topography of the area , [Grid reference of point A:SE94199 65825, B: TA 02286 58222].

Note: Vertical scale exaggeration to show the detail of the topography.

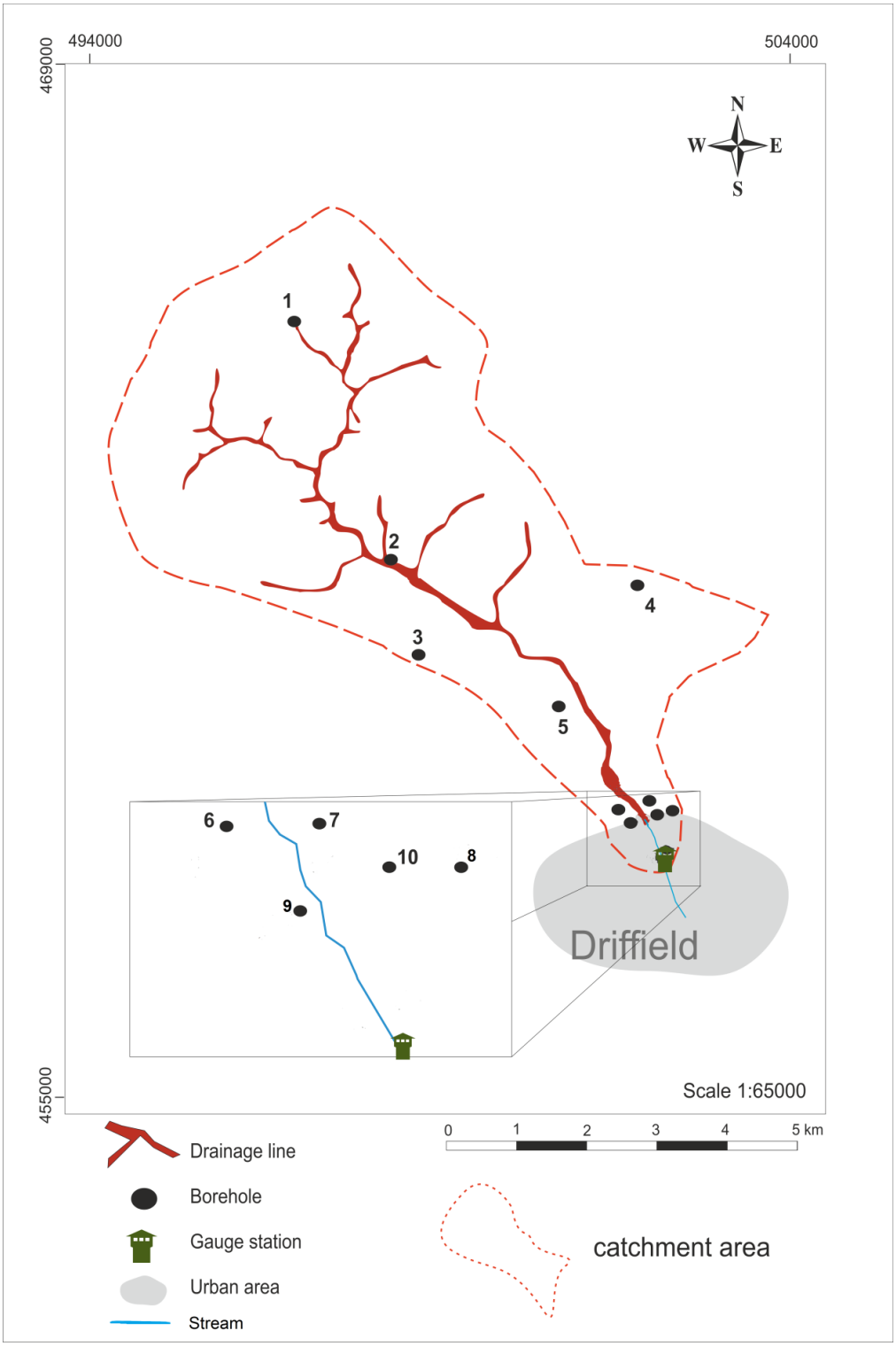

Figure 2-13. Map of the location of the boreholes which have been used for the geology of the Driffield catchment.

Table 2-1 NGR and elevation of the boreholes used in the Driffield Catchment.

Borehole #	BGS ID	Coordination		Grid reference	Elevation (m)
		Easting	Northing		
1	135323	496885	465479	SE 96885 65479	140.4
2	135329	498169	462234	SE 98169 62234	53.5
3	18534222	497690	460610	SE 97690 60610	86
4	460078	502440	461540	TA 02440 61540	67.4
5	459634	500614	459813	TA 00614 59813	54
6	459743	501880	458650	TA 01880 58650	23.4
7	459744	501920	458700	TA 01920 58700	24
8	459747	501990	458750	TA 01990 58750	25.67
9	459745	501930	458690	TA 01930 58690	24
10	459746	501950	458720	TA 01950 58720	24.2

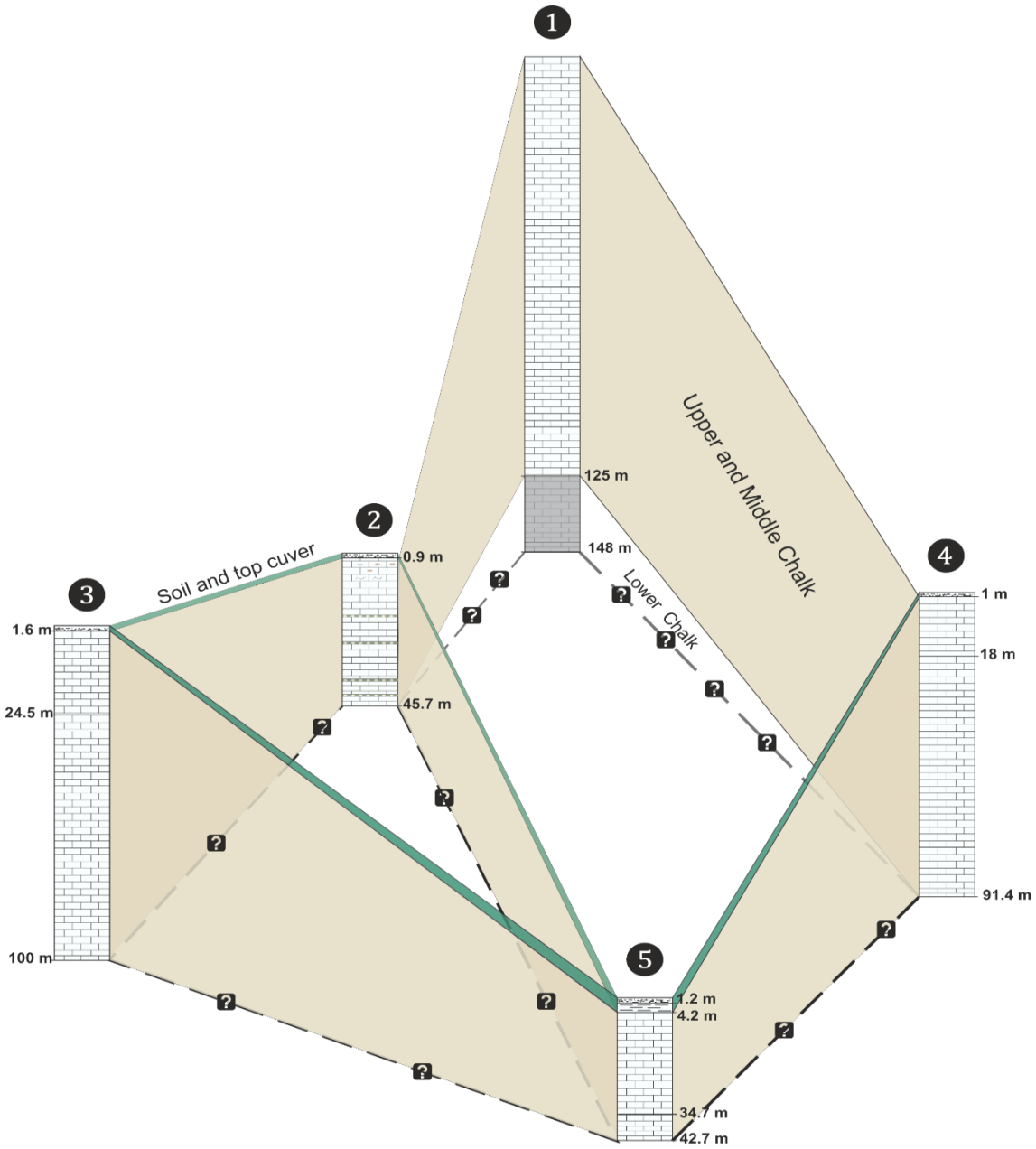

Figure 2-14 Panel diagram shows the geological profile of the Driffield catchment BGL, boreholes 1-5 from figure 3.14. The reports of the boreholes showed that the classification of the stratigraphic column in the boreholes was made using the old classification ; Lower, Middle and Upper Chalk. Therefore, in the constructed panel diagram the Chalk Formations were named accordingly instead of naming based on the chalk classification for the Northern Province (Burnham Chalk and Flamborough Chalk). [Flamborough Chalk and Burnham Chalk equivalent to Upper Chalk, Welton Chalk equivalent to Middle Chalk and Ferriby Chalk equivalent to Lower Chalk (Hopson, 2005)].

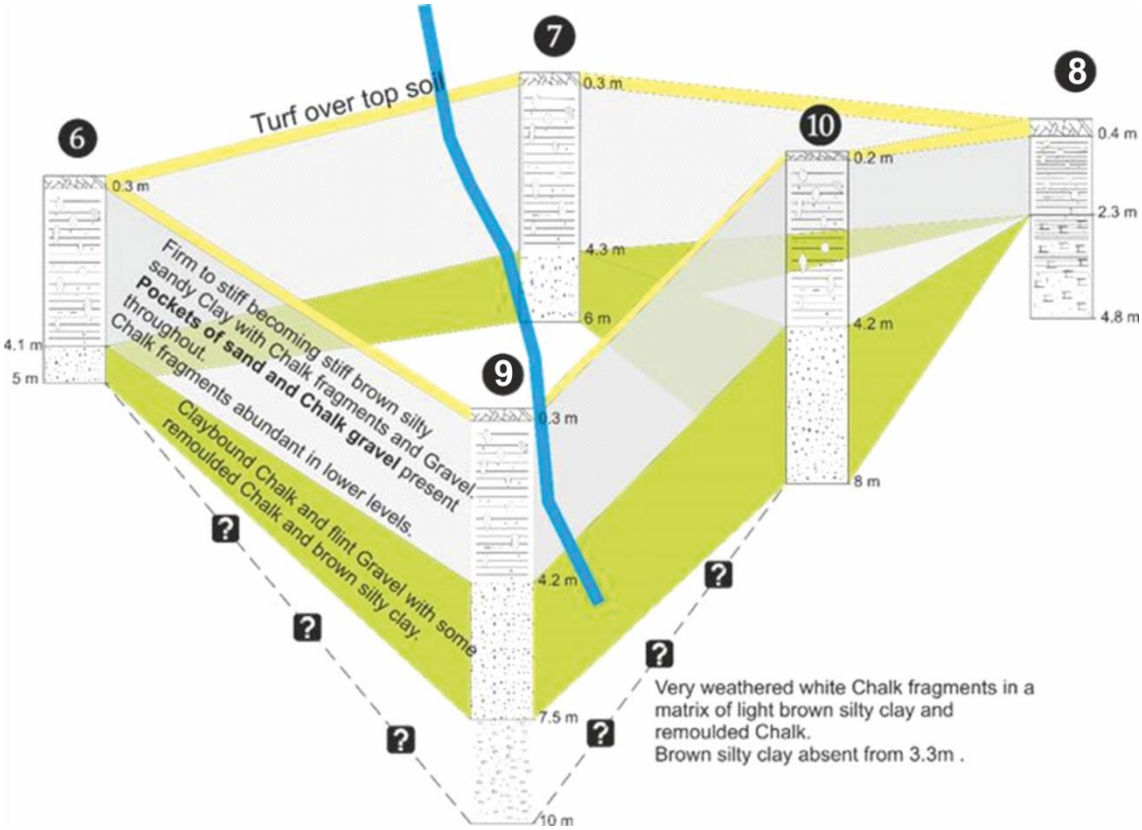

Figure 2-15 Panel diagram shows the geological profile of the Driffield catchment BGL, boreholes 6-10 from figure 3.14.

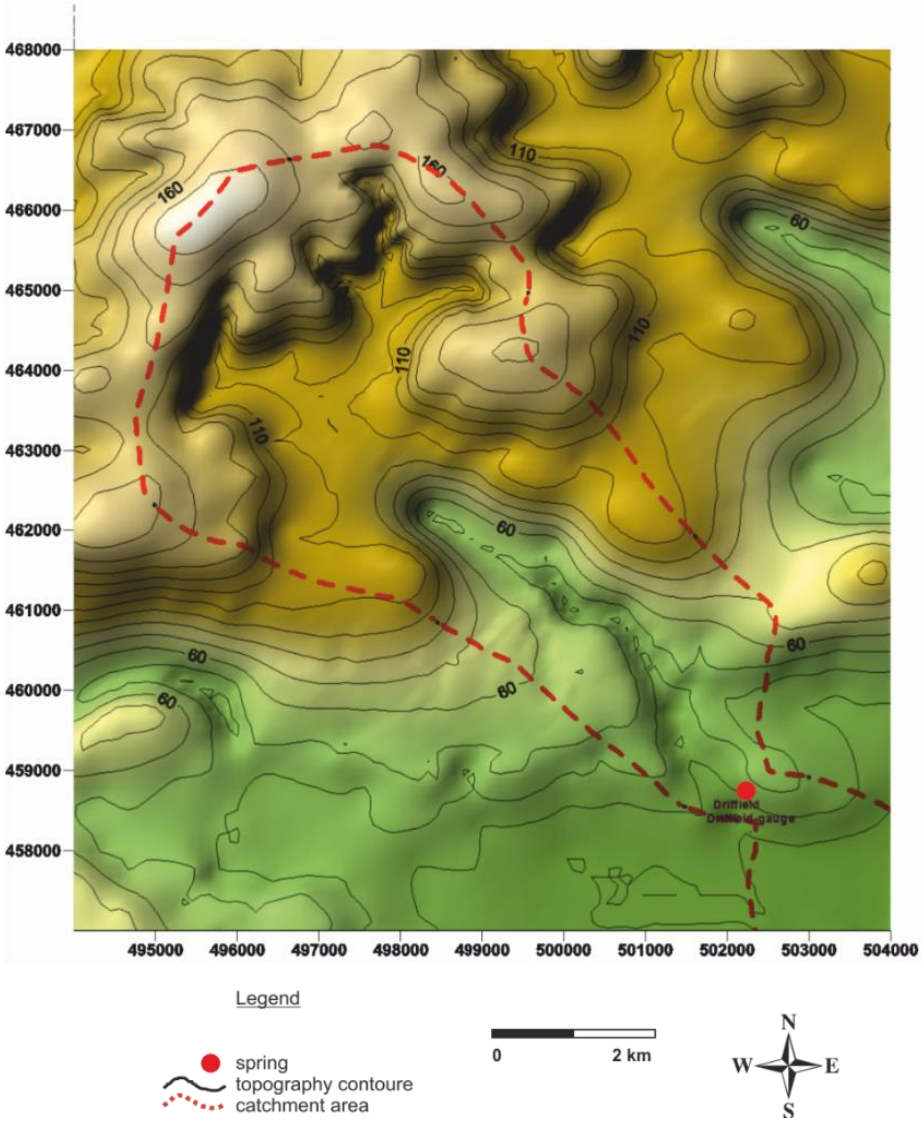

Figure 2-16 Topographic map of Driffield catchment area. Topographic map formed by Surfer (golden software), the catchment boundary from National River Flow Data on http://nrfa.ceh.ac.uk/data/station.

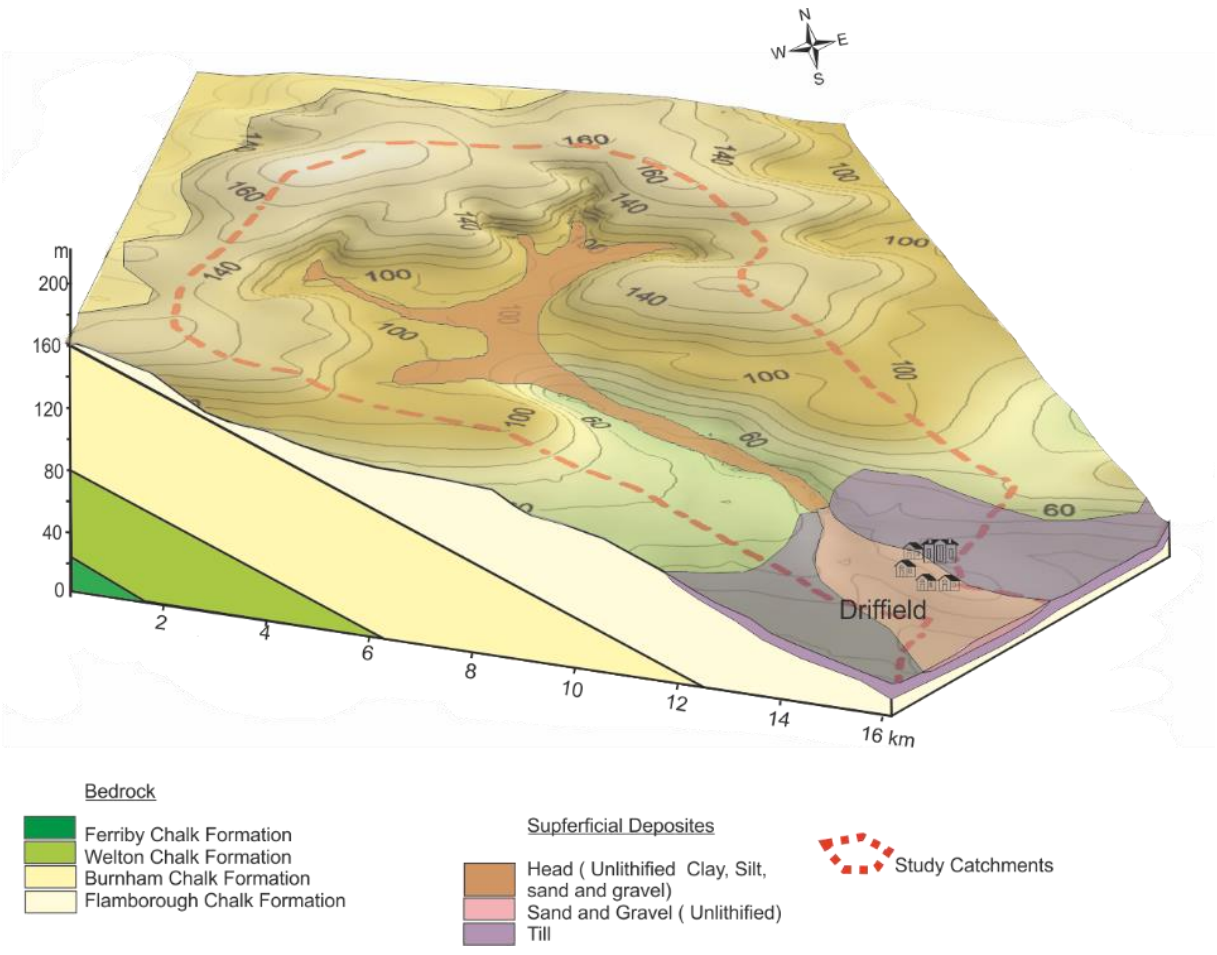

Figure 2-17 Three-dimensional geological model of the Driffield Catchment.

Note vertical scale exaggeration to show the detail of the topography.

2.4. Summary:

Geological cross sections and three-dimensional Geological models for Kirby Grindalythe and Driffield catchments have been constructed depending on the geological map of the area and borehole profiles. The models shown the surface topography and geological rock distribution, in addition to subsurface stratigraphy and geological structure.

The Chalk in the Kirby Grindalythe consists of three Formations; Ferriby Chalk, Welton Chalk, and Burnham Chalk. In general, the Chalk crops out in the area except for the valleys was filled by thin head deposits. The Driffield catchment is mainly composed of two Chalk Formations; Burnham Chalk and Flamborough Chalk Formations. Thin topsoil covers the majority of the Chalk and the head deposits covered the Chalk along the valleys. The southeastern border of the catchment is located at the contact between the unconfined and confined Chalk, where it becomes covered by thick superficial deposits (up to 10m or more).

The Chalk is underlain by Upper Jurassic Clay Formations. The contact surface between the Chalk Formation and underlying Clay Formations consists of an unconformable surface with the dip angle about 0.4 degrees on average, and dip direction NNE in Kirby Grindalythe Catchment, while its dip angle is about 0.8 degree SE in Driffield catchment. This surface crops out to the surface along the valleys in Kirby Grindalythe catchment and it buried deep below the ground in Driffield catchment (between 40-160 m).

In general the Chalk beds dip southeast with the dip angle 2.56 degrees. The dip angle of the Chalk beds is estimated at 0.5 degrees in Kirby Grindalythe catchment and 2.2 degrees in Driffield catchment.

The 3D geological models show that the thickness of the Chalk in Kirby Grindalythe range between 0 m below the valleys to 70 m bellow the interfluve. The thickness of the Chalk in Driffield catchment is about 160 m in the high topographic area and about 100 m inside the valleys.

Chapter 3. Hydrogeology of the study area: Development of catchment scale hydrological conceptual models:

In this chapter, the hydrogeology framework of the studied catchments will be discussed. In addition, the hydrogeological, geological and topographical information will be combined together to estimate the structure of the aquifers and their boundary and initial conditions.

3.1. General reviews:

3.1.1. Conceptual model of hydrogeology

In nature the behavior of real aquifers is very complex, moreover, for dual porosity aquifer, the system is even more complicated. For example, for fractured chalk, it can be noticed that the fractures distributed heterogeneously both in size and intensity vertically and horizontally (MacDonald and Allen, 2001).

Many factors make real aquifers complex. In nature, hydraulic properties of aquifer systems are heterogeneous and anisotropic spatially over the catchment area and vertically with depth. The factors like soil lithology and thickness which affect recharge are not uniform over the catchments. In addition, precipitation, temperature, and vegetation may be variable spatially and temporally over the catchment. Other factors such as geomorphology of the catchment may not be simple over the catchment area; slope and dip of the surface affects the thickness of soil cover and surface runoff.

In order to be solvable mathematically, complex systems need to be simplified in a conceptual model and generalizing the aquifer properties. A conceptual model is a schematic diagram presenting a simple version of reality. The conceptual model for

an aquifer will define how water enters, flows through and drains from the aquifer, also describes boundary and initial conditions. Every conceptual model starts with the very simple graphical format at the early stage of the modeling and become more detailed step-by-step during the model development. Mostly during the final state, it is represented by a detailed 3D diagrams (Rushton, 2003).

To achieve a conceptual model able to illustrate the real complex aquifer an approach can be followed called parameterization or generalization. Parameterization (which is sometimes known by generalization or simplifications) means presenting the system in the form that expresses our understanding of the system and its behaviour depending on a set of assumptions (Bear and Cheng, 2010). Transmissivity and hydraulic properties are the essential parameters in study any aquifer regime. Estimating a suitable value of these parameters to represent hydraulic characteristics in aquifer entirely (or part of the aquifer) makes the aquifer simpler and easier to understand.

Although the parameterization is required during model construction, but this will leads to rising uncertainty. Regional aquifers are more likely to subject to the uncertainty due to parameterization than small local aquifers, because logically large catchments likely to subject to more spatial variation in the parameters compared to small basins. Hence after the parameterization the conceptual models of small aquifers can represent the real system to a reasonable extent.

3.1.2. Catchment boundaries

Catchment area simply is an area where all surface and subsurface water contributing to the discharge at a particular point. The boundary of any catchment is determined by water divides. There are two type of water divide; surface and subsurface water divide. Surface water divides are the boundary between the watersheds where water flows overland toward different surface-water bodies, such as streams. This type of boundary is defined by the surface topographic heights. Groundwater divides are the boundaries of natural groundwater systems, where the groundwater on either side of

the groundwater divide flows away from divide. So groundwater divides consider as a no-flow boundary (Gannett and Lite,2004; Feinstein et al., 2005).

In many real cases these two types of divide do not coincide, because several factors have an important influence on the location of the groundwater divide; depth of the water table from the land surface, pumping groundwater from well, hydraulic properties of the aquifer, recharge, discharge, and geological factors (Kafri, 1970; Feinstein et al., 2005). In addition, some geological features like fault or facies changes maybe works as a barrier in the direction of the groundwater flow and affects the groundwater divides (Kafri, 1970). With a shallow water table it is more likely that the groundwater and surface-water divide coincide because both boundaries are controlled by the topography of the land surface. While in the case of deep water table, the ground water follows longer paths and may pass below local streams and topographic highs (Feinstein et al., 2005). In the Chalk aquifers, the variance in the thickness of the unsaturated zone between the interfluves and valleys could be a good example for explaining the poor relationship between topographic patterns and water table shape.

Several techniques have been suggested for estimation catchment area (Kreye et al., 1996) for example; topographic, geological, water balance , water chemistry, tracers, spring discharge hydrograph.

Topography and groundwater:

It is possible, using topographic maps, to trace the surface water divides or catchment boundary (Gannett and Lite,2004). As recharge generally occurs in upland areas, the highest water table and groundwater divide often tend to coincide with the surface divide (Harter and Rollins, 2008). The shape of the water table in unconfined aquifers is often assumed to be a subdued replica of the topography or land surface (Dingman, 2002;Toth ,1963), but the relief of the water table is not always the same magnitude as the land surface (Gregory, 1918). However, this statement may not be applicable for fractured rocks, as in many cases of fractured

aquifers the water table pattern and the surface topography appear poorly related (Moore and Thompson 1996; Blaskova et al., 2002; Desbarats et al. 2002; Shaman et al., 2002).

Geological structure and groundwater:

Generally, in the regional scale over the East Yorkshire, it can be noticed that the groundwater flow direction is co-incident with the general bedding direction, which is east and southeast. Regarding the surface water, the Gypsey Race stream can be considered as one significant example controlled by geological structure. The direction of the Great Valley where the Gypsey Race flows is controlled by the known directions of basement faults (Starmer, 1995)(see figure 2.5). In addition Smedley et al., (2004) claimed that the sudden change in the direction of Gypsey Race near Rudston to the west of Bridlington is because of the Hunmanby Monocline, this monocline is considered to be a surface expression of a deep basement fault, as its direction with the known directions of the basement faults.

3.1.3. Hydraulic Characteristics of the study catchments .

Little is known about the aquifer properties in the study catchments. Transmissivity contour map by Parker (2009), which is constructed based on 87-pumping tests results from 68 sites, is the most recent summary of transmissivity in the East Yorkshire Chalk Figure (3.1). From this map can be noticed that however there is significant difference in the transmissivity between the study catchments but within each catchment separately there is not a remarkable contrast in transmissivity. In Kirby Grindalythe transmissivity between 1000 - 500 m2day-1, and in Driffield Catchment is between 1000 – 1500 m2day-1, except the northeast border of the catchment where transmissivity increases to over 5000 m2day-1.

Information about the hydraulic properties of the aquifer in the study catchment has been obtained from borehole tests. In the Kirby Grindalythe catchment, the data was obtained from the borehole at Low-Mowthorpe, which is the only borehole in the

area has a pumping test information. This borehole showed that transmissivity is 450 m2/day, and the storage coefficient is 0.0016. In Driffield catchment the information was obtained from three boreholes ; Kilham Road off Scarborough, Great Kendal borehole ,and Elmswell Slack , see table (3.1).

The borehole data was obtained from the aquifer properties manual (APM) version 2.0.0 . APM is a browser (browser software) for the aquifer properties of the major and minor aquifer in England and Wales, prepared by the hydrogeology group of BGS.

Table 3-1 Hydraulic properties of the Chalk from three boreholes located in the Driffield catchment.

Borehole	Grid reference	Transmissivity (m^2/day)	Storage Coefficient	Elevation (m)
Elmswell Slack	SE999612	930	0.0074	42
Kilham Road off Scarborough	TA025615	1271	0.0004	67
Great Kendal	TA017602	1818	/	52

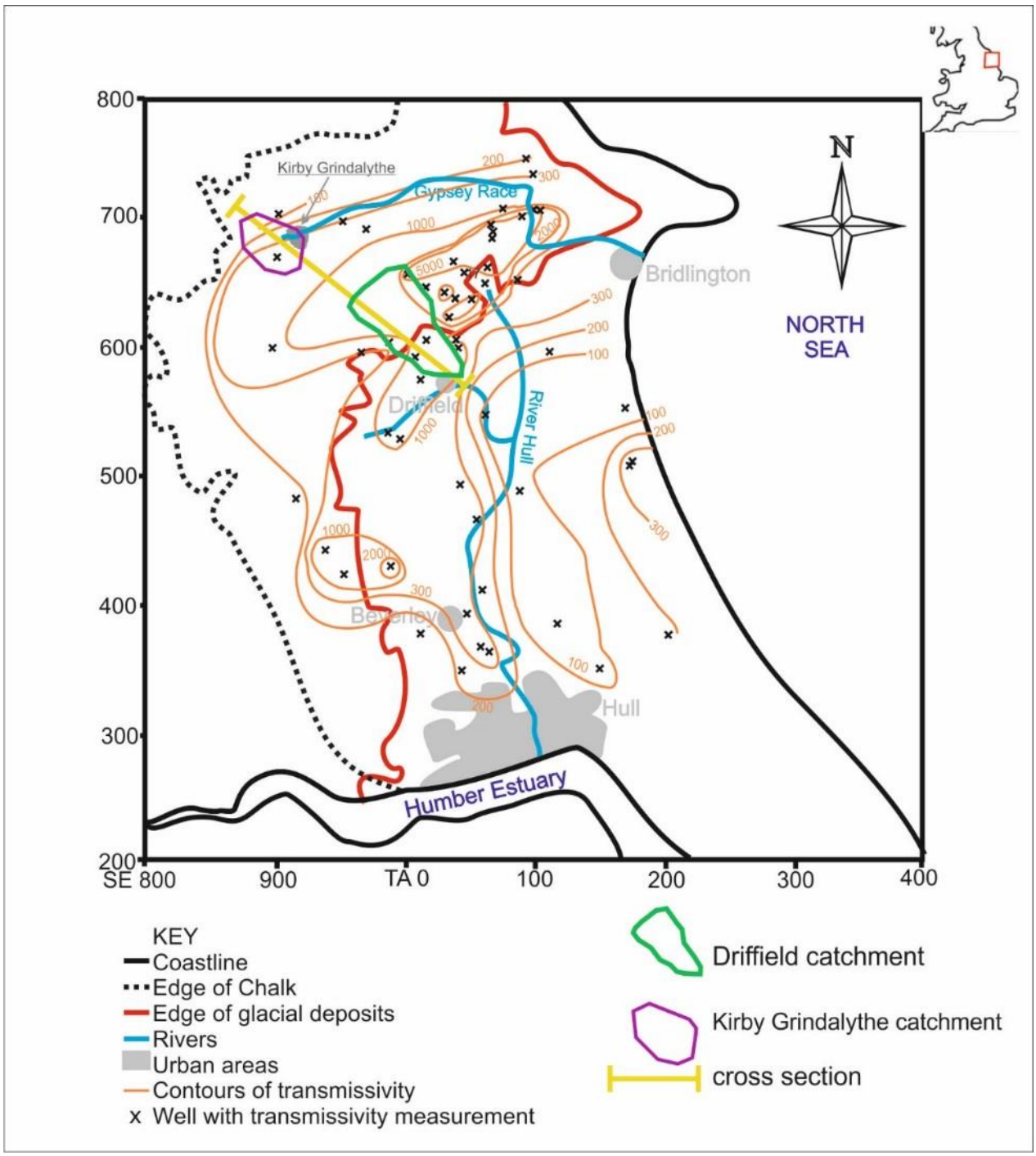

Figure 3-1 Transmissivity distribution (in m^2/day) measured from pumping tests (data supplied by Environment Agency of England and Wales). From Parker (2009).

3.2. Conceptual model for the study catchments:

The hydrogeological conceptual model for the study catchments has been developed from the geological models through importing hydrogeological parameters and according to some assumptions.

The imported hydrogeological information includes; catchment boundaries, water table, groundwater flow direction, groundwater- surface water interconnection, spring location and aquifer properties.

The conceptual model can be accomplished depending only on pre-existing information if it is available in enough quality and quantity to reflect all aquifer system characteristics. Whereas in some cases where there is a deficiency in information, investigations and data collection are required. The current study has depended on the set of existing information and data, including topography map of the area, borehole stratigraphy, aquifer hydraulic parameters that obtained from British Geological Survey reports. In addition, the field visits have been done for investigating the landscape of the catchments for checking the topography and its influence on groundwater flow, spring locations, and catchment boundary.

3.2.1. Determination the boundary of the study catchments

Geological factors and catchment boundaries:

The study catchments are not subjected to significant geological disturbances such as major faults and folding. Except a basement big east-west reverse fault pass near the southern border of the Driffield catchment which produced a wide and gentle slope regional syncline in the Chalk rocks see Figure 2.4 and 2.5. Therefore, the attitude of the bedding plane is expected to be the main geological structure affecting the groundwater flow regime.

In the Kirby Grindalythe catchment, the Chalk beds (found from the altitude of the outcropped contact surface between Ferriby Chalk and Welton Chalk Formation on the published maps) is dipping toward the east with the dip angle 0.5 degree, while the contact surface between the Chalk and the underlying Clay Formations is dipping toward northeast with the dip angle about 0.4 degree. In the Driffield catchment the Chalk dips toward the southeast (found from the altitude of the outcropped contact between the Burnham and Flamborough Chalk formations on the published maps) with dip angle 2.2 degrees , similarly the contact surface between the Chalk and underlying Clay Formations has same dip direction but with dip angle 2.6 degrees.

All these information explain that geological stratigraphy and structure do not have a significant impact on the catchment boundary in the study catchments.

Groundwater abstraction and catchment boundary in study area:

Groundwater abstraction in Kirby Grindalythe can be neglected (only from Low Mowthorpe borehole water is pumped in very small quantity for farming uses). In Driffield catchment a significant amount of groundwater is pumping from Elmswell Wold borehole (SE 998 613), which is located nearly at the middle of the catchment area. This means in Kirby Grindalythe the groundwater divide will not be influenced by pumping groundwater, while in the Driffield there is a possibility of influence of the pumping from Elmswell borehole on the water divide shape and location, however this well located in the valley where the transmissivity is likely to be very high (which is about 930m^2day^{-1} according to table 3-1), so the effect is probably small.

Furthermore, the evidence from section (3.1.2), here can be helpful in the identification of the catchment boundary depending on the topography of the area.

Based on the above assumptions in the conceptual models it has been considered that the groundwater divide coincides with the surface-water divides for both catchments.

Topography and catchment boundaries:

As explained in the literature review (section 3.1.2) the shape of the water table in unconfined aquifers is often assumed to be a subdued replica of the topography or land surface. A profile parallel to the regional groundwater flow direction along the Kirby Grindalythe and Driffield catchment has been constructed, see Figure (3.2). This cross section suggests that at the regional scale over the East Yorkshire Wolds there is a strong relation between the topography and groundwater flow direction.

In the Kirby Grindalythe catchment the interrelation between location of the springs and topography has been investigated for determining the effect of topography on the groundwater flow direction. Figure (3.3) shows the topographic map of the Kirby Grindalythe catchment and location of the springs. A dome shape hill (consisting of Chalk) exists at the west of Duggleby village; there is a series of the springs extended along the north, west and then south edges of the hill (Sp.O- 1 to 11). In addition, there is two spring on the eastern side of the hill (inside Duggleby) (Sp.I- 1 and 2) and another one at the southeast (Sp.I-3). Location of these springs indicates that the direction of the groundwater flow is following the topographic slope. The dip direction of the contact surface between the Chalk and underlying Clay Formations is toward the NE and the Chalk beds dip toward the east , but the springs at the western of the hill indicate that the groundwater flow is toward the west. This supports the above statement which suggested that the flow of the groundwater to the springs is significantly controlled by the topographic slope, rather than the geological structure. Further, there are another three springs in Kirby Grindalythe catchment, first one at the northwest of Duggleby and the other two south of Duggleby, which also follow with the slope of the local topography.

Regarding the Driffield catchment, two sets of information can be used as an evidence of the effect of the topography on the groundwater flow direction. First, the location of the Driffield spring, this spring is the only major spring in the catchment and it located where the topographic slopes in the area converge, see Figure (2.16).

Second, from the groundwater level and topographic elevation relation from four boreholes in the area, the groundwater contour map was estimated, which shows the groundwater flow direction, see Figure (3.4). Plotting the ground elevation of the boreholes and water table in the boreholes showed that the groundwater flow direction follows the topography of the area. The information from these boreholes was provided by the BGS, it consists of the monthly groundwater level for the period between 1979 to 2015.

3.2.2. The interconnection between the study aquifers and surrounding aquifers in the regional basin:

Kirby Grindalythe catchment is located at the western border of the Yorkshire Wolds but the border of the catchment does not coincide with the Wolds escarpment. At the western border, a small Chalk catchment is located between the Kirby Grindalythe catchment and the Wolds escarpment. The catchment is also surrounded at the northern, eastern and southern border by other Chalk catchments. This indicates that there is the possibility of interconnection between Kirby Grindalythe catchment and the surrounding catchments. Taking into consideration the attitude of the contact surface between the Chalk and underlay Clay Formations there a possibility of underground outflow from Kirby Grindalythe toward the catchment at the north and northeast, or gaining water from the catchment at the south and southwest. According to the attitude of the Chalk beds, the groundwater from the aquifer may flow subsurface toward the east catchments, this flow direction is coincidence with surface flow direction of the Gypsy Race. Furthermore, as it was explained previously that at the local scale the groundwater in the Kirby Grindalythe is also controlled by local topographic features. Therefore, there is the possibility of subsurface flow into the aquifer from surrounding aquifers at the north and south. In addition, based on the regional topography, there is the possibility of subsurface flow exiting the catchment toward the east.

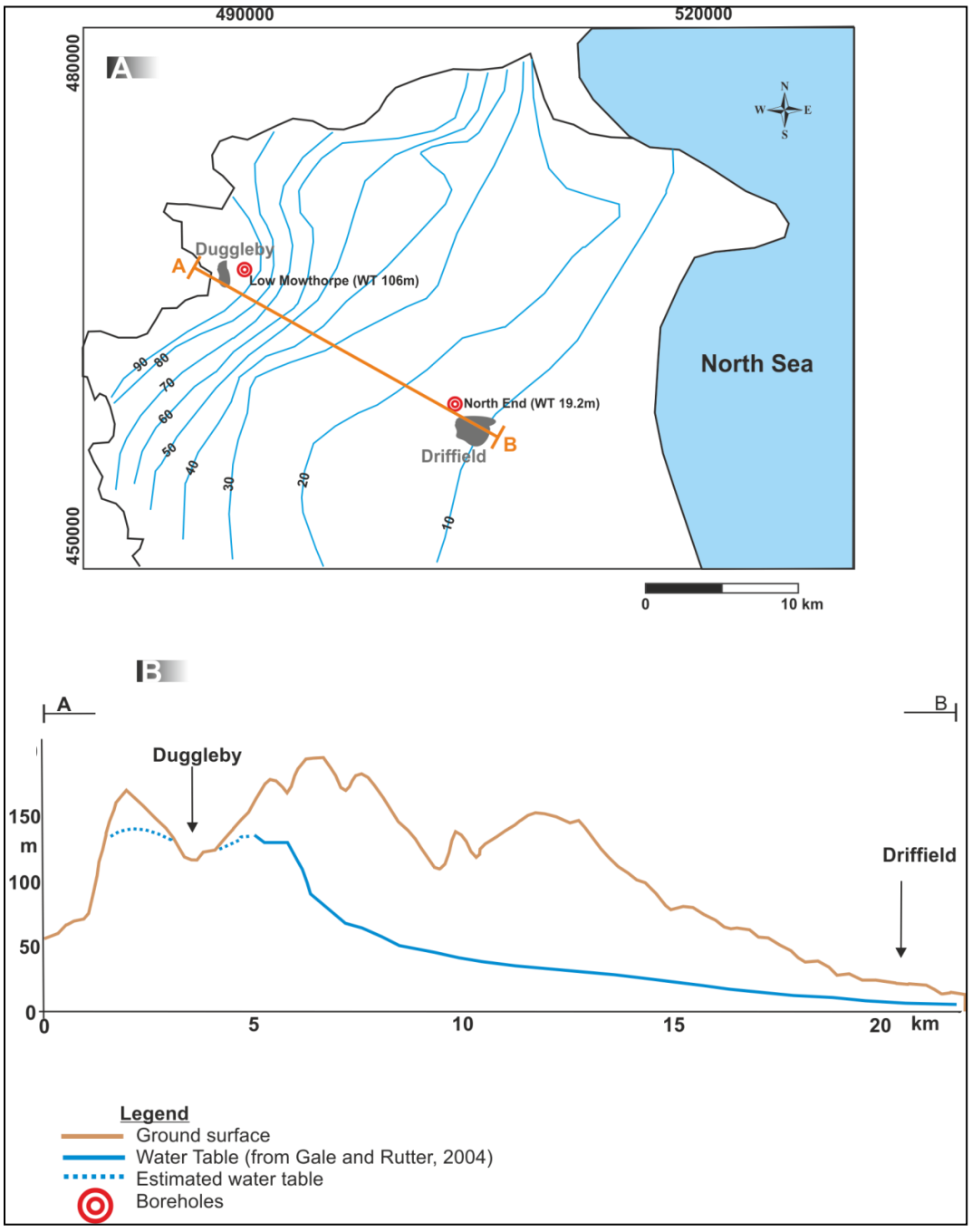

Figure 3-2 (A) Map showing groundwater level (in meters) in East Yorkshire Chalk, from (Gale and Rutter, 2006; ESI 2010 and 2015) represented by the blue contours. (B) cross setion from point A near Duggleby to point B near Driffield , showing pattern of the groundwater table and topography. The estimated water table in Duggleby based on the water table from Low Mowthorpe borehole and spring positions Note; vertical scale exaggeration to show the detail of the topography.

Figure 3-3 Location of the springs in the relation to the topography , Kirby Grindalythe catchment . The topographic contour map is from OS maps. The Sp.I refer to the springs inside the topographic catchment and Sp.O for the springs outside the topographic catchment.

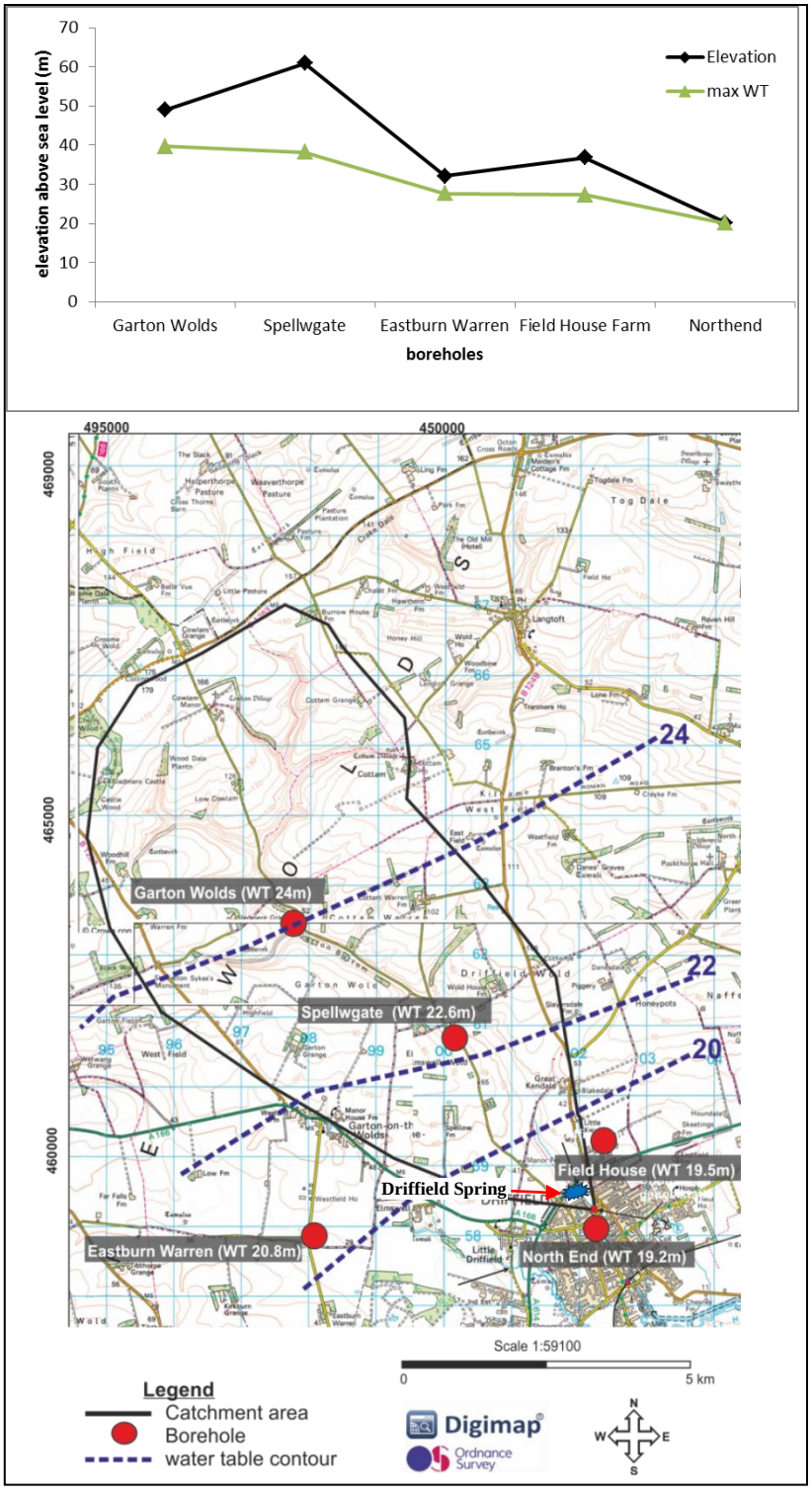

Figure 3-4 Water table contours estimated from the data of five boreholes based on average water level in the borehole (for the period 1979-2015).

The Driffield catchment is located nearly in the middle of the East Yorkshire Chalk province, at the border between the Yorkshire Wolds and Yorkshire Holderness Plane. This means it surrounded by other large Chalk catchments. The groundwater flows direction in the Driffield catchment almost same direction of the regional trend, which is east and southeast. Thus, there is a possibility of gaining or losing groundwater through subsurface flow with adjacent catchments.

The contact between the Chalk and underlying Clay formation is buried deep below ground (about 160 m in the high area and 100m in the interfluves) , consequently, the Clay Formation does not expect to have a great impact on the groundwater flow regime in the aquifer (as discussed in literature review; that the chalk well below the water table has low permeability and that you assume permeability is only developed down to the base level defined by the springs.).

3.2.3. Impact of geology and hydrogeology on catchment boundaries / subsurface discharge and interflow:

Kirby Grindalythe:

The discharge from all springs integrates to form the Gypsy Race stream which is gauged at Kirby Grindalythe village. The flow of the Gypsy Race at this location was initially assumed to represent a cumulative discharge from all springs.

During field investigation, it was noticed that at the eastern side of Duggleby village, the ground is muddy and has surface water producing a mire [NGR: SE884672] (see figure 3.5). The ground remains muddy downstream of Duggleby village until the small bridge at Duggleby, but downstream of this bridge toward Kirby Grindalythe village the ground is less muddy, and the stream flow becomes confined to a narrow channel. The geological map shows that the impermeable clay formations crop out at the surface along the valley between Duggleby village and the Duggleby bridge, whereas downstream of Duggleby bridge to the east of the Kirby Grindalythe village the stream extend along the Chalk rocks. Because the clay beds are impermeable it

prevents water from the stream to infiltrate to the ground between Duggleby village and Duggleby bridge, therefore the water saturate the head deposits producing the mire like feature. while because the base of the stream extend along the Chalk between the Duggleby bridge and Kirby Grindalythe village, therefore, there is a possibility of re-infiltrating of the water from the stream to the ground. This may be the most likely reason; why the area around the stream did not become muddy after the Duggleby bridge.

For the purpose of investigating whether the water is lost from the stream between Duggleby bridge and the gauging station, where the stream runs over chalk, discharge was measured under Duggleby bridge and also at the Kirby Grindalythe gauging station, using a current meter and the velocity-area method applied. Three measurements have been taken at three different flow rate stages.

Table (3.2) shows the result of the flow measurements that were taken at Kirby Grindalythe station and under Duggleby bridge (along Gypsy Race stream). The results showed that the discharge under Duggleby Bridge was higher than that at Kirby Grindalythe station by factor about 1.4 in average. This indicates that part of the water from the stream enters to the ground, and flows in the form of subsurface discharge beneath the gauging station.

Table 3-2. Flow rate within the Gypsey Race in two locations, first under the Duggleby bridge [NGR: SE884672] and second 2 km toward the east at the Kirby Grindalythe gauging station [NGR: SE903674].

	Duggleby bridge	Kirby Grindalythe village	Loss
	Q (L/sec)		(L/sec)
15/07/2015	17	9	8
11/03/2016	131	109	22
22/04/2016	91	83	8

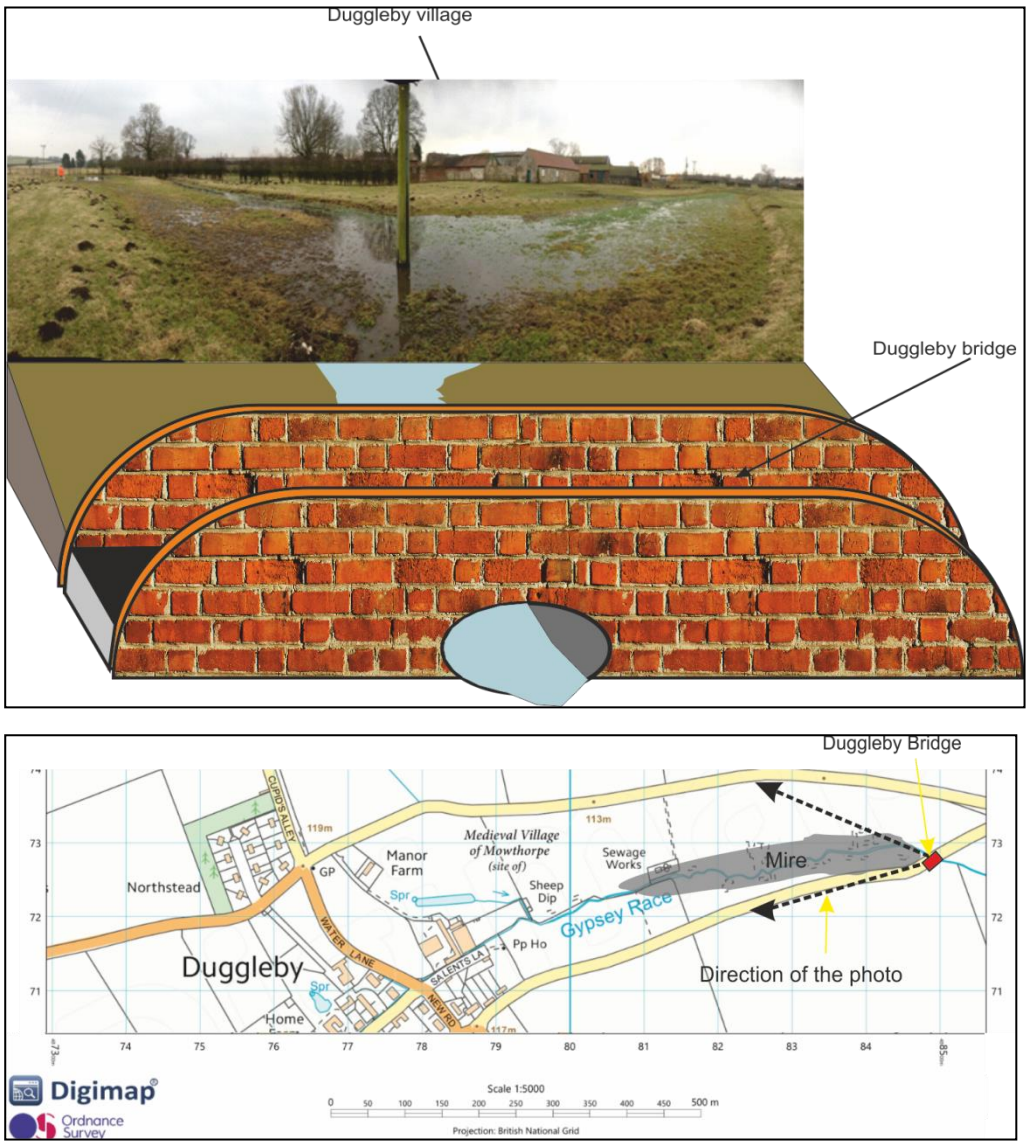

Figure 3-5. The photo shows the mire near Duggleby village, the map shows the location of the mire and direction of the photo.

Around a nearly symmetrical dome-shaped hill (consisting of Chalk) that exist at the west of the Duggleby village a series of springs arise (figure 3.6). About 8 to 9 springs located at the western and southwest side of the hill, flow westward in the direction opposite to the Gypsy Race (i.e. they are located outside the Kirby Grindalythe catchment). One spring arise at the eastern side of the hill inside the

Kirby Grindalythe catchment, (see Figure 3.3). Because all these springs arise from the same chalk aquifer, this indicates that the groundwater from this hill feeds two catchments, i.e. there is a groundwater divide within the hill. During this study, the flow from the western springs was measured (on two occasions; March and April 2016) simultaneously with the eastern springs (those which feed Gypsy Race), Figure (3.6).The aim of flow measurements on both sides of the hill was to estimate the location of the groundwater divide in this chalk block and to examine if congruent with the topographic divide. Because this hill has nearly symmetrical shape if the flow rate on the both sides is close it indicates that the groundwater and topographic divide are approximately matching, while if they not it means that these two water divides do not match.

Two measurements have been taken; the first after the peak flow on March 11th, 2016 which showed that the flow rate was 0.149 and 0.109 m^3/day at the western [SE854679] and eastern side [NGR: SE884672] of the hill respectively (see Figure 3.6 for locations). Meanwhile, the second measurement taken near the middle of the recession period on April 22nd, 2016, the flow rates was 0.092 and 0.091 m^3/day at the west and east side of the chalk hill respectively. The measurements show that during the early stage of the recession the discharge at the western side is 1.4 times the discharge at the eastern side, but by the middle of the recession period the discharge amounts became similar. This indicates that the Kirby Grindalythe catchment varies in size depending on the groundwater level; when the groundwater level in the aquifer is high more water discharges by the springs at the western side than those on the east side. This suggests the groundwater divide moves eastward when the water table is highest , but when the water table falls (i.e. by the middle of the recession period), the groundwater divide become matches the topographic water divide, Figure (3.6).

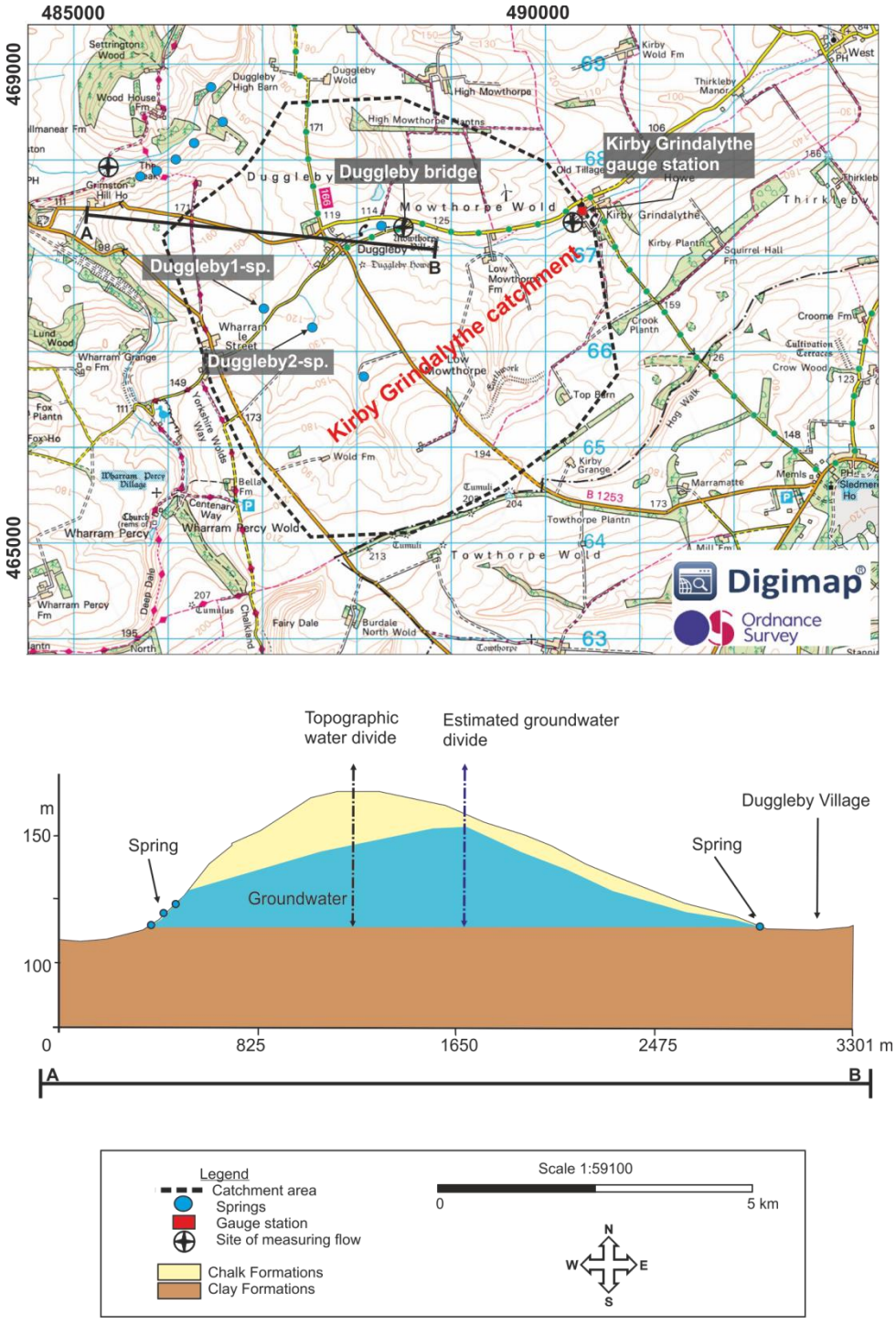

Figure 3-6 Conceptual model of variation in catchment area with hydraulic head, A is topographic map show location of the springs around the Chalk block east of the Duggleby. B conceptual model explain the relation between the head in the aquifer and location of groundwater divide when the water table is highest.

Driffield:

The situation of the Driffield catchment is different from that of Kirby Grindalythe, because the catchment is located at the down-dip side of the Chalk outcrop directly at the border between Wolds and Holderness Plane. Here the catchment surrounded at the north, west and south by big catchments, and the impermeable Jurassic Clay formations are buried deep below the Cretaceous Chalk rocks. Therefore there is a possibility of interconnection between this aquifer and surrounded aquifers.

From the geological model of the area it can be noticed that the spring emerge at south-eastern border of the catchment at the contact between Wolds and Holderness Plane, where the Chalk becomes buried bellow superficial deposits. During the field investigation it has been noticed that when the gauging station in Driffield Village shows zero flow, still there was water flowing in the stream channel downstream of the station, i.e. water enters the channel below the station, Figure (3.7). This means groundwater discharges from the superficial deposits (chalk gravels) which are permeable enough to allow groundwater flow. In addition, there is a possibility of groundwater flowing within the chalk below the superficial deposits entering the confined chalk aquifer to the south of Driffield. This situation can be considered as an evidence of interconnection between this catchment and surrounded aquifers.

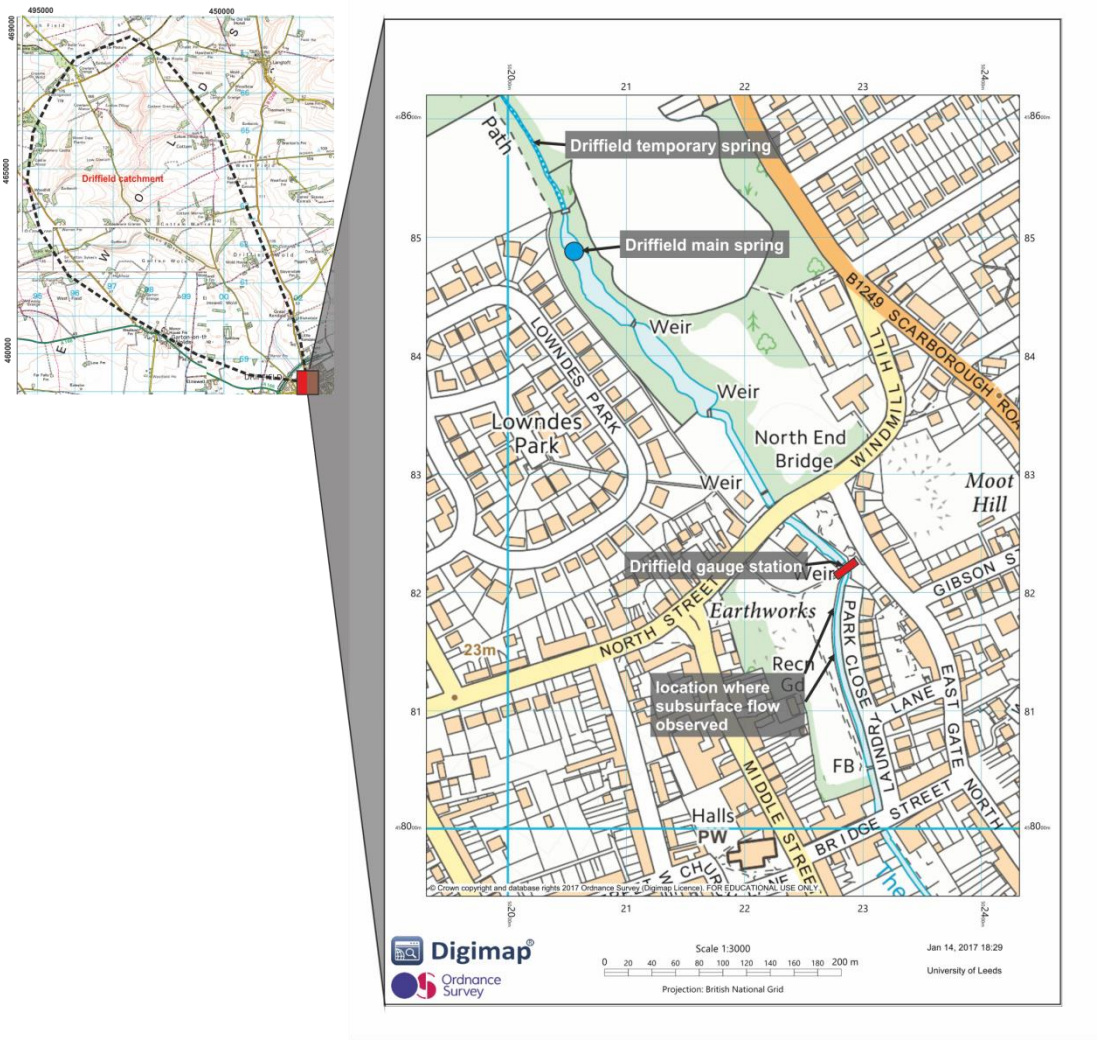

Figure 3-7 Map showing locations of Driffield spring, gauging station and site where subsurface outflow observed.

3.3. A conceptual model of Kirby Grindalythe:

3.3.1. The source of recharge:

Over the studied catchment area, the natural bodies of surface water such as rivers and reservoirs are absent; therefore precipitation is the primary source of the groundwater recharge.

3.3.2. Groundwater flow direction in Kirby Grindalythe aquifer:

Several factors may control the groundwater flow direction including the geology (stratigraphy and structure), the attitude of the base of the aquifer and topography.

From the structural point of view, folding and faulting which usually leads to significant variation in the fracture distribution, are not expected to have a significant influence on the groundwater flow direction in the Kirby Grindalythe catchment. The structural map of East Yorkshire shown that the area did not subject to significant mappable faults. In addition, the Chalk strata in the area did not subject to the complex folding system. The Chalk beds gently dip toward the southeast with a dip angle 2.2 degrees. Stratigraphically the aquifer consists of the Ferriby, Welton, and Burnham Formations, both Welton and Burnham Chalk Formations contain flints, which may act as a vertical groundwater flow barrier, e.g. tabular flints arranged parallel to the bedding surface.

The contact between the Chalk and Jurassic Clay Formations define the aquifer base, the shape and structure of this surface will have a role in the groundwater flow direction. In the geological model section, the contour map of this contact surface has been drawn and explained in detail. The dip direction of the surface has been estimated by north-northeast (NNE) direction and dip angle of 0.4 degrees. Because the dip angle of the contact surface is slight, it will probably not produce a significant influence on the groundwater flow direction.

in the topographic point of view, the catchment has two slope direction. Local based slope direction according to the hills that surrounded the catchment; at the north, west and south slope toward the valley in the middle of the catchment. On the regionally based slope direction with the East Yorkshire dominant slope which is eastward toward the North Sea. The eastward flow direction of the Gypsy Race is due to the eastward regional slope direction.based on the above information, in the Kirby Grindalythe catchment, groundwater flow has various directions. Regional groundwater flow direction is in the eastward direction, parallel to the regional dip slope of the Chalk beds and regional slope direction. Furthermore, the locally groundwater flow direction ; toward the southeast and north at the western and southern edge of the catchment area respectively, due to the topographic controls (see section 3.2.2).

3.3.3. Groundwater discharge from Kirby Gdrindalythe aquifer:

In Kirby Grindalythe the groundwater discharge through several springs, during field investigation 5 springs were detected (see Figure 3.6). These springs arise at a level which coincides with the elevation of the contact surface between the Chalk and Jurassic Clay Formations. As the Clay beds due to its hydrogeological characteristics does not allow groundwater to pass, so at the location where this surface intersects the ground surface groundwater naturally discharge to the surface in the form of the springs.

- One of these springs is located 1.3 km at the SW of Duggleby, and drains water from an isolated body [GR:SE868662]of the Chalk, which is located to the west of the catchment; in this study, this spring will be called Duggleby-1.
- The second spring [GR: SE877672] is located inside the Duggleby village, and drains water from the northern Chalk body.

- The third spring[GR:875662] emerges about 0.98 km SSW of Duggleby; the last spring located SE of the Duggleby [GR:SE880660] (this spring is called Duggleby-2 in this study); these last two springs deplete water from the southern Chalk body.

Water from all these springs is converging at the Duggleby Village to form the Gypsy Race stream, which flows eastward. Water discharge in the stream is gauged by Kirby Grindalythe gauging station.

3.3.4. Water table and saturated zone in the Kirby Grindalythe aquifer:

In the Kirby Grindalythe aquifer, the base of the saturated zone is defined by the elevation of the Clay beds of Jurassic Formations and the top determined by the elevation of the water table.

Usually the elevation of the water table measured through boreholes. Low Mowthrope is the only borehole that exists in the catchment, which is located near the catchment outlet (near Kirby Grindalythe village). Therefore, water table from this borehole individually does not represent the water table in the catchment. Hence, indirect approaches have been used for estimating the groundwater level. The first method was extrapolating the regional groundwater contour map to cover all Kirby Grindalythe catchment. The reason of extrapolation was because the groundwater contour map of the East Yorkshire only extended as far west as the Low Mowthrope borehole near the east border of Kirby Grindalythe catchment(did not covered entire catchment area). (figure 3.3). further technique has been used also for estimating the water table level in the aquifer which depended on the trigonometry and information about the inferred hydraulic head at various points. the used information included; water level at the Kirby Grindalythe station, the water table in the Low Mowthrope borehole, the water level at the spot under the Duggleby Bridge, the elevation of the springs upstream and the distance between these locations and

the estimated catchment boundary. The saturated thickness was estimated to be about **20 m** at the upstream catchment boundary, see Figure (3.8) with the water table sloping toward the east at about one degree. the maximum thickness of the unsaturated zone is about 35m based on the maximum topographic height and maximum water table elevation at the upstream catchment boundary.

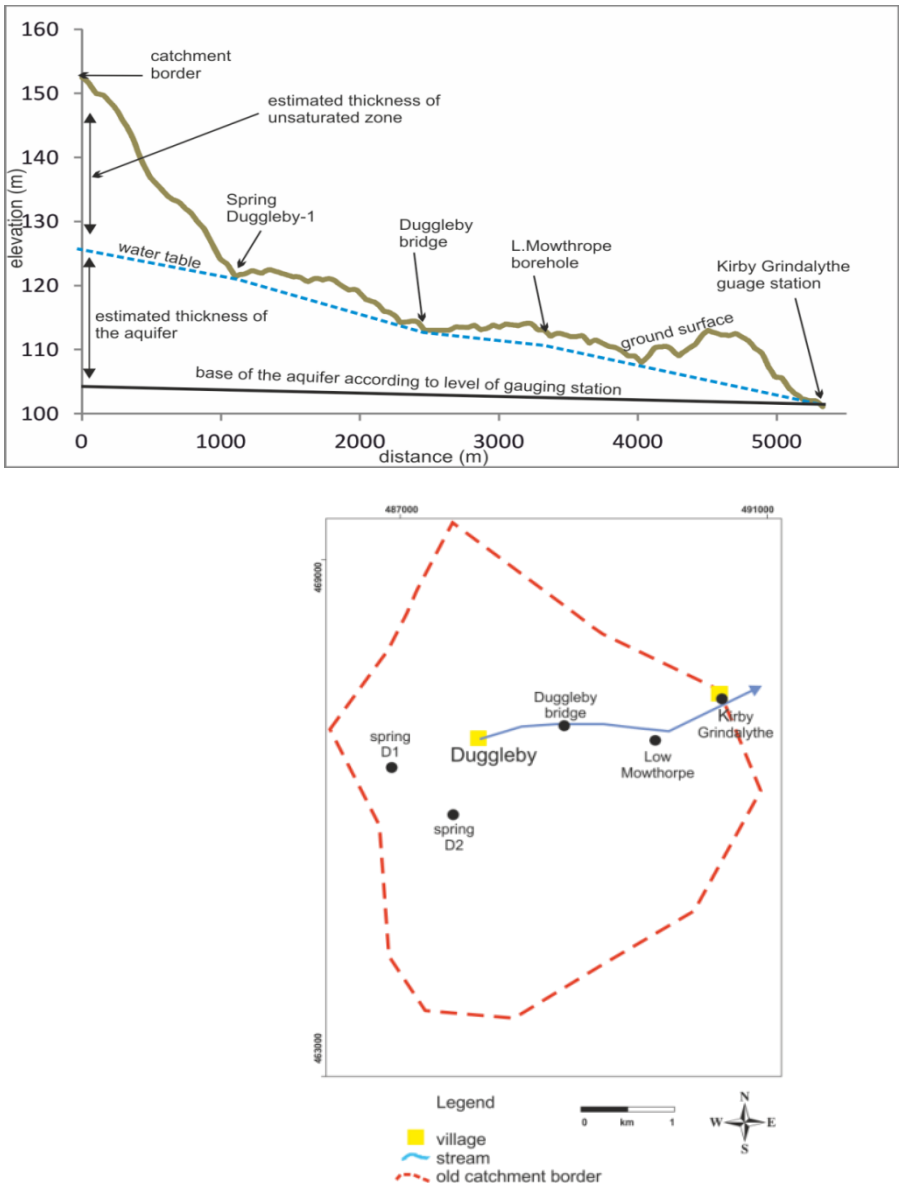

Figure 3-8 Estimating water table in the Kirby Grindalythe aquifer.

3.3.5. Hydrogeological conceptual model of Kirby Grindalythe aquifer:

Figure (3.9 A) is a hydrogeological conceptual model of Kirby Grindalythe aquifer which illustrates groundwater flow and hydrogeological framework of the aquifer. Figure (3.9 B) is cross section through the area in the NNW- SSE direction where most of the springs exist. The purpose of building the cross section was to explain the lithological profile and boundary conditions of the aquifer and the hydrogeological reason of existence the springs.

The Cretaceous Chalk represents the main aquifer in the area. The Chalk rocks crop out over the majority of the area, covered by highly permeable recent deposits (in the interfluves); this makes the Chalk an unconfined aquifer. The aquifer is underlain by impermeable Clay Formations of Jurassic age, which prevent the groundwater from penetrating deeper into the ground. Consequently, it can be concluded that the contact surface between the Chalk and Clay beds represent the base of the aquifer.

The overall catchment consists of three bodies of Chalk rocks; northern, western and southern blocks. Both northern and southern blocks are connected to the entire East Yorkshire Wolds Chalk, while the western block is an isolated body. Two west-east trending dry valleys separate these Chalk bodies, and these valleys intersect to the east of Duggleby village to form a greater valley which contain the very reach of the Gypsy Race stream.

The cross section of the area (see Figure 3.9 B) shows that the springs that are draining the isolated Chalk block are dip slope springs (e.g. spring Duggleby 1). While, the springs that arising from the hillside in the south of the study area are the scarp slope springs (e.g. spring Duggleby 2), i.e. they discharge along the escarpment of the Chalk (flow direction opposite to the dip direction). Also, there is a set of escarpment springs outside the eastern border of the study catchment, these springs flow to the west (i.e. not within the study catchment).

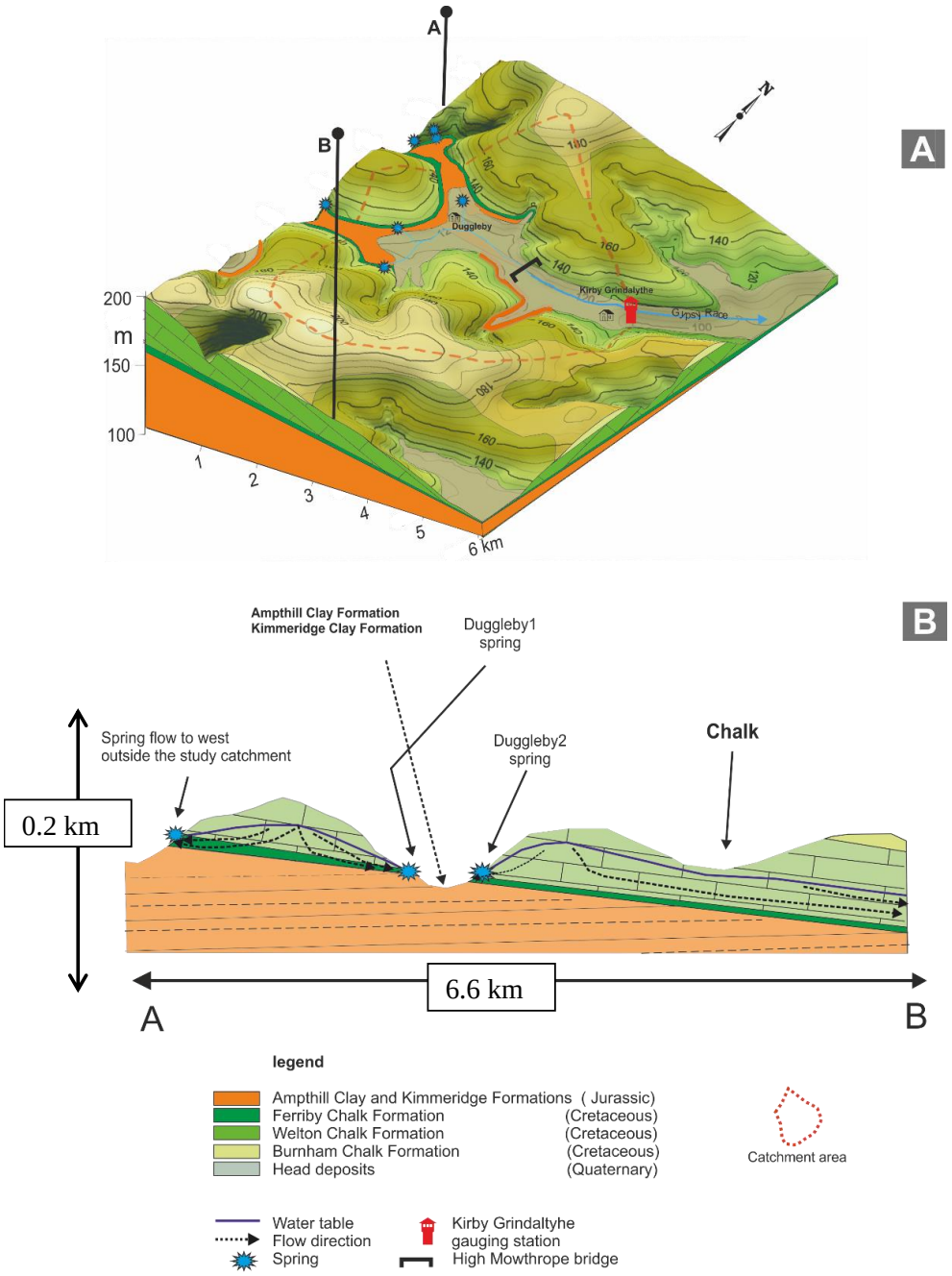

Figure 3-9 (A) Hydrogeological conceptual model of the Kirby Grindalythe (B) NW-SE cross section of the area through the springs Duggleby1 and Duggleby 2. Note: vertical scale exaggeration to show the detail of the topography.

3.4. Conceptual Model of Driffield:

3.4.1. The source of Recharge:

Water from rainfall is the main source for groundwater recharge, because of the absence of other water resources such as the watercourses and surface water stores.

3.4.2. Groundwater flow direction in the Driffield aquifer:

The aquifer is unconfined, therefore; the topography plays an important role in the groundwater flow direction. Groundwater flows through the aquifer from topographic highs that surrounded the catchment border from north, west, and south toward the location of the Driffield spring in the southeast of the catchment (see Figure 2.16). This pattern of groundwater flow is also confirmed by the water table elevation in four boreholes in the Driffield catchment, figure (3.4 and 3.12).

3.4.3. Groundwater discharge from the Driffield aquifer:

the Driffield spring, which is a spring emerge at the southeastern border of the catchment, is the main visible discharge point on the Driffield catchment. The factors that causes emerging this spring are differ from those for the springs in the Kirby Grindalythe catchment. Here the reason is not because of the cropping out the impermeable contact surface between the Chalk and underlying Clay Formation. The contact surface between the Chalk Formations and underlying Clay Formations at the spring location here is deep below the ground surface (the base of the Chalk is at a depth about 150 m below ground surface). The geological profile from boreholes in the Driffield catchment also confirms Chalk thickness of more than 150m (see figure 2.14).

The reason of the emergence of this spring is most probably due to the position of the edge of low permeability or impermeable superficial deposits. The area where the spring arises is located close to the west side of the paleo cliff line, at which the

superficial deposits due to glacial activity accumulated and covered the Chalk rocks. The thickness of these deposits increases toward the east and south and Chalk aquifer becomes confined. here and there along the edge of these deposits the groundwater in the chalk is flowing to the surface in the form of the springs.The spring in this area appears in the form of serial depression springs producing a pond. These springs are likely to be related to variation in the lithological composition of the superficial deposits. The spot at which the water discharge from the ground forms a pond with a depression of about 5x50m surface dimension and about 1 m in depth. this spring can be described as an overflow depression spring. The water discharges from the base and seeps from the sides of the depression producing a pond. The water from the pond is overflowing and flow to the south-southwest to form a stream called Water Forlorns, then the Driffield channel. The discharge rate from this spring is monitored by a weir station located in Northend Park in Driffield.

Two hypotheses can explain the existence of these ponds. The first explanation, is that the surrounding area and location where the pond exists consist of different types of superficial deposits. The top part consists of alluvium deposits, mainly of the mixtures of gravel, sand and contains a pocket of Chalk gravel that allows water to pass through. The bottom part of the superficial deposits consists of impermeable till deposits with some silt. Impermeable marl does not permit water to flow downwards, so when water discharges from the permeable gravel and sand, into the depression, it accumulates to produce these ponds. Geological map of the area shows that superficial deposit near the stream mostly consists of permeable river terrace deposits, while away from stream they become impermeable till deposits. This is supported by the geological profile NE-SW direction constructed from three boreholes around the spring; Figure (3.10), this figure illustrates existence the lateral variation in the recent deposits.

This hypothesis is possible because of the geographical location of the pond, it located at the end of the valley extending from the unconfined Chalk.

therefore because of the accumulationof the groundwater behind the superfical deposit at the contact between confined and unconfined Chalk. accumulation of the groundwater lead to water table to arise, then groundwater from the unconfined Chalk seeps to the supficial deposits through the permeable sediments near the top of the superficial deposits and produced this pond. Moreover, the water table in the North End borehole (southwest of the pond in the confined chalk) lies below the water level in the pond which indicates that water in this pond is not connected directly to the confined Chalk aquifer immediately below. A second explanation suggests that the existence of the pond may be related to depletion of the groundwater from confined Chalk through permeable windows in the glacial till. There are several ponds and springs distributed in the Holderness Plain where the Chalk is confined (evidence of existence of permeable windows through the glacial till) such as Blue Keld spring [GR: TA051499] at the southeast Hutton. However the location of the pond in Driffield indicates more probably the water comes from the unconfined Chalk, as it been explained in the previous paragraph (first scenario).

Figure (3.11) show the conceptual model of the Driffield spring based on the first scenario.

3.4.4. Water table and Thickness of the saturated zone:

The maximum thickness of aquifer in the catchment has been estimated to be 40m approximately from the water table elevation and the spring level, assuming that the thickness is equal to the vertical distance between the maximum level of the water table at the upstream catchment boundary, and the level of the spring. The information about the water table obtained from the groundwater contour map and from the boreholes in the catchment.

Figure (3.12) the green line shows the maximum groundwater table elevation in the Driffield catchment while the black dashed line is ground surface. The maximum water table has been extended to the NW border of the catchment and the thickness

of the aquifer has been determined here. The vertical distance between the green/red/purple and black lines represents the unsaturated zone thickness, it can be noticed that unsaturated zone thick under the high topography and thinner below lowland areas.

The groundwater fluctuation zone in the aquifer estimated from the water table fluctuation in the boreholes. Figure (3.12) shows the maximum and minimum water table in the aquifer, the vertical thickness between the maximum and minimum groundwater level represents the groundwater fluctuation zone in the aquifer.

3.4.5. Hydrogeological conceptual model of Driffield aquifer:

The Driffield aquifer has been embodied in a conceptual model in order to describe hydrogeology of the area, Figure (3.13 B); Figure (3.13 A) is a longitudinal cross section through the area in the NW-SE direction. The aquifer consists of the Burnham Chalk and Flamborough Chalk Formations of Cretaceous age. The Chalk crops out over the majority of the area, and is covered by highly permeable recent deposits along the valleys; this makes the Chalk an unconfined aquifer. The Chalk Formations are underlain by the impermeable Clay beds of the Jurassic (not shown on the models as more than 100 m below sea level in the area). Also the figure showed the groundwater fluctuation zone. this zone is considered to contain the highest permeability in the aquifer. In general, the aquifer below the fluctuated zone is likely to be less permeable (according to previous studies in the literature review), as illustrated (see section 1.3.4).

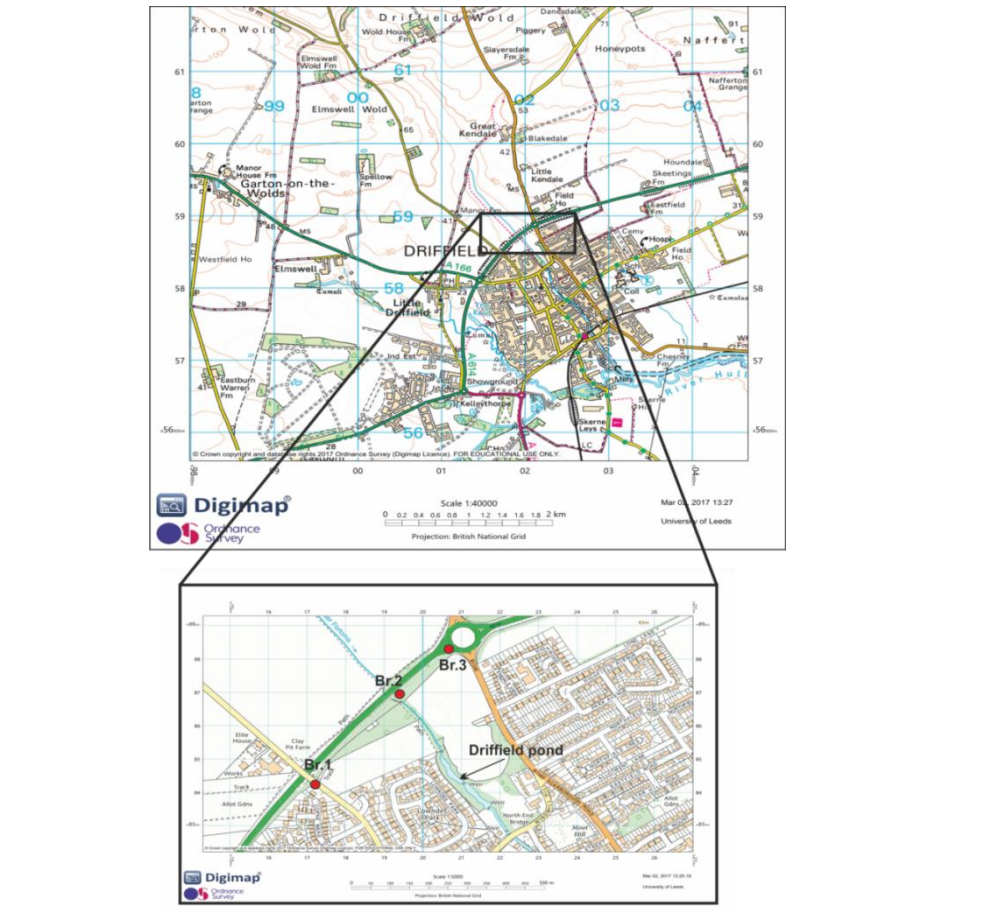

Figure 3-10 Soil and subsurface deposits from three shallow boreholes from BGS borehole records.

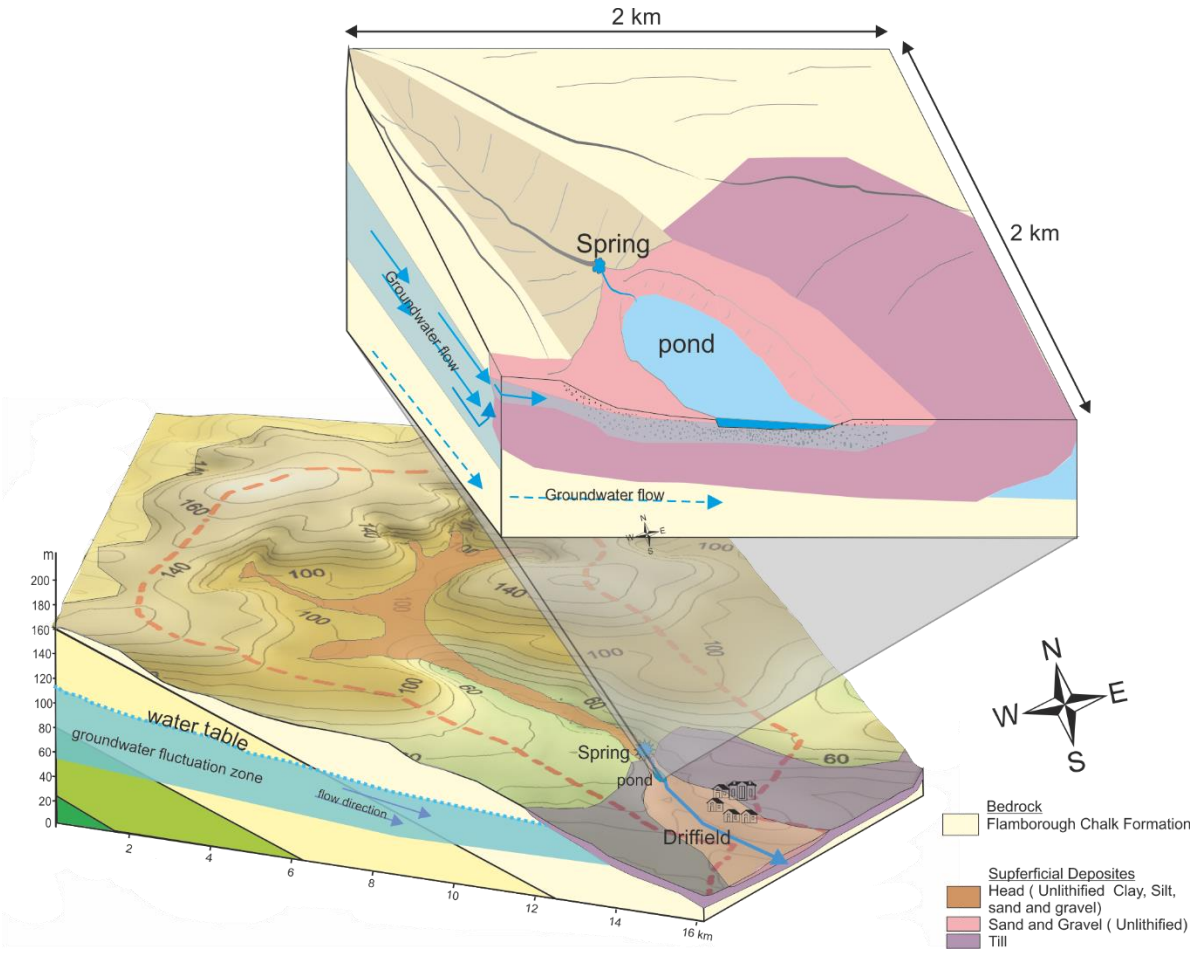

Figure 3-11 Diagram conceptualizing the reason of existence the Driffield spring in the form of the pond.

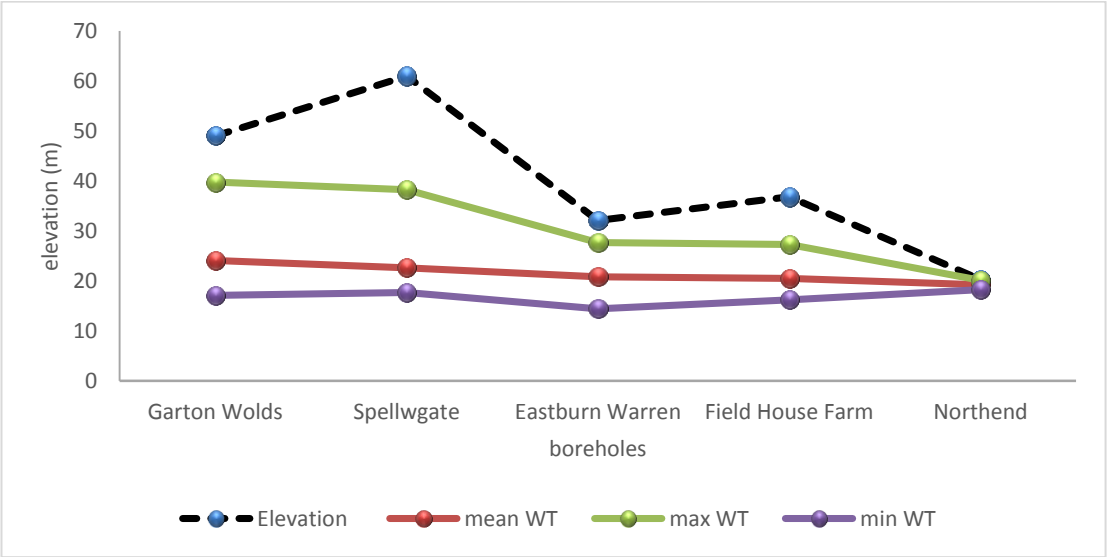

Figure 3-12 Graph show the maximum and minimum groundwater level in the Driffield catchment based on the water level data from boreholes for the period (1979-2015). the elevation represent height above sea level. Location of the boreholes appeared in figure (3.4).

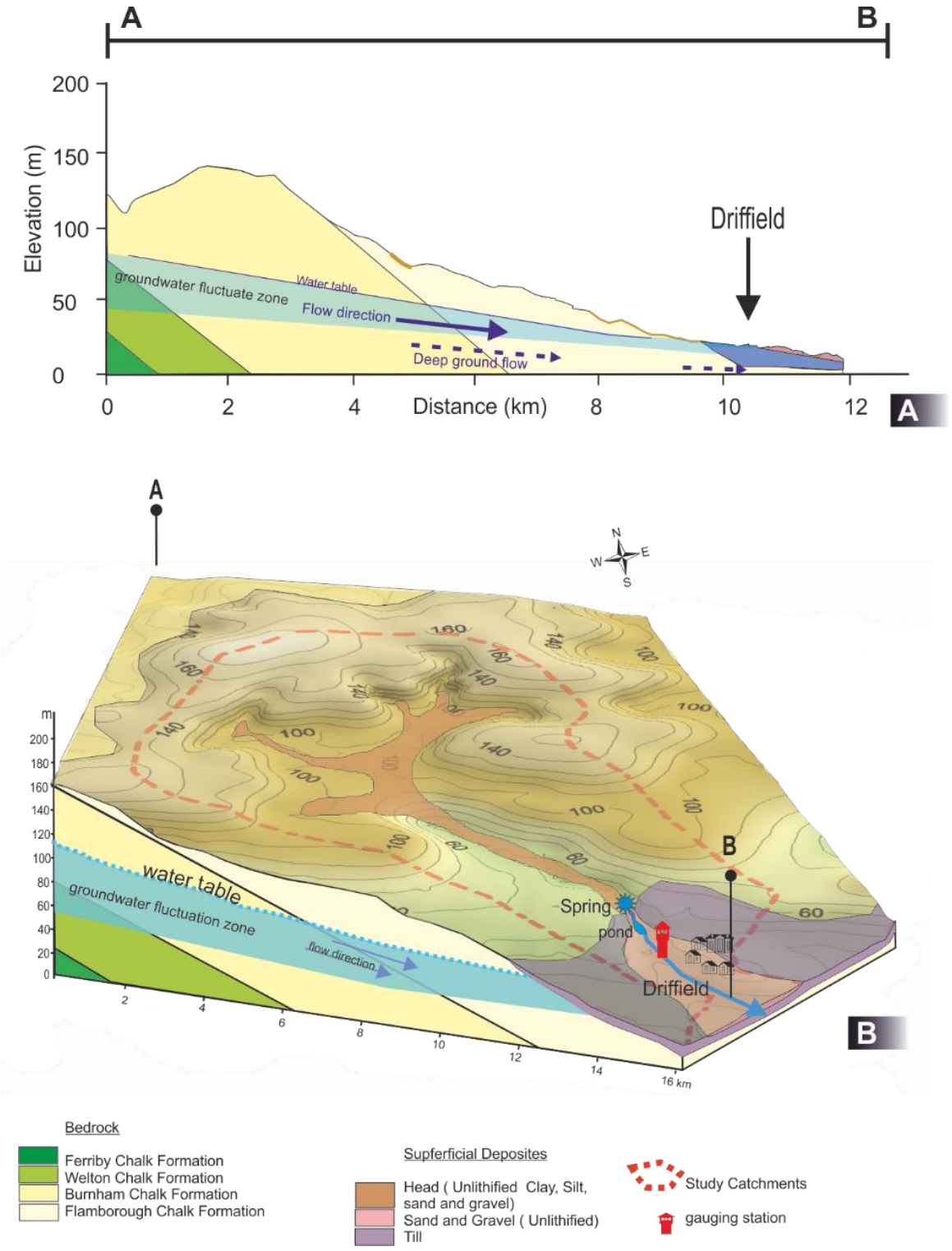

Figure 3-13 Hydrogeological conceptual model of the Driffield catchment area.
[Grid reference of point A:SE94199 65825, B: TA 02286 58222].

3.5. The sensitivity of the conceptual models:

In the conceptual model has been assumed that the topographic water divide (catchment boundary) is a no-flow boundary, so the groundwater divide coincides with the topographic catchment boundary. However, the models showed that unsaturated zone is much thicker under the interfluve than the lowland and valleys; this means the water table surface may be flatter relative to the topography. Therefore, there is a possibility of groundwater inflow into or outflow from the study catchments to adjacent catchments. Thus the size of the catchment may be either bigger or smaller than that defined by the topographic catchment boundary. The sensitivity of the water balance calculations to resulting errors in catchment size is discussed in the following chapters.

In the Kirby Grindalythe conceptual model was assumed that the contact surface between the Chalk and underlay Clay Formations does not affect the groundwater flow direction as it is nearly flat and has small dip angle (0.4 degrees). This contact surface dipping toward the northeast, which is not the same direction of the Chalk beds. Therefore, there is the possibility of underground water flow from Kirby Grindalythe to the catchment to the north and northeast, in the direction of dip of the Chalk/ Clay contact boundary. Again, the sensitivity of water balance calculations to any resulting errors in the catchment size (as defined by the topography) is discussed in subsequent chapters.

3.5.1. The conceptual models for the study catchments were constructed based on some assumptions:

- This study is aiming to examine spring discharge behavior during the period when the recharge is absent. Therefore, the factors that control the recharge such as such evapotranspiration, rainfall and soil cover has been neglected.
- The studied catchments occupy a relatively small area, thus the spatial variation in the hydraulic parameters has been neglected.

- The topographic and groundwater divide are coincident. At this stage, because we are making a simplified model of the catchment the possibility of the connection between catchments has been neglected (except the possibility of subsurface flows from the aquifer with the direction coincident with the stream direction). therefore the catchment boundary has been drawn according to the topographic water divided.
- The unconformable contact surface between the Chalk and underlying Clay Formations in Kirby Grindalythe represents the base of the aquifer, and is responsible for the spring locations that issue in the area. The contour map of this contact surface for the study area and surrounded areas, which was constructed during this study, showed that this contact surface is not flat. However, the map showed that under the study catchment, the unconformable surface almost flat, therefore, in the conceptual model this surface will be treated as a flat surface.
- In Driffield catchment assumed that the base of the aquifer determined by the level of the spring. Because the chalk well below the water table has low permeability and assumed that permeability is only developed down to the base level defined by the springs.

3.6. Summary:

In this chapter, a 3D hydrogeological conceptual model for Kirby Grindalythe and Driffield catchments has been constructed. The conceptual models have been developed from the 3D geological model which was constructed for the same catchments during this study (see Chapter 2) through importing hydrogeological information.

Main findings revealed by conceptual model development are:

- In the study catchments, the groundwater flow direction is predominantly controlled by the topography.

- Springs in Kirby Grindalythe catchment area of two types; for example spring Duggleby-1 is dip-slope spring and Duggleby-2 is escarpment-slope spring. The main spring in Driffield catchment is a dip-slope spring.
- Springs from in Kirby Grindalythe catchment arise where the contact surface between Chalk Formation and underlay impermeable Clay Formations intersect the ground surface. Whereas, the spring at Driffield arise where impermeable or low permeable superficial deposits onlap onto the Chalk (i.e. at the border between unconfined and confined chalk); where the groundwater level intersects the ground surface it emerges in the form of springs.
- Thicknesses of the unsaturated zone changes concordantly with the topographic elevation, as in the high topographic area the unsaturated thickness thicker and reduce with decreasing topographic elevation.
- Depending on the constructed conceptual models the maximum saturated thickness estimated to be 20 m in the Kirby Grindalythe, whereas in the Driffield catchment the maximum thickness of saturated estimated to be about 40 m.

Chapter 4. Recharge and Water Balance

- In this study, water balance for Kirby Grindalythe and Driffield catchments has been calculated and analyzed. the water balance has estimated based on the following set of information:Rainfall (P) data from the Meteorological Office (Met Office) and actual evapotranspiration (AE)data for years 2010 to 2015 in mm/ day from the Met Office Rainfall and Evaporation Calculation System (MORECS) grid square 94 (The AE data are for the MORECS reference crop 'grass'). Figure (4.1) shows the grid map from MORECS and location of grid square 94 which includes the study catchments.
- The daily mean discharge in m^3/sec for Kirby Grindalythe (Gypsey Race at Kirby Grindalythe) and Driffield (Water Forlornes at Driffield) gauging stations at grid reference SE904675 and TA023583 respectively. These stations are operated by the Environment Agency UK (Yorkshire).
- Groundwater abstraction for years 2010 to 2014 provided by the Environment Agency.
- information about catchment area; see section 4.1 below.

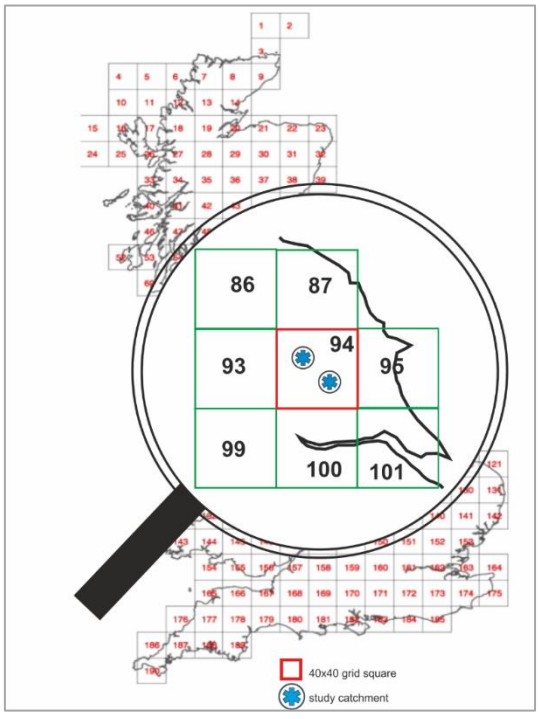

Figure 4-1. Map showing the MORECS grid squares and location of grid square 94 which includes the study catchments.

4.1. Water balance general review:

The water balance calculation in the aquifer system is a very important issue in many groundwater studies (Gebreyohannes et al. 2013; Mohammadi et al. 2014). Water balance is based on the principle of the law of conservation of mass. Fundamentaly two parameters included in the water balance; inflow and outflow. The inflow consists of all the water that recharges the system including water comes from precipitation and irrigation. The outflow represents all water leaves the aquifer system which is mainly in the form of the discharge, evapotranspiration, and artificial abstraction.

A simple version of water balance equation states that:

$$\text{inflow} = \text{outflow} + \Delta S \qquad \text{Equation 4-1}$$

$inflow = groundwater\ recharge\ \left(\frac{m^3}{\text{year}}\right)$

outflow=groundwater discharge $\left(\frac{m^3}{\text{year}}\right)$

ΔS=change in groundwater storage $\left(\frac{m^3}{\text{year}}\right)$

The traditional soil moisture balance equation which is based on the studies done by Penman (1948) and Grindley (1969) is one of the widely used equations for estimating recharge.

$$\Delta S_S = (P + sw) - (R_f + AE + R) \qquad \text{Equation 4-2}$$

ΔS_S = change in soil storage $\left(\frac{\text{m}}{\text{year}}\right)$

P = precipitation $\left(\frac{\text{m}}{\text{year}}\right)$,

$$\text{sw} = \text{ surface water input (river , stream or storage)} \left(\frac{\text{m}}{\text{year}}\right)$$

$$\text{R}_\text{f} = \text{surface runoff} \left(\frac{\text{m}}{\text{year}}\right), \text{AE} = \text{Actual Evapotranspiration} \left(\frac{\text{m}}{\text{year}}\right)$$

$$\text{R} = \text{groundwater recharge} \left(\frac{\text{m}}{\text{year}}\right),$$

The change in soil storage over a hydrological year is negligible as usually it close to zero (Ernst, 2000). In this study the water balance calculated over a whole water year therefore it been assumed the ΔS_S is zero, so;

$$(\text{P} + \text{sw}) = (\text{R}_\text{f} + \text{AE} + \text{R}) \qquad \text{Equation 4-3}$$

Direct Recharge represents that part of the surface water which percolates into the ground and reaches the groundwater. It happens when the amount of the precipitation is enough to infiltrate below the root zone. Basically, it occurs mainly during wet seasons when the soil moisture is at or above the field capacity level and AE significantly smaller than precipitation amount, (Hudak, 2001).

Water that reaches the earth surface percolates through the soil and rocks. Factors like soil texture, soil compaction and soil moisture influence the infiltration. Slow infiltration rate usually happens in compacted wet clay soil, while in the loose, dry and sandy soil the infiltration is fast. Cracks and other openings in soil can significantly enhance infiltration rates (Hudak,2001).

Estimating recharge is a complex process; it is extremely difficult to measure recharge directly. Alternative methods were usually taken for measuring recharge, the alternative methods depend on parameters such as precipitation rate, air temperature, soil moisture situation and actual evapotranspiration. Soil water balance approach is one of a widely used method for calculating and estimating the water available for recharge.

Evapotranspiration (ET) releases water from ground surface to the atmosphere in the form of vapor by processes of evaporation and transpiration. In general, evapotranspiration is calculated instead of estimating evaporation and transpiration separately; separating evaporation and transpiration is very difficult and both calculating and measuring evapotranspiration is more practical, (Fetter,2000). The value of the ET is influenced by several parameters. The Food and Agriculture Organization (FAO) grouped these parameters into weather parameters, crop factors, management and environmental conditions (Allen, et al., 1998).

ET is classified into two types; Potential Evapotranspiration (PE) and Actual Evapotranspiration (AE). PE is the amount of water would evaporate or transpire if the adequate water was available in the soil to meet the demand; PE is considered the maximum possible evapotranspiration (Schwartz and Zhang, 2003).

AE is the portion of the rainfall water which evaporates/transpires under the field conditions, for this reason, it represents the real ET. AE is smaller than PE except for short time periods during and after rainfall or snowmelt events when AE will be equal to PE (Hauser, 2009). AE participates in the soil water balance equation (eq.4.2) for estimating the portion of precipitation available for recharging aquifers.

ET is measured either directly or estimated indirectly based on empirical budgeting approaches (based on crop coefficients and soil water balance models) and analytical models (Penman – Monteith model). Measuring ET using physical measurements (e.g., soil moisture balance and weighing Lysimeters) is more accurate; however, availability of data usually means ET is estimated. The estimating methods are based on the meteorological data such as maximum and minimum daily temperature, solar radiation Ra, wind speed and humidity (Hauser, 2009).

The FAO invented an approach for estimating ET called Crop Coefficient method. This method estimates crop evapotranspiration (ET_C) by multiplying the reference crop evapotranspiration(ET_0), by a crop coefficient (K_C) , (Allen, et al., 1998).

$ET_C = K_C * ET_0$ Equation 4-4

Where $ETc\ crop\ evapotranspiration\ [mm\ d^{-1}]$

$Kc\ crop\ coefficient\ [dimensionless]$

$ETo\ reference\ crop\ evapotranspiration\ [mm\ d^{-1}]$

The ET_0 is an evapotranspiration rate from a hypothetical grassland (reference surface). K_c is the factor used for distinguishing the effects of different field crops from grass on the evapotranspiration rate. The type of the land use supposed by MORECS for calculation AE matches the characteristics specified by the FAO for the calculation of ET_0. The K_c of the Rapeseed (which is a type of Oil crops) is 1.15, (Allen, et al., 1998).

4.2. Water balance in the study catchments

The hydrograph recession curve of the stations shows that most of the years during the late stage of recession period the stream discharge reduces greatly or became zero. This means that the annual change in the aquifer storage, between hydrological years measured from 1 October – 30 September, when water levels are at their lowest, is probably small. As a consequence, it is possible to remove ΔS from the water balance equation for our study catchments when considering the hydrological year as a whole. Hence,

$inflow = outflow$

So here the inflow will be represented by rainfall recharge, and the outflow will be represented by the natural discharge (which consist of springs in the study area as well as any subsurface drainage), groundwater abstraction, and any discharge through the shallow soil zone above the bedrock (interflow discharge).

$Discharge(Q) = Recharge\ (R_v)$ Equation 4-5

$Q = Q_S + q_A + q_{in}$

$$R = P + R_{interflow}$$

So in more detail the equation will be in the form ;

$$Q_S + q_A + q_{in} = P + R_{interflow} \qquad \text{Equation 4-6}$$

$where$:

$\boldsymbol{Q_S} = spring\ discharge\ \left(\frac{m^3}{year}\right), \boldsymbol{Q} = total\ discharge\ \left(\frac{m^3}{year}\right)$

$\boldsymbol{q_{in}} = interflow\ discharge\ \left(\frac{m^3}{year}\right), \boldsymbol{q_A} = artifical\ asbstraction\ \left(\frac{m^3}{year}\right)$

$\boldsymbol{R} = total\ recharge\ \left(\frac{m^3}{year}\right), \boldsymbol{P} = rainfall\ \left(\frac{m^3}{year}\right)$

$\boldsymbol{R_{inflow}} = interflow\ recharge\ \left(\frac{m^3}{year}\right)$

4.2.1. Water balance components

Catchment size

To assess water balance, the amount of recharge water needs to be expressed in volumetric units, which requires the area of the aquifer catchment. The catchment area of the Kirby Grindalythe and Driffield catchments are stated as 15.9 km^2 and 32.4 km^2 respectively according to the Environment Agency (the information on http://nrfa.ceh.ac.uk/data/search); these values are estimated according to the topography of the area. However, groundwater divides are not typically coincident topographic catchment divides.

In principle, water balance is a suitable approach for estimating (or at least placing limits on) the size of a catchment area, but it does not provide information regarding the location or the boundary of the catchment area. Therefore, here in this study, the

result from water balance will be used for evaluating the accuracy of the size of the studied catchments. If the result shows that catchment size according to topographic water divide appeared not match with the groundwater divide, Ideally, approaches like water levels from the borehole and tracer tests can be used for determination the location of the groundwater divides . Unfortunately, in this study because of absence of boreholes (especially in the Kirby Grindalythe catchment), these approaches cannot be used, alternatively the catchments will be adjusted using information from the geological and hydrogeological conceptual models outlined in the previous chapters 2 and 3.

The approach used for revising the catchment areas (from their initial values supplied by the Environment Agency) is broadly as follows. It can be considered that the volume of water which enters the system over a water year is same as the volume of water which leaves the system in that year, i.e. the system is approximately in steady state. Thus, the annual recharge (precipitation minus evapotranspiration) volume should be approximately equal to the discharge volume. Where the outflow volume vastly exceeds recharge, this suggests the catchment area has been underestimated; in contrast when the volume of recharge vastly exceeds outflow, this suggests catchment area has been overestimated. However, the interconnection between neighboring catchments may leads to underground water flow from one to another, so catchment area cannot be determined precisely using the above approach, as discussed further below. However, comparison of recharge and outflow over a water year is a useful first step in refining the catchment models.

Rainfall:

Rainfall is the primary and fundamental hydrological input to groundwater. In general, rainfall is spatially and temporally variable. The spatial variation in the rainfall over the East Yorkshire is shown in Figure (4.2). The long-term average (LTA) which was taken over 1970-2000 showed that approximately for Kirby Grindalythe was 730 mm/year , and for Driffield it was 657 mm/year. The

difference in the annual rainfall between Kirby Grindalythe and Driffield most probably arises because of the difference in the topographic elevation. The temporal variation shown in figure (4.3) represents the average monthly rainfall in mm for the period 2010 to 2015 in the MORECS's grid square 94, which includes both study catchments. The average annual rainfall for grid square 94 was 659 mm for the years 2010 to 2015 see figure (4.4). The figure showed that there is a different in the rainfall amount over the study catchments, while the data from MORECS showed no variation in the rainfall over the study catchments (because the MORECS grid square is vast). This study used the rainfall data from MORECS in the water balance calculation. Although the figure (4.2) showed there is some variation in the rainfall over the study catchments, this study calculated water balance assuming that the total rainfall amount was similar over both study catchments. The reason of using MORECS inserted of the information from the map in figure (4.2). because the data from the map was in the form of LTA annual rainfall, while the information from MORECS was in the average daily format, which was more useful to use with daily AE and Q in studying water balance.

Evapotranspiration (ET):

The MORECS AE, which is used the current study, assumed that the area is grassland, when in fact not all the catchment areas are grassland, but a mixture of grasslands and cropped lands. This means that the AE from MORECS will be slightly smaller than the real AE rate in the area.

Long-term average (LTA) potential evapotranspiration between the year 1969 to 2007 for the MORECS grid square 94 is 515 mm/y (ESI, 2015). The average annual actual evapotranspiration for the MORECS grid square 94 (for reference crop 'grass') was about 214 mm/yr for water years 2010-2015. Figure (4.5) shows monthly Actual Evapotranspiration pattern in the study area.

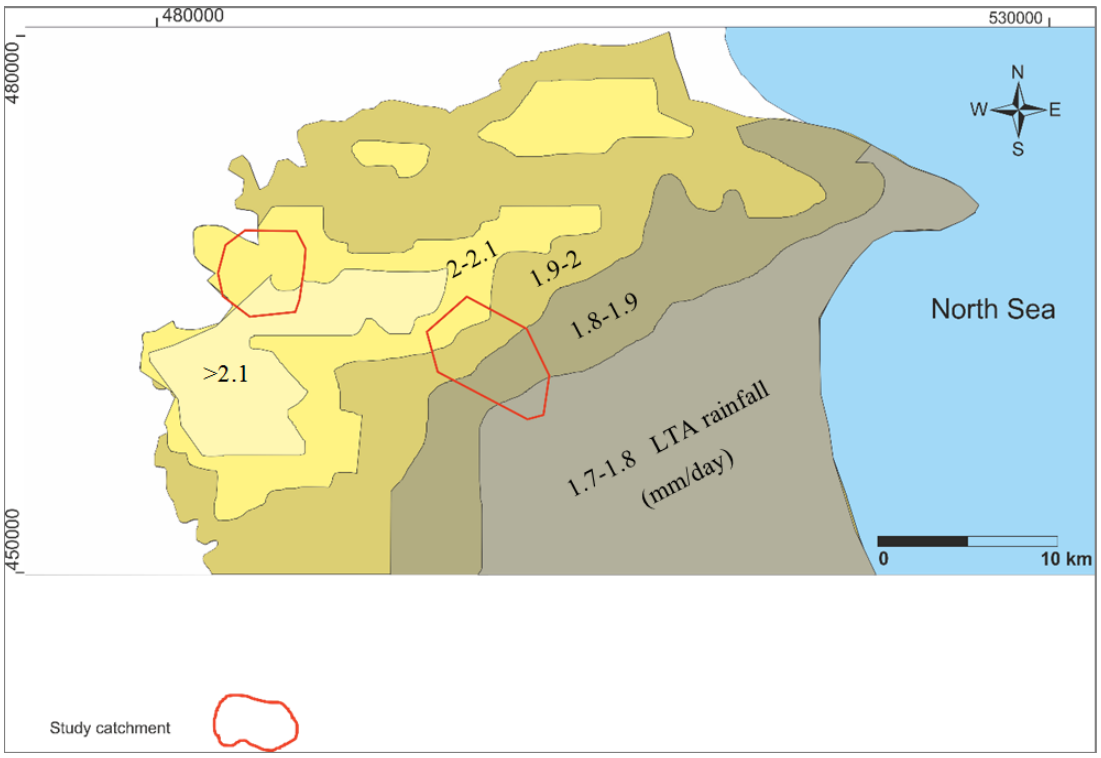

Figure 4-2Map showing the long-term average of rainfall distribution in East Yorkshire, (ESI, 2010).

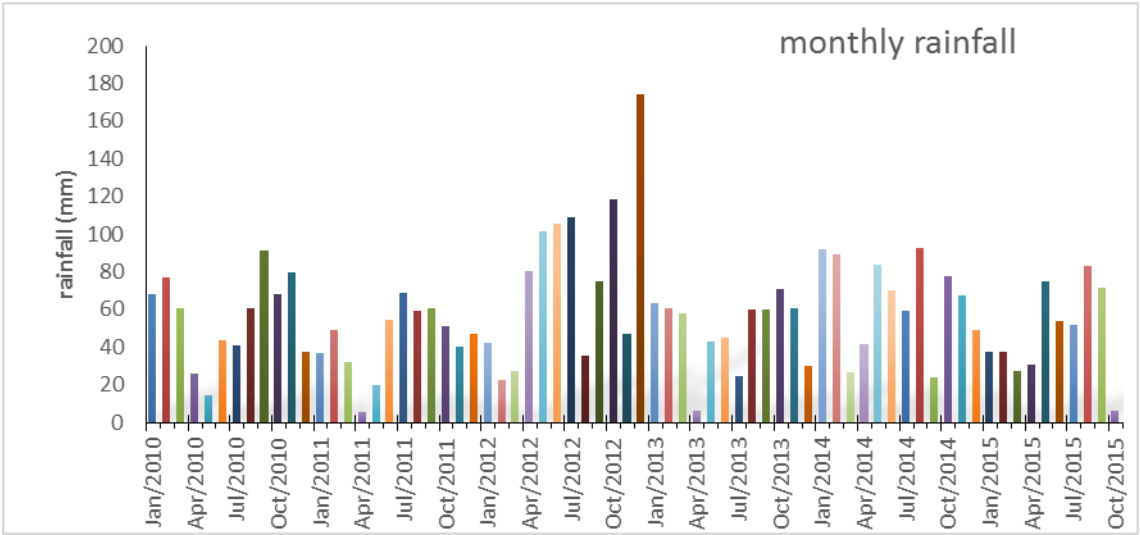

Figure 4-3. Monthly rainfall in the study area, based on the information from MORECS grid square 94.

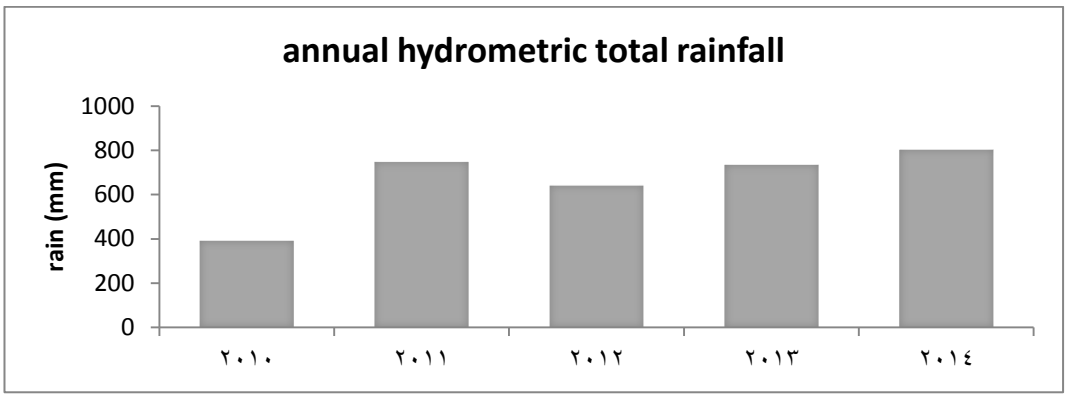

Figure 4-4. Annual rainfall in the study area (MORECS grid square 94).

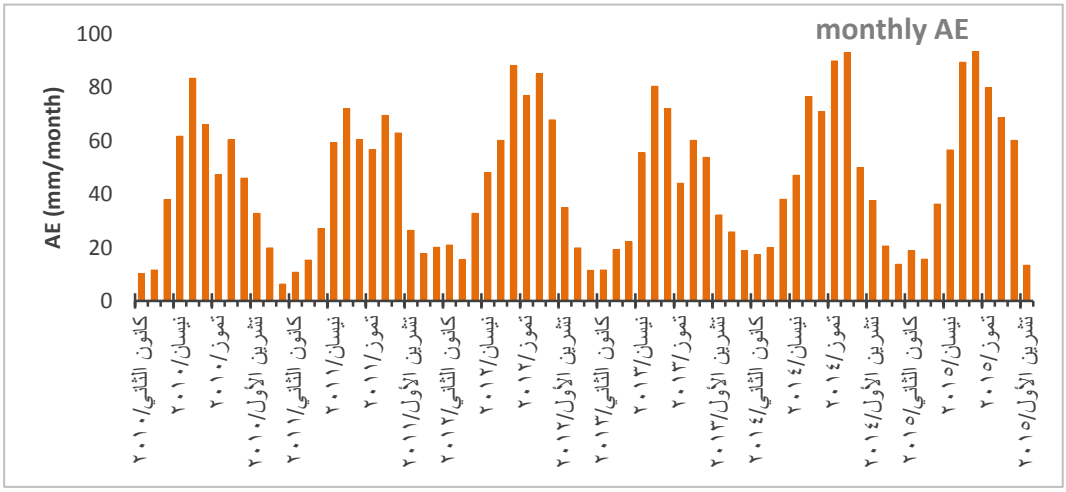

Figure 4-5 Actual evapotranspiration in the study area, from MORECS grid square 94.

Recharge

The recharge has been calculated using equation 4.3. Surface runoff can be removed from the equation when the incidence of the surface runoff is seldom. The study catchment area consists of unconfined chalk rocks, and the Chalk crops out over the

majority of the area. Occasionally highly permeable head deposits cover the area along the river beds. As a consequent, the geological and hydrogeological properties of the catchment area do not usually lead to a surface runoff. When the water in soil storage surpasses the field capacity of the soil, the extra water will try to percolate to the groundwater as a recharge (Jackson and Rushton, 1987).

Rainfall is considered as a primary source of recharge in the area, especially for the unconfined aquifers. No significant natural indirect recharge source such as river, stream, and lake neither an artificial source such as basin and pools are available.

Hence for the study catchments, over the whole annual scale the equation for groundwater recharge R_v (m^3/year) (i.e. R times A, the area of the catchment) can be written as a follows:

$$R_v = (P - AE) * A \qquad \text{Equation 4-7}$$

R_v *is volumetric recharge in* m^3/day

A is *catchment area* (m^2)

This equation has been used to estimate the volume of the recharge water (in m^3/year) have been estimated for the Kirby Grindalythe and Driffield catchments for five successive years (years 2010 to 2014).

The graph in the figure (4.6) show that AE is similar for most years but rainfall more variable. Which explains that the recharge variation between water years in study area mostly control by the rainfall in the comparing to the AE. This also confirmed from the relation between rainfall and stream discharge see figure (4.7). This figure showed that the variation in the duration and shape of the recession curve between water years was significantly influenced by the contrast in the rainfall.

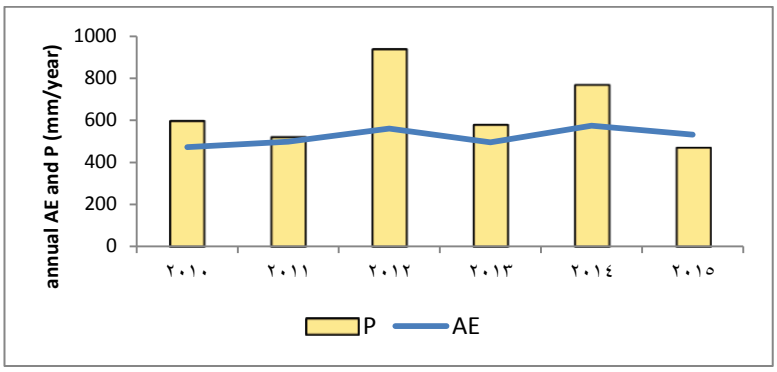

Figure 4-6 Average annual actual evapotranspiration (AE) and rainfall (P) in the study area (MORECS data).

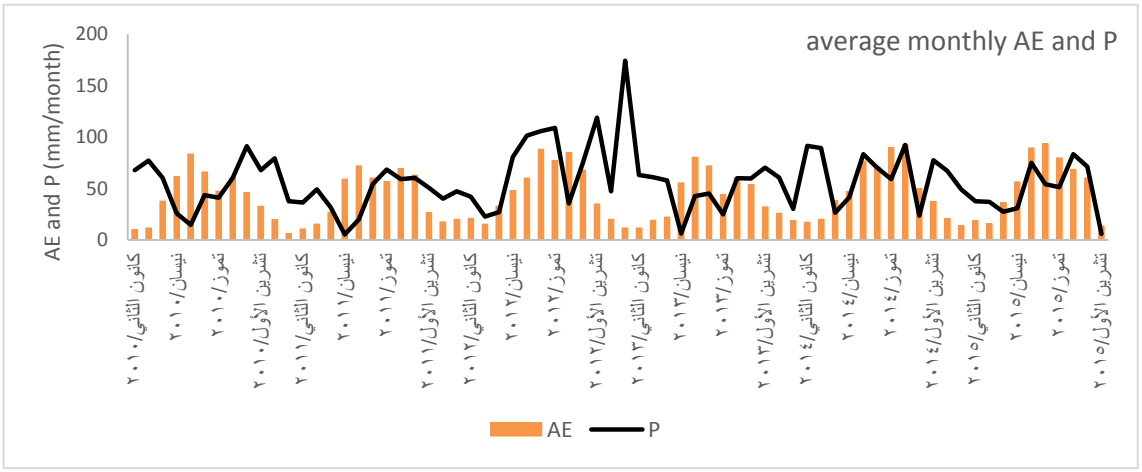

Figure 4-7 Average monthly actual evapotranspiration (AE) represented by bars and rainfall (P) represented by a black curve (MORECS data).

Groundwater abstraction:

During the calculation, the water balance for the Kirby Grindalythe catchment effect of the artificial pumping of groundwater was neglected. Two abstractions licensed boreholes areexist within the area, but significant amount of abstraction has not been reported to the Environmental Agency. These two boreholes are farming boreholes, they are used occasionally but not intensively for irrigation but mainly for cleaning the farm storage area (this information was obtained from the Low Mowthrope

farming staff). In contrast in Driffield, catchment groundwater was abstracted from five boreholes [TA 019 612 , SE 9984 6136, TA 0255 5945 , TA 0170 6020 ,TA 024 615] , approximately in the middle of the catchment. The Environment Agency provided the annual groundwater abstraction for the period between 2010 to 2014 (see table 4.1), which was used to find the water balance. The abstraction amount from these boreholes represents the actual pumped water from the borehole according to the EA. However, there is a possibility of abstraction from the aquifers through the unlicensed boreholes, because based on the Environmental Agency policy, abstractions of less than 20 m3/day do not need a license.

Annual estimated recharge simultaneously with the annual abstraction from Driffield catchment were plotted on the time series graph, see figure (4.8). The result showed that pattern of the annual abstraction to some extent reflects to the pattern of the annual recharge.

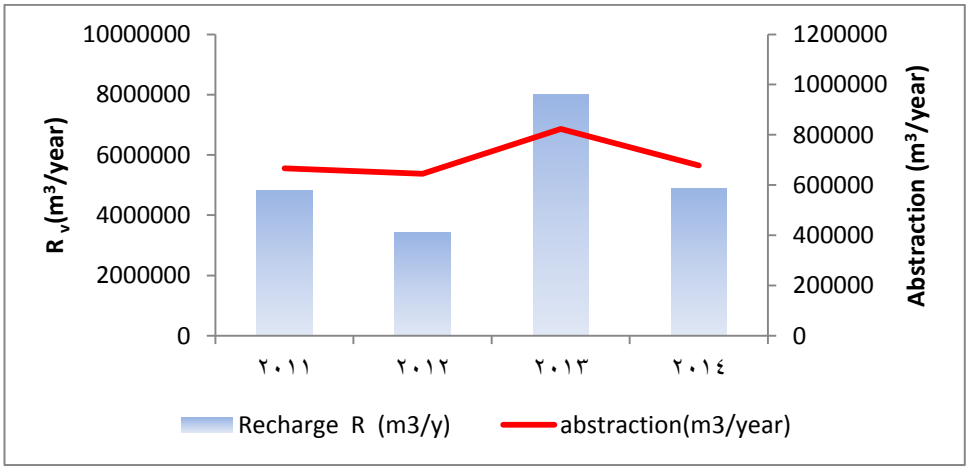

Figure 4-8 Shows time series comparison between annual groundwater recharge (R_v) and groundwater abstraction (Ab) from Driffield catchment.

4.2.2. Assumptions in calculating water balance for the study area

In this study the water balance for the study catchments was undertaken based on some assumptions:

- There is no interflow recharge and discharge.
- Depending on EA policy for borehole abstraction license, any borehole with the pumping rate less than 20 m^3/day does not need a license, so the abstraction from these boreholes not included in the water balance calculation.

4.3. Results

Water balance has been calculated for both Kirby Grindalythe and Driffield catchments for the years 2010 to 2014. The result showed that there is a difference between the volume of inflow (direct recharge, R_v), and gauged discharge Q, i.e. discharge measured at the gauging station table (4.1). The R_v was greater than Q by factors between 1.9 - 4.4 for Driffiend and 3.5 - 6.9 for Kirby Grindalythe.

4.4. Interpretation of the water balance results:

The result of the water balance calculation for years 2010 to 2014 for both Kirby Grindalythe and Driffield catchments showed that the volume of the annual recharge was bigger than annual discharge measured at the gauging stations. Three scenarios have been suggested for interpreting the reason for this difference.

Table 4-1. Summary of water balance at Kirby Grindalythe and Driffield catchments.

	year	annual rainfall (mm)	annual AE (mm)	Abstraction (m^3/yr)	Recharge R_v (m^3/y)	Discharge Q (m^3/year)	R_v/Q
Kirby Grindalythe (15.9 Km^2)	2011	747.4	578.2	/	2690280	399513.6	6.7
	2012	639.1	513.7	/	1993860	371174.4	5.3
	2013	733.1	460.4	/	4335930	1225275.3	3.5
	2014	801.9	629.8	/	2736390	398019.9	6.9
	year	annual rainfall (mm)	annual AE (mm)	Abstraction (m^3/y)	Recharge R_v (m^3/y)	Discharge Q (m^3/year)	R_v/Q
Driffield (32.4 km^2)	2011	747.4	578.2	666112.19	4815967.8	1359244.8	3.5
	2012	639.1	513.7	644278.02	3418681.9	932601.6	3.6
	2013	733.1	460.4	823508.02	8011971.9	4059719.1	1.9
	2014	801.9	629.8	677949.33	4898090.6	1111893.8	4.4

4.4.1. First scenario: overestimation of annual recharge due to unrepresentative climatic data :

During the period when the water balance calculated for the catchment (2010-2014) rainfall recharge always exceeded gauged outflow. This indicates that there is a possibility of overestimation of the amount of the rainfall or underestimation of actual evapotranspiration which was used in the water balance. The MORECS grid square is 1600 km square (40 km x 40 km) is very vast area comparing to the study area which is 10 km square. As a result, the MORECS data might not represent the study area correctly due to spatial variation over the 1600 km square area which occupied by each MORECS grid square. The map of rainfall distribution for East

Yorkshire showed that there is a small spatial variation in the rainfall between the Kirby Grindalythe and Driffield catchments. Consequently, the overestimation in the climatic data may have influenced the inflow/outflow ratio, but the ratio of the inflow/outflow which appeared is so large, it is unlikely that an overestimate in rainfall or underestimate in the AE alone produced this big difference.

4.4.2. Second scenario: overestimation of the catchment area due to uncertainty in the catchment boundary:

The volume of recharge was estimated by multiplying the depth of effective precipitation available for recharge by the area of the catchment. So, an overestimation of the catchment area means overestimate in the recharge value and the ratio of the inflow/outflow exceeding unity.

As for all water years 2010 to 2014 used in this study the amount of inflow was bigger than the gauged outflow for both Kirby Grindalythe and Driffield catchments, there is a possibility that catchment size was overestimated.

As explained in the Chapter 3 section (3.6) the boundary of the study catchments was estimated according to the topography. So the recharge-discharge ratio from the catchments indicates that the hydrological catchment may not match exactly with the topographic divide. However this over-estimation would have to be very large if it was the only factor responsible; such a large overestimation of catchment area seems unlikely.

4.4.3. Third scenario: Subsurface flow beneath the gauging stations e.g. flows through conduit system

A third possible explanation for the discrepancy between recharge and stream outflow is that a portion of the ground water flow through a conduit systems or superficial deposits parallel to and/or beneath the streams, bypassing the gauging stations. In this case, the water balance equation can be expressed as follows:

Recharge R_v = gauged outflow+ underground flow

The result of the Gypsy Race flow measurement at the Kirby Grindalythe station and Duggleby Bridge shown that the flow rate at the Duggleby Bridge was higher than the Kirby Grindalythe (see table 3.2 in chapter 3). The distance between these two positions is 2 km, there is no abstraction from the stream between these two locations. This means that the flow rate reduces in the stream is unlikely to be due to artificial processes. Losing water from the stream within 2 km length while the width of the stream less than 1 m suggests evapotranspiration is unlikely to be responsible, which indicates that a portion of water in the stream after Low Mowthorpe bridge flows into the ground, either entering the Chalk or a superficial deposit. At Kirby Grindalythe beneath the gauging station, the aquifer consists of Ferriby and Welton Chalk formations; the Welton Chalk contains bands of flint which may be responsible for creating a high flow zone in the shallow aquifer.

In the Driffield catchment during the field investigations it was noticed that during the very late period of the recession period when the flow rate at the gauging station become zero, there was water flow in the stream channel downstream the station. This also indicates the existence of groundwater flow at the shallow depth, exiting the catchment below the gauging station. Hence, in both catchments, subsurface flow exiting the catchment below the gauging station explains the discrepancy between recharge and gauged outflows.

4.5. Sensitivity of groundwater pumping from small boreholes and subsurface inflow on the water balance in Kirby Grindalythe and Driffield catchment:

The assumptions that are used for calculating water balances ignored the effect of any pumping from boreholes with pumping rates less than 20 m^3/day and water entering the defined catchments below the ground surface. Here in order to

understand how these two factors affect the water balance result (expressed in the form of recharge/gauged discharge ratio) a sensitivity analysis has been done.

In order to understand the effect of the boreholes with daily pumping rate lower than 20 m^3 on the ratio of the recharge/discharge the sensitivity test has been done. In the sensitivity test, the effect of up to 12 boreholes, each with pumping rate of 20 m^3/day, on the recharge/discharge ratio was found, see figure (4.9). The figures show that the ratio of recharge/discharge not affected significantly by pumping water from this number of boreholes. The effect in the Kirby Grindalythe is bigger than in Driffield catchment, due to the difference in the catchment size.

Furthermore, the effect of recharge to the aquifer through inflow of groundwater from surrounding aquifers on the recharge/discharge value, a sensitivity analysis for inflow was accomplished. In the sensitivity test, it has been assumed that an additional recharge equal to 1% up to 10% of the total annual recharge that came from precipitation has entered the aquifer in the form of inflow from surrounded catchments. Figure (4.10) is showing the result from the inflow sensitivity test. The result showed that in the Kirby Grindalythe catchment, with value of inflow recharge equal to the 10% of total annual recharge the recharge/gauged discharge ratio increased by factor of 0.4, while for the Driffield catchment the ratio increase by factor of 0.28. So the presence of additional subsurface inflow causes the recharge/gauged discharge ratio to rise further above unity; the presence of any such recharge thus cannot explain the observed discrepancies highlighted in table 4.1. It can be concluded that, as stated previously, subsurface discharge below the gauging stations is the most likely explanation for the observed ratios, and this result is robust with respect to the errors inherent in the data used.

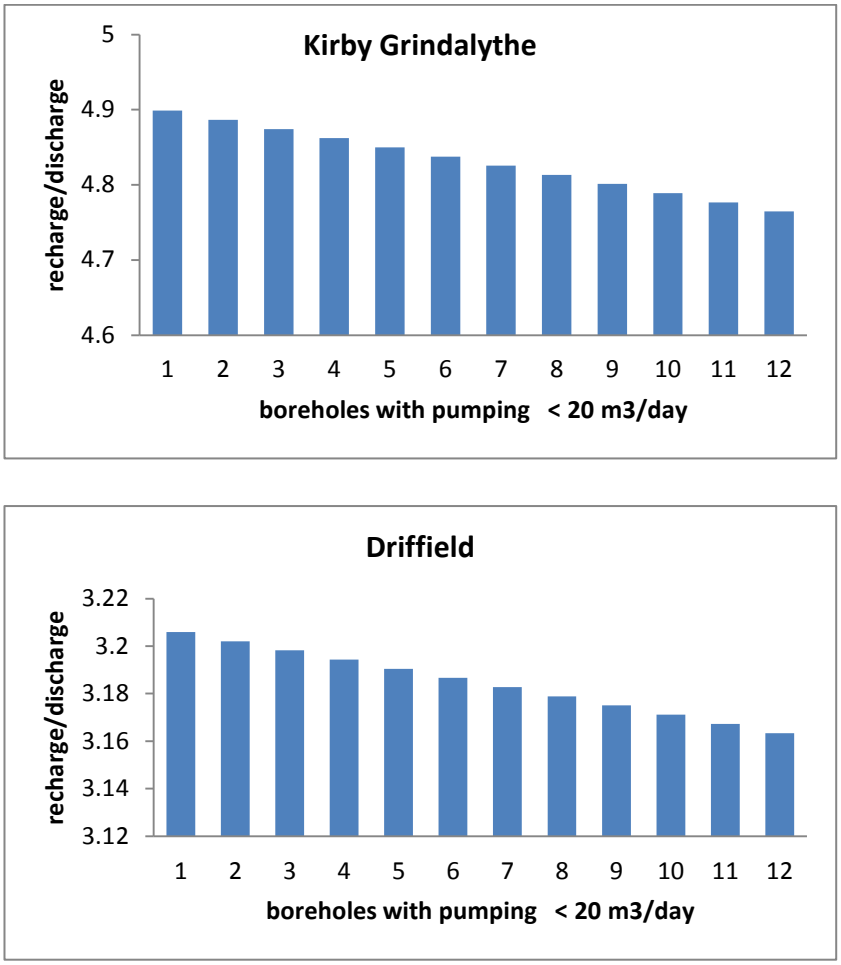

Figure 4-9 Effect of groundwater pumping from additional hypothetical boreholes with pumping rate of 20 m^3/day on the water balance result of Kirby Grindalythe and Driffield catchments.

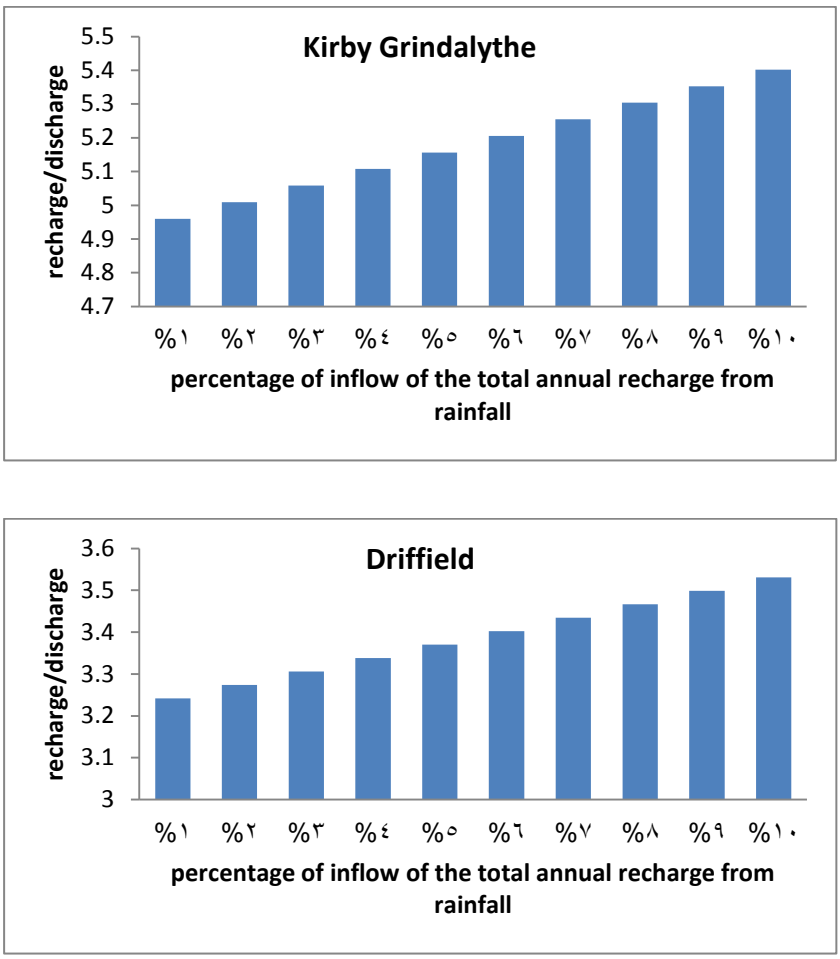

Figure 4-10 Effect of the additional recharge from surrounding areas on the water balance result of Kirby Grindalythe and Driffield catchments. Y-axis represent the inflow /gauged outflow ratio, and X-axis represent the percentage of additional inflow recharge (these percentages represent an extra water above the total annual recharge from precipitation).

4.6. Summary:

A local water balance equation was established for the study catchments, this equation was derived from the generic water balance equation, which works base on the principle of the law of conservation of mass. The result from water balance calculation found that the amount of the recharge (inflow) is greater than the amount of the measured discharge (outflow) from the aquifers through the gauged streams. In average, the recharge-gauged discharge ratio for Kirby Grindalythe was 5.6 and for Driffield was 3.4.Three possible scenarios have been suggested for explaining the different between the annual recharge to gauged discharge. First, an overestimate in the climate data used for calculation water balance, the climate data from MORECS used for calculation, which covers 40X40 km^2 this data, assumed there is not spatial variation in rainfall and actual evapotranspiration. While the rainfall distribution map of East Yorkshire showed that there is a small spatial variation in rainfall amount between Kirby Grindalythe and Driffield catchments, this is nowhere near enough to account for the discrepancy. Second, an overestimate in the catchment size, the boundary of the study catchments were estimated according to the topography, but in nature more likely the groundwater divide does not match with the topographic divide exactly. However, based on the recharge-discharge ratios the catchment sizes according to groundwater divides would need to be very much smaller than the topographic catchment boundary; this seems unlikely. Third, previous works revealed subsurface flow in the Chalk aquifer, the field investigation during this study also confirmed subsurface flow beneath the gauging stations is likely in both study catchments. So, one of the most likely reason for the difference between recharge and measured discharge volume is that big portion of the catchment discharge occurs in the ground, bypassing the gauging stations. This result is likely to be robust to errors caused by undocumented small abstractions or subsurface inflows to the catchments.

Chapter 5. Monitoring groundwater and stream water

During the study, stream water temperature, stream water electrical conductivity (EC), water table and groundwater temperature at selected wells and streams were monitored continuously at 15 minute time intervals during the period from March 2013 to July 2015.

5.1. Review of related literature

5.1.1. Groundwater Water and stream water temperature:

The daily and seasonal fluctuations of groundwater temperature are smooth compared to those of the atmospheric and surface-water temperature, and they become more smooth or even stable with increasing depth of groundwater. The temperature of the groundwater at depth typically fluctuates within less than one Celsius degree. Meanwhile, the temperature of the surface water varies on a daily basis, fluctuating by a few Celsius degrees, simultaneously with the atmospheric temperature because of their direct contact (Stallman, 1965; Baskaran et al., 2009), provided that the stream water has time to equilibrate with the atmosphere. In this study, the temperature of the stream water was monitored to investigate its use as a tracer for investigating the relative contributions of groundwater versus more direct inputs from rainfall such as runoff and interflow (quickflow components) (Anderson, 2005; Rau et al., 2010; Stonestrom and Constantz, 2003) (Stallman, 1965)(Baskaran et al., 2009). Silliman and Booth (1993) used this method for mapping gaining and losing reaches of a stream in Indiana. Within groundwater, Oberlander and Russell (2005) revealed that the temperature profile within the borehole in carbonate rock during pumping tests showed a steep temperature gradient, and they related the sudden reduction in the groundwater temperature to flow of the water to the borehole through big fractures. Stream water temperature monitoring along the stream channel

allows identifying of quickflow through the soil or surface runoff to the stream (Lee et al., 2013). However, this requires longitudinal stream temperature profiles. In this study time series monitoring of single sites was used in order to investigate whether the source of the spring-fed streams changes seasonally or following storm events.

If a stream gain waters from long residence time groundwater, its temperature is expected to be fairly stable (assuming that the groundwater component entering the stream does not reside in the stream long enough to equilibrate with the atmospheric temperature). In contrast, a sudden change in the stream water temperature after a rainfall event indicates quick flow from the catchment to the stream through soil or runoff, or possible rapid groundwater flow through big conduits.

5.1.2. Stream water conductivity:

Electrical conductivity is the susceptibility of a material for carrying an electrical current. In the case of water, this value depends on the purity of water, temperature, type and concentration of dissolved ions. Freshwater relatively has very low conductivity compared to saline water. Temperature is another factor which influences the water conductivity, through conductivity increasing slightly with rising temperature (Ritter 2010).

The conductivity of groundwater is typically higher than the conductivity of rain water due to higher concentrations of dissolved ions; groundwater in chalk specifically is fairly conductive owing to its saturation with calcium. In nature, ions dissolve in the water during percolation and transportation of groundwater through soil and rocks before discharging to the stream channels. Dissolved solids in the natural groundwater as a result of dissolution activity, particularly calcite, in this case cause both the ions concentration and the EC of the groundwater to increase (Hem, 1985; Freeze and Cherry, 1979; Peters, 1984). EC is temperature dependent; generally speaking as the water temperature increases the solubility of the minerals increases (Garrels and Christ ,1965; Stumm and Morgan, 1970; Garrels and Mackenzie,1971). Increasing the water temperature will cause a decrease in its

viscosity and an increase in the mobility of the ions dissolved in the water (Barron and Ashton, 2005). For instance, the measured conductivity of the solution of 0.01 KCl at 20^{o}C is 1.273 mS/cm, while within the same solution the conductivity increases to 1.409 mS/cm at temperature 25^{o}C (RA, 2004). However, the role of carbonic acid on mineral weathering complicates the relation between water temperature and solubility rate. Reynolds and Johnson (1972) confirmed that the processes of carbonate reaction and dissolution due to carbonic acid are more rapid in cold regions than in warm regions. This is because water in equilibrium with gaseous carbon dioxide (CO_2) contains more CO_2 at low temperature than at higher temperatures (Peters, 1984). Sweeting (1966), in a study of groundwater draining limestone in northern England, observed an increasing dissolution rate of the carbonate mineral with decreasing stream water temperature, and further detected that with decreasing stream water temperature, the pH of the water also decreased. This type of change can be called a seasonal change of conductivity driven by seasonal temperature change; nevertheless, this type of change is relatively gentle and concurrent with a change in the seasonal atmospheric temperature.

5.1.3. The relation between groundwater EC and temperature:

In general, the relation between EC and temperature is nonlinear in natural water (Millero, 2001); however, this nonlinearity is relatively small in the temperature range from 0-30 ^{o}C (Sorensen and Glass, 1987). Groundwater conductivity can change over time as a result of physical and chemical processes such as oxidation, reduction, precipitation and ion exchange (Radtke et al., 1988). The EC of groundwater in carbonate rocks is primarily controlled by the concentration of the Ca^{2+} and HCO_3^- ions in the water. The concentration of Ca^{2+} depends on the solubility of the calcium carbonate, which is mainly controlled by temperature, total and partial CO_2 pressure and pH (Coto et al., 2012).

Carbon dioxide is the most soluble atmospheric gas. Its solubility is proportional to its partial pressure (Henry's Law) and inversely proportional to temperature. For dissolution of CO_2 in water, Henry's Law may be written as follows (Ford and Williams, 2007):

$$CO_2 = C_{ab} * P_{CO_2} * \ 1.963$$

Where CO_2 gL^{-1}, l.963 is the weight of 1 liter of CO_2 in grams at 1 atmosphere pressure and 20°C, and C_{ab} is temperature-dependent absorption coefficient.

The $CaCO_3$ solubility is controlled by the following equilibrium

$$Ca^{2+} + 2HCO_3^- \rightleftarrows CaCO_3 + CO_2 + H_2O$$

When the temperature at the water table increases, the partial pressure of CO_2 reduces, thus CO_2 is lost from solution to the gas phase. Consequently, according to the above equilibrium equation the driving force leads to precipitation of $CaCO_3$ or reduced dissolution of $CaCO_3$ (Mackay, 2003).

Secondly, reducing CO_2 in the water causes decreasing carbonic acid concentration, thus pH of the water increases (Roy et al., 1984).

$$CO_2 + H_2O = H_2CO_3 \rightleftarrows HCO_3^- + H^+$$

P[CO_2] may increase in the soil atmosphere as a result of biological activity in the rooting zone. This has a great role in the solubility process in carbonate rocks because the root zone CO_2 may entirely replace O_2 and increase the concentration of CO_2 to 21% (Ford and Williams, 2007). When recharge water infiltrates through soil saturated with CO_2 it becomes oversaturated with CO_2; subsequently when this water enters the aquifer it will enhance the solubility of the $CaCO_3$ and increase the EC.

Travertine (calcareous deposits) occurs predominantly in springs and spring-fed lakes (Chafetz and Folk, 1984). Precipitation of travertine indicates that the groundwater is supersaturated with calcium carbonate with respect to calcite and supersaturated in CO_2 with respect to air. Precipitation of calcium carbonate can occur at the mouth of the spring and in the stream (when groundwater is exposed to the atmosphere), due to loss of CO_2 as a result of the higher temperature outside the aquifer (Boggs, 2009). This indicates that the EC of groundwater in contact with the atmosphere changes when air temperature is higher than the temperature at the water table. However, the intensity of the change in EC in the stream water depends mainly on the temperature, total and partial CO_2 pressure and pH (Coto et al., 2012).

When the relation between the T and EC of the water is examined, the temperature of the environment that surrounds the water, and the temperature of the water itself must be considered. Each of these two temperatures affects the EC of the water in a different way. There is a direct relation between the temperature of the water and EC, because with increasing temperature the viscosity of the water reduces and the mobility of the dissolved ions in the water increases; consequently, the EC increases. However, there is an inverse relation between the temperature of the environment surrounding the water system and EC of the water. For example, if CO_2 is taken into consideration, increasing the air temperature near the water-air contact surface causes decreasing partial pressure of CO_2, leading to loss of CO_2 from the water through the CO_2 changing from solute to gas phase. This reduces the ability of the water to dissolve $CaCO_3$ and reduces the concentration of Ca^{+2} in the water owing to precipitation of $CaCO_3$. Consequently, the EC of the water decreases.

The direct effect of water temperature variation on EC can be eliminated by applying temperature calibration, usually to 25°C. As it is important to calibrate the EC measurements to a specific temperature, the following equation is used to calibrate EC readings to 25°C (Mantynen, 2001; Hayashi, 2004):

$$C_{25} = \frac{C_m}{1+0.02(T_m-25)} \qquad \text{Equation 5-1}$$

$where: C_{25}\ is\ corrected\ conductivity\ value\ adjusted\ to\ 25^oC$
$C_m\ is\ actual\ conductivity\ measured\ before\ correction$
$T_m\ is\ water\ temperatuere\ (in\ C)\ at\ time\ of\ C_m\ measurment$

The units of conductivity are (1/ohm-m) or Siemens (S) per meter. In the International System, (SI) units of conductivity are reported as millisiemens per meter (mS/m).

However, this equation cannot eliminate the effect of the seasonal temperature-$P[CO_2]$ relation on the EC of the groundwater in open systems and streams. Therefore a smooth EC fluctuation can be commonly detected in the groundwater.

The effect of the air temperature fluctuation on the $P[CO_2]$ can be determined from the following equation (Sullivan, 2000):

$$\log_{10}(P_{CO_2}) = 0.03 * T - 2.48$$

5.1.4. Carbon dioxide (CO2) in recharge water

Carbon dioxide is the most common source of water acidity. CO_2 dissolves in the rainwater through equilibrium with the atmosphere. Besides the atmospheric CO_2, more CO_2 enters the rainwater while it percolates the soil during the recharging journey. The source of CO_2 in the soil is mostly from autotrophic respiration by roots and heterotrophic respiration by microorganisms (Metcalfe et al., 2007). The spatial heterogeneity of land use and microorganism activity causes heterogeneity in the CO_2 in the soil. A spatial variation in the pH of the Chalk groundwater has been reported in East Yorkshire. Smedley et al. (1996) discussed this variation and noted that the pH is generally higher in the scarp-slope springs than the dip-slope springs. Smedley et al. (1996) connected this variation to the groundwater $P[CO_2]$, and suggested that this variation is controlled by variation in the thickness of the unsaturated zone and land use. This author claimed that when the unsaturated zone is

thick the system is more likely to behave as a closed system, so the CO_2 concentrations in the groundwater will be lower. Meanwhile, when the unsaturated zone is thin, the groundwater will be in contact with the atmosphere (and thus behave as an open system); consequently, the concentration of the CO_2 will be higher.

In general, the EC in streams which are fed mainly by chalk groundwater will be expected to exhibit steady seasonal fluctuation in relation to the seasonal temperature fluctuation in the sense that higher atmospheric temperatures reduce the EC. Unexpected rising or falling of stream conductivity beyond the expected effects of CO_2 solubility may be due to external sources that influence the concentration of dissolved ions. For instance, increasing conductivity may arise from pollution by chemical substances (e.g. land fertilizer) (Divya and Belagali, 2012; Shabalala et al., 2013). A study carried out in Poland by Fronczyk et al. (2016) to monitor contaminants in groundwater (from springs and wells) due to fertilization showed that significant increases of EC ranging from 551 to 1,441 µS/cm resulted from adding chemicals to the ground. Meanwhile, decreasing conductivity could happen due to dilution of spring water by recharge from direct rainfall via quick flow through soil and surface runoff.

5.2. Field measurement methods and instrumentation

The measurements were recorded using three sets of automatic data loggers: Rugged Troll, Rugged Baro Troll, and CTD-Diver, see details below. A short time interval was selected in order to monitor input of short rainfall events on the groundwater and stream water temperature. Four boreholes and three spring-fed streams were selected as monitoring sites in the Wolds area of East Yorkshire, Figure (5.1) and Table (5.1); many of these were outside the study catchments of Driffield and Kirby Grindalythe for the reasons explained below, see section 5.2.2. The information was downloaded from the data loggers every 5 to 6 months as the built internal memory of the diver

has a capacity to record data for up to 6 months continuously at the 15 minute time intervals selected for this study.

5.2.1. Equipment:

The following three sets of hydrogeological monitoring instruments were used:

- CTD-Diver (Van Essen instruments/Schlumberger), this probe is used for measuring stream water EC and T (Figure 5.2).
    - EC range 0 to 120 mS/cm and accuracy +/- 1% of reading.
    - T range -20 to 80^{o}C, and accuracy +/- 0.1^{o}C.
- Rugged Troll (In-Situ Inc.). Mini-Diver used for measuring water column pressure (P in mH2O) and borehole water temperature (T in C), (Figure 5.2).
    - P range to 76 mH2O, and accuracy +/- 0.1%.
    - T range -20 to 50 C, and accuracy +/- 0.3 C

- Rugged Bari Troll (In-Situ Inc.) used for measuring atmosphere pressure.
    - P range to 20.4 mH2O, and accuracy +/- 0.1%.

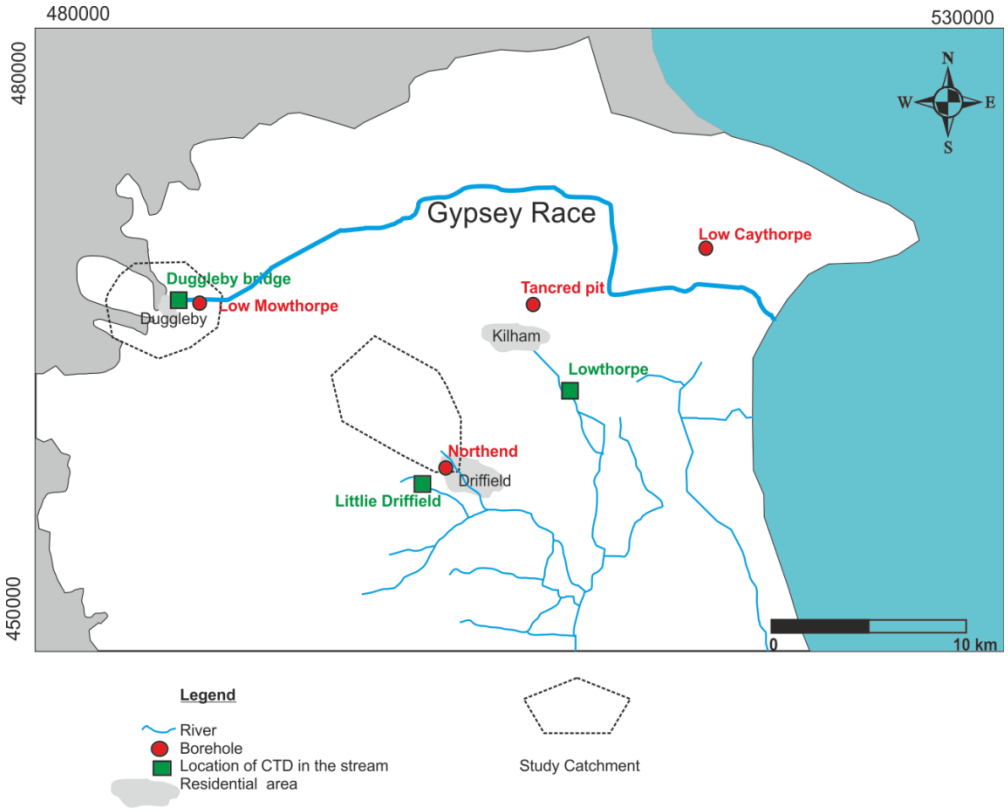

Figure 5-1. Map showing the location of the boreholes and streams monitored in this study . CTD divers installed in the stream and Trolls in the boreholes.

Table 5-1 demonstrates the coordination of the divers and Figure (5.1) illustrate the location of the monitoring sites on the map.

Description	water source	Grid Reference
Lowthorpe	Stream	TA088603
Duggleby bridge	Stream	SE884672
Church Lane, Little Driffield	Stream	TA009575
Low Mowthorpe	Borehole	SE893670
Northend Park, Driffield	Borehole	TA022582
Low Caythorpe	Borehole	TA124677
Tancred pit	Borehole	TA069660

Figure 5-2. CTD diver and in-Situ Troll data loggers.

5.2.2. Field site:

Three locations were selected for monitoring stream water temperature and conductivity, see Table (5.1) and Figure (5.1):

- Under the Duggleby bridge, ~1.9 km downstream from the springs (Kirby Grindalythe catchment).
- Under the bridge in Little Driffield, 1.6 km downstream from the springs (site is located in the Little Driffield catchment which is adjacent to the west of the Driffield Catchment shown by the red outline in Figure (5.1)).
- Under the bridge at Lowthorpe, 2.97 km downstream from the most remote springs at Kilham (Bellguy spring), although the large springs feeding the same stream at Bellguy and Bracey Bridge are closer, see Figure 5.1 and inset (site is located in the Kilham catchment which is adjacent and to the east of Driffield catchment).

At each stream location, a CTD diver was installed by lowering it onto the streambed and securing it with a metal cable for retrieval to the bridges at these sites. The divers were set up to read stream water EC and T continuously at 15 minute intervals.

The reason for selecting three stream monitoring sites was that each stream drains a different catchment. The locations where the CTD divers were installed in the stream were a few hundred meters to km downstream from the locations of the springs feeding the streams. Devices were located no closer to the springs for reasons of security and access, i.e. locations nearer the springs were not considered safe for leaving equipment. Therefore, the nearest bridge downstream from the lowest spring location was selected for installing the equipment. The bridges are built from solid material (typically masonry) which facilitated attaching the recording device via a metallic cable, and placing it hidden from view beneath the bridge. In addition, the water in the stream at the measurement locations consists of aggregation of the waters from several springs arriving from the same catchment, so it was expected that the EC at these places in the stream would represent the EC throughout the entire catchment area.

The bridge near Duggleby is located in the Kirby Grindalythe catchment. The Little Driffield and Lowthorpe bridges are located southwest and northeast of Driffield catchment respectively (in Little Driffield and Kilham catchments). The reason for not monitoring the stream within Driffield catchment was because this stream is located in an urban area which was not considered secure for installing the probes. The logistical selection of these catchments adjacent to Driffield was considered acceptable because they are similar catchments, and were therefore likely to represent the Driffield stream.

Unfortunately, despite such careful selection of the location of the devices, several were subjected to interference or theft during the period of observation. The device at Little Driffield was pulled out of the stream during February and March 2013. The hydro-diver at Duggleby was pulled out of the stream for a period between October and November 2013. At Duggleby, the device was found broken in June 2014(although the data up to this date was extracted from the broken diver by the manufacturing company after they were sent the broken diver). The diver at Lowthorpe was stolen in October 2014.

Four boreholes were selected for monitoring the groundwater hydraulic head:

(See Table 5.1 and Figure 5.1)

- Low Mowthorpe borehole to the west of Kirby Grindalythe village near the western border of the Yorkshire Wolds (Kirby Grindalythe catchment).
- Northend Stream borehole in Driffield town (Driffield catchment).
- Tancred Pit borehole located to the north of Kilham village (about 10km northeast of Driffield). This borehole is located in Kilham catchment.
- Low Caythorpe borehole, located on Low Caythorpe farm to the west of Boynton village. The borehole is located near the eastern border of the Yorkshire Wolds, near to where the Gypsey Race stream leaves the area.

5.2.3. Field measurements:

Monitoring in streams:

CTD divers were placed in streams on the streambed, and secured in place by connecting them with the bridges through a steel cable. Downloading the data from the divers to the computer was achieved in the field (at the location of the probes), through a specific adapter and software. The adapter was constructed to read the divers and able to connect with a laptop (or PC) through a USB. When the probes were connected to the laptop the software allowed downloading of the recorded data from the diver to the computer, and also allowed clearing of the diver's memory. The EC measurements did not need calibration for temperature variation because the transducer was factory formatted to calibrate readings to the temperature 25^{o}C. Figure (5.3) shows the CTD diver in situ and the process of downloading the data.

The measurements were taken from March 2013 to September 2015.

Figure 5-3. Downloading data from the data logger to the computer in the field.

Monitoring in boreholes:

In each borehole, two hydrologic probes were installed. A Rugged Troll was installed below the water table in the borehole to record the pressure due to the column of water above it, and a second device (Rugged Baro Troll probe) was installed in the borehole just below the ground surface but at about water level, to record atmospheric pressure. This allowed recording of changes in water pressure due to changes in groundwater level above the level of the lower probe.

The pressure due to the column of water above the submerged device was found by removing the effect of atmospheric pressure. This was achieved by subtracting the value of the pressure recorded by the baro diver from that recorded on the submerged hydrological diver (Eqn. 5-2). Figure (5.4) is a schematic diagram showing

installation in the borehole. The following equations were used for calculating the water level above the reference level WL (m.a.s.l.) from the recorded pressures (Schlumberger Water Services, 2014):

$$\boldsymbol{WC = 9806.65 * \frac{P_{troll} - P_{baro}}{\rho . g}}$$ Equation 5-2

WC= the water column above the device in meter (m)

$$\rho = density\ of\ water = 1000 \frac{kg}{m^3}$$

$$g = acceleration\ due\ to\ gravity = 9.81 \frac{m}{s^2}$$

P=pressure (cmH_2O)

$$\boldsymbol{WL = TOC - CL + WC}$$ Equation 5-3

WL= water level (above the reference level)

TOC=top of the casing (height above reference level, i.e. sea level)

CL= cable length used for suspended diver.

The same probe which was submerged in the borehole water has the capability for measuring the temperature. So simultaneously with the pressure, the temperature was recorded, which represented the well water temperature and was therefore assumed to represent groundwater temperature.

The monitored boreholes are located along a trend from the west to the east in East Yorkshire, see Figure (5.1). This trend was selected because the hydrogeological map from the British Geological Survey (BGS) shows that the regional groundwater flow is in this direction, see Ch.3 figure 3.2.

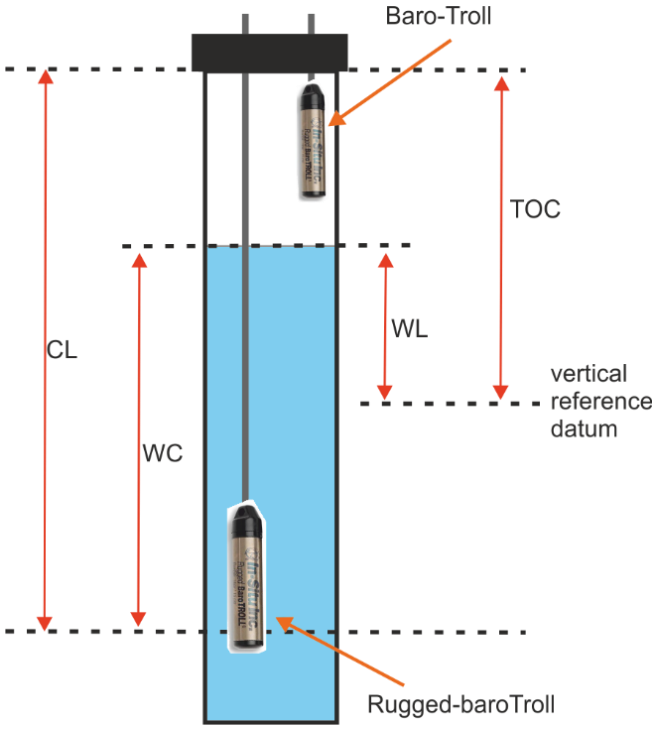

Figure 5-4. Schematic diagram showing installation of devices in the borehole.

5.3. Result and discussion of the field measurements:

5.3.1. Result and discussion of the stream and borehole temperature:

The measurements from the probe inside the boreholes show that the temperature of the well water is nearly constant throughout the year in the range between 9^{o} and 10^{o} C, with the exception of Low Mowthorpe which shows larger fluctuations, see Figure (5.5). The magnitude of temperature fluctuations is most probably due to the depth of the devices below the water table. Table (5.2) shows the depth of the probes bellow the water table. Deeper devices showed steadier water temperature fluctuations. In general, the temperature during the period when most of the recharge happens (November to March) is about 9.5 C. Consequently, water temperature measured at depths a few meters below the water table probably represents the temperature of the water resulting from groundwater circulation in adjacent

formations (as suggested by Michalski, 1989). The Low Mowthorpe borehole showed bigger fluctuations in the groundwater temperature than those from other boreholes. This is more likely because in Low Mowthorpe the troll (hydro-diver) was installed in the shallowest depth below water table compared to the other boreholes (see figure 5.5 B).

The temperature of the stream water showed fluctuations similar to those of air temperature, see Figure (5.6).The magnitude of stream water temperature recorded by the device in the stream at Duggleby was almost the same as that of the air temperature, which was 20^{o}C as a maximum and -2^{o}C as a minimum seasonal fluctuation. The temperature recorded by the devices in the streams at Little Driffield and Lowthorpe fluctuated in a narrower range, which was 15^{o}C as a maximum and 5^{o}C as a minimum seasonal fluctuation. This similarity in the temperature variation leads to the conclusion that the stream water temperature more likely reflects the air temperature rather than the groundwater temperature, and the stream water temperature appears to be in equilibrium with the air temperature at the Duggleby site, where the stream is relatively small. The factors influencing whether the stream water temperature reaches equilibrium with air temperature can be related to factors including the depth of water in the stream and the locations of the devices relative to the outlet of the springs.

Variation was observed in the magnitude of the seasonal fluctuations between the streams in Duggleby versus Little Driffield and Lowthorpe. This variation could be related to the depth of the CTD diver in the stream. The average depth of the stream at Duggleby was 0.2m, while at Little Driffield and Lowthorpe it was 0.62 m and 0.72 m respectively. The effect of the stream depth on the stream temperature can be noticed clearly in the data from Duggleby (see Figure 5.7). The stream temperature at Duggleby during May 2013 was higher than in May 2014, while the air temperature was similar during these two periods. But during May 2013 the stage of the water flow in the stream was about 0.1m, while in May 2014 the stage was 0.25 m. Accordingly, it can be concluded that the lower the flow rate the closer the water

temperature comes to equilibrium with the air temperature, and the very high flow rates most probably show the groundwater temperature.

Comparing the temperature from the borehole and the temperature from the stream clearly confirms that the water temperature recorded in the streams in the study area does not represent the groundwater temperature. As the stream water temperature at all three sites is strongly affected by atmospheric seasonal and daily temperature fluctuations, it was difficult to use stream temperature as a tracer for examining the quickflow versus groundwater contributions to stream flow.

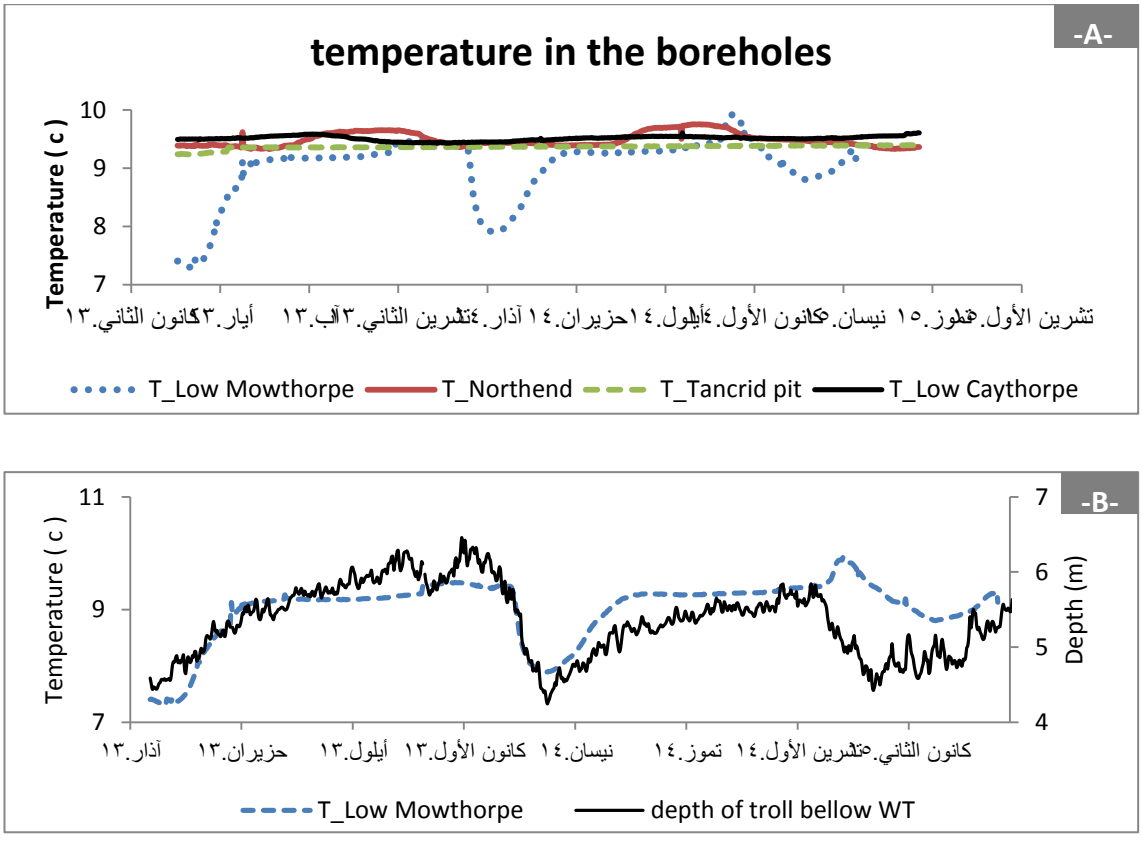

Figure 5-5 A-Average daily temperature from boreholes. B- Show the relation between large fluctuations of water temperature in the Low Mowthrope borehole and depth of the troll bellow the WT.

Table 5-2 Average depth of hydrologic diver (Troll) below the average water table level.

boreholes	depth of diver below WT
Low Mowthorpe	6.5 m
Northend Stream	9.5 m
Tancrid Pit	33 m
Low Caythorpe	17 m

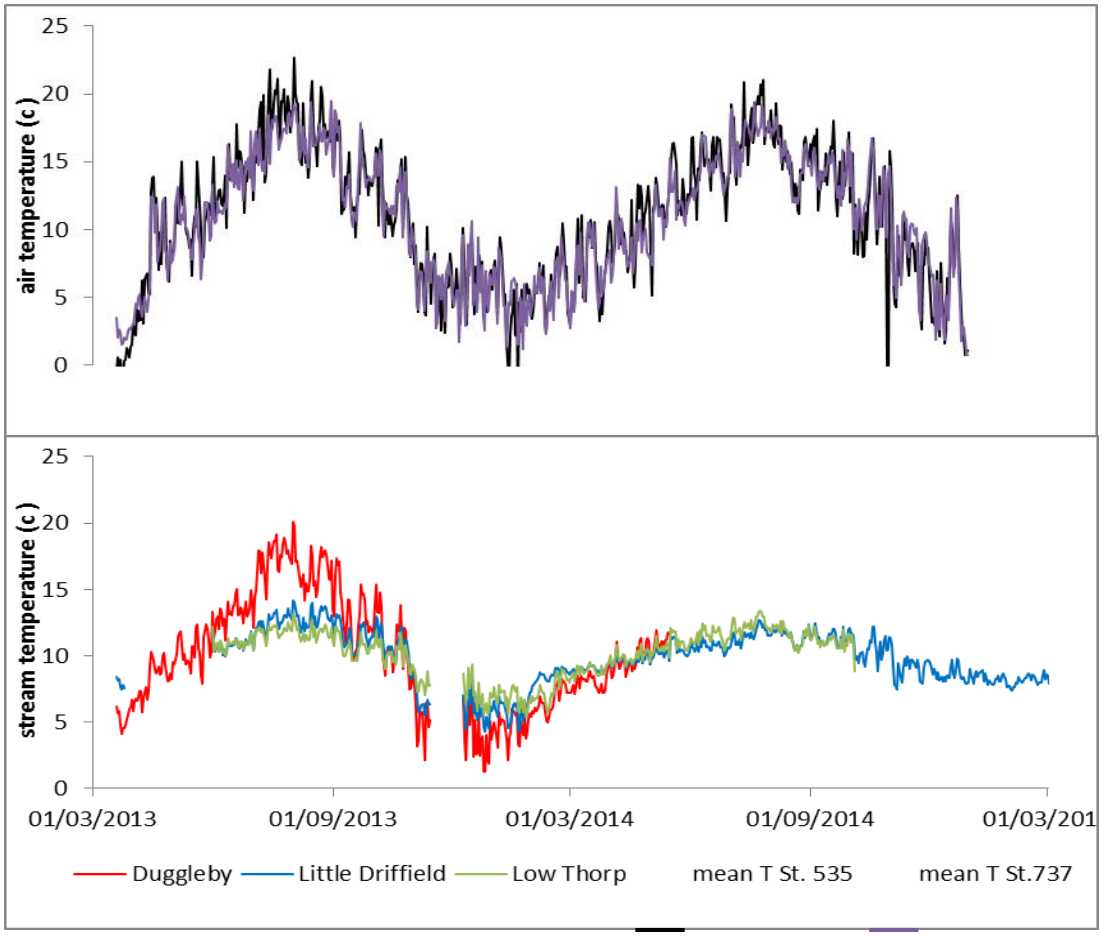

Figure 5-6 Stream and air temperature. The air temperature was obtained from the British Atmospheric Data Centre (BADC) for Station Bridlington MRSC 373 [GR : TA 193679] and Station CAWOOD 535 [GR: SE 561371] which are located in East Yorkshire.

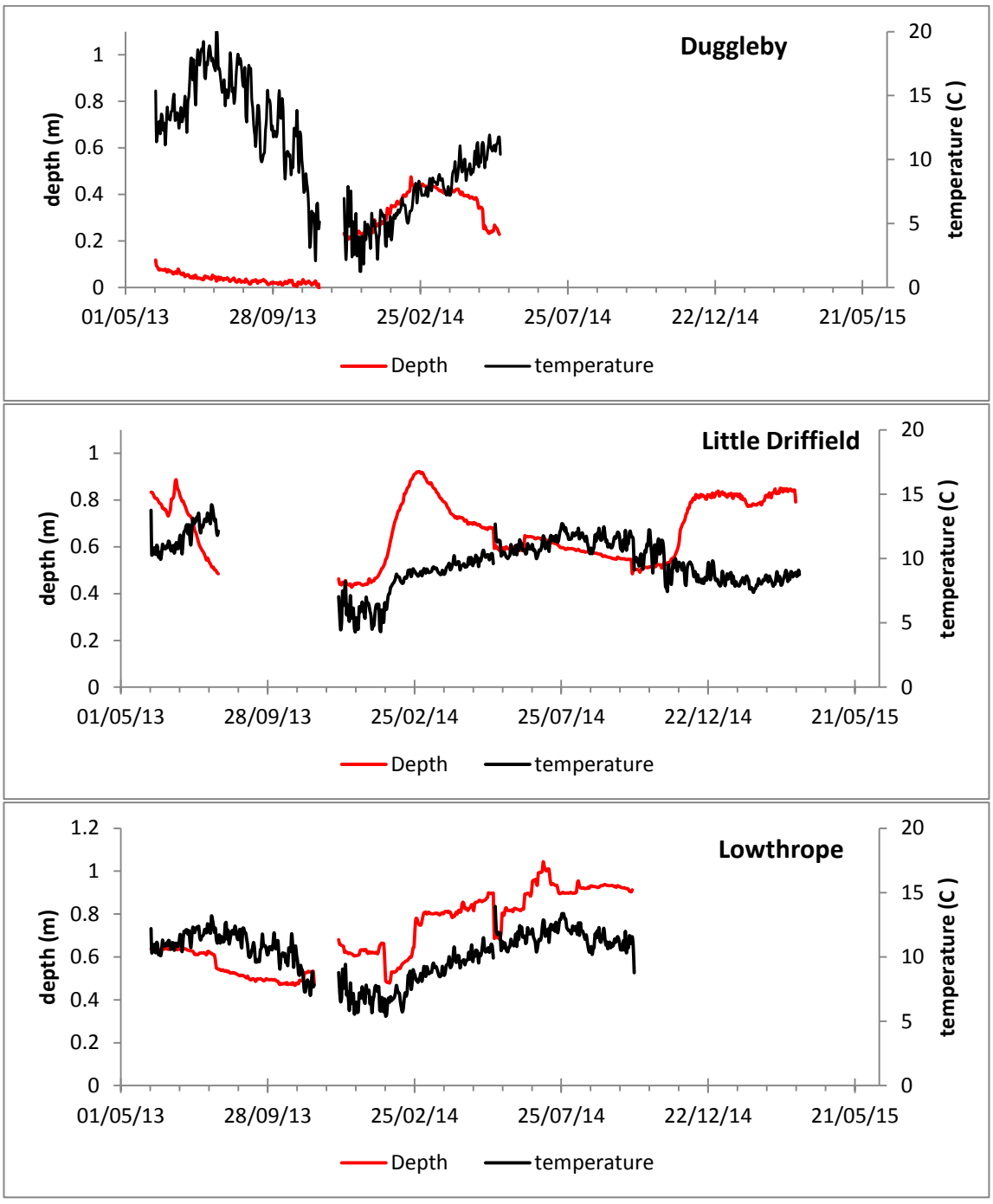

Figure 5-7 Show relation between stream water temperature and depth of the CTD devices below the stream water surface. The data based on 15 minutes interval.

5.3.2. Results and discussion of the water level from monitored boreholes:

Monitoring groundwater levels in boreholes provides hydrogeological and hydrological information. Determination of groundwater flow direction and interconnection between groundwater and surface water can be determined from groundwater levels (Grannemann et al., 2000; Taylor and Allen, 2001).

In this study the main target of the groundwater level measurement from the boreholes was to determine the regional groundwater flow direction and seasonal hydraulic head range. This information would help in developing the conceptual hydrogeological catchment models for use as the basis for numerical modelling.

The water level in the boreholes which were monitored during this study are illustrated in Figure (5.8). The groundwater levels in Tancred Pit and Low Caythorpe show bigger annual change than those in Northend Stream and Low Mowthorpe boreholes. The average groundwater level change during the recession period in the Tancred Pit borehole was 8.5 meters and in the Low Caythorpe borehole it was 6.5 m, whereas in Northend Stream and Low Mowthorpe boreholes it was about 2m. From Figure (5.1) it can be noticed that the boreholes at Northend Stream and Low Mowthorpe are located close to springs, while the Tancred Pit and Low Caythorpe boreholes are located further from springs. It is therefore clear that the areas located close to discharge points are not subjected to big changes in groundwater level and boreholes located further upslope record larger seasonal fluctuations.

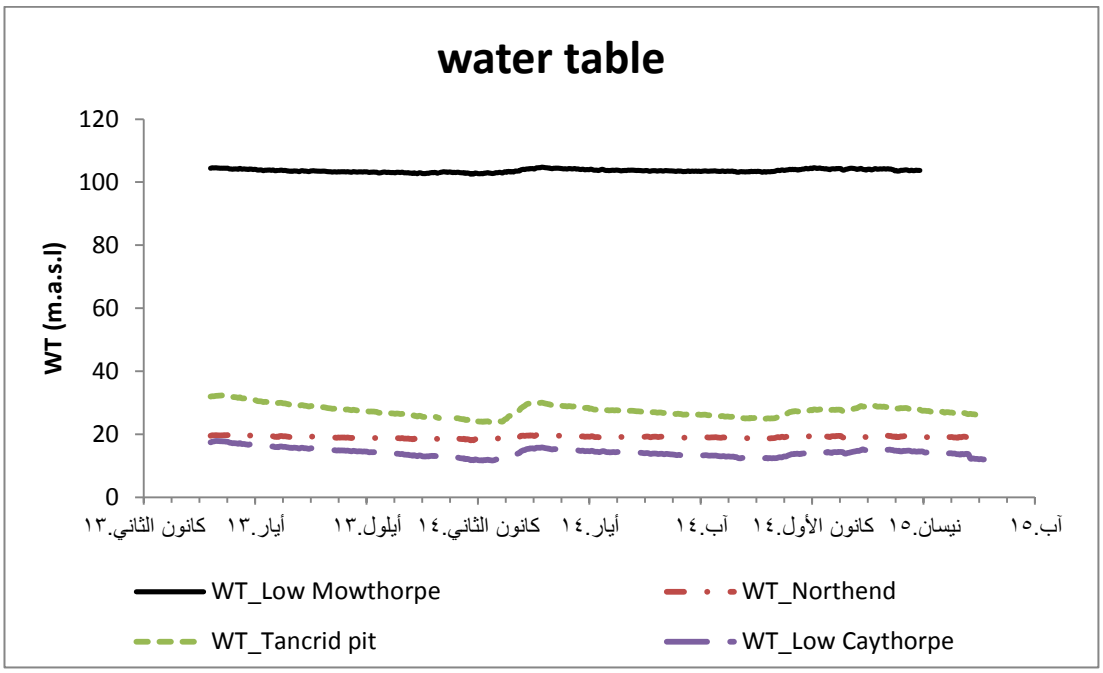

Figure 5-8. Water levels in the monitored boreholes (the elevation is in meters above sea level, m.a.s.l).

Results and discussion of stream water electrical conductivity:

Investigation of whether measured stream water EC represents that of Chalk groundwater-fed springs:

It has been mentioned previously that the selected monitoring locations in the streams (where CTDs were installed) were relatively far downstream from the locations of the springs (1.9km distance between Duggleby1,2 springs and Duggleby bridge in Kirby Grindalythe catchment, and 2.97 km between Bellguy spring and Lowthorpe spring in Kilham catchment). Hence, the EC of water at the CTD sites might differ from that at the springs. This difference most probably emerged because of degassing or ingress of atmospheric CO2 which may occur between the springs and the CTD sites, and arises from a difference between the temperatures of spring water and ambient air, as discussed previously in section 5.1.3. Where the ambient temperature is higher than that of the spring water, degassing of CO_2 will lead to

calcite precipitation and fall in EC; conversely where the ambient temperature is below that of the spring, ingress of CO_2 may raise the EC if the calcite dissolves, e.g. from stream bed sediments. Degassing or ingress of CO_2 may also change the pH. Furthermore, water at the CTD sites may represent spring water mixed with water from other sources, for example other springs, or base-flow to the stream below the spring, which may lead to changes in EC.

To investigate whether the EC of the stream water as recorded by the devices represents groundwater discharging at the main spring, EC and T were simultaneously measured at the spring locations and CTD locations. The measurements were taken four times in 2016 at the spring and CTD sites at Duggleby and Lowthorpe. The measurements were taken at Duggleby1 spring and Duggleby bridge CTD monitoring site, Bellguy spring and Lowthorpe bridge monitoring site. After collection all the EC measurements were calibrated to a temperature of 25^{o}C, see Table (5.3) .

The results showed that EC at the spring locations was typically greater than in the streams at the CTD sites downstream, by a relatively small amount. In the Kirby Grindalythe catchment, EC at the Duggleby1 spring was higher than in the stream under Duggleby bridge by 12 to 16 µS/cm, when monitored on four occasions between April and December 2016 (note that the offset between successive measurements was about 1 or 2 µS/cm, i.e. essentially zero within error, as the EC instrument accuracy is ±1%, so larger than these differences). In the Kilham catchment, the data showed that EC at the Bellguy spring was higher than in the stream under Lowthorpe bridge on the first three monitoring occasions, by 15,18 and 29 µS/cm successively. The final reading (December 2016) showed a small change in the other direction, i.e. that EC in the stream under Lowthorpe bridge was smaller by 12µS/cm, than in the water at Bellguy spring. Hence, there are significant offsets between differences at successive monitoring dates (i.e. +3 µS/cm between first and second reading and +11 µS/cm between the second and third reading, then - 41 µS/cm to the final reading in December 2016).

The differences in the water EC at the springs and the CTD sites may have arisen because of the degassing/ingress of CO_2 from the water due to change in the temperature of the water. Alternatively, ingress of low EC water from the shallow subsurface via the stream base and banks may be responsible. The latter explanation is supported by the fact that the Kilham catchment feeding the spring at Bellguy (and Lowthorphe CTD site) is bigger than the Kirby Grindalythe catchment feeding the Duggleby spring and monitoring site (see Figure 1.2, Introduction chapter). The larger size of the catchment may lead to more variability in EC and the quantity of shallow subsurface water which may enter the stream between the spring and the CTD site, creating larger and more variable EC offsets. In contrast, the Kirby Grindalythe catchment is relatively small, so a more homogeneous change between emergent springwater and the monitoring site was seen. Further, the distance between the location of the spring and the CTD may be another factor responsible for the size of the difference in EC values between the springs and CTD and the offset between successive readings. The distance between springs Duggleby1 and Duggleby2 and CTD location is 1.9km, while the distance between Bellguy spring and Lowthorpe bridge is 2.97km. Thus, there is more possibility of shallow subsurface water entering the stream at Lowthorpe than at Duggleby.

As only minor variations in the EC between the spring sites and CTD locations in the stream fed springs were identified, it can be concluded that the stream water is predominantly chalk-derived groundwater with not much quick flow component.

Regarding the temperature, only the measurements taken in November 2016 at the springs were within the groundwater temperature range of between 9 and 10°C (see section 5.3.1). All the other temperature measurements at the spring and in the stream at CTD sites were either above or below the range seen in the groundwater boreholes, which suggests the temperature of water emerging from the springs is already in equilibrium with the atmospheric temperature. At Duggleby, this may be because the spring is rather small and emerges into a pond, which is where temperature was measured. At Bellguy, spring flows are generally higher and the

spring outflow was measured directly, so equilibration with atmospheric temperature suggests that it may not tap deep groundwater flows, but rather water which has previously flowed at or close to the surface further upstream. That the spring waters are already near atmospheric temperature again supports the hypothesis that any changes in EC downstream of the springs are due to mixing with other EC waters, rather than degassing/ingress of CO2.

Electrical Conductivity as an Indicator of Hydrologic Processes

It has been explained in the beginning of this chapter that measuring EC is a suitable approach for monitoring stream water chemistry. There is a difference in the EC of the water from groundwater, rainwater and runoff water from farms and agricultural land (water from farms and cultivated land may wash off different chemicals into the stream or the ground) because of the variation in the concentration of the ions. This study aimed to use EC as an indicator for studying the hydrologic processes of the stream water. For this purpose time series variations in the relations of stream EC, EC- effect rainfall and EC-discharge were examined. These relations were used to determine the dominant source of water in the stream. For Kirby Grindalythe and Little Driffield the Q and EC from the same catchment were used, but for Lowthorpe, because the flow is not gauged, the discharge Q from the adjacent Driffield catchment was used. The distance between Driffield and Lowthorpe streams is approx.7 km.

Table 5-3 Water EC and T measurements at selected springs and CTD stream sites in stream at Duggleby and Lowthrope at Kirby Grindalythe and Khilham catchment respectively.

Measurement date	Kilham catchment				Kirby Grindalythe catchment				High Mothorpe station		Difference in the water EC between Spring and CTD location	
	Bellguy Spring		Lowthorpe Bridge		Duggleby1 Spring		Duggleby Bridge		Air T (C)			
	EC (µS/cm) at 25 °C	Stream T. (C)	EC (µS/cm) at 25 °C	Stream T. (C)	EC (µS/cm) at 25 °C	Stream T. (C)	EC (µS/cm) at 25 °C	Stream T. (C)	max	min	Kilham catchment	Kirby Grindalythe catchment
22/04/2016	477	12.2	462	11.7	599	13.2	587	12.9	10.5	3.4	15	12
16/05/2016	459	13	441	12.5	578	14.8	565	14.2	16	7.4	18	13
23/11/2016	426	9.9	397	9.1	446	9.8	432	8.7	9.5	5.5	29	14
21/12/2016	422	6.3	434	6.3	457	9.4	441	6.3	7	2.8	-12	16

Result and discussion of the stream water EC:

Figure (5.9) shows the results of stream water EC monitoring at Duggleby[1], Little Driffield and Lowthorpe streams respectively (all the measurements are corrected to 25^{o}C).

The EC in the stream under Duggleby bridge (which represents the upper reach of the Gypsey Race), Figure 5.9, showed an average 'baseline' value of around 575 µS/cm, but there were many short duration events when the EC fell below the average value (troughs), as well as many spikes. The majority of the troughs happened during the period from August - October 2013, with EC values falling to 310-430 µS/cm, (see Duggleby in Figure 5.9). In addition, a lot of spikes of EC values higher than the base level were recorded in the stream. These spikes generally happened during winter time when the rainfall and flow rate is high (Duggleby in Figure 5.9). In the stream at Duggleby, the relation between EC-Q and EC-EP showed in general no correlation of the average daily EC with the Q and EP , see Figures (5.10 and 5.11), although EC spikes and troughs were more common at low flow.

Apart from short periods (EC troughs) the EC results for the stream at Little Driffield were broadly similar during the monitoring period from May 2013 to March 2015 (Figure 5.9). EC did not vary much, remaining in the range 375 – 475

[1] Little Driffield record showed some significant decreases in EC from August to November 2013, but these values do not represent the EC of the stream water because it was found that the device had been pulled out of the stream and left by the stream in a wet muddy area. There was also a sudden fall from 10 to 23 April 2014, suggesting that maybe the device had been temporarily removed and then replaced by an unknown person. The data for these periods when the device was likely removed have been deleted from the plot.

µS/cm, with an average 'baseline' of around 410 µS/cm. Three short term events of lower EC were recorded from 20-30 January 2014 EC at Little Driffield it dropped to around 150 µS/cm, with other drops in value to around 180 and 120 µS/cm occurring during 27-30 March 2014, and 6-8 April 2014 respectively, see Little Driffield in Figure 5.9.

The EC record from Lowthorpe (Figure 5.9) did not show any large EC spikes and troughs, and generally fluctuations were between around 400 and 450 µS/cm, with the average being 430 µS/cm. Similar to the stream at Duggleby, no correlation between the EC-Q and EC-EP relation was observed in the stream at Lowthorpe or Little Driffield, Figures (5.10 and 5.11), although for Little Driffield EC troughs occurred at low flow.

Interpretation of the stream water EC:

The EC of the streams was generally at about the same level during low and high flow rate. The Q-EC relation showed that the high EC spikes which were identified on EC-time series graphs appeared during the low flow stage of the stream. Similarly, the EC troughs appeared during the low flow stage of the stream. The relation between EC and effective rainfall (EP) showed that the EC spikes coincided with periods of little rainfall, while EC troughs appeared co-incident with both high and low rainfall.

The reason for the EC spikes and troughs will now be discussed, considering the EC time series graphs, EC-Q, and EC-EP relations. The EC spikes appeared in winter (when evaporation is very low) and during the very low flow stage of the stream. These spikes likely appeared due to contamination of the stream water by slurry wash off from the cowshed (observed to be full of cow manure) in Duggleby village, located 700m upstream of Duggleby bridge. EC troughs that appeared during low flow stages of the stream were likely due to intrusion of water with lower EC, which has greater effect at low flow stages. This means that those short-term decreases in

EC were probably due to dilution of the stream water by water of lower EC, e.g. rain water flowing into the stream via quickflow. This is supported by the fact that EC troughs also may coincide with periods of rainfall (Fig. 5.10). [Note: EC troughs cannot be considered as errors in the recording because according to the 15 minute interval time data records these trough events lasted for 5 to 8 hours, see expanded timescale plot, Figure (5.12).]

Comparison of EC at Duggleby with Little Driffield and Lowthorpe

In general, the records showed that the average 'baseline' EC (i.e. the average value excluding the short term peaks and troughs) in the stream water at the Duggleby site was higher than those at Little Driffield and Lowthorpe (575 µS/cm versus 410 – 430 µS/cm). This difference probably arises from either differences in the biological activity in the soil zone, or in the average thickness of the unsaturated zone within each catchment. Most notably, the unsaturated zone in the Kirby Grindalythe catchment feeding the Duggleby stream is likely to be much thinner than those feeding the other two sites, which are adjacent to, and similar to, the Driffield catchment (unsaturated zone estimated as 35m in Kirby Grindalythe and 100m in Driffield, see section 3.3.4 and 3.4.4). This in turn leads to greater calcite dissolution and higher EC in the Kirby Grindalythe catchment, because of the ease with which soil- or atmosphere-derived CO_2 can reach the saturated zone.

5.1. Summary:

EC was measured at the springs and in the stream at points 2 to 3 km downstream at Little Driffield, Lowthorpe, and Duggleby (bridges where CTD divers were installed for monitoring stream EC and T during this study). The measurements showed a slight difference in the water EC between the spring and CTD sites (-12 to +29 µS/cm, see Table 5-3). The springwater temperature measurements suggest that this variation probably does not arise due to the effect of the difference in springwater and air temperature. It probably arises because the water in the stream

at the CTD sites consists of aggregated water from several sources of varying EC, so the EC in these sites represents balancing of mixed water rather than water from a specific spring. However, water in the stream at the location of the CTD is broadly representative of the water from the springs upstream.

The EC measurements recorded by the CTD showed little variation in the EC in each stream, which indicates that the streams are dominated by Chalk-derived groundwater with not much quick flow component. Exceptions to this pattern were seen in EC troughs at low flows that are suspected to have been caused by dilution of the chalk-derived groundwater by quickflow at Little Driffield and Duggleby, while in the case of the Duggleby stream (which is by far the smallest), the EC spikes were probably caused by wash-off of contaminated water from farms, for example cow manure from a cowshed upstream.

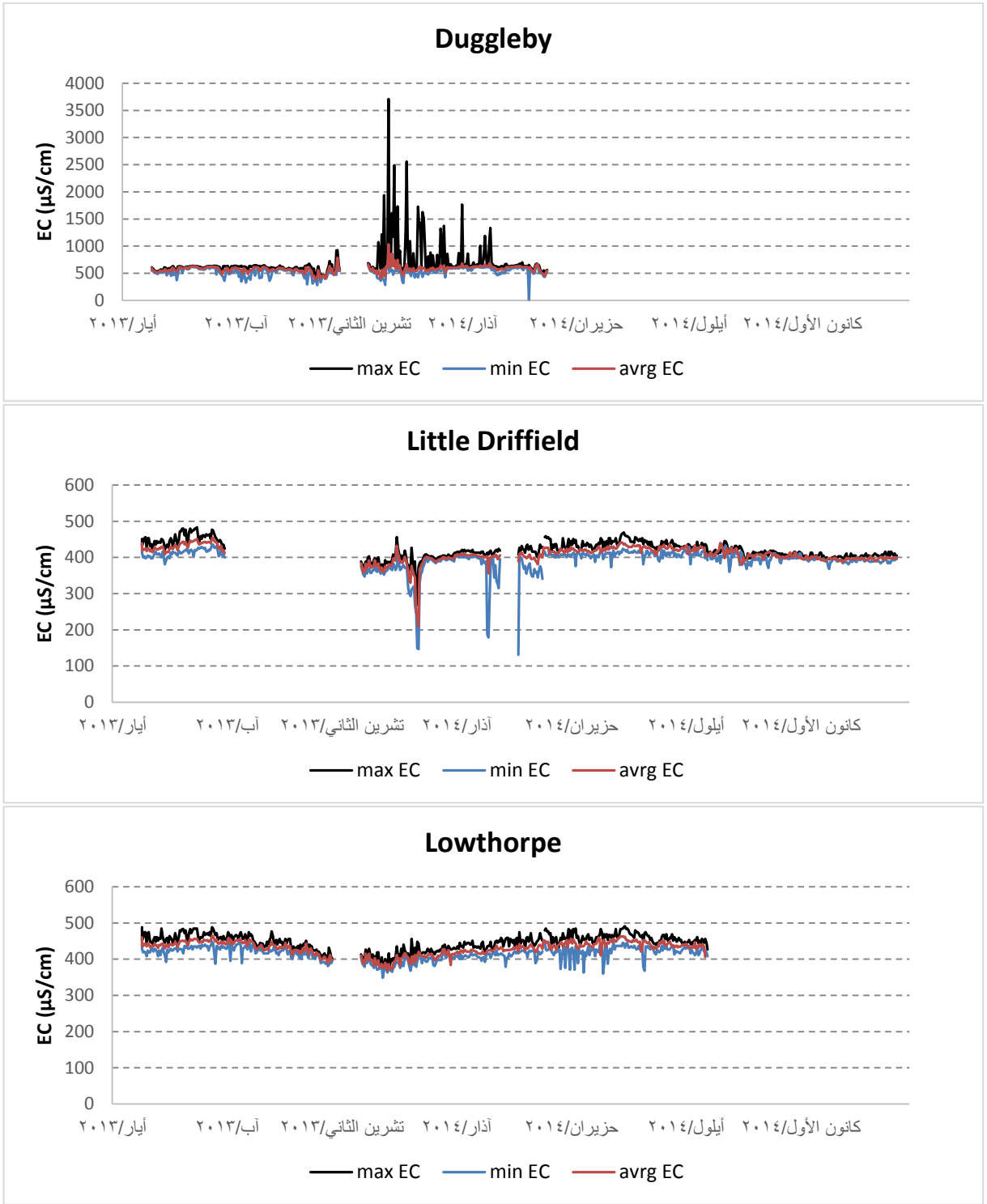

Figure 5-9Time series Electrical Conductivity in the stream under the Duggleby bridge, Lowthorpe bridge and Little Driffield bridge (EC in daily min, max and average).

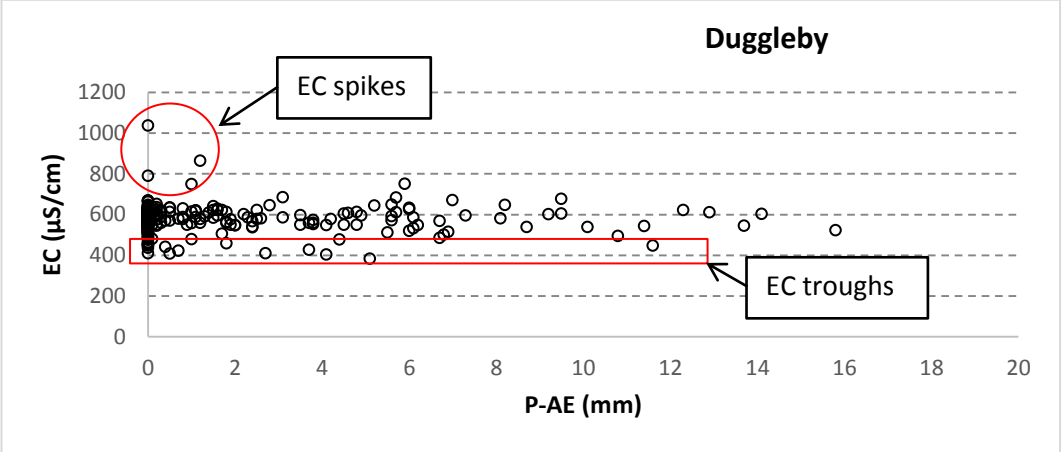

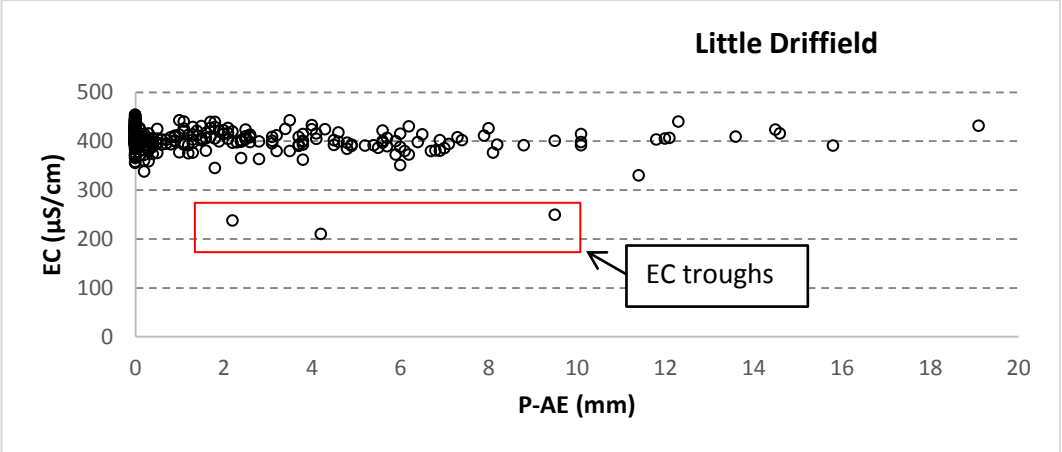

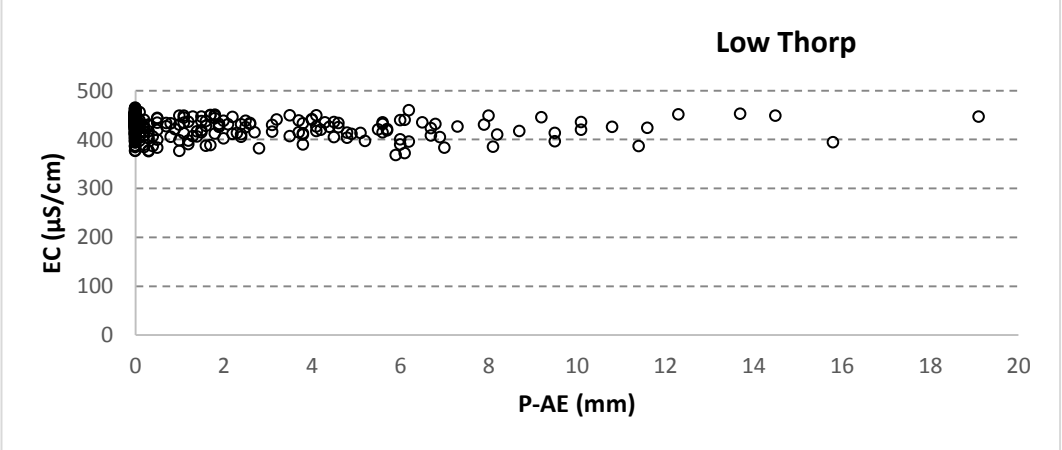

Figure 5-10 show the relation between the EC in the monitored streams and effective rainfall.

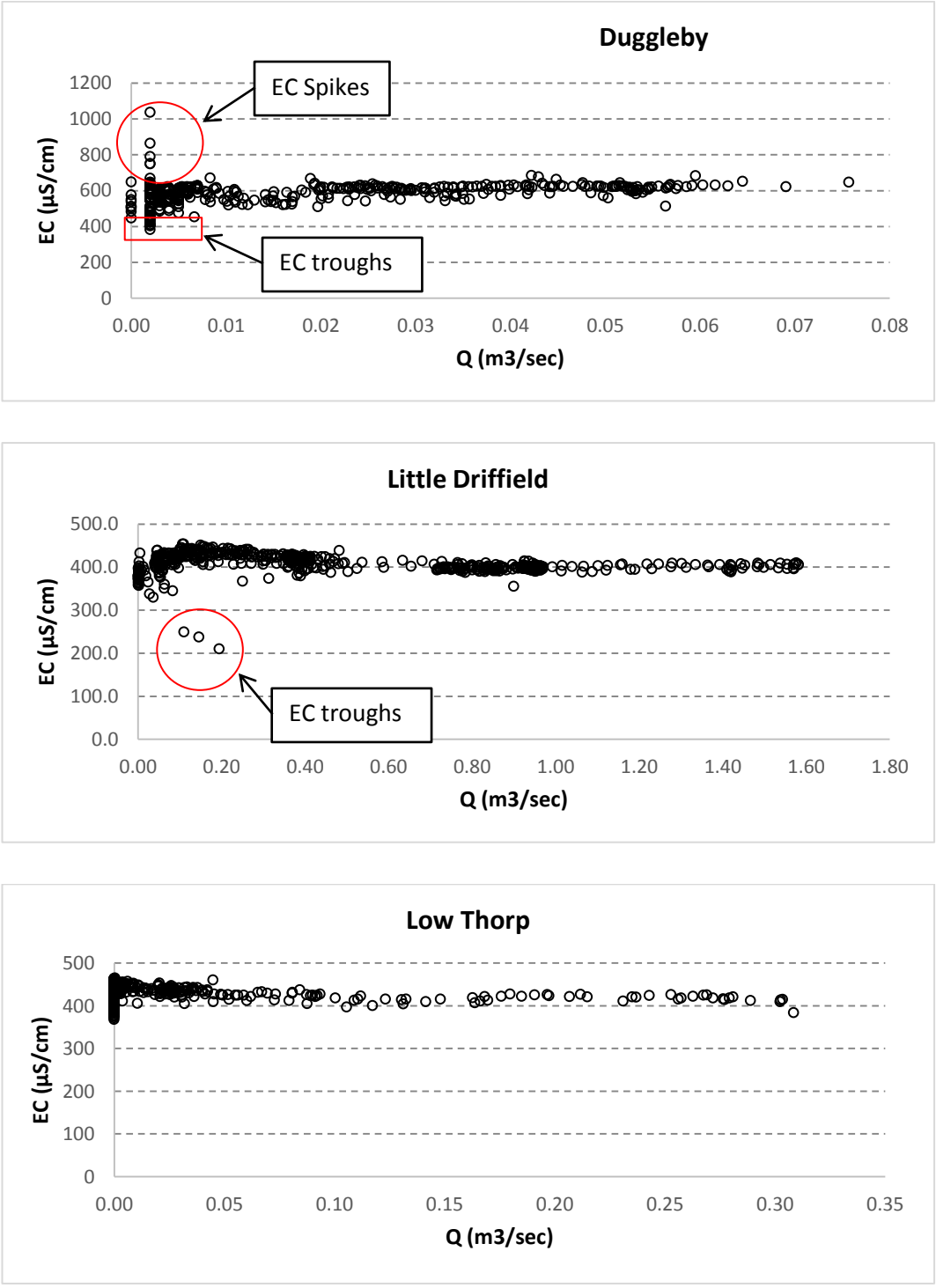

Figure 5-11Relation between the stream water EC and flow rate of the stream (note that for Low Thorpe and Little Driffield the Q values are from the adjacent gauged Driffield catchment).

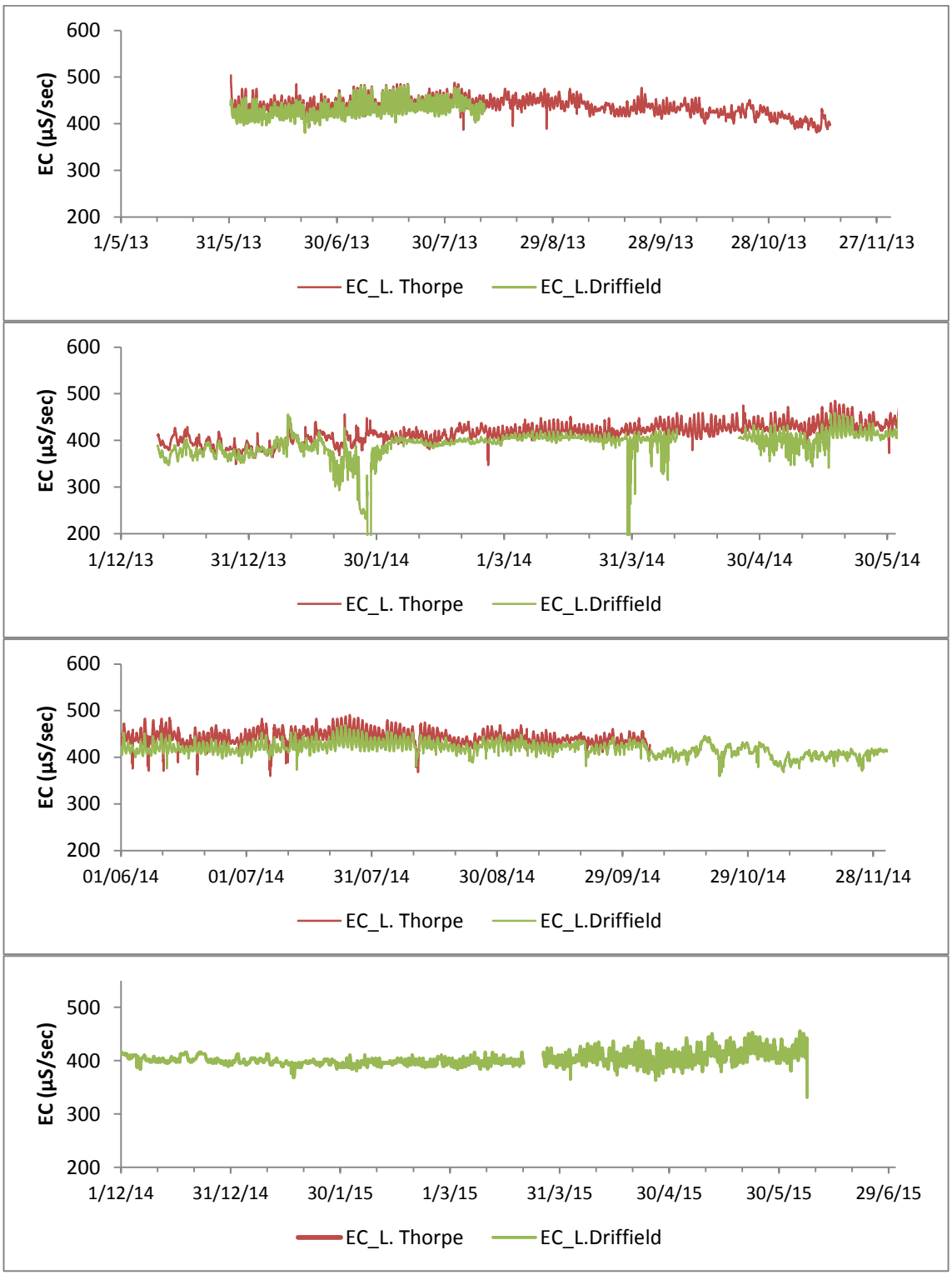

Figure 5-12Electrical Conductivity at the Lowthorpe and Little Driffield stream sites (data at 15 minutes sampling interval).

The EC records showed that the baseline EC (suspected to represent the signature of chalk-derived groundwaters) in the stream waters at Kirby Grindalythe catchment (Duggleby site) was higher than at Kilham (Lowthorpe site) and Little Driffield catchments (575 μS/cm versus 410 – 430 μS/cm). This difference was possibly either due to differences in biological activity in the soil zone, or to difference in the average thickness of unsaturated zone within each catchment, which would mean that the Kilham and Little Driffield groundwater is effectively more confined and less accessible to soil- and atmosphere- derived CO_2.

The temperature measurements of both the emergent spring water and stream water at the monitoring sites suggest strong influence of atmospheric air temperature, i.e. these particular springs do not tap deep groundwater, but water that is already in equilibrium with air. This makes it difficult to use the temperature of stream water as a tracer for investigating groundwater. The records from the data logger in the boreholes show that the groundwater temperature is nearly constant at between 9 and 10^{o}C, with the average seasonal variation not exceeding one degree.

Annual groundwater fluctuations from Northend Stream and Low Mowthorpe boreholes were small, whereas the variation between the Tancred Pit and Low Caythorpe boreholes was bigger. The reason derives from the location of the boreholes relative to the location of the springs and streams, i.e. Low Mowthorpe and Northend Stream boreholes are located close to the streams, while Tancred Pit and Low Caythorpe are located at a greater distance from the streams. Consequently, those at a greater distance provide a useful guide for setting boundaries and initial conditions for the groundwater simulation reported in chapter 8.

Finally, the water table level in the boreholes indicates that the regional groundwater flow direction is from NW toward the SE in East Yorkshire.

Chapter 6. Analytical interpretation of spring recession curve results for the Yorkshire Wolds

This chapter reviews the spring hydrogeology and methods used for measuring the flow rate in open channels. Literature on approaches used in hydrograph recession curve analysis is also reviewed. Sources of error in the flow rate data and the analytical and statistical methods used for evaluating data and estimating uncertainty are discussed.

This chapter also examines the reliability of the discharge data, and determines the margin of error in the flow rate. The recession curve of each water year is estimated and the master recession curve (MRC) constructed. Then, based on the most popular analytical models, the MRC is analysed and interpreted.

6.1. General background about spring-flow measurement and analysis of flow-recession curves:

6.1.1. Discharge

In hydrology, discharge is the volume of water passing through a cross-section area of the channel in a certain amount of time. Discharge information is required for a variety of hydrogeologic, hydrologic, environmental and engineering studies (Vogel and Kroll, 1992; Asawa,1999; Wittenberg and Sivapalan, 1999; Rahman and Goonetilleke, 2001; Robert H., et al 2001; Dewandel et al., 2003; Covington et al., 2012; Humphries et al., 2012; Gan and Luo, 2013; Chang, Wu and Liu, 2015; Fu, Chen and Wang, 2016).

Several approaches are used for measuring flow discharge in open channels, the most commonly used methods being: Volumetrical method (Richard and Gary,

2007), Area-velocity method (Chanson, 2004; Das, 2008), Area slope method, and Dilution method (Rantz et al., 1982; Kilpatrick and Ernest, 1985; Dutillet, 1993; Moore, 2004).

More detail about these methods and hydraulic gauging can be found in appendix (2)

6.1.2. Rating Curve

At the weir, because the discharge of water that passes the structure is a function of the stage of the water flow over the weir crest, the relation between stage and discharge can be constructed. This relation is constructed by taking long-term measurements of flow and stage simultaneously at different flow rate phases (from very high to very low during the water year of the stream). The relation between stage (h) and discharge (Q) could be represented by different means, for instance, graphic, table, or equation (Braca, 2008). Graphical and equation representation are the more popular methods for illustrating the stage-discharge relation. The stage-discharge relation is known as the rating curve and the equation by the term rating equation.

Stage is defined as the height of a water surface above an established datum. Stage is recorded by measuring the height of the water surface inside channels or water measurement structures above a selected datum level (Dodge, 2001).The stage measurement technique has been used since the late 1800s and it is preferred because it is quite easy to measure water stage continuously using this method compared to direct measurement of water discharge (Birgand, 2012).

Constructing a rating curve has many advantages in the hydrological analysis process. For example, it makes it possible to identify the relation between stage and discharge (Salkind, 2010), allows prediction of the trend of relation below and above the measurements, and permits direct conversion between stage and discharge. Many studies have confirmed that using the stage discharge method is a practical and cheap method for deriving water discharge that allows continuous and easy measurement

of fluctuation of water discharge inside open channels (ASCE, 1996; Clark, 1999; Braca, 2008; Dottori et al., 2009; Birgand, 2012).

The rating curve is a model curve that is often fitted with a linear regression equation (SEFE, 1996). Usually, the stage-discharge data scatter about the fitted line; this scatter most probably arises from the uncertainty that accompanies the measurements. To overcome this problem, a curve of best fit is used to represent the rating curve, see figure (6.1).

The rating curve is analytically represented by an equation called the rating equation (6.1).

$$Q = C(h - h_0)^b \qquad \text{Equation 6-1}$$

C = constant which is numerically equal to the discharge when the $(h-h_0) = 1.0$

h = water stage

h_0 = water stage of zero flow, or the water stage height of effective zero flow for a channel control or a section control of irregular shape b = slope of the straight segment of the rating curve (rating curve may consist of one segment or more than one segment depending on the type of weir) .

Plotting Stage vs. Discharge on arithmetic coordinate paper helps in identification of the point of zero flow and recognising abrupt changes in both stream profile and changes in channel control (e.g. if control section is submerged). In addition, plotting stage vs. discharge on log-log paper enables calculation of rating parameters, for instance from slope variations in the control section and for extrapolating the rating curve (Gordon et al., 2004).

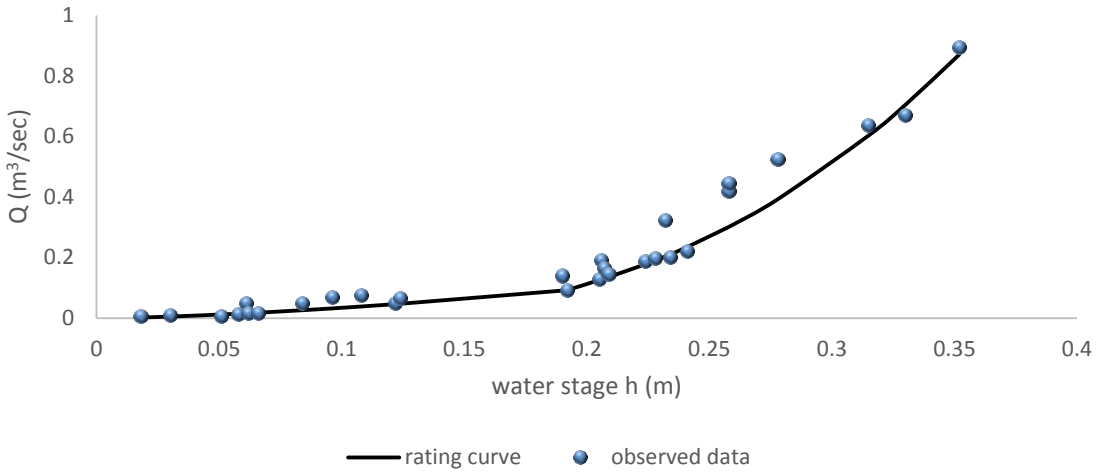

Figure 6-1 Example rating curve for a stream gauging station.

Stage of zero flow (h_o):

The stage of zero flow (h_0) is a value which makes the stage-discharge relationship (from the rating equation) on logarithmic paper appear as a straight line, also called the factor of datum correction. It is not considered as a stage at which the channel is dry, rather that required for an effective zero flow. Normally, the value of this stage does not coincide with the zero of the gauge except in cases where this level is set to the lowest level of an artificial control or the crest of a hydraulic gauging structure. h_0 may be positive or negative in value, and the factors which cause the value of h_0 to be positive or negative are illustrated by Gordon, et al. (2004) and Herschy (2009).

Stage of zero flow can be measured directly in the field and also can be identified from the rating curve. In the field, zero flow is determined by measuring water at the deepest place on the control structure, e.g. the weir, and subtracting this depth from the gauge height at the time of measurement (Herschy,1985; Birgand, 2012). Practically, the point of zero flow is best identified at the time of low water flow.

Determining the stage point of zero flow is also possible graphically from the rating curve; however, this method involves several steps (Braca, 2008; MBCHS, 2009).

Extrapolating the slope of the lower end of the rating curve to intersect the stage axis of the stage-discharge relation will determine the point of zero flow (Holmes et al., 2001). Shifting in the low-flow stage of the rating curve is the consequence of change in the gauge height of effective zero flow (WMO, 2008). During this study, four measurements of stage and discharge were taken during the recession period, to represent the lower end of the stage-discharge rating curve. The reason for taking stage-discharge measurements during the spring recession stage specifically is because this study is based on the flow during this recession period. Further, the data from the lower end of the stage-discharge rating curve is used for estimating the stage of zero flow. Also, the main aim was to predict rising uncertainty in the rating curve, which can be estimated from evaluating the stage of zero flow rather than having to validate the entire rating curve. If the observed stage-discharge measurements are above or below the slope of the lower end of the stage-discharge of the original rating curve (EA rating curve) it would imply that a change has happened to the original stage-discharge relation and create uncertainty in relation to the data. The low end of the relation was tested as this is most likely to be affected by, e.g., silting behind a constructed weir (Fenton and Keller 2001).

6.1.3. Uncertainty and Source of error in the rating curve:

The purpose of error or uncertainty analysis is to determine the precision of the data which will be used in the study. The flow data that are utilised in this study do not derive from direct flow measurements, but from stream stage according to the rating curve. Therefore, any uncertainty in the rating curve will propagate to the discharge data. Uncertainty over the discharge data arises from the components of the rating curve, which are stage and discharge of the stream.

In the analysis of the data the observed measurements are not distributed at a constant distance around the model curve and thus the residual values will not be the

same at all stages (Peterson-Overleir, 2004; Di Baldassarre et al.,2012). In some cases, the lower stage may contain high uncertainty (at lower water levels, the roughness of the channel surface makes it difficult to measure water level correctly) and in another state higher stages may contain high uncertainty (water surface more turbulent with higher flow).

Clarke (1999) and Clarke et al. (2000) concluded that uncertainty in the rating curve arises due to two main groups of errors. The first group arises due to uncertainty in rating curve construction, such as inaccuracy in the estimation of rating parameters, and due to unexpected random errors due to exceptional variation owing to the device. Also, uncertainty in the rating curve will increase considerably with rising uncertainty over the estimated value of h_0 (Clarke, 1999; Clarke et al., 2000). These types of error usually appear in the form of scattering around the rating curve. The second group (systematic error) refers to changes that may happen in the channel geomorphology due to erosion or deposition during the data collection period (Fenton and Keller, 2001)(this latter group was tested within this study by additional measurement).

An analytical method for Calculating error:

Several statistical analysis and mathematical approaches have been used for the purpose of computing error in observed data (Dymond and Christian,1982). However, systematic errors cannot be eliminated by statistical analysis, as such methods can describe only random errors. Therefore the data will continue to contain some errors (Jarraud, 2008). A recommendation by the International Standards Organization (ISO) for dealing with analysis uncertainties was that the random and systematic error should no longer be treated separately in the process of uncertainty analysis because there are no characteristic differences between the uncertainty components arising from random and systematic effects. This assumes that the standard deviation of the scatter of points around the fitted curve will take into account all elements of uncertainties (Herschy, 2002).

The least square regression method is the most popular and acceptable statistical approach for fitting stage-discharge data.

The amount of such error is reduced as the goodness of fit (which is measured by the coefficient of determination R^2 between observed data and fitting curve) increases. Clarke (1999) has estimated that when R^2 is higher than 0.95 on the rating curves it is possible to extrapolate discharges with a high degree of precision.

Dymond & Christian (1982) produced a detailed literature review of uncertainty in rating curve estimation, which highlighted several statistical methods used for estimating error and margin of error of the rating curve. The standard error of the residual (equation 6.2) is the most widely used method for calculating the error in the rating curve (Herschy 1994; Clarke,1999; Peterson-Overleir, 2004).

$$\mathbf{S_e} = \sqrt{\frac{\sum(\mathbf{y_i}-\hat{\mathbf{y}})^2}{\mathbf{n}-\mathbf{2}}} \qquad \text{Equation 6-2}$$

Where:

y_i *and* x_i *variables ,* $\hat{y}$ *estimated value of* y_i, *is standard deviation of residual ,*

Although each stage has its error value for presenting error in a dataset, commonly a single value has been preferred to represent the estimated error in the original data. Clarke et al. (2000) claimed that when calculating error interval in the dataset, it is possible to assume that residuals about the fitted relation have a normal distribution with a constant value.

6.1.4. Spring hydrograph:

Spring hydrographs are graphical representations of the time series flow rate, which usually consist of a single or successive peaks. Each peak principally consists of three main segments, namely, rising limb, peak and falling limb, Figure (6.2). Each of these three segments represents a special stage of recharging, infiltration and discharge respectively. The falling limb also comprises two main segments, the first

of which is usually steeper and comes directly after the peak, and is referred to as the flood event or recession in the presence of recharge. The second segment is less steep and represents the base flow or recession curve with minimal or absence of recharge.

Hydrograph recession curve and recession coefficient:

In this study, the term "recession curve" will be used for the second segment of the falling limb, which represents the depletion of the groundwater from storage in the absence of (or with minimal) recharge (Toebes and Strang, 1964).

In analytical studies, the recession curve is described by a factor called the recession coefficient (α). Based on the mathematical models, the recession coefficient has been used for estimating the physical characteristics of the aquifer (Bagaric´,1978; Civita, 2008; Dewandel et al., 2003; Farlin and Maloszewski, 2013; Kovács et al., 2005; Kovacs and Perrochet, 2008; Kresic, 2006). (Kowalski 1984, 1987from Buczyński and Rzonca, 2011) ,(Rorabaugh,1964 and Berkaloff,1967 in Geyer, T et al., 2008), These studies show that the recession coefficient is directly related to the transmissivity and inversely related to the storage property of the aquifer. Also, Raeisi (2008) has used α for computing storage in the karst aquifer.

In this study, of primary interest is the long timescale (i.e. monthly) recession curve that follows annual winter recharge. Thus, as described later, a master recession curve (MRC) will be produced for each catchment to remove the influence of short timescale individual quick flow events.

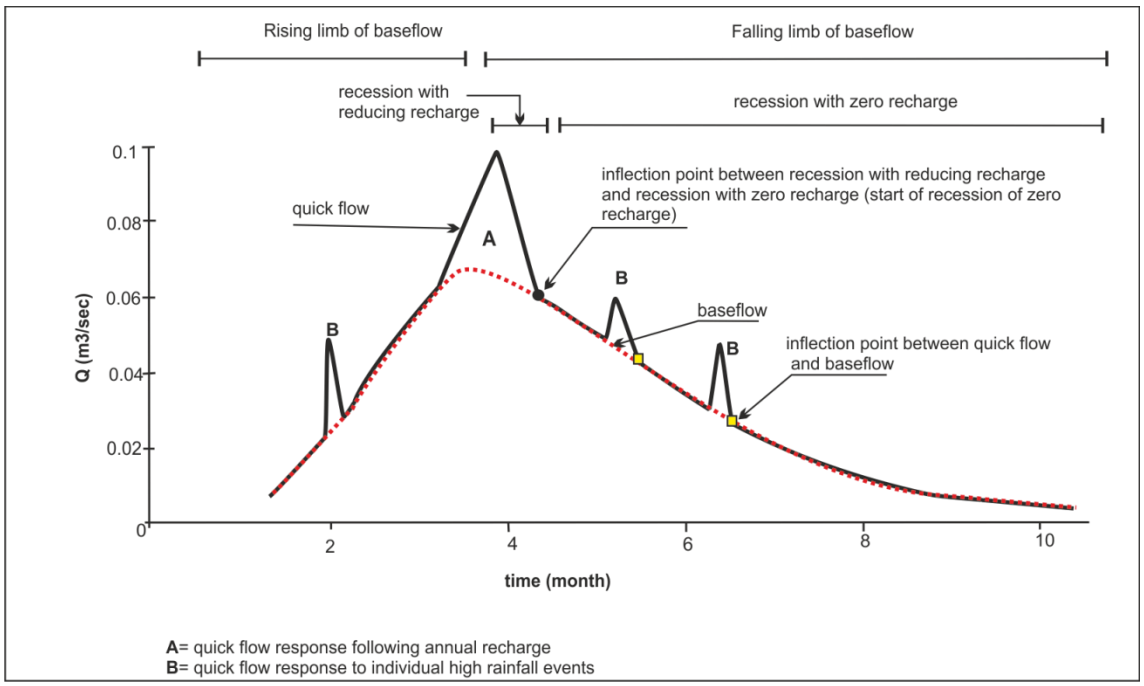

Figure 6-2 Schematic diagram showing the hydrograph components.

6.1.5. Factors that influence recession curves:

The shape and the degree of steepness of the recession curve of the spring hydrograph differ significantly from one spring to another; even recession curves for the same spring are not the same for successive hydrologic years.

The shape and pattern of a spring hydrograph are functions of many factors including hydraulic properties of the aquifer, lithology, geometry of the aquifer, rainfall intensity, shape and size of catchment area, moisture content and evapotranspiration (Karanjac and Altug, 1980; Tallaksen, 1995; Amit et al., 2002; Delleur, 2007; Kova´cs and Perrochet 2008; Fiorillo , 2009; Fiorillo and Guadagno, 2010). According to Covington et al. (2009), the shape of a spring hydrograph is a reflection of both aquifer geometry and the recharge process. Even if the two have the same degree of permeability, a larger aquifer will show smoother recession

curves than a small aquifer, owing to travel through the larger aquifer requiring a longer time.

It has been reported from the comparison between the spring hydrograph recession curve of different springs of a fractured aquifer that the recession curve's steepness and shape are mainly governed by the intensity and geometry of the fracture system (Kovács et al., 2005). Amit et al. (2002) found variation in the recession coefficient for the same spring between different water years to be slight, although there was a significant change in the discharge rate between water years. This conclusion implies that the value of the recession coefficients is affected by hydraulic properties of an aquifer, whereas the variation of the discharge depends on precipitation rate. This indicates that the main factors influencing the recession curve are lithological and geometrical characteristics of the aquifer. Laboratory experiments by Liu and Li (2012) modelling spring hydrographs revealed variation in the slope of recession curve for the same hydraulic environment under different rainfall intensity and that this variation is reflected in the quick flow segment (quick flow refers to increase in flow due to a single individual short timescale rainfall event) of the recession hydrograph. Delleur (2007) found that the same aquifer under higher rainfall intensity showed steeper quick flow recession curves.

The hydraulic properties of both matrix (and small fracture) and larger fracture systems influence the pattern of recession curve (Kovacs, 2003). Lee et al. (2006) illustrated this effect by explaining that in the well-developed fracture system water flows faster, while in the poorly developed fracture system the water needs more time to drain. As a result, in a slow draining aquifer successive rainfall events become integrated into one big storm peak on the hydrograph because the responses to these successive events become superimposed and appear as one integrated flat peak. Whereas, with a well-developed and well integrated fracture flow system, individual events are transmitted rapidly to the spring (producing a "flashy" hydrograph response). The degree of moisture content and rate of evapotranspiration also has a strong effect on the relation between rainfall event and the response of the

spring discharge (Barfield et al., 2004). As a consequence, information on the ET and moisture content increases the accuracy of the recession curve interpretation.

Delleur (2007) grouped spring hydrographs into three types based on their response to a storm pulse. The first group is fast response aquifers, a type in which each event is represented by a single hydrograph peak, because the storm pulse passes quickly and the curve decays completely and returns to base level. The second group comprises slow responding aquifers; with this type the recession curve takes far longer to return to its base flow level because of the slow response and the long time taken for a light storm to produce a shallowing in gradient that does not show up clearly on the hydrograph. With this type, a sequence of recharge events is mostly recorded as superimposed peaks and the response appears as one pulse. The final group is located between group one and two, and in this case, while there is some structure to the hydrograph, it is not possible to resolve each single pulse. In general, the spring hydrograph is created through superimposing of single hydrographs corresponding to separate rainfall or recharge events (Kresic and Stevanovic, 2009).

Consequently, because the spring drains water from vast areas of the aquifer, the discharge is governed by an accumulative effect that integrates the flow systems that exist in the aquifer. Therefore, study of the spring recession curve is preferred over other geological and geophysical methods (Dreiss,1982; Bakalowicz, 2005). In contrast, other geological and geophysical methods can only represent the aquifer locally at the investigation points.

6.1.6. Master Recession Curve (MRC) for Kirby Grindalythe and Driffield catchments:

Although the recession curves of different hydraulic years for the same aquifer may be different and include spikes, they generally follow the same trend.

Variation of recession curves for the same aquifer may result from several factors:

- Since recession periods do not start at the same time every year, vegetation and evapotranspiration (which influence the recharge) will affect the recession curves.
- Intensity and duration of precipitation vary across water years, which will influence the groundwater level in the aquifer.
- Size and shape of the catchment may change depending on the groundwater level in the aquifer. The shape of aquifers is not simple or geometric, so groundwater level and volume of water in the aquifer are not linearly related. A rise in groundwater of a few meters may cause an increase in the size of the catchment; based on this perspective the difference in the maximum head in the aquifer between water years will affect the recession curve.

As the recession curve for a single year may be interrupted by short recharge events, the recession curves for successive water years may be slightly different. Hence, the recession curve needs to be re-arranged to produce a single curve called a master recession curve (MRC). Several approaches have been invented for constructing a master recession curve, e.g. matching strip, correlation and tabulation method (Brownlee, 1960; Toebes, 1969; Brutsaert and Nieber,1977; Toebes and Strang, 1964; Sugiyama, 1996; Raghunath, 2006).

According to the strip method, the recession curve divides into segments depending on the recharge events. Then the segments superimpose and adjust horizontally until

the main parts overlap. The MRC will be the average line that passes through the overlapping segments (Toebes and Strang, 1964), see figure (6.3).

In the tabulation method, recession data gathered at regular intervals of time will be tabulated in columns, with each recession in a separate column. The columns are then adjusted vertically until the discharge values agree horizontally (Figure 6.4, 6.5). Finally, the average of the agreed discharge values between the columns is calculated, and the average values will represent the MRC.

6.1.7. Analytical Models for interpretation of recession curve:

Analytical models are used for calibrating the observed data empirically based on analytical solutions (Fiorillo, 2014). Fundamentally, analytical models describe recession curves according to the discharges–storage relationship in the simple aquifer (equation 6.3). (Horton, 1935, 1937; Langbein, 1938; Brustsaert and Nieber, 1977; Troch et al., 1993; Wittenberg, 1999; Wittenberg and Sivapalan, 1999) considered that the water discharge from the aquifer is a function of the aquifer storage volume:

$S = aQ^b$ Equation 6-3

Where: S is the storage (m^3), Q is the discharge (m^3/sec), the factor a has the dimension of $m^{3-3b}s^b$ and b is the nonlinearity factor (dimensionless).

The relation is linear when b=1 and nonlinear when b≠1

Since the last century, extensive investigations have been conducted to analyse and predict the recession behaviour of spring hydrographs. Boussinesq (1904) and Maillet (1905) are considered pioneers among the researchers who proposed mathematical solutions for interpreting spring recession (Bailly et al., 2010).

The Maillet model or Maillet exponential model is the most popular model and assumes that the aquifer consists of a single reservoir that behaves linearly (Kovac, 2003, 3005). According to this model, discharge can be estimated by equation (6.4):

$$\boldsymbol{Q_t = Q_o e^{-\alpha t}}$$ Equation 6-4

Where Q_t is the discharge [L^3T^{-1}] at time t, and Q_0 is the initial discharge [L^3T^{-1}] at an earlier time, $\boldsymbol{\alpha}$ is the recession coefficient [T^{-1}] usually expressed in $days^{-1}$.

If the Maillet model is followed the recession curve will appear as a straight line with slope α on a semi-logarithmic graph (Atkinson 1977; Dewandel et al., 2003; Kovacs, 2003).

More detailed information and description about other analytical models can be found in appendix (2).

6.2. Evaluating the discharge data from the Kirby Grindalythe and Driffield gauging stations and estimating error boundaries:

Discharge data used in the current work consist of the mean daily flow rate in m3/day for the period from 1998 to 2015, using data from Kirby Grindalythe and Driffield gauging stations. These data are provided by the Environment Agency (EA) in the form of Microsoft Excel sheets.

First, the raw data are collected by the gauging stations in the form of stage measurements. Later the EA converts the stage data to flow rate data according to the rating curves built for each station separately. In the appendix (2.3) the EA stage-discharge data for Kirby Grindalythe and Driffield station are expressed. Any uncertainties in the rating curve components (stage-discharge) are propagated to the

derived discharge data. Therefore, in this study in order to assess the accuracy of the discharge data, the EA-rating curves have been subjected to error estimation analysis. The processes of evaluating the flow rate data and error estimation were achieved through accomplishment of the following actions.

- Checking the accuracy of the EA rating curve and estimating the error in the rating curve.
- Finding the amount of uncertainty and margin of error in the EA rating curve.

6.2.1. Checking the precision of the EA rating curve and estimating the error in the rating curve:

The process of checking the accuracy of the rating curve was conducted in different stages:

- Testing the shift in the stage of the zero flow (h_0) through measuring the stage-discharge at the low stage of the stream and then finding the goodness of fit between these measurements and rating curve at low stage.
- Checking whether the rating curve represents the curve best fitted to the stage-discharge (H-Q) data.

Stage-discharge measurement:

During this study flow rate and stage of the stream were measured. The main reason was to evaluate the stage-discharge data on the low stage rating curve, which were provided by the EA.

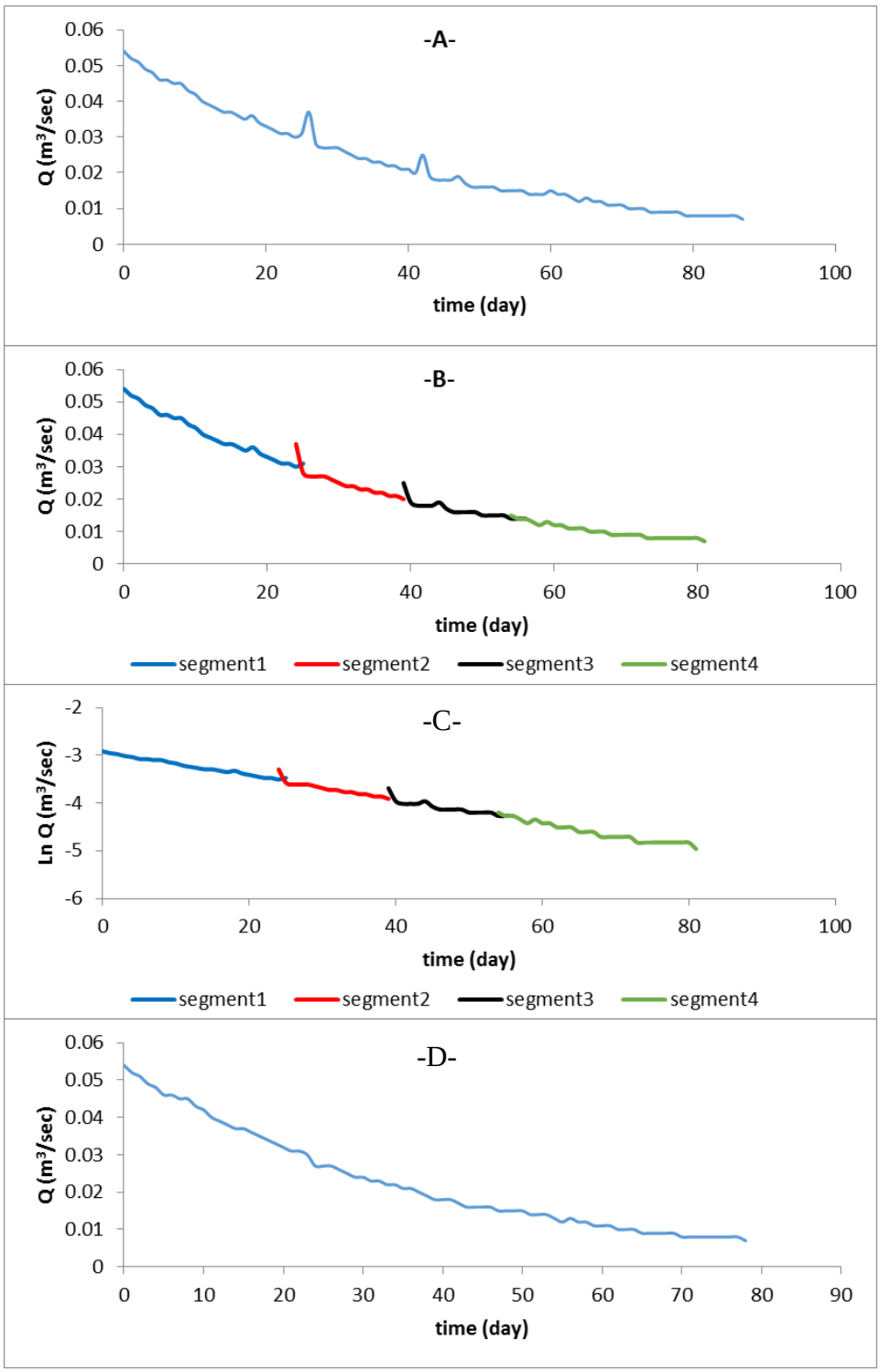

Figure 6-3.Matching strip method for construction MRC. The recession curve is from Kirby Grindalythe 2000.

time	Q (m3/sec)						mean Q
	Q2000	Q2001	Q2002	Q2003	Q2004	Q 2014	MRC
0	0.103			0.103	0.103		0.103
1	0.102	0.102		0.102	0.102		0.102
2	0.101	0.101		0.101	0.100		0.101
3	0.099	0.099		0.100	0.099		0.099
4	0.097	0.096		0.099	0.098		0.098
5	0.096	0.096		0.097	0.098		0.097
6	0.094	0.095		0.095	0.095		0.095
7	0.093	0.087	0.088	0.093	0.092	0.094	0.091
8	0.090	0.083	0.077	0.091	0.089	0.091	0.087
9	0.087	0.080	0.075	0.087	0.085	0.089	0.084
10	0.083	0.078	0.072	0.085	0.082	0.087	0.081
11	0.079	0.074	0.070	0.081	0.078	0.084	0.078
12	0.076	0.071	0.065	0.078	0.077	0.081	0.075
13	0.072	0.069	0.062	0.075	0.074	0.073	0.071
14	0.069	0.067	0.059	0.072	0.076	0.070	0.069
15	0.066	0.066	0.056	0.070	0.071	0.067	0.066
16	0.067	0.062	0.055	0.069	0.067	0.065	0.064
17	0.061	0.060	0.052	0.065	0.064	0.062	0.061
18	0.058	0.058	0.050	0.062	0.063	0.059	0.058
19	0.055	0.056	0.048	0.060	0.065	0.056	0.057
20	0.055	0.054	0.048	0.058	0.062	0.055	0.055
21	0.051	0.051	0.045	0.056	0.057	0.052	0.052
22	0.047	0.050	0.043	0.054	0.054	0.049	0.050
23	0.045	0.047	0.042	0.052	0.053	0.048	0.048
24	0.043	0.046	0.039	0.049	0.051	0.048	0.046
25	0.040	0.044	0.038	0.048	0.048	0.045	0.044

Figure 6-4. Diagram illustrating the tabulation method for calculation of MRC using, recession curve from Driffield.

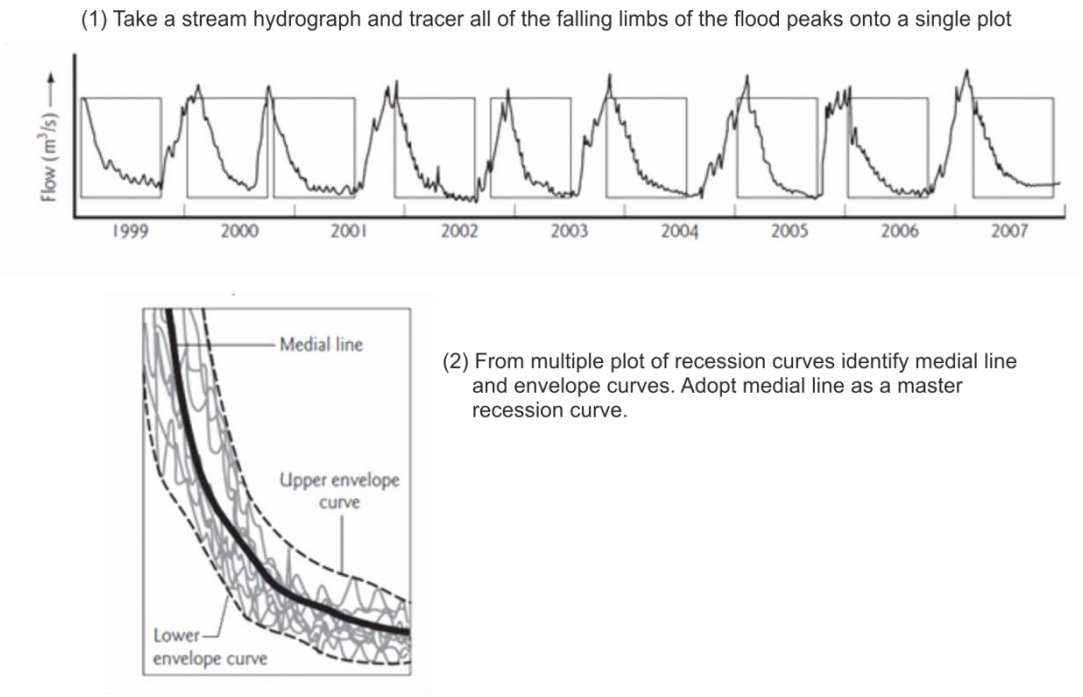

Figure 6-5 Derivation of a Master Recession Curve (MRC) from declining limbs of hydrographs (by Pettyjohn 1985a,b From Younger, 2009).

Fieldwork schedule for stage-flow measurement:

- Selecting a good location for taking measurements along the river, which means a location that has an appropriate cross section. This will allow the depth and area of the channel to be measured easily and accurately, and consequently the water stage measurements and calculations of the average discharge will be more precise. Selecting an appropriate method for measuring discharge.
- Measurements to be taken during the low stage of the recession period of the springs' hydrologic year in 2014 (from March to May 2014).

Flow measurement locations:

The gauging stations at Kirby Grindalythe and Driffield were selected as locations for measuring the stage and water velocity. The reason for choosing the gauging stations were: (a) the stage and flow measurements could be used to assess the accuracy of the rating curve of these stations, (b) a gauging station is a hydrological structure which has a geometrical shape, which gives an opportunity for calculating the cross section area of the stream more precisely compared to any other location along the stream channel.

Discharge measurement method:

The velocity-area (Mid-Section) method was used for measuring flow rate. This approach was selected because the locations chosen for taking measurements are geometrical in shape, which makes it easier to measure the internal dimensions. Additionally, this is one of the most widely used and acceptable methods for stream discharge measurement (Shrestha and Simanovic, 2010; Turnipseed and Saure, 2010), and recommended by the USGS as an active method for measuring discharge of most streams and rivers (Hauer and Lamberti, 2011).

Equipment used for measuring flow:

The main tools used for taking measurement by mid-section method are:

- Current meter - for measuring water velocity in (m/sec).
- Tape measure - for splitting the channel into equal vertical cells
- Top setting rod - for measuring the depth of the water.

A current meter, the "Digital Water Velocity Meter", was used for measuring the velocity of the water. Figure (6.6) shows the Digital Water Velocity Meter, or Global Water Flow Probe. The Global Water Flow Probe is an accurate water velocity instrument for measuring flows in open channels and partially filled pipes. The Flow Probe is ideal for storm water runoff studies, sewer flow measurements, measuring

flows in rivers and streams, and monitoring water velocity in ditches and canals. The water velocity probe consists of a protected water turboprop positive displacement sensor coupled with an expandable probe handle ending in a digital readout display. The water flow meter incorporates true velocity averaging to provide the most accurate flow measurements.

General characteristics of this device**:**

- Its low weight, of about 0.9 kg, makes it easy to use.
- The accuracy of this device is about 0.03 m/sec.
- The measurement range of this device is between 0.1 and 6 m/sec.
- It has capability to save measurements from up to 30 readings.

Figure 6-6 Digital Water Velocity Meter.

Results of the stage-discharge measurement

The work schedule was to take stage and flow measurements every 30 days during the stream recession period (March to September). However, only four measurements were taken at each gauging station, and the readings were taken from

March to June. The reason relates to the water stage in the stream. During this period of the year, the water level in the stream becomes so low that the height of the water is less than the total diameter of the Turbo-Prop sensor of the flow-meter. Tables (6.1 and 6.2) show the results of the stage and flow measurements taken during the spring recession discharge in the water year 2014.

Table 6-1 shows the stage-discharge measurement at Kirby Grindalythe station.

Date of measurement	width (m)	velocity m/sec	the depth of water h (m)	Q m3/sec	Total Q (m3/sec)	Average h (m)
21/03/2014	0.15	0.7	0.095	0.009975	0.05229	0.099
	0.15	0.71	0.105	0.011183		
	0.15	0.71	0.105	0.011183		
	0.15	0.7	0.10	0.0105		
	0.15	0.7	0.09	0.00945		
04/05/2014	0.15	0.55	0.0525	0.004331	0.023408	0.0538
	0.15	0.6	0.0525	0.004725		
	0.15	0.6	0.055	0.00495		
	0.15	0.6	0.0545	0.004905		
	0.15	0.55	0.0545	0.004496		
22/05/2014	0.15	0.5	0.045	0.003375	0.0162	0.045
	0.15	0.45	0.045	0.003038		
	0.15	0.45	0.045	0.003038		
	0.15	0.5	0.045	0.003375		
	0.15	0.5	0.045	0.003375		
29/06/2014	0.15	0.4	0.03	0.0018	0.00945	0.03
	0.15	0.4	0.03	0.0018		
	0.15	0.4	0.03	0.0018		
	0.15	0.4	0.03	0.0018		
	0.15	0.5	0.03	0.00225		

Table 6-2 shows the stage-discharge measurement at Driffield station.

Date of measurement	width (m)	velocity m/sec	the depth of water (m)	Q m3/sec	Total Q (m3/sec)	Average h (m)
21/03/2014	0.2	1.55	0.22	0.0682	0.209	0.22
	0.2	1.6	0.22	0.0704		
	0.2	1.6	0.22	0.0704		
04/05/2014	0.2	0.5	0.085	0.0085	0.02805	0.085
	0.2	0.6	0.085	0.0102		
	0.2	0.55	0.085	0.00935		
22/05/2014	0.2	0.5	0.08	0.008	0.024	0.08
	0.2	0.5	0.08	0.008		
	0.2	0.5	0.08	0.008		
29/06/2014	0.2	0.45	0.03	0.0027	0.00828	0.0307
	0.2	0.45	0.032	0.00288		
	0.2	0.45	0.03	0.0027		

Checking the shifting in the ho:

Given the availability of stage-discharge data for the low stage of the stream flow, the stage of zero flow can be determined from the rating curve (Braca, 2008). This entails plotting stage-discharge data on the log-log paper (as the rating curve appears as a straight line) and then extending the stage-discharge line to intersect the stage axis, with the location of the intersection on the stage axis representing the stage of the zero-flow. As it was explained in the earlier section (stage of zero flow), uncertainty in the rating curve can be checked through examining the change in the location of the stage of zero flow on the rating curve. To examine the shifting in the $h_{0,}$ the stage-discharge data at the low stage of the stream needed to be checked. For this purpose, the stage and discharge at the gauging stations at Kirby Grindalythe and Driffield were measured during the recession period when the stage was low, tables (6.1 and 6.2).

The measured flow-stage data together with the EA flow-stage rating data were plotted on the same graph Figure (6.7). As it appears in the figure, there is a good overlap between EA rating curve and measured stage-discharge data. In order to examine the degree of matching between these data, the Log values of the measured stage-discharge and EA stage-discharge data were plotted on the same graph because log values of the rating data usually appear as a straight line, making it easier to check overlap of these data visually and analytically, see figure (6.8). As it appears from the figures, there is good agreement between the rating data. This confirms that the EA rating curve, which was used for deriving discharge, had not undergone a systematic change between initial calibration and these test measurements (at low discharge).Furthermore, to determine the goodness of fit between the measured stage-discharge and EA rating curve, the r-squared between these two sets of data was calculated. From the EA equation representing the rating curve for each measured value of the stage, the value of discharge was calculated. Then, from the same equation for each measured value of the discharge, the stage value was calculated. Next, the measured and calculated discharge values were plotted against each other (see figure 6.9), and similarly the measured and calculated stage values were plotted against each other (see figure 6.9). Eventually, the r-squared for the plotted values was calculated. The value of the r-squared for all the plotted values was 0.99. This value indicates a good fit between the measured stage-discharge and the EA rating curve. This leads to the conclusion that the $\mathbf{h_0}$ of the rating curve had not been subject to change between initial calibration and the tests undertaken (of low discharge) as part of this study.

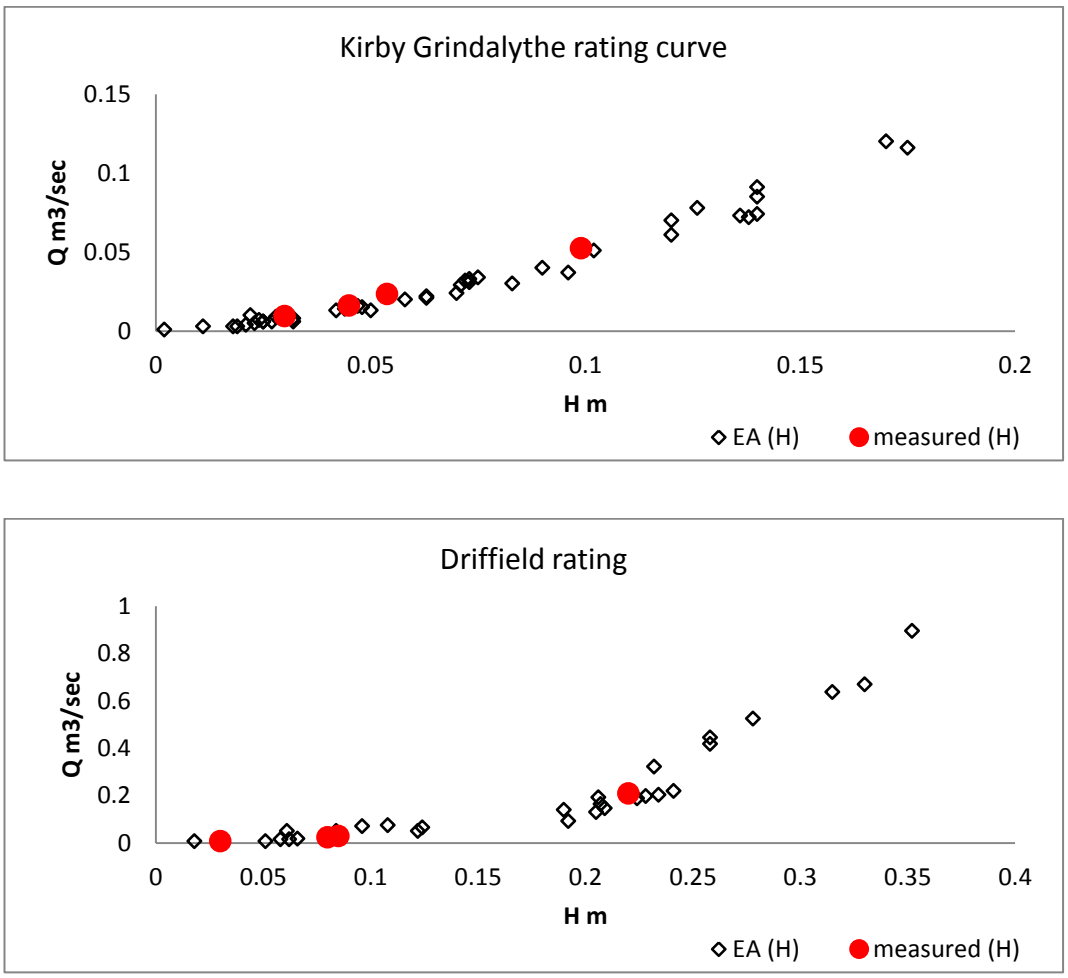

Figure 6-7 checking the accuracy of rating curves. Black dots are the EA stage-discharge data, red points are the stage-discharge measured in this study.

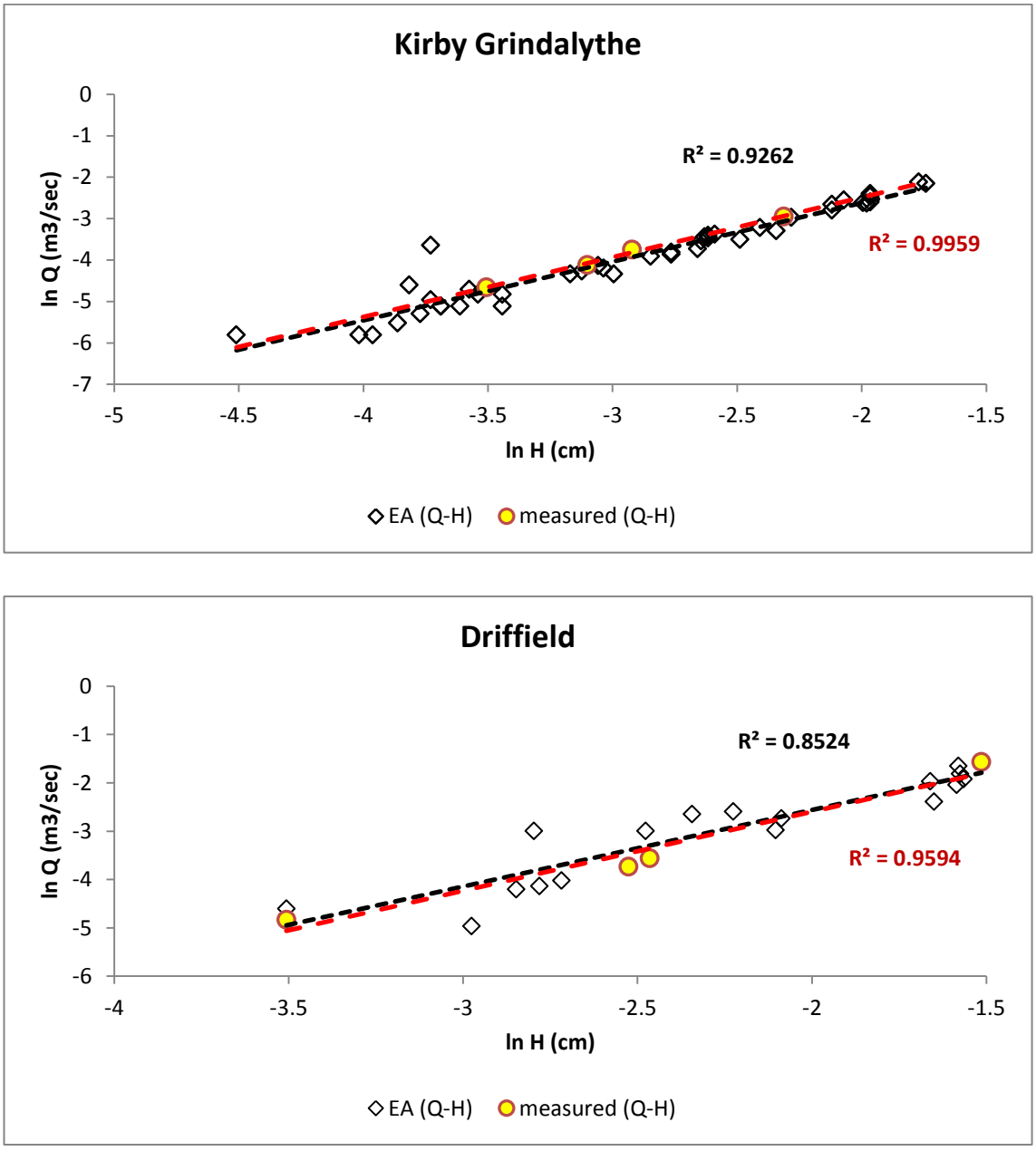

Figure 6-8 plotting log value of EA rating curve together with the log value of the measured stage and discharge data (which measured during this study).

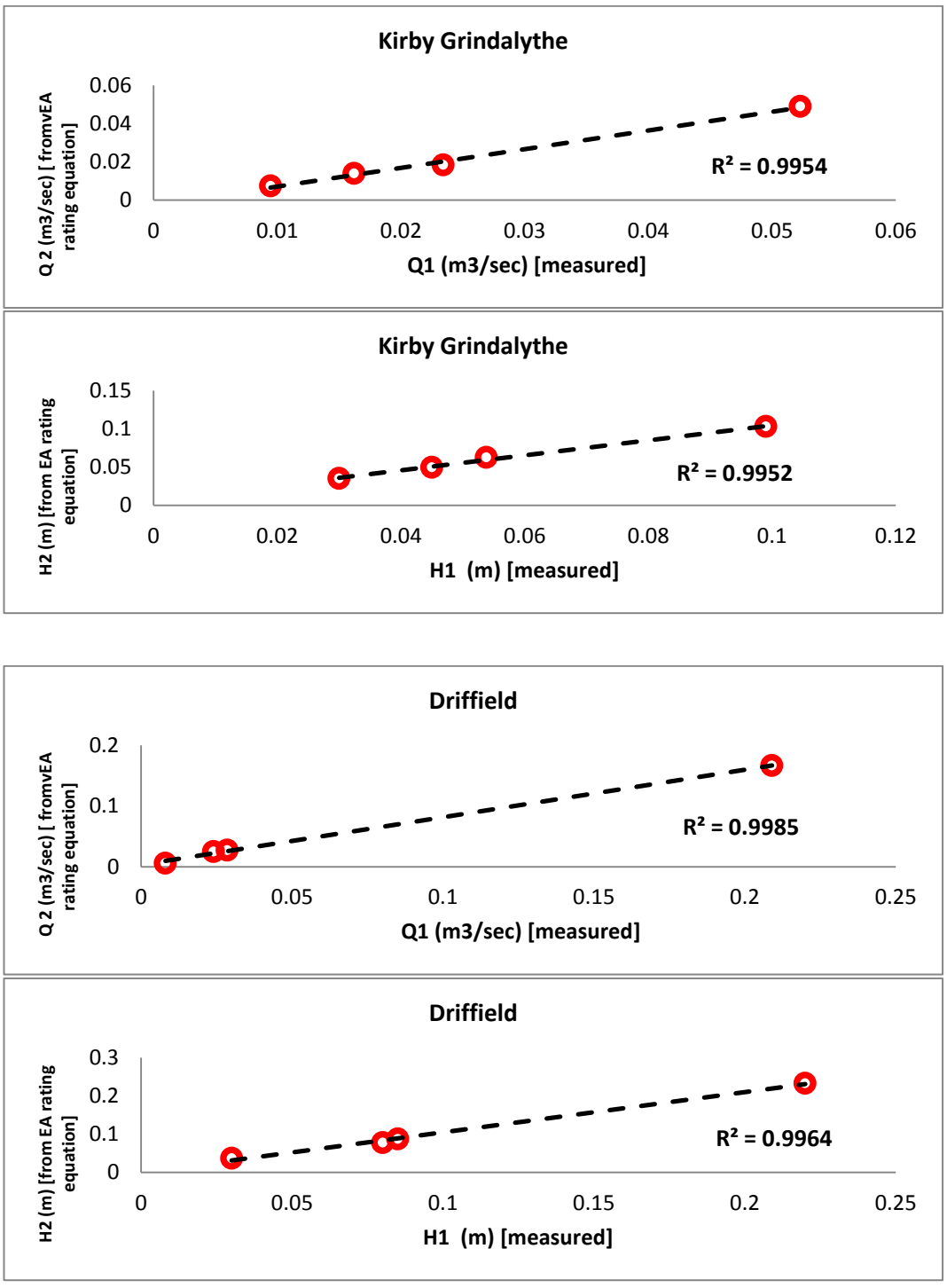

Figure 6-9 Show the result of testing the goodness of fit between the measured stage-discharge and the EA rating curve from r-squared . Q1and H1 represents the discharge and stage that measured by this study. Q2 and H2 represent the discharge and stage value from EA rating curve.

Checking if the EA rating curve represents the best fitting curve to the stage-discharge (H-Q) data from the stations:

The rating curve represents the best fitting curve to the stage-discharge data. From the EA stage-discharge data the rating curve for the stations was reconstructed. Then the reconstructed rating curve was compared with the EA rating curve to find if the EA rating curve was capable of representing the stage-discharge data properly.

The rating curve was reconstructed by plotting the stage-discharge data on a log-log graph and then finding the best fitting curve to the plotted points by using the least square regression method.

Principally, the relation between water stage and discharge in open channels is represented by the power law relation equation (6.5).

$$\boldsymbol{Q = c(h - h_o)^b}$$ Equation 6-5

C = constant which is numerically equal to the discharge when the $(h-h_0) = 1.0$

h = water stage

h_0 = water stage of zero flow, or the water stage height of effective zero flow for a channel control or a section control of irregular shape b = slope of the straight segment of the rating curve (the rating curve may consist of one or more than one segment depending on the type of weir) .

The R-squared (r^2) between the EA rating curve and reconstructed rating curve was calculated. If the original rating curve does not show a good match with the new rating curve this means that the original rating curve is not a good representative for the gauging station. In this case the derived discharge data would need to be calibrated. However, if the two rating curves show good agreement it indicates that the discharge data derived from the original rating curve are reliable. ***For Kirby***

Grindalythe, the rating curve was drawn based on equation (6.6) which is provided by the EA. This rating curve will be called the Environment Agency rating curve. Then the rating curve was re-constructed for the station using the new data as well as the original data.

$$\boldsymbol{Q = 2.162 * (h - 0.002)^{1.6514}} \qquad \text{Equation 6-6}$$

The plot of both the calculated rating curve and EA rating curve on the same graph showed good agreement between the two, particularly in the lower stage. This indicates that the stage of the zero flow did not change. The R-squared for the EA rating curve for all the data was 0.97, which confirms the validity of the EA rating curve, see Figure (6.10).

For Driffield: using rating equations (6.7 and 6.8), provided by EA, the rating curve for Driffield gauging station was drawn. The Driffield rating curve consists of two segments (each segment represents a different phase of the weir because the Driffield station consists of a compound weir). In this study this rating curve will be called the EA rating curve for Driffield.

Then the rating curve was re-constructed for the station using the new data as well as the original data.

$$Q = 1.126 * (h + 0.001))^{1.1516} \qquad when\ stage < 0.19\ m \qquad \text{Equation 6-7}$$

$$Q = 23.24 * (h - 0.074)^{2.566} \qquad when\ stage\ 0.19 \text{ to } 0.4\ m \qquad \text{Equation 6-8}$$

Plotting the EA and calculated rating curve on the same graph visually revealed good agreement between the two, Figure (6.11). The R-squared between Q values from each curve was 0.98, which shows that the curves are quite similar. Based on this result the original rating curve was used.

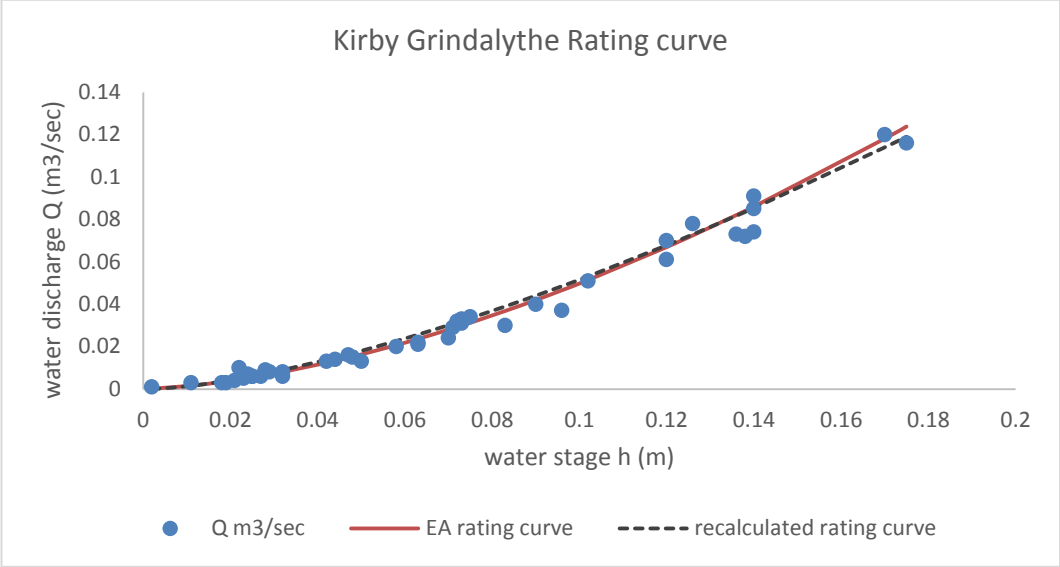

Figure 6-10 show the rating curve for the Kirby Grindaltyhe gauging station, the orange color line is the rating curve prepared by environment agency and the black dash line is the rating curve calculated by this study.

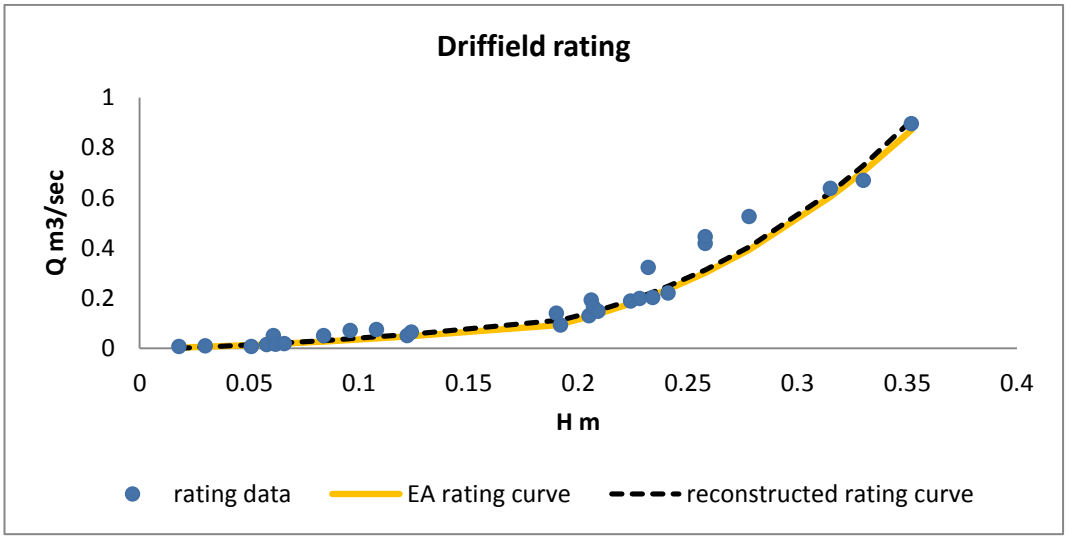

Figure 6-11 illustrate rating curve of the Driffield gauging station, the orange dash curve is the rating curve prepared by environment agency and the black dash line is rating curve calculated by this study.

6.3. Calculating uncertainty (margin of error) in the rating curve:

For estimating error in the discharge data of the Kirby Grindalythe and Driffield stations, error in the rating curve was calculated depending on the method “standard error of estimate".

From the stage-discharge data and model rating curve the standard deviation of residual S_e was computed using the following equation:

$$\mathbf{S_e} = \sqrt{\frac{\sum(\mathbf{y_i}-\hat{\mathbf{y}})^{\mathbf{2}}}{\mathbf{n-2}}} \qquad \text{Equation 6-9}$$

Where y_i represent measured discharge (m^3/sec), $\hat{y}$ is estimated discharge from OLS

The estimated error in the discharge from the Kirby Grindalythe rating curve was 0.005 (m3/sec). Δq was added to and subtracted from the discharge values by using equation (6.10). The discharge after adding and subtracting Δq was plotted to show the margin of error in the discharge of the Kirby Grindalythe station, Figure (6.12).

$$Q_{est} = q_{est} \pm 0.0055 \qquad \text{Equation 6-10}$$

q is the discharge of the stations.

Similarly, the value of the error was estimated for the Driffield station from the rating curve. The predicted value of error in the Driffield rating curve was 0.05 (m3/sec). Figure (6.13) shows the error bounds for the Driffield rating curve.

$$Q_{est} = q_{est} \pm 0.016 \quad \text{if } h < 0.19\,m \qquad \text{Equation 6-11}$$

$$Q_{est} = q_{est} \pm 0.033 \quad \text{if } h < 0.4\,m \qquad \text{Equation 6-12}$$

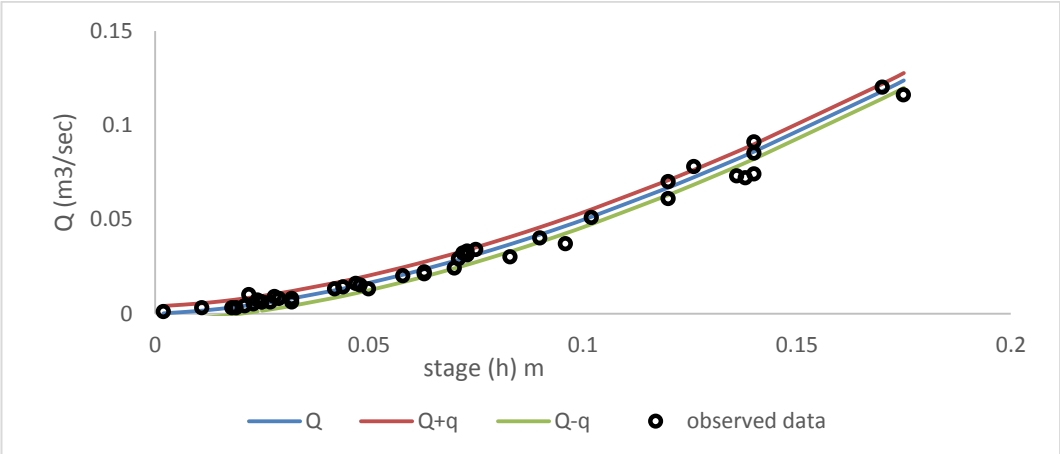

Figure 6-12 Shows margin of error in the Kirby Gridndalythe rating curve base on the standard error of estimate formula.

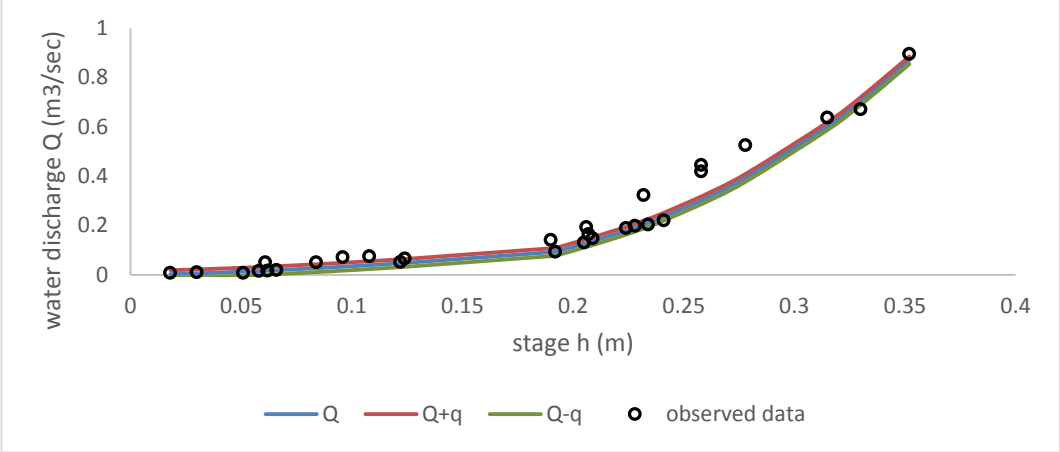

Figure 6-13 Shows margin of error in the Driffield rating curve base on the standard error of estimate formula.

From the margin of error, it was observed that the flow rates at the very end of the recession period are the least reliable. This probably resulted from the uncertainty in the stage measurements. Because of the roughness of the channel base when the water level in the channel reduces, the water flow in the channel becomes more turbulent and consequently uncertainty in the stage measurements increases. The margin of error in some recession curves of the Kirby Grindalythe and Driffield catchments is shown in Figure (6.14).

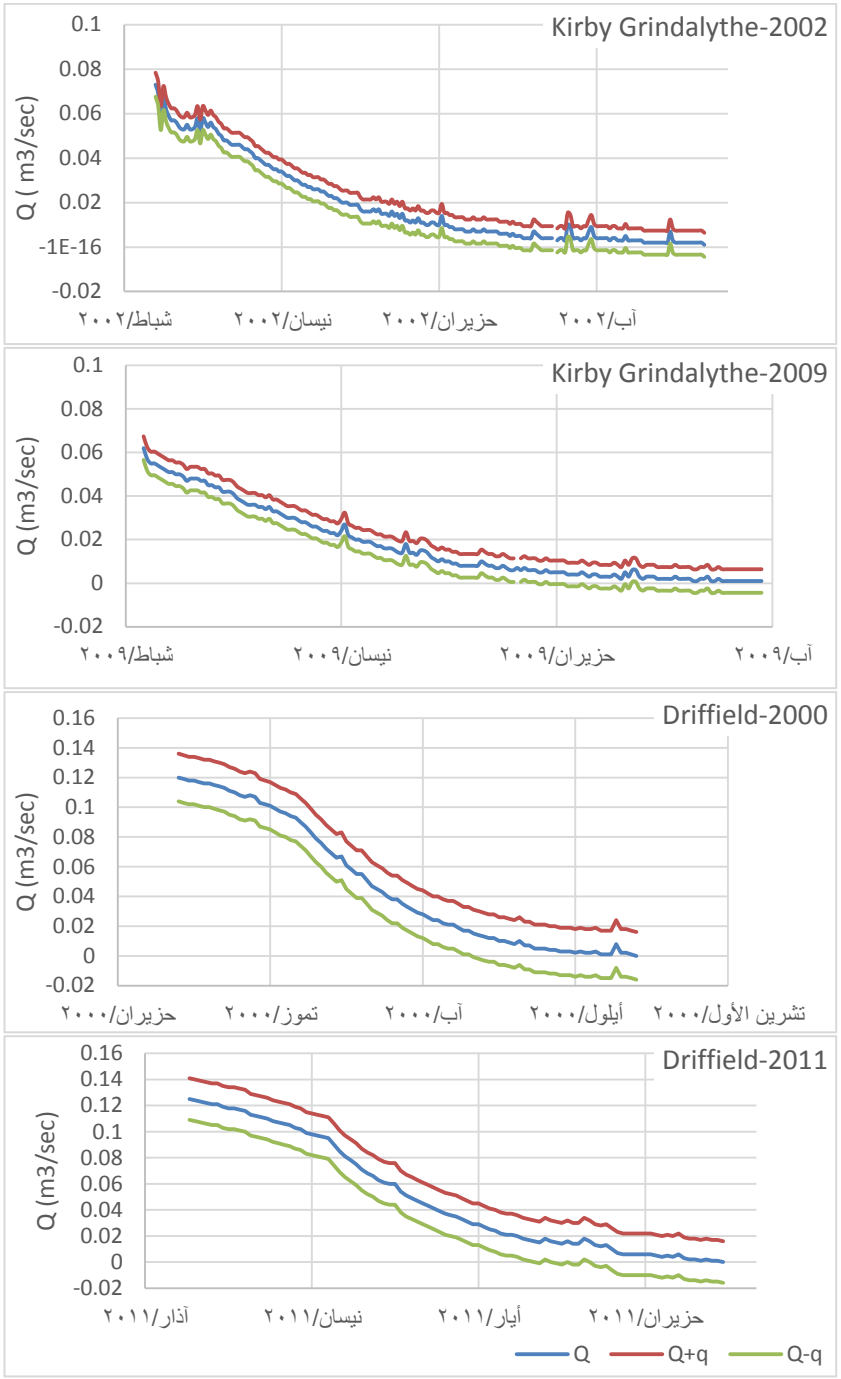

Figure 6-14 show the margin of error in two recession curves (as an example) from Kirby Grindalythe and Driffield station.

6.4. Analysis of the recession curves

6.4.1. Determination of the start of the recession period

Hydrograph recession curves represent the segment of hydrograph which comes after the peak flow. However, recharge and discharge data show that the time when the recharge stops does not match the peak flow. Nevertheless, after the peak flow the recharge reduces until a critical point when the evapotranspiration exceeds the rainfall, after which the rainfall does not recharge groundwater significantly. This study is aiming to interpret the recession curve in the period of absence of recharge when the behaviour of the flow rate is more dominantly under the influence of the aquifer system rather than external factors. The beginning of the recession period (corresponding to absence of recharge) was estimated using rainfall and actual evapotranspiration data. Daily rainfall was subtracted from the actual daily evapotranspiration (AE-rainfall), with a positive result characterising the periods where the actual evapotranspiration exceeds rainfall. When the value of AE is smaller than rainfall this means that part of the rain water has the chance to percolate deeper into the ground if the soil water content is at the field capacity (i.e. there is no soil moisture deficit (SMD)). If the rainfall is greater than AE but the soil's water content is below the field capacity the rainfall will be retained in the soil rather than percolating into the ground. The result of AE-P was plotted simultaneously with the discharge data and SMD on a time series graph, see Figure (6.15). From the figure, it can be noticed that the values of AE-rainfall during the recession period of stream discharge become positive a short time after the peak flow. Also, it can be noticed that the time when AE-P becomes positive is coincident with the time when SMD becomes positive. Therefore, the point at which the AE started to become positive was chosen as the start of recession period without recharge or effective recharge (because there may be a short event of increasing discharge due to bypass flow of rainfall water to the spring). The SMD was derived from the Metoffice data for grid square 94.

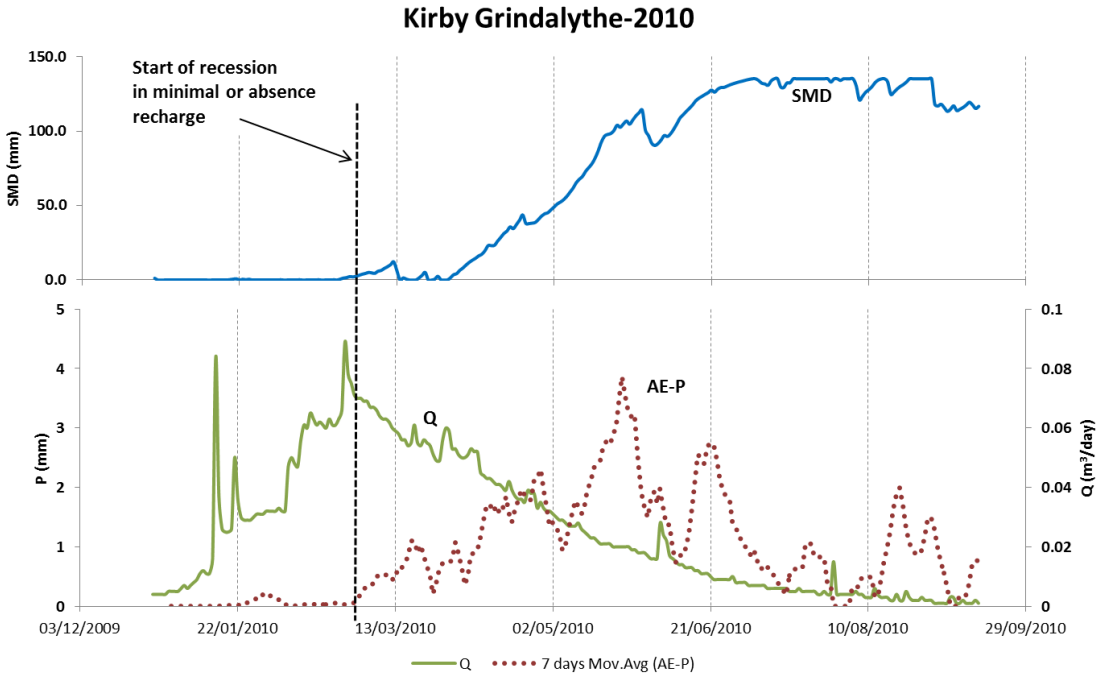

Figure 6-15 shows estimating start of recession curve in the absence of the recharge. The value (AE-P) simultaneously with discharge (Q) and Soil Moisture Deficit (SMD) plotted on same time series graph.

6.4.2. Master Recession Curve (MRC) for Kirby Grindalythe and Driffield catchments:

Since the recession curve for the same spring may vary between different water years, using data for several water years will better represent the aquifer recession curve than using data for a single year. The current study used recession curves for successive water years instead of using the recession curve for a single year. Figure (6.16) shows recession curves of successive water years from Kirby Grindalythe and Driffield catchments.

Two steps were used for constructing the MRC: matching strip and tabulation method. During the recession period, sometimes short-term recharges may happen, mainly due to transitory rainfall events. These short recharge events will appear in the shape of a short spike. Consequently, these recharge events distort the recession curve and prevent its continuous development into a complete curve. It is necessary to remove these short recharge events from the recession curve to better represent the groundwater diminishing from the aquifer in the absence of or minimal recharge. To overcome the problem of short event recharge during the recession period a master recession curve (MRC) for each water year was constructed using the strip method.

As the recession curves of successive water years are different the recession curve for a single water year cannot represent the complete recession period of the aquifer system. In some years recession starts with higher flow rate and extends for a longer time (e.g. Driffield 2007), while in another year it starts with lower discharge and continues for a shorter period (e. g Driffield 2002). To overcome this problem of variation between recession curves from different years master recession curves (MRC) were developed according to the tabulation method (Toebes and Strang, 1964). This method was selected as the most appropriate technique for constructing an MRC for a range of years.

Figure 6.17 shows the construction of a master recession curve for Kirby Grindalythe and Driffield.

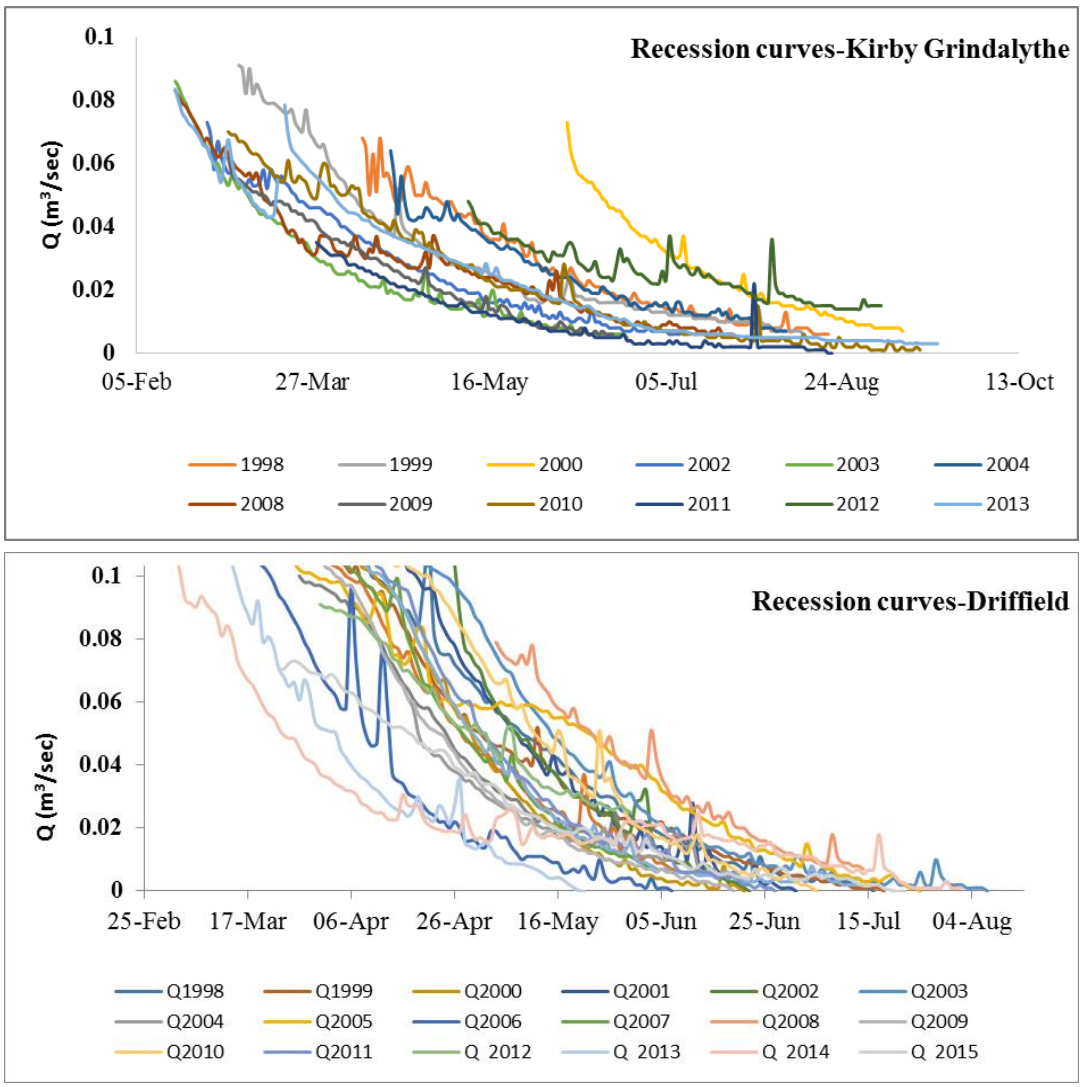

Figure 6-16. Hydrograph recession curves from Kirby Grindalythe and Driffield gauging station for selected years 1998 to 2014.

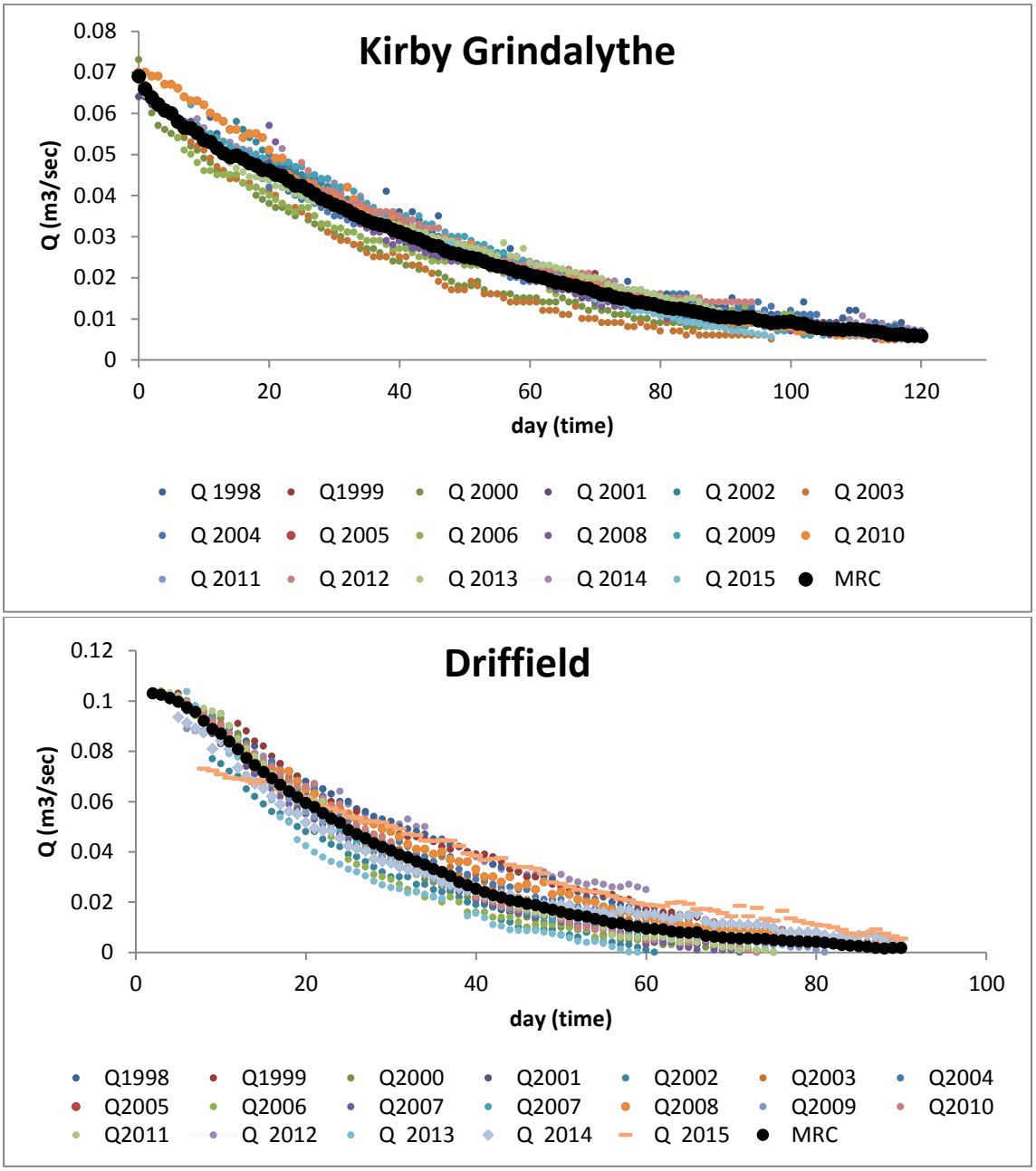

Figure 6-17 Master recession curve of Kirby Grindalythe and Driffield. The process achieved in two steps; first, the Matching strip method used for construction MRC for each single water year to remove the effect of short timescale individual rainfall events. Then the tabulation method used to construct MRC for recession curves from successive water years.

6.4.3. Analysis of the MRC of the Kirby Grindalythe and Driffield catchments:

Three approaches were applied for interpretation of the MRC of Kirby Grindalythe and Driffield catchments: Maillet exponential (or multi-exponential models if the curve consists of more than one segment), Boussinesq quadratic and Horton double exponential.

Discussion:

For testing the MRC based on the Maillet method the flow rates of Kirby Grindalythe and Driffield were converted to logarithms and then plotted on the time series graph. The MRC for Kirby Grindalythe appears as a single straight line, see Figure (6.18), while recession data for Driffield do not appear as a single straight line, see Figure (6.19). An inflection point was detected on the Driffield MRC, dividing the curve into two segments, with each segment fitted by a straight line.

Since the MRC of Kirby Grindalythe appeared as a straight line, according to the linear method it was interpreted as consisting of a single reservoir. Despite appearing as a straight line it was also tested with non-linear methods to identify whether it could be fitted by a non-linear model and to determine which of the models was able to fit the curve better. The analysis results for the Kirby Grindalythe MRC are presented in Figure (6.20) and table (6.3). It appears that the model curves from both the linear and non-linear model were a good fit with the MRC. It can be noticed that the Maillet and Boussinesq models fitted the entire curve completely, but the Horton model did not fit the very early stage of the recession curve, only starting to match the MRC completely after 8 days.

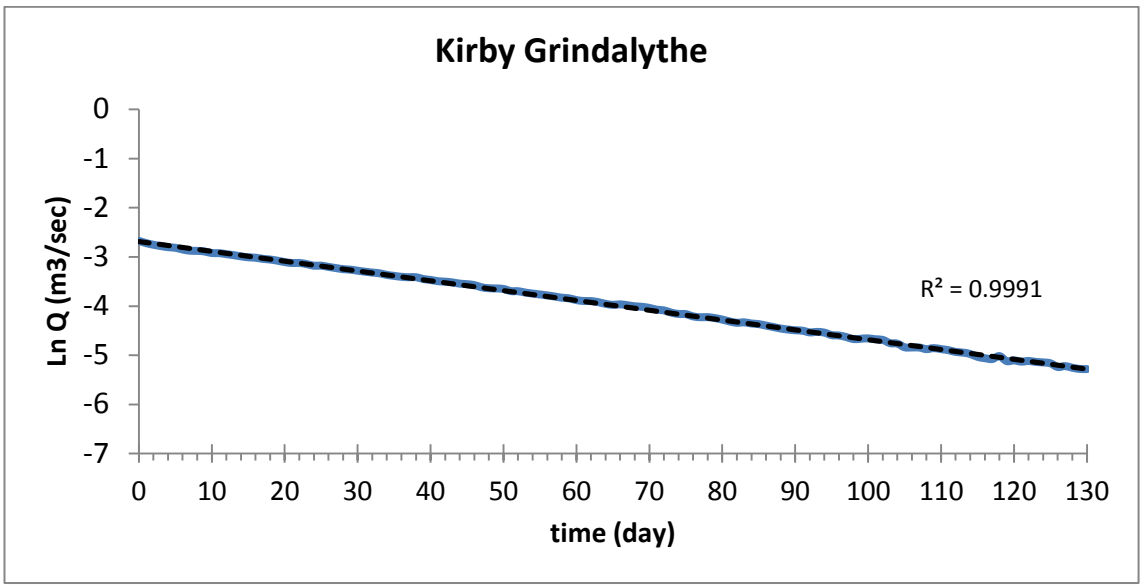

Figure 6-18 The MRC from Kirby Grindalythe plotted on the semi-log paper.

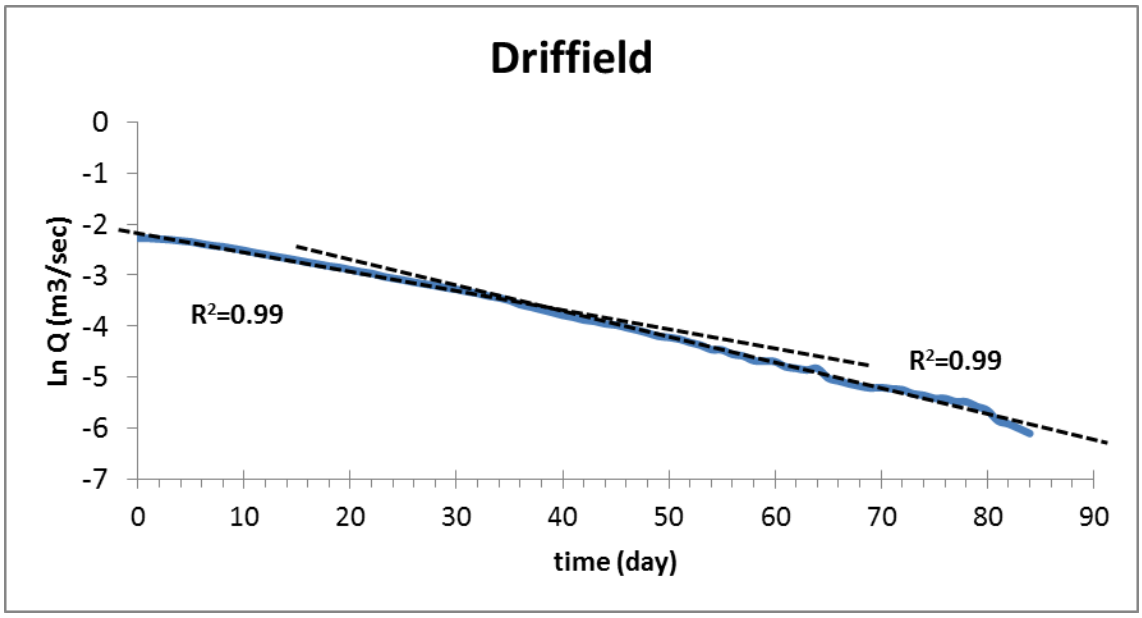

Figure 6-19 The MRC of the Driffield station on the semi-log paper.

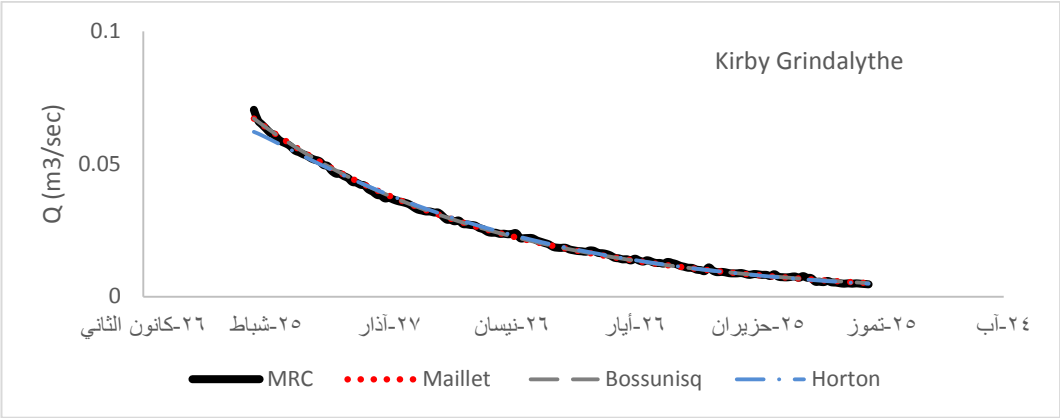

Figure 6-20 Shows the MRC of the Kirby Grindaltyhe and analytical result from both linear and non-linear models.

The results obtained from the analytical interpretation of the Driffield MRC are shown in Figure (6.21). Also, table (6.3) expresses the recession coefficient (alpha value) of the fitting curves to the observed recession curve. The result reveals that the Maillet model fitted the recession curve well. The exponential segment that fitted the real flow rate recorded a recession coefficient of 0.037day^{-1} for the first segment after peak flow, and 0.051 day^{-1} for the second component. The Horton model also shows good agreement between the model recession curve and MRC. The Horton model curve shows the same pattern but the flow value is higher than the value of real discharge at the early stage of the recession. However, from the middle to the end of the recession period it fitted the recession curve well. The Horton model curve fitted the real data with alpha of $0.0034day^{-1}$. The result of the Boussinesq model also fitted the real data but not as well as the multi- exponential and Horton models. The overall pattern of the model curve from Boussinesq appeared to be similar to the pattern of the observed MRC. However, the model discharge value was bigger than the observed value at the early stage of the recession, fell below the real value at the middle stage of the recession, and then became higher again during the late period of the recession.

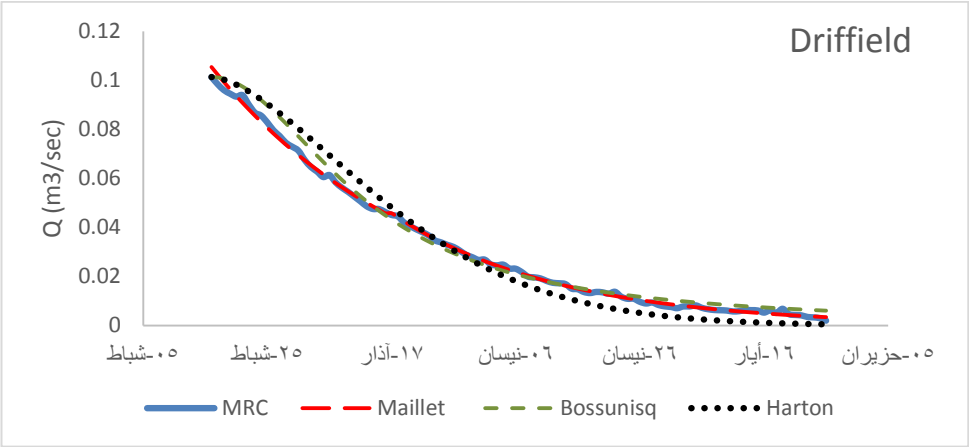

Figure 6-21 Illustrates the MRC of the Driffield station and analytical result from both linear and non-linear models.

Table 6-3Analytical result for Kirby Grindalythe and Driffield MRC.

Kirby Grindalyhte		
analytical approach	alpha of Segments	
Maillet	0.02 [T^{-1}]	
Boussinesq	0.0103	
Horton	0.0022 1/t	
Driffield		
analytical approach	alpha of Segments	
	first	second
multi-exponential	0.037 1/t	0.05 1/t
Boussinesq	0.04	
Horton	0.0034	

Interpretation:

Based on the analytical models for the linear aquifer the springs from Kirby Grindalythe deplete from a single reservoir aquifer. The MRC of Driffield on semi-log paper decomposed to more than one component with different slopes.

There are two possibilities for explaining the case of the recession curve for Driffield MRC when it does not appear as a straight line on semi-log paper: (a) the water flowing from an aquifer consists of cumulative influx from several linear reservoirs with different hydraulic characteristics. According to the multi- exponential model this aquifer consists of parallel reservoirs with various hydraulic properties, and each reservoir behaves linearly; (b) the water flow from the single aquifer behaves nonlinearly (relation between discharge and aquifer storage is nonlinear).

The result from the multi-exponential model showed proper fitting of the model to the Driffield MRC. The result from the multi-exponential method showed that the MRC decomposed into two segments with recession coefficient ($\alpha 1$) and ($\alpha 2$), 0.037and 0.051 day^{-1} respectively. The trend of the recession coefficient was $\alpha 1 < \alpha 2$. Most studies have expected that if the recession curve divides into more than one segment, the first segment which starts from the peak flow will most probably have an alpha value bigger than the alpha values of successive segments. Usually the slope of the recession segments descends toward the end of the recession period (Bonacci and Magdalenic, 1993). In the current study this pattern of the recession coefficient may be related to the existence of one of the two following scenarios:

(a) The aquifer is a fracture dominated flow system. The size and density of the fractures decrease significantly with depth. As a consequence, this fracture pattern in the aquifer produces abrupt vertical variation in the transmissivity or storage coefficient with depth, see Figure (6.22). This scenario is based on the assumption that the recession coefficient is inversely related to the volume of the water stored in the aquifer, as is shown in the following equation (Kresic and Stevanovic, 2009):

$$\boldsymbol{\alpha = \frac{Q_t}{V_t}} \qquad \text{Equation 6-13}$$

Q_t is discharge at time t
V_t is the volume of groundwater store in the aquifer

(b) Assuming that there is no significant difference in the hydraulic properties through the aquifer, changes in the recession coefficients are due to decreasing size of the reservoir (Figure 6.23). This assumption also can be demonstrated by equation(6.13), showing that reduction of the area of the reservoir with time causes the storage volume to reduce more rapidly towards the end of the recession; therefore, the value of the recession coefficient increases with time.

The Chalk Aquifer has a highly permeable zone around the water table, and permeability decreases abruptly below the water table fluctuation zone (Gale and Rutter 2006). Hence, case (a) is the more likely scenario to describe the behaviour of the Driffield chalk aquifer.

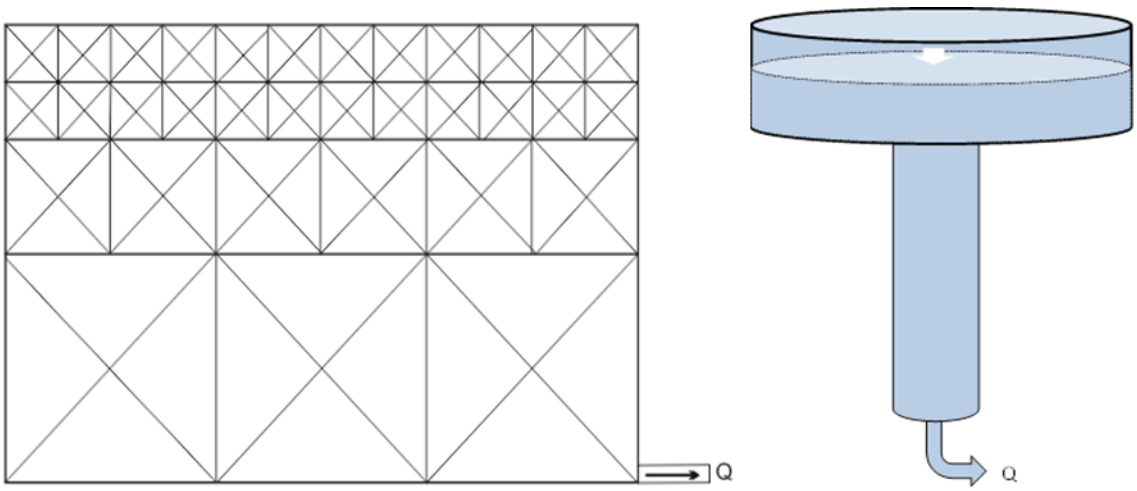

Figure 6-22, conceptual model show an estimation of fracture system in the Chalk aquifer in the study area.

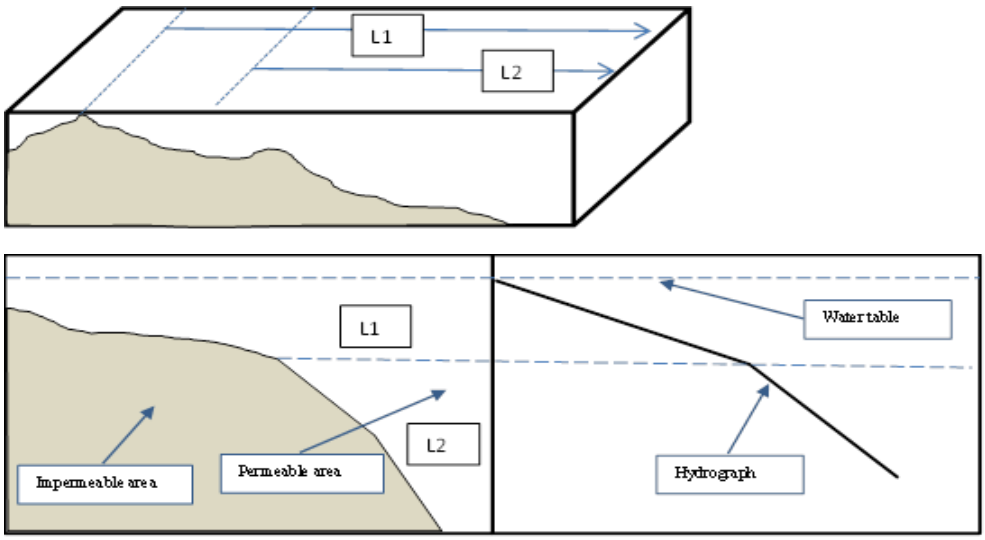

Figure 6-23, conceptual model shows the relation of recession curve to the recharge area.

6.4.4. The karstic behaviour of the Chalk in the study aquifers based on recession curve:

The recession period of the typical karstic system is characterised by variation in the discharge rate, which appears in the form of successive peaks and recessions. The rapid variation in the spring discharge is due to the quick flow through a highly permeable karstic network of fractures toward the spring (Kiraly and Perrochet, 1995; Florea and Vacher, 2006).

In the recession curve of both Kirby Grindalythe and the Driffield catchments, spikes appeared due to the increasing discharge rate. The spikes that appeared on the recession curves represent a quick short-term recharge responding to transitory rainfall events that were superimposed on the long-term recession curve.

Bonacci, (1993) conceptualized the spring hydrograph outcome according to the development of the fracture system in the aquifer. This conceptualization reveals fracture development in the aquifer in terms of sharpness of the hydrograph, duration of the recession period and lag-time between rainfall and responding

discharge. Consequently, in the typical Karst with a highly developed fissure system, the recession period appears in the form of successive peaks of short duration and sharp recession curves, due to the quick infiltration and flow through the big conduits and rapid drain of the recharged water. On the other hand, in the aquifer with small fractures, network flow is slow and draining of groundwater requires a longer time, meaning that the recession overall takes a long time and the flow decreases gradually (slope of the recession curve will be more gentle compared to that of the large-scale fracture system).

Using the assumptions suggested by (Bonacci, 1993) for interpretation of the recession curve, the long-term recession curves in the study catchments (130 days and 90 days in Kirby Grindalythe and Driffield respectively) indicate that in general the aquifers consist of small-scale fracture systems. Meanwhile, the events of increasing discharge, which appeared in the form of spikes during the recession period, are indications of the existence of rapid flow systems. Most probably, these rapid flow systems occur in the shape of small fissures or conduits. Figure (6.24) shows the relation between rainfall and hydrographs in the study areas. It appears that the discharge spike rose quickly in response to the rainfall. This confirms existence of quick bypass flow in the study aquifers.

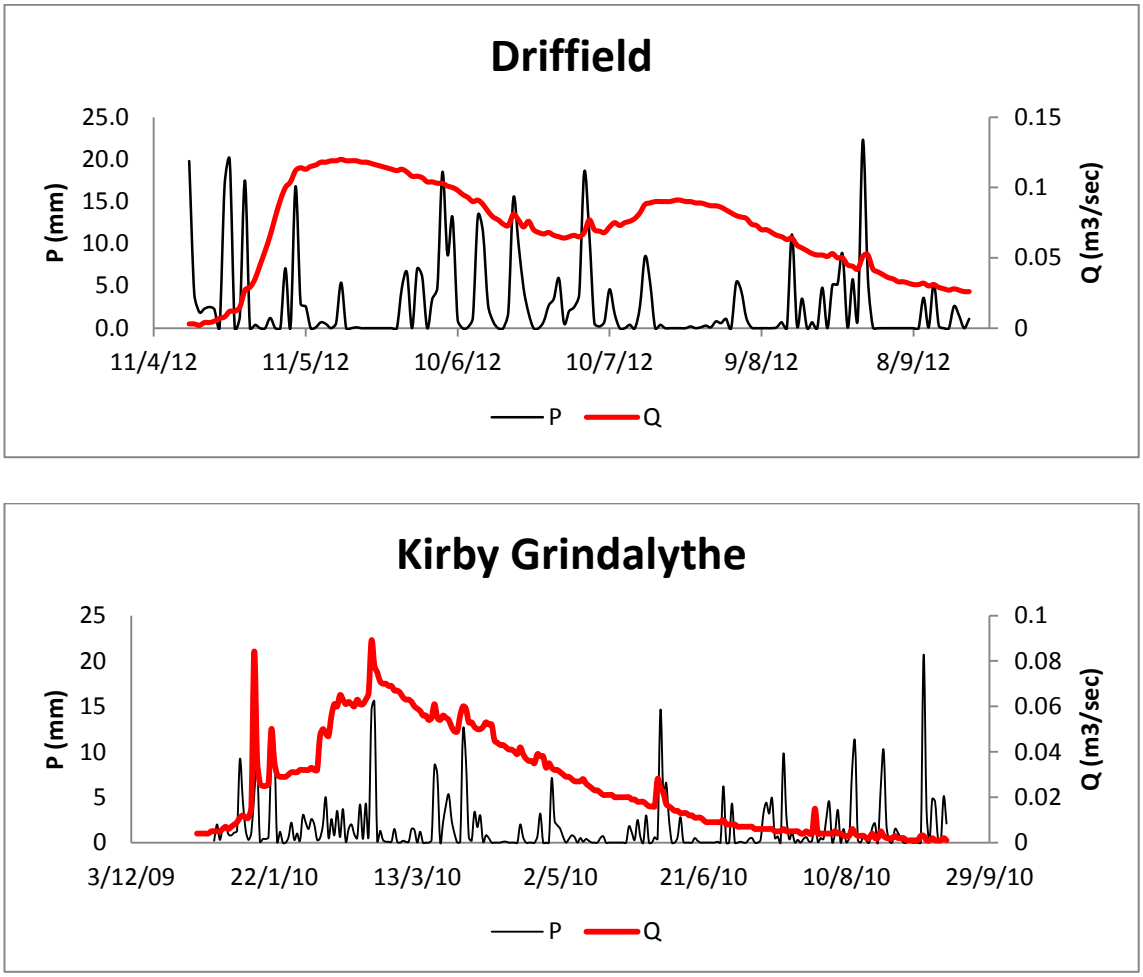

Figure 6-24 spiks of increasing discharege during the long term flow recession stage from the Kirby Grindalythe and Driffield catchment.

6.5. Summary:

This project measured flow and stage for the recession period of the water year 2014 at the gauging stations located in the study catchments. The goodness of fit between pre-existing and measured rating data shows no evidence of significant variations in the channel at the gauging station that would influence the effectiveness of the rating curve. This indicates the reliability of the flow rate information obtained from the EA monitoring stations.

The recession curve from the Kirby Grindalythe and Driffield Springs was interpreted according to linear (using Maillet equation) and non-linear (using the Bossunisqu and Horton) analytical models. The linear models showed a better fit to the recession curves from both catchments. The Maillet and Multi-exponential models revealed that the Kirby Grindalythe aquifer probably consists of single reservoir aquifer. Meanwhile, the Driffield aquifer contains two reservoirs or flow systems.

Short events of increasing discharge appeared on the recession curves in the form of sharp spikes. These spikes emerged coincident to the rainfall events or a short time after these rainfall events. The existence of these discharge spikes during the recession at the time when the AE is larger than the precipitation amount is an indication of existence of a fast flow system in the aquifer, which could comprise enlarged fissures. It might be possible to describe this phenomenon as a karstic behaviour of the Chalk.

Chapter 7. Groundwater CFC concentration

7.1. Chlorofluorocarbons (CFCs)

Chlorofluorocarbons are a group of chemically stable compounds containing chlorine and fluorine and produced artificially. . These chemical compounds have been produced in large quantities in three types CFC-11 (CCl_3F, trichlorofluoromethane or freon-11), CFC-12 (CCl_2F_2, dichlorodifluoromethane), and CFC-113 ($C_2Cl_3F_3$; 1, 1, 2 trichloro-trifluoroethane). The large-scale production of CFC-12 began in the early 1940s, followed by CFC-11 in the 1950s and CFC-113 in the 1960s. Since the 1930s these compounds have been involved in several industrial applications, being used widely as coolants in air conditioners, refrigeration, propellants in aerosol cans, blowing agents in open- and closed-cell foams, insulation, packing material, and as solvents. CFC-11 and CFC-12 have been used mainly as coolants, while CFC-113 was used as a solvent (Glass, 2002; Darling et al., 2010; Singhal and Gupta, 2010).

The impact of these gasses on stratospheric ozone has caused global concerns. Consequently manufacturing of most CFCs was curtailed since 1987 according to international agreements that are known as The Montreal Protocol to protect the stratospheric ozone layer.

CFCs in the environment are measured in the unit picomole per liter (pmol/L) or picomole/kg.

7.1.1. CFCs as a tracer:

During the last 50 years, a huge number of substances were introduced into the atmosphere and hydrosphere by human activities. Movement of the relatively stable substances (stable physically and chemically) through the ground can help to determine when and where water recharged, the flow path and flow velocity.

There has been widespread release of CFCs gasses to the atmosphere. In the atmosphere, due to the relatively high solubility of CFCs in water, the CFCs dissolve into the condensate water vapor. Rainwater containing CFCs from the atmosphere falls to the ground and becomes integrated into the hydrological cycle. Also, water that exposes to the atmosphere continuously is subjecting to the contamination by these substances (CFCs) via atmospheric exchange.The solubility of different CFC compounds is not similar.; USGS reported that despite the fact that the concentration of CFC-11 in the air is smaller than that of CFC-12 by the factor of two, but its concentration in water is greater. The solubility of CFC-11 in water in equilibrium with 1999 air is approximately 1,300 picograms per kilogram (pg/kg), at the same time and situation the solubility of CFC-12 was about 520 pg/kg (assuming a recharge temperature of 2°C (Glass, 2002). The concentration of these gasses in water depends on several factors based on Henry's Law. Henry's Law is one of the gas laws which was formulated by the British chemist, William Henry in 1803.This Law states that; at a constant temperature, the amount of a given gas dissolved in a given type and volume of liquid is directly proportional to the partial pressure of the gas in equilibrium with that liquid.

$$p = k_H * C$$

$$where\ p\ is\ parital\ pressure\ of\ the\ solute\ above\ the\ solution$$

$$C\ is\ the\ concentration\ of solute\ in\ the\ solution$$

$$k_H\ is\ the\ Henry'sLaw\ constant, which\ has\ units\ such\ as\ \ Pa.m^3$$

When surface water and precipitation percolate to the ground to recharge groundwater, at some point it will lose contact with the atmosphere; from this point the amount of the CFCs in the recharge water will be preserved at the same concentration, reflecting the concertation at the recharge time. This behaviour means that CFCs can potentially be used as a tracer for estimating the age of the groundwater and its residence time.

It is possible to use CFCs as a tracer for aging groundwater in this way, as the concentration of these compounds in the air has varied with time since their first production and release for the past 50 years. The historical variation in the concentration of CFCs can be used in the estimation groundwater recharging time. It can be used in the groundwater aging anywhere on earth because of its capability of mixing and diffusion in the air easily. The USGS confirmed that atmospheric CFCs concentrations at Barrow north Alaska show similar amounts to those in Colorado (Glass, 2002). Due to different patterns of emission there are differences in the CFCs concentration between the North and South hemisphere. Recharge time of groundwater can be determined by relating the measured concentrations of these substances in the groundwater back to known historical atmospheric concentrations and (or) to calculated concentrations expected in water in equilibrium with air (Plummer and Friedman ,1999).

Figure (7.1), shows the historical concentration of CFC-11 and CFC-12 in water in equilibrium with the air.

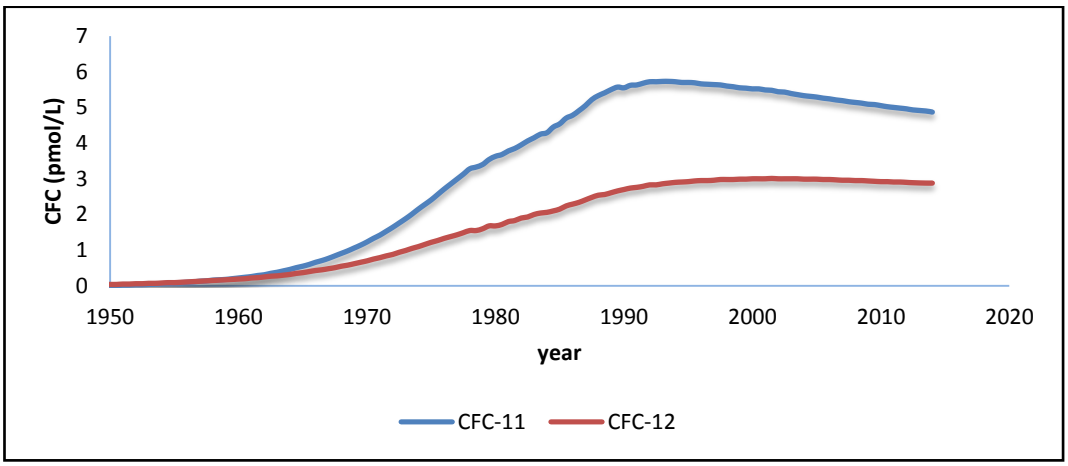

Figure 7-1 Concentrations of chlorofluorocarbons CFC-11 and CFC-12, in northern hemisphere groundwater recharged between 1950 and 2010 at a temperature of 10°C and elevation near sea level (Gooddy et al., 2006). Data based on Plummer and Friedman (1999) and from the National Oceanic and Atmospheric Administration Climate Monitoring and Diagnostics Laboratory.

Three reasons make dating groundwater depending on CFCs possible (Plummer and Friedman,1999). (1) these gases are an artificial product and do not have any natural background, their concentration in the atmosphere over the past 50 years has been reconstructed, (2) their differences in the solubility capacity in the water is known, and (3) their concentration in the atmosphere and modern water are sufficient to be quantified reliably. The feasibility of using CFCs as tracers in groundwater investigation goes back to the 1970s (Thompson et al., 1974; Schultz et al., 1976; Randall and Schultz, 1976; Thompson, 1976; Hayes and Thompson, 1977; Randall et al., 1977; Thompson and Hayes, 1979; Schultz, 1979), as the CFCs were used for tracing recent recharge and identification the groundwater residence time.

Thompson et al., (1974) confirmed that CFCs could be used as a tracer when they managed tracer test by injecting fluorescein dye and a solution containing 100 mg/kg CFC-11 into an intergranular poorly sorted sand and gravel aquifer. They found that fluorescein dye was not recovered while they detected CFC-11 at the adjacent monitoring borehole. The result of this study indicated the potential for using CFC-11 as a useful tracer in a porous system, whereas other kinds of tracer could be absorbed in such system. CFC-11 has been used by Schultz et al., (1976) as the tracer in groundwater investigations near Tucson, Arizona; they used CFC-11 in tracing groundwater recharge of sewage discharge to river beds.

A new method for dating groundwater was suggested by (Randall and Schultz , 1976), based on CFC-11 concentration in water samples. They estimated the age of water sample by measuring the concentration of the CFC-11 in the sample and related it to another water sample of known age. They also realized that for reliable dating of groundwater recharge using CFCs, reconstruction of the atmospheric concentrations over time for CFCs would be required.

7.1.2. Groundwater contamination by CFCs:

One of the limitations faced by CFCs as a tracer in groundwater dating is contamination of groundwater with chlorofluorocarbons from sources that add to the concentrations present at the recharge. Only a miniscule amount of additional CFCs (e.g. parts per trillion) is sufficient to cause severe contamination; CFCs are present in the formulation of several organic compounds. Because the concentration of CFCs in those organics is higher than that in modern air, leaking one of these organics into the ground will cause rising concentration of CFCs in the groundwater to level above that in the modern atmospheric level (Thompson and Hayes, 1979; Jackson et al., 1992; Busenberg and Plummer, 1992) .

Because CFC is an artificial compound, human activity is the main source of contamination. Groundwater contamination by the CFCs comes from three primary sources:

1) Contamination due to emitting CFCs into the air due to industrial activity or leaking gas from machines containing one or more of these gasses. This creates a local air concentration anomaly leading to recharge of rainfall with an unusual CFC concentration.
2) Contamination due to leaking of CFCs into the ground directly through seepage from landfills.
3) Contamination may arise because of the sampling equipment and sampling bottle, if the equipment is contaminated by CFC compounds this will lead to propagating this contamination to the collected water sample. This may also occur if the sampled groundwater contacts the air because of leaking through the bottle cover.

The data from atmospheric monitoring stations worldwide network confirmed that CFC gases have the greatest ability to mix and spread in the atmosphere. However CFC concentrations in urban areas are higher than in rural areas, since CFC release is related to the density of population and industrial activity. Ho et al. (1998), for

example, detected significant CFC excesses in the New York metropolitan area. Local atmospheric excesses of CFC-11 and CFC-12 have been reported by (Oster et al. 1996) downwind of an industrial area in Germany. Also, Ho et al. (1998) described how wind direction has an influence on seasonal variation in CFCs concentration.

Despite the existence of local atmospheric concentration anomalies, Schultz et al., 1976 found that concentration of CFC-11 in precipitation in and around urban and industrial areas is in the equilibrium with the global atmospheric distribution rather than the local near surface anomalies. They reached this conclusion based on analysis of the solution of gas in raindrops during precipitation mechanisms. There are two mechanisms in the establishment of precipitation, rainout, and washout. Rainout is the process of condensation within a cloud to form raindrops; washout is the acquisition of gas by raindrops after leaving the cloud. The solution of gasses into precipitation happens in both stages. Studies of the behaviour of other gasses (e.g. SOx and NOx) in precipitation showed that dissolution of gasses takes place predominantly in the rainout stage and is less affected by the local near-ground anomalies. This CFC contamination of groundwater is more likely to happen due to subsurface contamination rather than local near surface atmospheric release of CFC gasses.

7.1.3. Uncertainty in CFCs results:

Sensitivity of CFCs in the estimation groundwater residence time depends on the rate of change in the CFC concentration in the atmosphere with time. Small changes in the CFC concentration in the air leads to rising uncertainty in the groundwater age determination according to CFCs. Solubility of the gas according to Henry's Law principles is the function of temperature and pressure, in the groundwater depends on temperature and pressure of the recharge water at the water table. Consequently, uncertainty in the recharge water age estimation depending on CFCs concentration may arise due to uncertainty in these factors.

Temperature strongly affects the solubility of CFC gasses in the water. Therefore, it is necessary to know the recharge temperature of groundwater for interpretation CFC data. Recharge temperature is the temperature at the water table during recharge when water is last in contact with a gas phase. Figure (7.2) shows the estimated concentration of CFCs under different temperature conditions (5^{o} to 25^{o} C) between years 1940 and 1998; these values estimated at sea level and in equilibrium with North American air (Plummer and Busenberg, 2000). This figure clearly illustrates the result of uncertainties in recharge temperature (for instance 5^{o}C) will make a difference in the apparent age of several years. Another factor that influences gas solubility is the barometric pressure. Nevertheless, uncertainty in the pressure does not produce significant error compared to temperature; uncertainty in catchment area elevation of 1000 m results in age uncertainty of a few years or less (Busenberg et al., 1993). This means that pressure effects will only be significant in mountainous regions.

Excess air in the groundwater could also produce uncertainty in age determination of the recharge water (Plummer and Busenberg, 2000). Excess air is "atmospheric air (gases), beyond the amount that can be attributed to air/water solubility that is incorporated into shallow groundwater during or following recharge" (Shapiro et al., 2012). Excess air enter into the groundwater by entrainment air during infiltration and (or) by water-table fluctuations. However, the relatively high solubility of CFC gases means that the amount present in excess air is small in the relative to that already present in the water. This led (Busenberg and Plummer, 1992) to conclude that uncertainty in the age interpretation due to the uncertainty in the excess air could be ignored in most groundwater cases because of its small effect.

The thickness of the unsaturated zone (UZ) could also influence the interpretation of CFC ages. In a porous medium there is a time lag for the diffusive transport of CFCs, which increases proportionally with the thickness of unsaturated zone (Weeks et al., 1982; Cook and Solomon, 1995). Therefore when the UZ is thin the trace-gas composition in the groundwater at the water table is almost the same as of the

atmosphere. While, for a deep water table the age of trace-gas could be greater than the age of trace gas in the atmosphere at the time of recharge (Cook & Solomon 1995). In fractured aquifers, the thickness of UZ does not influence CFC age interpretation. Where there is rapid transport through fractures in the UZ, the concentration of CFCs in the groundwater effectively represent residence time only since recharge water reached the saturated zone (Darling et al. 2005).

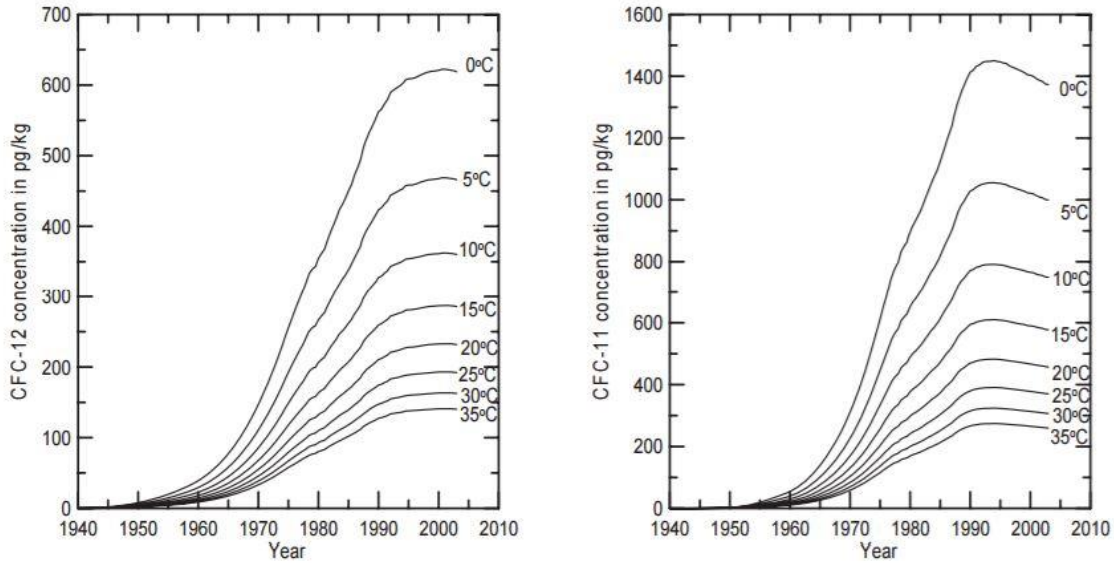

Figure 7-2 concentrations of CFC-11 and CFC-12 in groundwater recharged between 1940 and 2000, at sea level, and in equilibrium with the North American atmosphere at 5–30° C. http://www-pub.iaea.org/MTCD/publications/PDF/Pub1238_web.pdf

7.1.4. Estimating groundwater age from the concentration of CFCs:

The CFC age estimate can be made simply by comparing the measured concentration with the computed historical concentration for CFCs (given estimated recharge altitude and temperature) to obtain the year of recharge. The CFC concentration in

groundwater will relate to the equivalent air/water equilibrium concentration. This process achieve by plotting the value of the CFC in the water samples on the historical concentration CFCs curve. This will lead to acquire the apparent age of the groundwater (Warner and Weiss, 1985; Bu and Warner, 1995).

However, this method presupposes that the water in springs is the result of piston flow in the aquifer. In nature, the water in the ground most likely consists of a mixture of younger and older waters (water of different age). This more predominant in the fractured aquifers, where younger water (with higher CFC concentration) flow fastly in the larger fractures while older water (i.e. recharged earlier and with lower CFC concentration) flow slower in the small fractures or by diffusion through the matrix porosity.Consequently, the young water mixes with the older water. To account for this, an approach has been proposed for estimation of the flow process by plotting one CFC against other or plotting CFC against SF_6 (Sulfur hexafluoride gas) (Gooddy et al., 2006; IAEA 2006). There are four theoretical mixing models: piston flow (PFM), exponential piston flow (EPM), exponential mixing (EMM) and binary mixing (BMM) (Cook and Bo¨hlke, 2000; Zuber, 1986). These models used to describe the variation in the resulting groundwater mixtures. Gooddy et al. (2006) developed a conceptual model for groundwater movement in part of the lowland Chalk catchment in the UK based on the hypothetical mixing models from the combined use of CFCs and SF_6 data. Figure (7.3) shows a plot of CFC-11 vs. CFC-12, with the piston flow curve and the modern–old binary mixing line. The area which surrounded the mixing curve divided into zones, each zone defines the contamination in the water sample regarding the CFC11 and CFC12 (IAEA 2006).

A further approach has been suggested for age determination of groundwater from CFCs. When the water sample contaminated with one of the CFCs the age of the groundwater can be estimated by plotting the ratio of two CFCs, for example, CFC-11 and CFC-12 (IAEA, 2006). CFC ratios are preserved in simple binary mixtures of young water diluted with old water (of pre-CFC or low CFCs concentration), the ratios of CFCs can determine the age of the young fraction (IAEA, 2006). A

historical atmospheric ratio of CFC-11/CFC-12 in the North American air is illustrated in figure (7.4). The CFC-11: CFC-12 ratio has a dating range of approximately 1947 through 1976. The CFC-11/ CFC-12 ratio in the air was nearly constant from 1976 to 1990 and more recently has declined.

However, where the water samples have CFC concentrations greater than the amount in modern air-water equilibrium, groundwater dating is impossible.

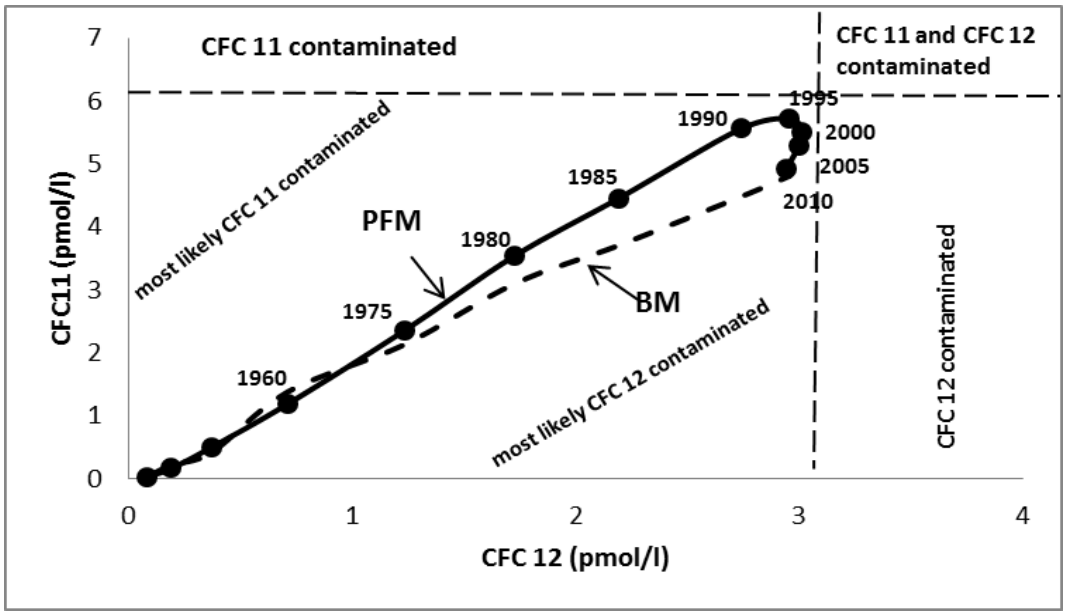

Figure 7-3 CFC-11 vs. CFC-12, with the piston flow curve and the modern–old binary mixing line from (IAEA 2006).

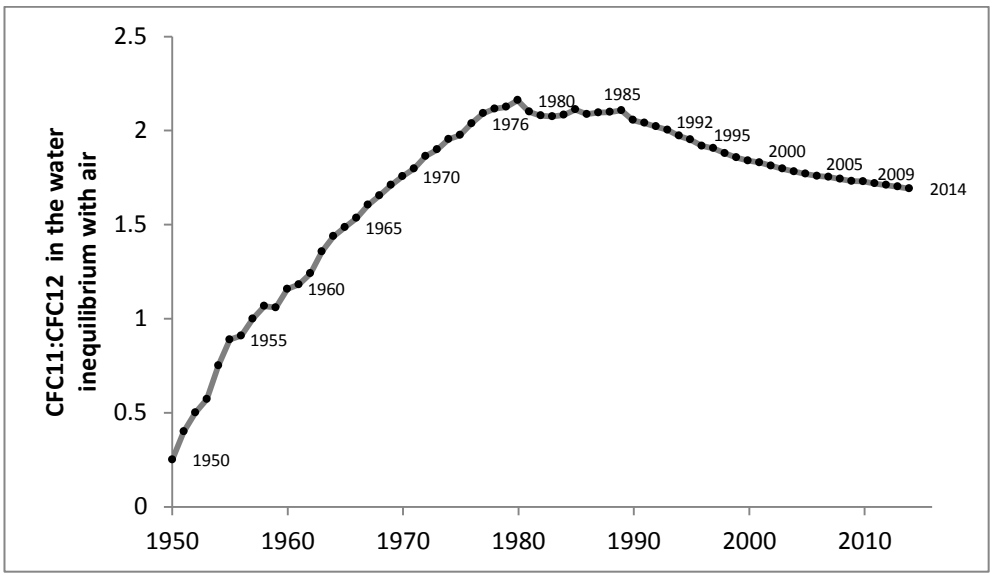

Figure 7-4 Historical ratios of CFC-11/CFC-12 in groundwater in equilibrium with air.

7.2. Methodology

7.2.1. CFC sampling methodology:

Spring-waters were sampled using the specific procedure developed by USGS for sampling water for CFC test, the method is called CFC bottle filling. Because of presence the CFCs in the atmosphere, any water, which contacts the atmosphere directly, is subject to contamination by the CFC present in contemporary air (because of the ability of the CFCs to dissolve in the water even in the normal atmospheric condition). The sampling technique developed by USGS uses a pragmatic approach to preventing contact between the water-sample and air by using excess pumped sample water as a barrier between the sample bottle and air. The following is a systematic description of the sampling process.

- Before beginning to pumping water in the bottle, the water has been run for sufficient time so that the water cleans out the hose and pump.

- The bottle was cleaned by allowing water to flush out inside of the bottle completely and then dump the contents prior the sampling.
- Fresh water from the sampling source was sampled to fill the bucket in which the CFC sample bottle is submerged for sample collection.
- The discharge end of the hose was placed at the bottom of the sampling bottle, then filled from the bottom up (This process will displace the water and air already in the sampling bottle).
- Before capping the CFC sampling bottle, it allowed the water to overflow the bucket for about 30 seconds (about 7 litres based on the pump discharge rate, this amount of overflow is more than the suggested amount by USGS which is one litre).
- The submerged sampling bottle is capped in the bucket, then checked for any air bubble before sealing the cap/bottle joint securely with electrical tape (if there are bubbles the sample should be retaken).
- After each sampling, the bottles were labelled with the name of location, date and time of collection.
- The CFC bottles have been stored at room temperature (about 22^{o} C) before shipping to the CFC lab. In this study the bottles before shipping to the lab; the first group of samples was stored for about four months and the second group of samples after three months. According to USGS, CFC water samples can be stored for up to 6 months.

Figure (7.5), shows schematic diagram explaining the USGS CFC bottle-filling procedure.

The material used for collecting CFCs samples:

- A caravan water tank submersible pump was used for pumping water from the sources, Figure (7.6). The pump that was used was operating at 12V electricity; this made using it easy as only a small 12V battery was needed while it was employed in the field. In addition, the pump was designed to be

lightweight (with external dimensions were 102 X 35 mm) and low power consumptions. The pump outlet sleeve designed to connect with 11mm hose.

- An 11mm diameter flexible plastic water hose was used for conveying water from the pump to the sampling bottles.
- 12V portable power bank was used for operating the pump.
- A nylon rope was used for hanging weight, water hose, and pump. The nylon rope was used to connect together pump, hose and weight while the pump was thrown into and pull out from the pool.
- Weight; 2 kg weight iron disc was used for submerging and fixing the pump in the water pool.
- A small size fishing float ball was used for suspending pump in the water pool. If the submersible pump touches the bottom of the pool, the dirt, which aggregates at the base of the pool, will block and damage the pump.
- Water sampling bottle. The water was sampled in a glass bottle which has a prevent screw cap, see Figure (7.7). It is important to use bottles with preventing cap for preventing exchange CFCs between sampled water and atmospheric air. Bottles were provided by the CFC analysis laboratory and have been tested for suitability.
- Plastic tape. A plastic tape has been used to the cap/ bottle joint to eliminate the probability of leaking from the bottle's cap.
- Plastic bucket. A plastic bucket (with dimensions 25cm diameter X 27cm depth) was used as a container for collecting water in which the sampling bottles were submerged.
- Sticking labels and permanent pen.

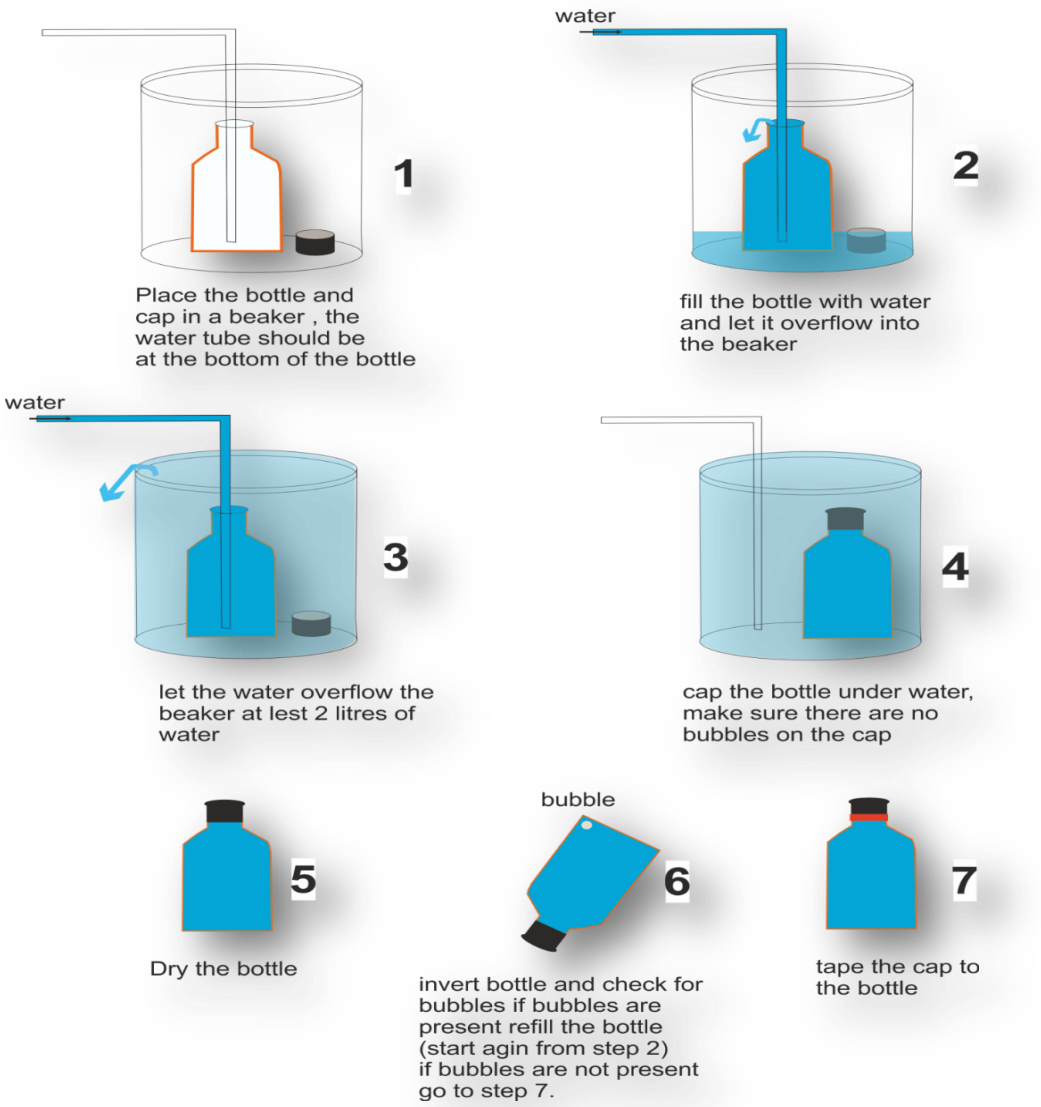

Figure 7-5 the CFC bottle filling procedure.

Figure 7-6 small size submersible pump.

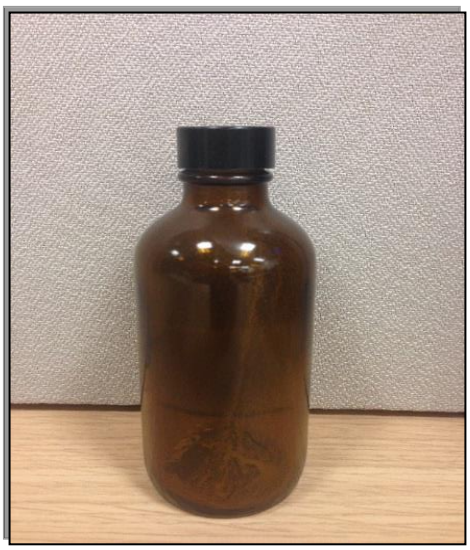

Figure 7-7 sampling bottle.

Describing the locations of springs:

Duggleby-1 is a spring drains an isolated body of the Chalk Rock (consisting of Welton Chalk Formation and Ferriby Chalk Formation) west of Duggleby village. The spring located 1.12km the southwest of Duggleby village, at grid reference SE 86858 66263 or coordinate East 502121, North 458404.

Duggleby-2 is a spring deplete from a body of Chalk rocks (consist of Welton Chalk Formation and Ferriby Chalk Formation) south of Duggleby village. This spring located 0.93 km southwest of Duggleby, at grid reference SE SE 87508 66220 or coordinate East 486858, North 466263.

Driffield pond is the location where water from a Chalk catchment northwest of the Driffield town is draining. This site consists of the pond located on the northwest side of Driffield, 0.33 km from the Northend Park, at grid reference TA 02121 58404, or coordinate East 502121 , North 458404 (see Figure 3.7).

Sampling schedule:

The sampling started in the middle of February 2015 and finished by October 2015; the sample collected at one-month intervals. In total 21 spring-water samples were collected during this time. The period from February to October during the year was chosen for collecting the spring water samples in order to observe the variation which may exist in the CFCs concentration during the recession period of the spring discharges.

The collected samples were sent to the BGS laboratory Wallingford for measuring the concentration of the CFC-11 and CFC-12. The concentration of the CFCs in the water samples was measured by gas chromatography using an electron capture detector (GC-ECD) with the detection limit 0.01 pmol/L. Then the CFC calibrated to the air standard collected at an AGAGE (Advanced Global Atmospheric Gases Experiment) atmospheric monitoring station, and the sample analyzed assuming that the recharge temperature was 10^{o} C (IAEA 2006; Darling et al., 2012).

7.2.2. Correction and calibration:

The temperature of groundwater at the water table during recharge and elevation of the catchment area are a possible factor that produces a significant influence on the dissolution of the gases in the water. For this reason, a correction is required during the calculation of equivalent air concentrations from the CFCs data.

From the calculation, the water balance and estimating the recharge in the study catchments it been estimated that mostly the recharge happens during the period between October to March, and some intermittent short recharge events were recorded up to June. This means that the recharge in the area happens over the long period of the year, so the average annual temperature in the ground can represent the temperature at the water table during the recharge.

Data from the stations in the area for years between 1910 to 2015 (from Met Office) showed that the maximum and minimum monthly mean air temperature during the year were 14.9 ℃ and 3℃ respectively, with average annual 8.5 ℃, see Figure (7.8). The mean monthly groundwater temperature in the study area, which was recorded in four boreholes using CTD see section (5.3.1) during this study, for years 2013 to 2015 showed that the groundwater temperature was more stable and slightly higher than the air temperature. The mean monthly groundwater temperature was seasonally fluctuated with the minimum value of 9.1ºC and maximum value 9.5ºC, with average annual value 9.4ºC, see Figure (7.8). Figure (7.9) is an example showing the comparison between annual air and soil temperature variations for (Halesowen) near Birmingham, UK. It also showed that the temperature in the soil was slightly higher than the air temperature.

When the spring water samples analyzed in the BGS lab the temperature at the water table during the recharge was estimated to be 10℃. It has been explained, that the mean groundwater temperature in the study area about 9.4℃. Because the estimated and actual temperature of the groundwater is so close no further temperature correction has been applied.

Another factor that affects the dissolution of gases in water is the elevation. Regarding the CFCs sampling in the current study, the variation in elevation between recharge and discharge locations does not exceed 60 m meters, as a consequence effect of altitude will not produce significant uncertainty in the groundwater age interpretation and the correction will not be needed.

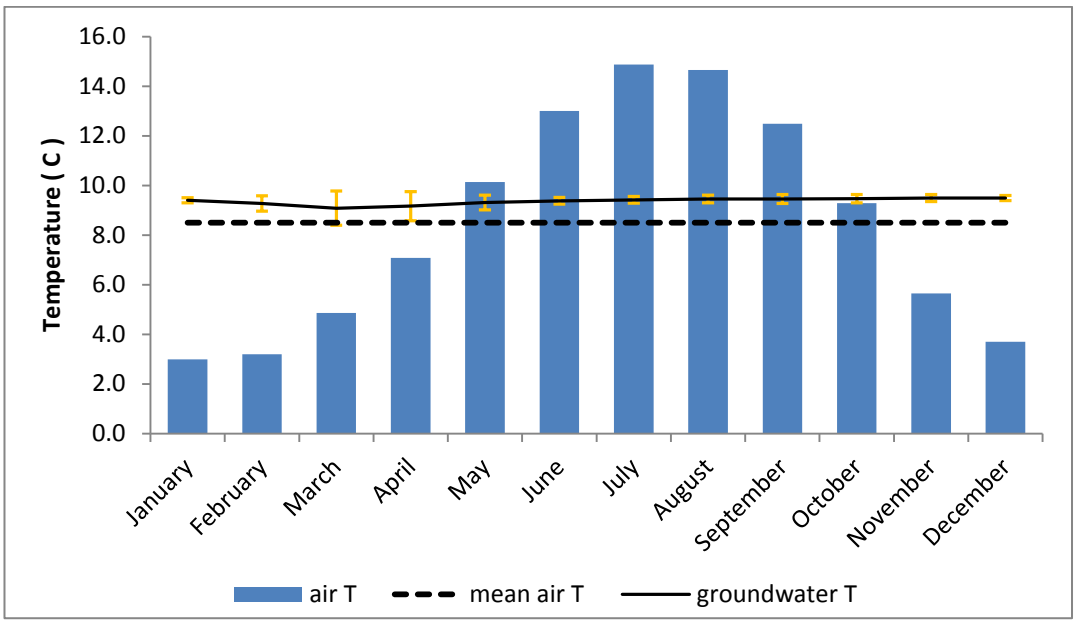

Figure 7-8 blue bars are average monthly air temperature for years between 1910 to 2015 for the north England. The data obtained from the Met Office archive online. The dash line represent mean air temperature. Black dots represent the mean monthly groundwater temperature (from three boreholes in the study area) for years 2013 to 2015.

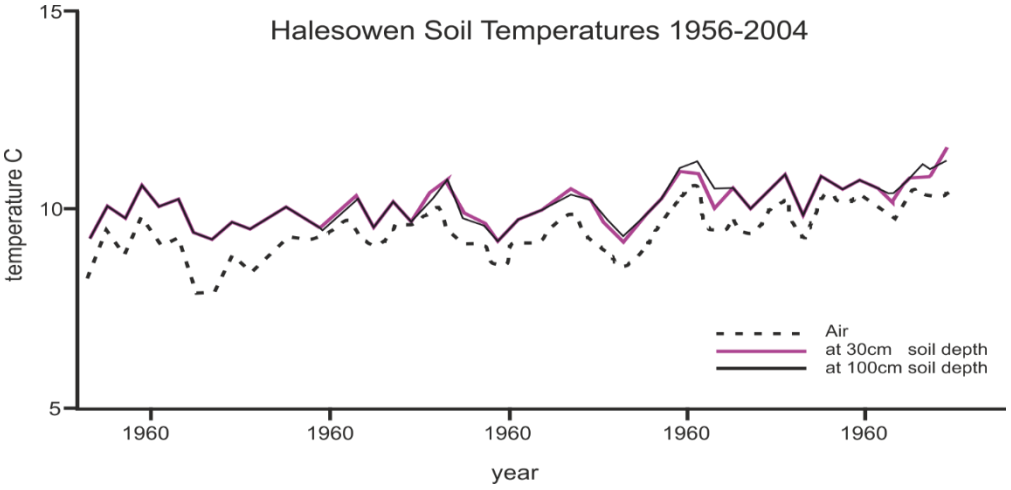

Figure 7-9 show the fluctuation in the temperature of the air and in the soil (at depth 30cm and 100cm), from [http://www.halesowenweather.co.uk/soil_temperatures.htm].

7.2.3. Methodology for Analysis of the CFC result

CFC testing for the water samples has accomplished in the BGS laboratories. Concentrations of the CFC in the groundwater samples were measured by stripping the gases from the water samples and then injecting the gas into a gas chromatograph equipped with an electron capture detector (Bullister and Weiss, 1988)

Analysis of the CFC results has been done in several stages:

The concentration of the CFCs in the water sample has been used for investigating groundwater age, groundwater mixing, and groundwater flow processes.

- Analysis uncertainty in the CFCs data.
- CFCs in the water samples have been plotted against the historical concentration of the CFCs for estimating groundwater age.
- CFCs plotted against each other for investigating groundwater flow system and mixing process.
- The ratio of the CFC-11:CFC-12 plotted on the historical CFC-11:CFC-12 time series relation for estimating groundwater age and mixing process.

Among the entire collected samples, only one sample contained CFC lower than the recent air/water equilibrium value. Thus all water samples were contaminated with CFC except one sample (for CFC-12 only). Consequently, the only non-contaminated sample could be used for estimating the groundwater residence time.

For the contaminated samples:

- The samples plotted on the time series graph to investigate the pattern of the CFC concentration in the contaminated samples.
- Flow rate plotted against the CFC concentration on the ordinary graph. The purpose was for exploration the relation between the discharge and contamination rate.

- The ratio of CFC11: CFC12 plotted on the time series graph and has been compared to the CFC11: CFC12 ratio in the modern water fraction.

7.3. Results and discussion

7.3.1. Results of groundwater age determination:

The water samples from the springs at both Duggleby and Driffield were found to contain measurable concentrations of CFC-11 and CFC-12. Table (7.1) presents the concentrations of the CFC-11 and CFC-12 in the spring water samples. The values are plotted on the historical air/water equilibrium concentration curves in Figure (7.11 and 7.12). This shows that the CFC-11 concentration in all the water samples were greater than the values in the modern air/water equilibrium. Similarly, the concentrations of CFC-12 in all water samples except one sample from the Duggleby2 were greater than the modern air/water equilibrium.

The water sample from Duggleby2 that was taken during June 2015 has a concentration of CFC-12 of 1.99 pmol/L. Plotting the data on the CFC-12 curve shows that this sample would return an apparent recharge date of 1983 (see Figure 7.13). This is the only sample with a concentration of CFC-12 explicable by atmospheric level sources alone. Therefore there is a strong possibility that this sample does not represent a "real" groundwater recharge age, e.g. due to mixing with contaminated water, see further discussion below.

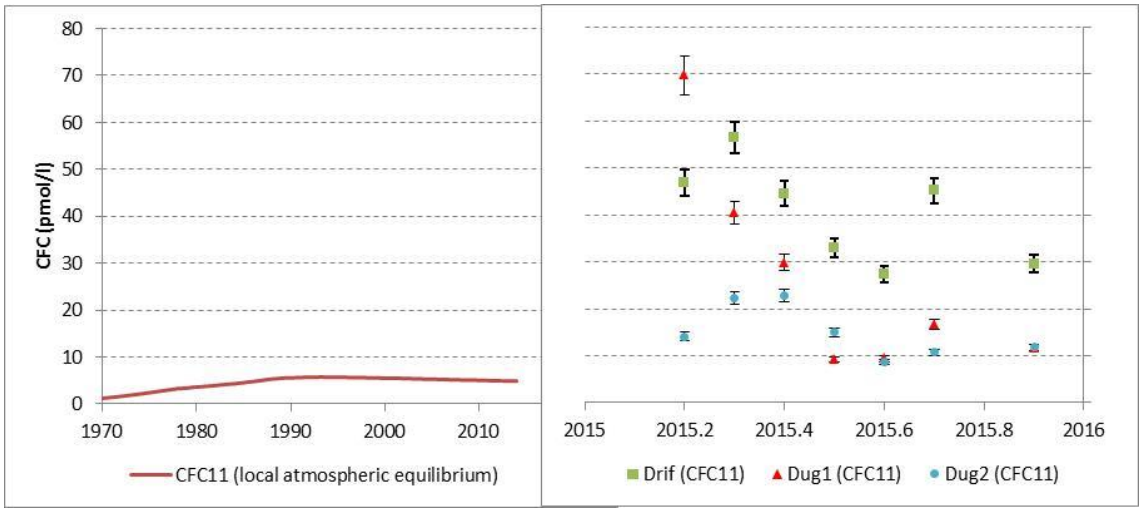

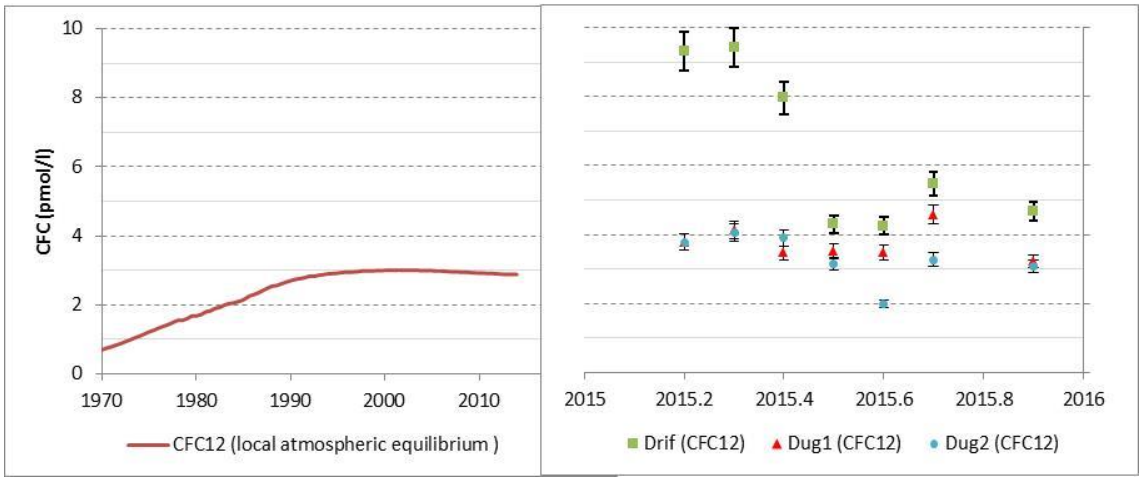

Figure 7-10 shows error boundary of the CFC in the samples due to estimated uncertainty in the temperature and analysis processes. The left side of the graph shows the historical concentration of CFC in the groundwater in equilibrium with the air since 1970. Moreover, the right side of graph expanded to show the concentration of the CFC11 and CFC12 in the collected water samples during 2015.

The CFC-11 and CFC-12 in the collected samples from Duggleby1, Duggleby2, and Driffield springs are plotted on the CFC-11-CFC-12 historical mixing curve (Figure 7.14). Comparing the concentration of the CFCs in the water samples to the mixing curve indicates that all water samples are contaminated with CFC-11 and CFC-12, except one sample from Duggleby-2, which appeared to be contaminated only by CFC-11, see Figure (7.14). Similarly plotting the CFC11: CFC12 ratio of the water samples on the historical ratio of the CFC11: CFC12 showed that ratio in the samples is higher than the historical ratio, Figure (7.15).

In most of the samples the concentration of CFC-11 ranged from 1.5 to 4.8 times bigger than in the modern fraction. Also, the concentration of the CFC-12 in the spring water ranges up to 2.8 times higher than the modern fraction. This indicates that the spring water is contaminated with CFCs beyond equilibrium with modern or recent air. In Figure 7.14 all of the analyzed samples lie well away from the curves that correspond to the Piston Flow Model (PFM) and Binary Mixing (BM). Therefore, the method of binary mixing model applied to the CFC-11: CFC-12 ratio cannot be used for estimating the apparent groundwater age.

It is also clear in Fig. 7.14 that Duggleby 1 and Duggleby 2 show similar extents of CFC-12 contamination, but there is far greater CFC-11 contamination in some Duggleby 1 samples compared to Duggleby 2. The Driffield samples are generally the most heavily contaminated with CFC-12 and are more heavily contaminated with CFC-11 than any of the Duggleby 2 samples but lie within the CFC-11 concentration range of the Duggleby 1 samples. All samples, bar one, are heavily contaminated with both CFC-11 and CFC-12.

Table 7-1 Concentration of CFC-11 and CFC-12 (pmol/L) in spring water from Kirby Grindalythe and Driffield catchment.

Sampling date	Driffield		Duggleby 1		Duggleby 2	
	CFC-12	CFC-11	CFC-12	CFC-11	CFC-12	CFC-11
13/02/2015	9.32	46.89	3.78	69.73	3.78	14.11
26/03/2015	9.42	56.51	4.14	40.56	4.06	22.29
27/04/2015	7.96	44.54	3.46	29.89	3.91	22.91
26/05/2015	4.3	32.91	3.52	9.13	3.15	14.95
23/06/2015	4.24	27.38	3.48	9.36	1.99	8.79
15/07/2015	5.47	45.18	4.57	16.62	3.27	10.71
04/09/2015	4.68	29.61	3.22	11.68	3.08	11.81

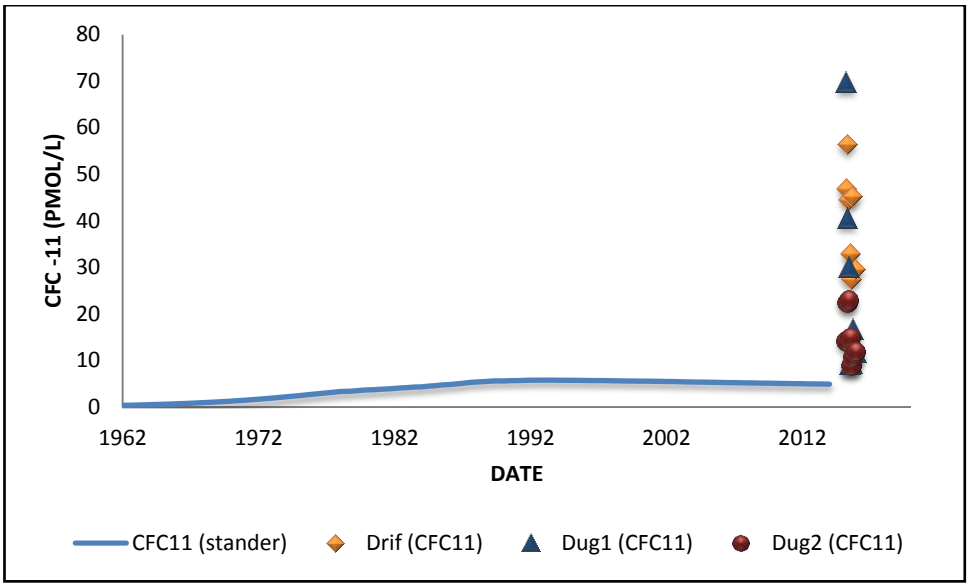

Figure 7-11 plotting the analysis result of the CFC-11 of the water samples from Driffield, Duggleby1 and Dubbleby2 springs on the historical CFC-11 concentration in the air/water equilibrium.

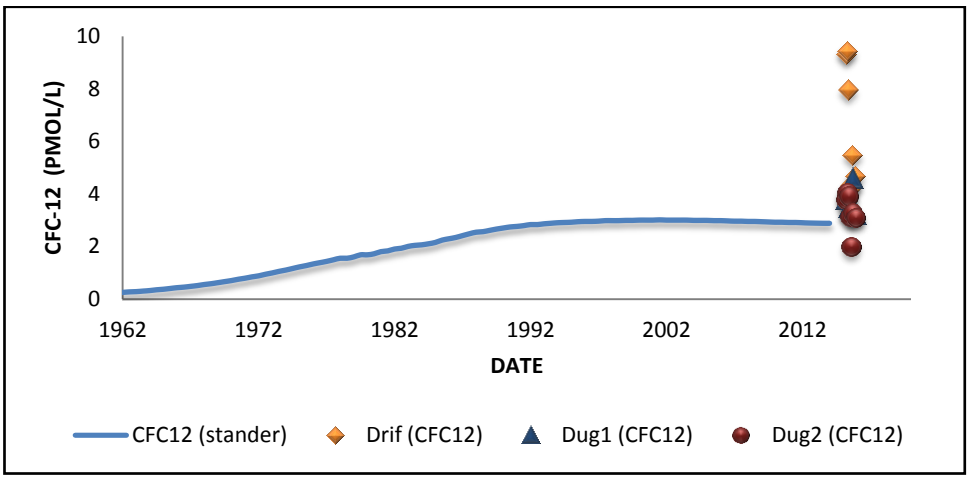

Figure 7-12 plotting the analysis result of the CFC-12 of the water samples from Driffield, Duggleby1 and Dubbleby2 springs on the historical CFC-12 concentration in the air/water equilibrium.

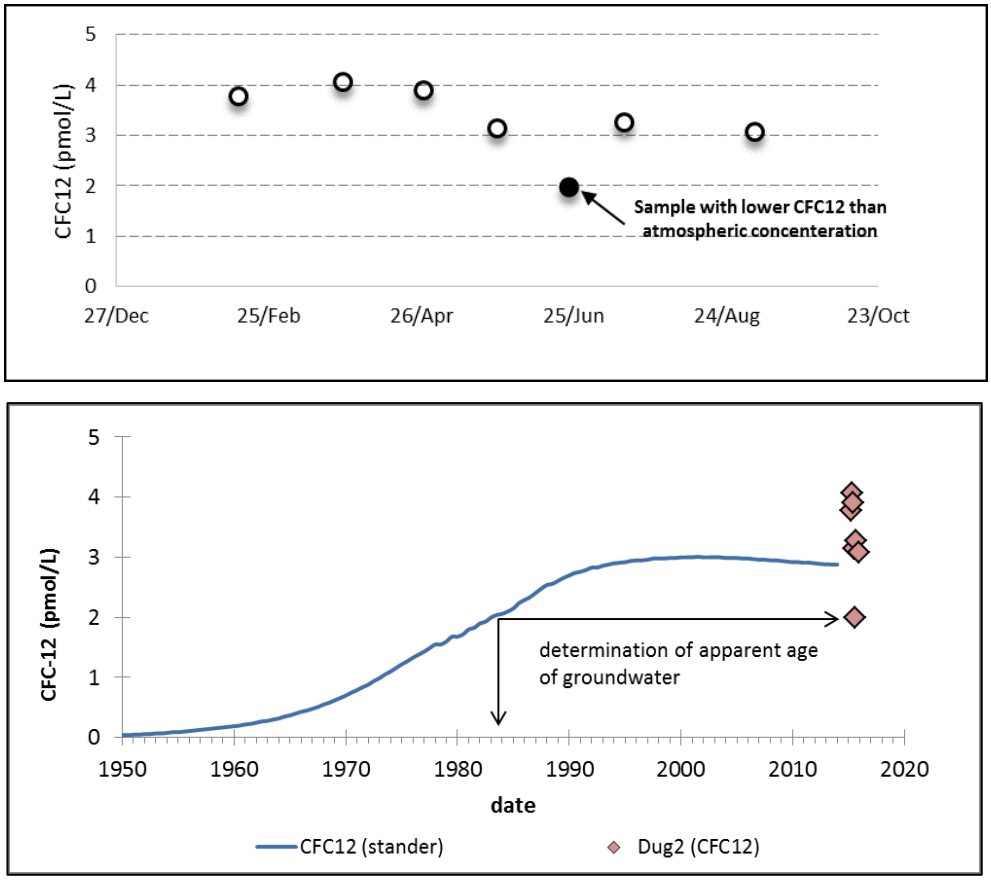

Figure 7-13 estimating groundwater age from the concentration of the CFC12 in a water sample.

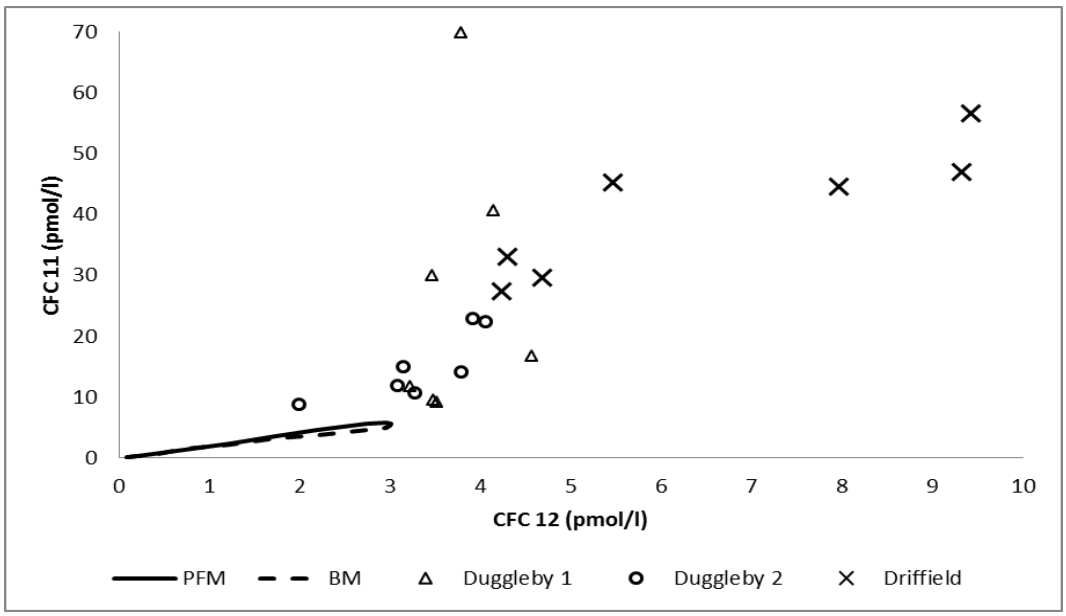

Figure 7-14 samples from Duggleby1, Duggleby2, and Driffield springs on the CFC-11-CFC-12 historical mixing curve. Note PFM (Piston Flow) and BM (Binary Mixing).

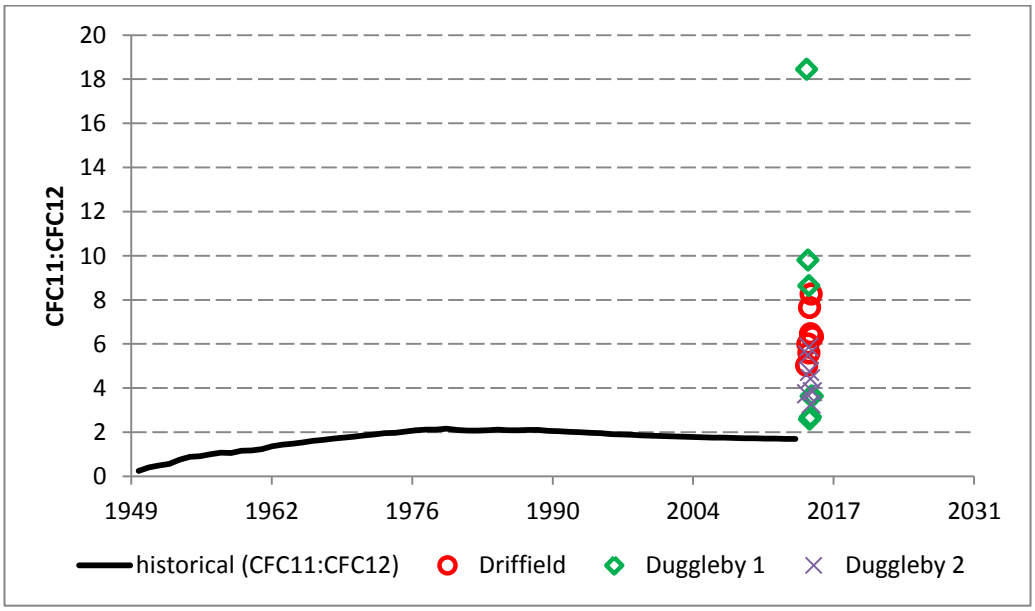

Figure 7-15 the CFC11: CFC12 ratio of the water samples from Duggleby1, Duggleby2, and Driffield springs on the historical ratio of the CFC11: CFC12

7.3.2. The result from CFC- Discharge relation:

The majority of the water samples showed that the groundwater is contaminated with both CFC-11 and CFC-12. The concentration of the CFCs in the water samples are plotted on the time series graph to understand the pattern of the concentration. The trend of the concentration of the CFCs in the contaminated water samples can potentially reveal information about the flow system in the aquifer.

Figs 7.16 and 7.17 show two types of trends with time in the water samples:

1) The water samples that collected at earlier months (February to May) of the year (early stage of the recession, with higher flows) contained higher CFC concentration and the concentration reduced with time toward the end of the recession (July to September). This is typified by CFC-11 in Duggleby 1 and CFC-12 in Driffield.
2) CFC concentration shows no large change across the recession period – there is variation between individual samples but no significant difference between the earlier and later parts of the time-series, i.e. Duggleby 2 for CFC-11 and both Duggleby 1 and Duggleby 2 for CFC-12. CFC-11 at Driffield shows a wider range of variation than these examples but no clear difference between early and late parts of the recession due to the high July value.

To understand if the concentration pattern of the CFCs in the samples can reveal anything about the predominant flow systems in the aquifer, the concentration of the CFC was compared to the flow rate.

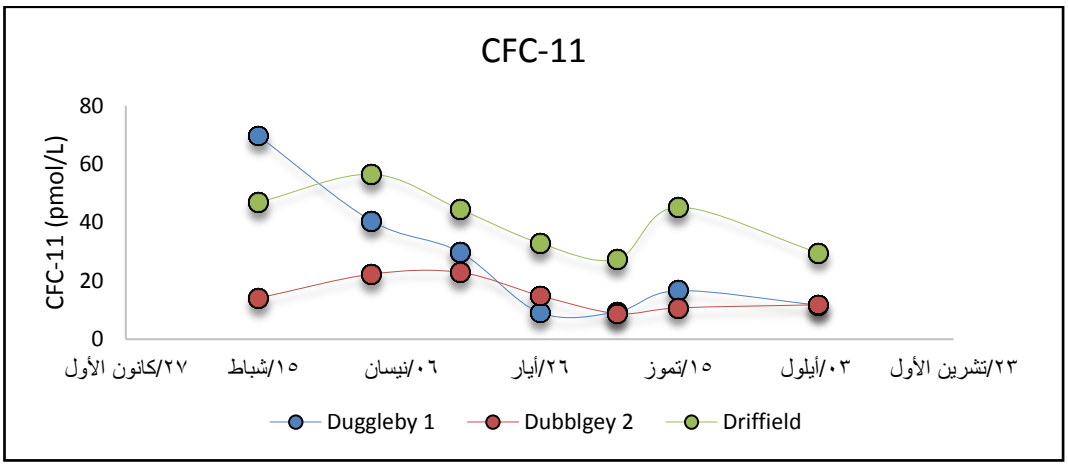

Figure 7-16 concentration of the CFC-11 in the Duggleby1, Duggleby2, and Driffield springs during the February to October 2015.

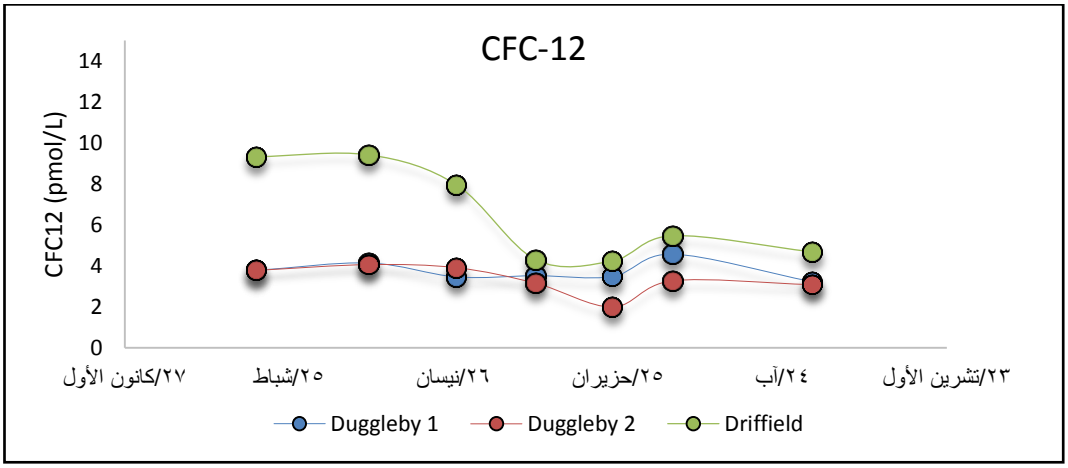

Figure 7-17 concentration of the CFC-12 in the spring water samples from Duggleby1 , Duggleby2 and Driffield springs during the February to October 2015.

CFC-11 and flow rate:

For better understanding the relation between the discharge (Q) and CFCs, they are plotted against each other, see figure (7.18). The relation showed that CFC-11 and Q in the Duggleby-1 spring are directly related with r-squared = 0.86 and CFC-11 concentration varies from ~10 pmol/L at lowest flows to 70 pmol/L at highest flows. By contrast, plotting CFC-11 vs. Q from Duggleby-2 shows no relation (the r-squared of their relation was 0.1), the concentration of CFC-11 fluctuated slightly (between 8 and 24 pmol/L) during the recession period of the spring. CFC-11 and Q from Driffield showed that there is a weak direct relation between them with r-squared 0.6. The concentration of the CFC-11 reduced from 55 to 35 (in average) pmol/L from early to late parts of the spring flow recession.

CFC-12 and flow rate:

For better describing the relation between CFC-12 and Q, CFC-12 and Q were plotted against each other.

For the Duggleby 1 and Duggleby 2 springs there is little relation between the CFC-12 concentration and the flow rate. The r-squared of the CFC-12 vs. Q relation from was 0.03 and 0.27 from springs Duggleby-1 and Duggleby-2 respectively, Figure (7.19). It is also apparent from this plot that the one low value of CFC-12 concentration in the Duggleby-2 data is not part of any consistent trend with discharge. Rather, it appears to be an outlier from the other data that would otherwise form a single group with no relation between CFC-12 concentration and Q with closely similar CFC-12 concentrations to the Duggleby 1 samples.

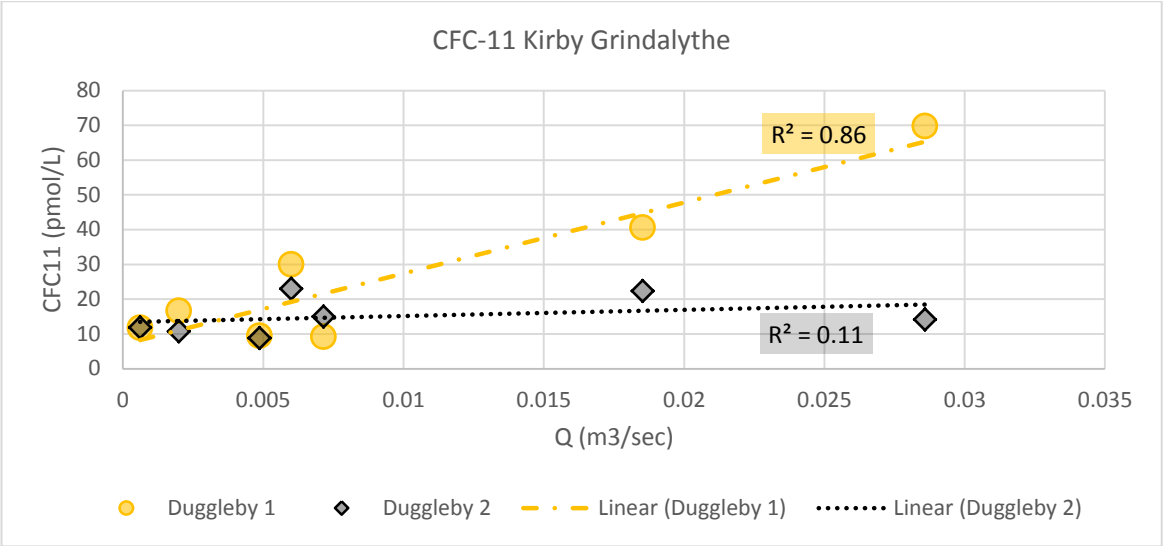

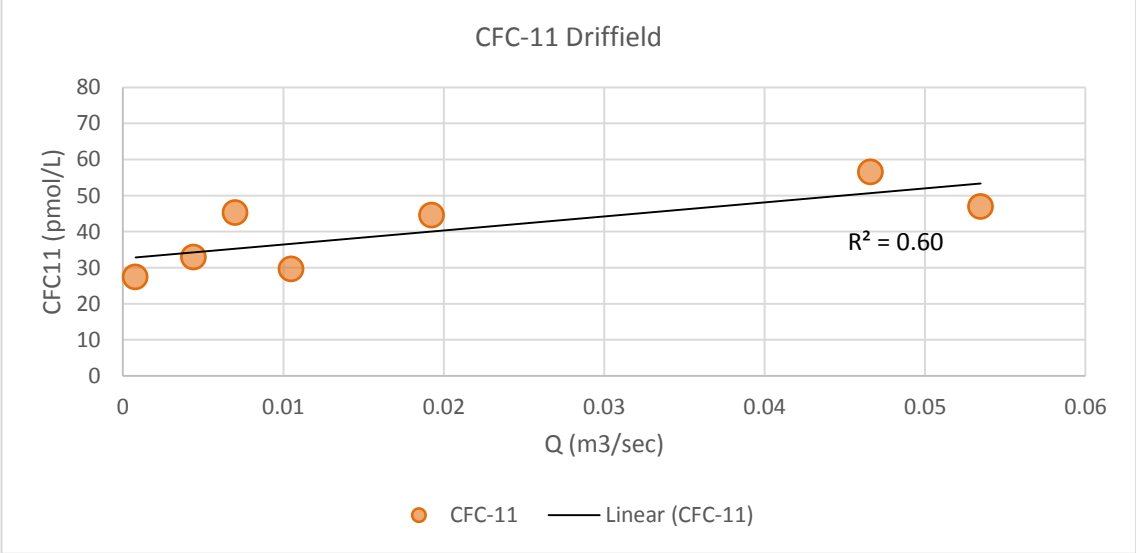

Figure 7-18 show the CFC11-discharge relation of the Duggleby-1 and Duggleby-2 springs from Kirby Grindalythe catchment.

However the relation from Driffield spring shows strong covariance of CFC-12 with Q (r-squared = 0.8784), with lower concentration during low flow and higher concentration during high flow rate. Under the flow rate, 0.02 m^3/sec the concentration of CFC-12 was between 4 and 6 pmol/L. The concentration of CFC-12 was increased, which was ranging between 8 and 10 pmol/L when the flow rate increased and exceeded 0.02 m^3/sec, see Figure(7.20).

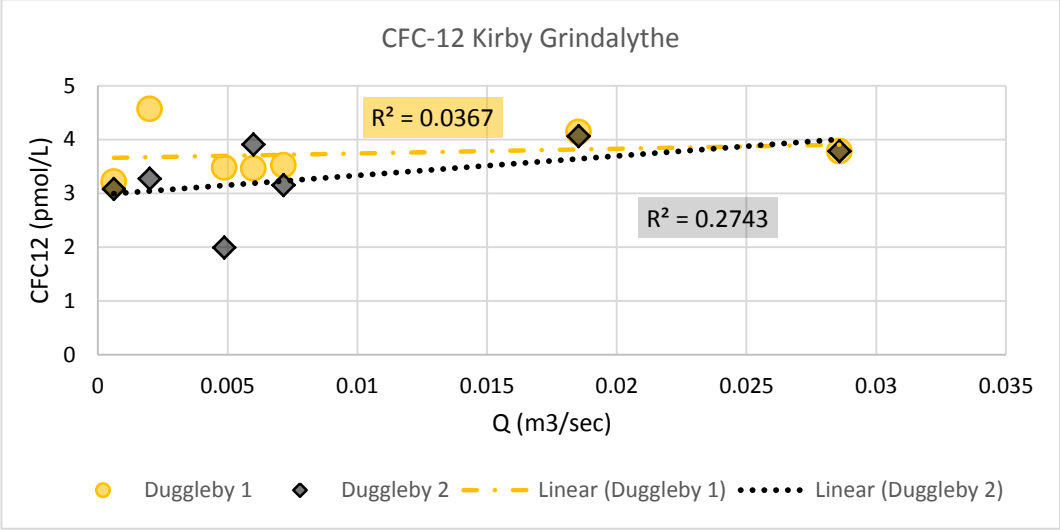

Figure 7-19 demonstrate the CFC12- discharge relation of the springs Duggleby-1 and Duggleby-2.

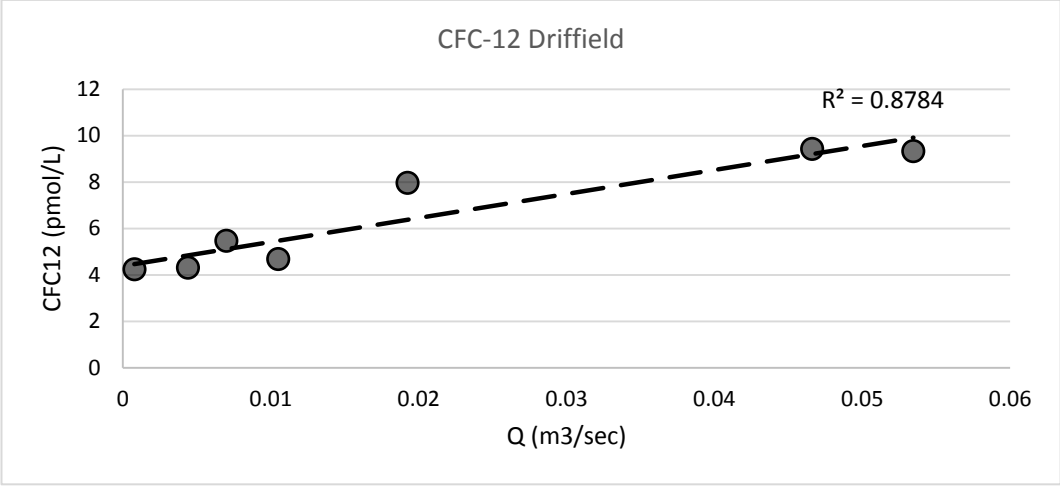

Figure 7-20 illustrate CFC-12 and discharge relation of the Driffield spring.

7.3.3. Result and interpretation of the ratio CFC11: CFC12:

Using CFC11: CFC12 ratio for estimating groundwater mixing in the aquifer:

Although this study did not benefit from CFCs ratio method for the groundwater age estimation, this method has been used for estimating mixing of the old and new groundwater. If the ratio in all water samples is the same, this means that mixing has not happened and all water came from the same source (and same recharge event) with a single CFC ratio. Significant changes in this ratio would mean that either the groundwater is a composite of the mixing of water from different sources (with different CFC ratios) or different recharge events when CFCs concentration was significantly different.

For the purpose of estimating the mixing groundwater between old and young water recharge the ratio of the CFC-11: CFC-12 from the spring water samples compared to the same ratio in the atmosphere with the equilibrium the groundwater, Figure (7.21). The historical concentration of the CFC-11 and CFC-12 in the atmosphere with the equilibrium to groundwater since 1990 and up to 2014 the ratio of CFC-11:CFC-12 showed very slight changes (appears as a near-horizontal line) from value 2 to 1.69. The ratio of CFC-11: CFC-12 in the water samples from Duggleby2, Driffield and 4 samples from Duggleby1 fluctuated within a horizontal envelope. While three samples from Duggleby1 showed a marked decrease in the ratio. In conclusion, the pattern of the CFC-11:CFC-12 ratio revealed that the water from Duggleby2 and Driffield more likely did not show the groundwater mixing as the ratio fluctuated within only a narrow range (which indicate that the CFCs from same source). While the pattern of the ratio of the CFC-11: CFC-12 from Duggleby-1 showed that the groundwater discharged by the spring is likely derived from two different water sources characterized by different CFC-11:CFC-12 ratios.

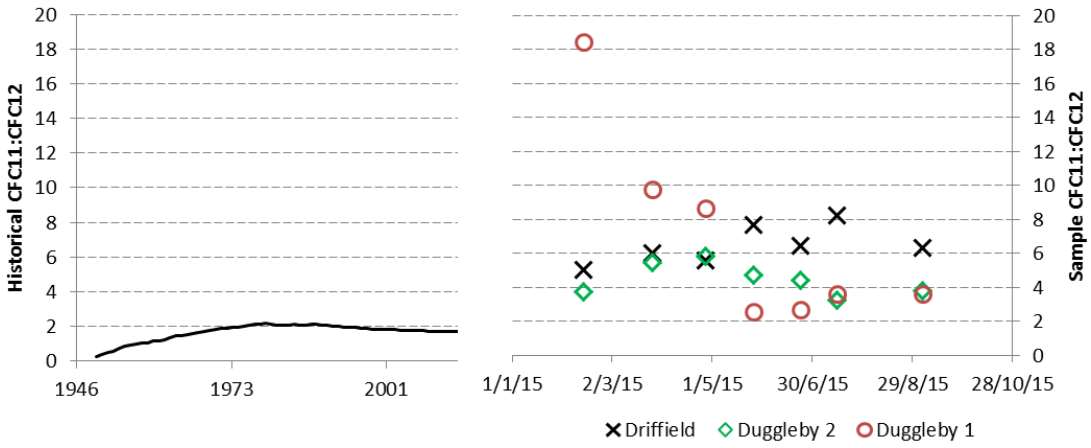

Figure 7-21 the pattern of the CFC11:CFC12 ratio in the atmosphere with the equilibrium of water and in the water samples from springs Duggley1, Duggleby2 and Driffield.

7.4. Uncertainty estimation:

Error due to estimating recharge temperature, excess air, uncertainty in the atmospheric input functions and errors caused by diffusion and dispersion would likely result in accuracy of apparent age ±4 years (Cook and Solomon, 1997). Based on the historical data records of the CFCs concentration in the groundwater in equilibrium with the air the ± 4 year for the period over 1990 this uncertainty is equivalent to about ± 3% of the equilibrium CFCs concentration.

In the groundwater samples, the concentration of the CFCs is measured by stripping the gases from the water sample and then injecting the gas into a gas chromatograph equipped with an electron capture detector (Bullister and Weiss, 1988). The accuracy of the analyis is approximately ± 3% for concentrations above 50 pg /kg; this threshold is equivalent to 0.36 pmol/L for CFC-11 and 0.41 pmol/L for CFC-12 (the units reported in Table 7-1) i.e. all measured samples are significantly above this threshold and a 3% analytical uncertainty is appropriate. Consequently, the total amount of uncertainty can be approximated by about 6% of the CFCs concentrations. Figure (7.10) shows the simultaneous plotting of time series CFC-12 and CFC-11 in

the Driffield spring with the error bar of 6% and the historical concentration of the CFC-11 and CFC-12 in the groundwater in equilibrium with atmospheric level. It can be seen that with the amount of 6% errors still the concentration of the CFC-11 in the groundwater much larger than the historical level. Similarly, the concentration of CFC-12 in the samples from Driffield spring and Duggelby-1 spring was bigger than the historical level. While with the 6% of the error in the data beside the sample from June 2015, which was already below the modern level, another two samples fall below the modern CFC-12 concentration. The sample from September 2015 returns to the recharge during 1994 and sample from May 2015 is from recharge during 1998.

The majority of the samples even after the estimated amount of error due to the uncertainty in the temperature and analysis processes still showed the CFCs concentration much higher than the modern level. This result concludes that the high concentration of the CFCs in the spring samples more likely came from contamination rather than the uncertainty in the samples.

7.5. Conclusions from CFCs analysis result:

Figure (7.22) has been constructed to show the general conclusion of the CFC-11 and CFC-12 concentration patterns, the relation between the CFCs and flow rate, and the relation of CFC-11 vs. CFC-12 in the collected spring water samples. This figure has been constructed according to the results from Figures (7.3, 7.14, 7.18, 7.19 and 7.20).

The samples from Duggleby 2 showed that the groundwater was subjected to the contamination with both CFC-11 and CFC-12 and that this contamination is characterized by a closely similar ratio of CFC-11:CFC-12 in all samples. In addition, there was not a noticeable relation between CFC-11 and. CFC-12 and flow rate. The concentration of the CFC-11 and CFC-12 fluctuated but regardless of the flow rate. Because the change in concentration of CFCs was not significant during the recession discharge the most probable explanation is that the source which feeds

the spring during a recession period is a single source, contaminated with both CFC-11 and CFC-12.

The water samples from the Driffield spring showed that the concentrations of CFC-11 and CFC-12 in the samples are proportionally related (in a similar ratio to Duggleby 2). However, in this case, they are also proportionally related to the spring discharge. The relation between CFC-11 and CFC-12 and flow rate may indicate the existence of two groundwater reservoirs that feed the spring one with lower CFC concentrations prevalent at low discharge and another with higher CFC concentration that contributes to flow during high flow. The fact that all these waters have similar ratio of CFC-11: CFC-12 may indicate a widespread source of contamination, but affecting different waterbodies to different extents..

The Duggleby 1 data shows a very different distribution to Duggleby 2 and Driffield data. At Duggleby 1 there is a relatively restricted range of CFC-12 concentrations but a wide range of CFC-11 concentrations, up to values higher than measured at the other sites. There is therefore a much wider range of CFC-11: CFC-12 ratios in the Duggleby 1 data, ranging to much higher values than at the other sites. There is also a relation between CFC composition and flow rate; at the high flow rate, the relation of CFC-11 and. CFC-12 in the spring water samples changes, the groundwater becomes intensively contaminated with CFC-11 compared to the CFC-12, and the latter does not show a significant change in concentration. This result implies that two sources of groundwater feed the Duggleby 1 spring – one with lower CFC-11: CFC-12 ratio predominant at low flow and a source with a much higher CFC-11: CFC-12 ratio contributes at high flow. The lower CFC-11: CFC-12 ratios at Duggleby 1 are similar to those at Duggleby 2 and may represent the same widespread contamination source.

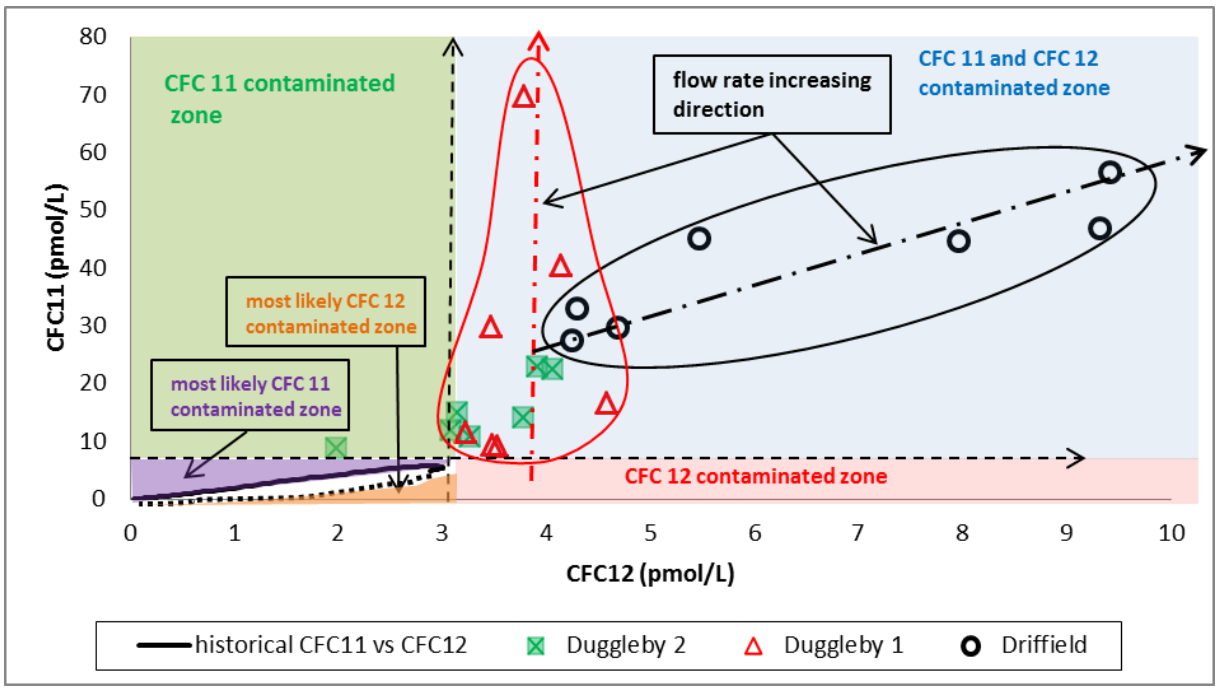

Figure 7-22 The solid black curve represent the historical CFC11 vs. CFC12 in the water in equilibrium with air, the circle, triangle and square marker points represent CFC11 vs. CFC12 in the water samples.

7.5.1. Evaluate the reason of the contamination:

The source of the contamination expects to be rise either from landfilling, contaminated near surface atmospheric air locally enriched in CFCs or from contaminated equipment.

Contamination due to the sampling bottle and sampling equipment will not produce a significant change in the pattern of the CFC in the groundwater. Flushing water during the sampling process helps in removing the CFC on the equipment due to its contact with the air. As a result, the possibility of the contamination of the bottle and sampling equipment is little.

Even if the trace of contamination with CFC remained on the equipment after flushing and transformed into the sampled waters, this contamination will not

produce a change in the general pattern of the CFC in the ground water. The concentration of the CFC in the modern atmosphere is higher than the old groundwater, and the groundwater contains a certain amount of the CFC. So if the groundwater during sampling contaminated with the CFC from the equipment, the original value of the CFC in the groundwater would enhance by the CFC which came from the equipment according to the mixing ratio principles.

$$CFC_{in\ water\ sample} = CFC_{in\ groundwater} + CFC_{in\ equipment}$$

In The Kirby Grindalythe catchment, groundwater contamination with CFC due to the local activity is unusual. It is located in a rural area where the probability of the air contamination by the CFCs due to local activity is rare. However, there is a possibility that the contamination through leaching CFCs from a point source, e.g. from a broken refrigerator has been thrown in the area.

The Driffield catchment, even though it located close to the urban area but it located upward side of the groundwater flow direction considering the location of the Driffield town. Which means any contamination of the groundwater in the town due to the leaking gas from equipment or buried equipment does not affect groundwater at the Driffield catchment.

Indeed, the source of contamination is not clear; the prospects of contamination indirectly from the air and directly from the ground will take in consideration as two possible scenarios.

First scenario the contamination comes from the ground:

There are no significant landfill sites in and around the catchments for the burial of wastes, especially near Kirby Grindalythe catchment, see Figure (7.23). Unless the residents are throwing and bury refidgeration equipment (such as a refrigerator) randomly in the area. Simple mass balance reveals that less than 1/10th of the amount of CFC-12 existent in a single domestic refrigerator could contaminate a

moderately sized aquifer to more than 10 times current atmospheric levels Morris et al. (2005).

According to the geological and hydrogeological situation of the catchments that feed springs Duggleby 1, Duggleby 2 and Driffield, it is not likely that all three catchments contaminated with same source of CFCs via ground. Assuming that there is landfilling area and caused the contamination, how could all the three springs is contaminated at the same time? The Kirby Grindalythe catchment is far from the Driffield aquifer, so the probability of hydrological interconnection between these two catchments is weak. Even in the case where these two aquifers were interconnected, the geological model of the area shows that the springs Duggleby1 and Duggleby2 in the Kirby Grindalythe catchment are flowing from two separated Chalk bodies. So the probability of contamination due to the landfilling might not describe the contamination of the three springs concurrently.

Second scenario the contamination comes from the air:

Based on information from the National Recycling Campaign for England called Recycling Now, several locations are available in East Yorkshire for recycling fridges and freezers. Figure (7.23) shows a map of sites for recycling fridges and freezers in East Yorkshire. Because of the wind, CFCs at the recycling sites from broken freezers or from industrial activity that happens in the industrial zone might spread to the surrounded areas and contaminate the air with the CFCs.

The analysis of CFC contamination (Section 7.4 above) showed a contaminant source with a low CFC-11: CFC-12 ratio that was widespread across all three catchments and a source with high CFC-11:CFC-12 ratio that affected Duggleby 1 only. The most likely (though not proven) explanations are:

A widespread airborne CFC source with low CFC-11: CFC-12 ratio that affects different catchments (and parts of catchments) differently. This has highest

concentrations at Driffield (compared to the Kirby Grindalythe catchment), which may be closer to the source.

A more local source with high CFC-11: CFC-12 ratio that affects one spring (Duggleby 1) in the Kirby Grindalythe catchment and may be the result of a local point source due to improper disposal, see figure (7.24).

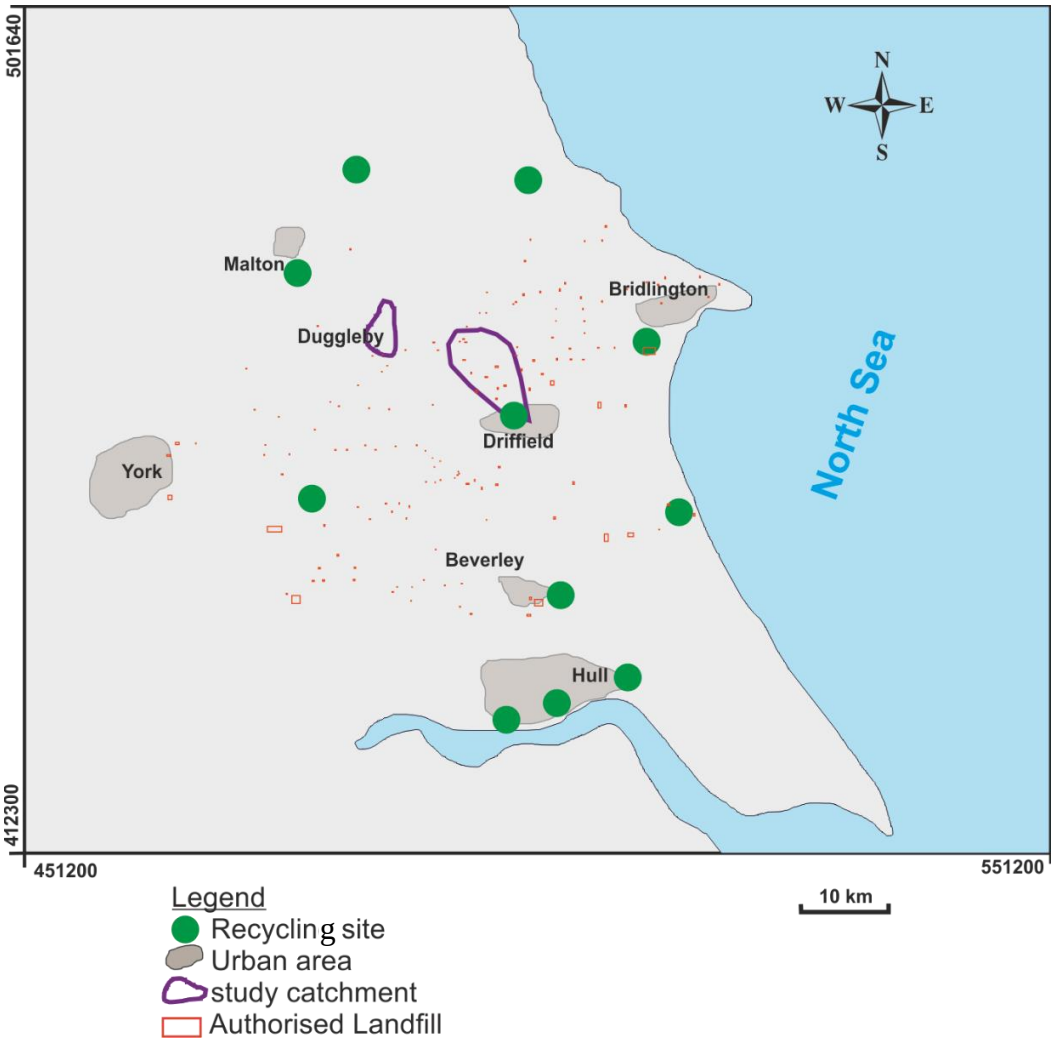

Figure 7-23 location of the Recycling fridges and freezers in the East Yorkshire. Locations of the recycling site from the map by the Recycling Now a national recycling company, the landfill locations from Environment Agency pam.

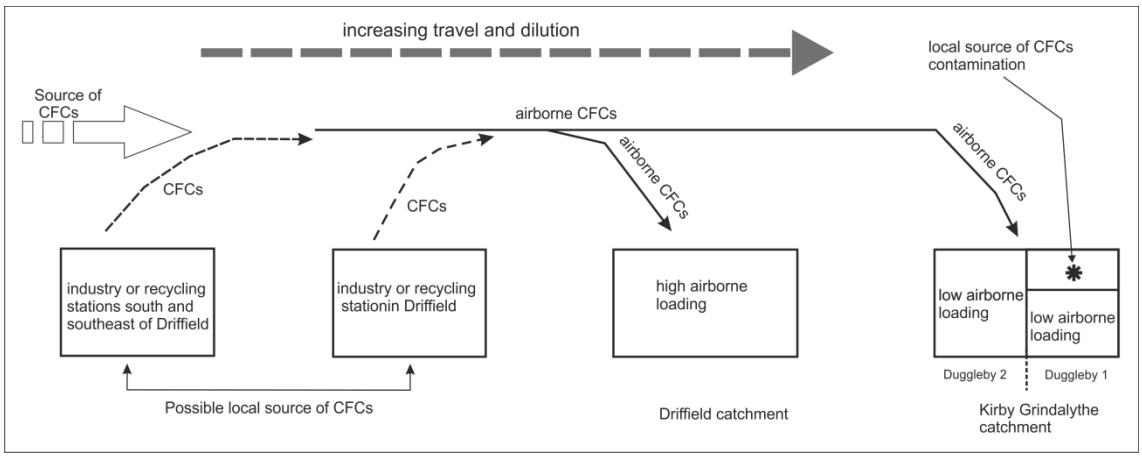

Figure 7-24 conceptual model explain the possible source of the groundwater contamination by CFCs in the study catchments.

7.6. Interpretation:

7.6.1. Interpretation of the sample which contains CFC-12 less than the Modern air/water equilibrium value:

Interpretation the non-contaminated water samples:

Only one sample among all collected samples contained the CFC-12 lower than the modern air/water equilibrium value. The sample was from the Duggleby2 spring in the Kirby Grindalythe catchment collected during the low flow stage on 23 June 2015. Plotting this sample on the historical concentration curve of the CFC-12 compound in the air in the equilibrium with water shows that the water sample returns to the water recharged during 1983. This means the resident time of the water in the aquifer is about 32 years (or more because there is a contamination component).

However evidence showed that this sample more likely appears as an outlier because:

- First; the sample which showed CFC-12 concentration lower than the atmospheric level (in equilibrium with groundwater) was from June which is nearly during the middle way of the recession period. While the samples in August and September, which are near the late stage of the discharge recession, showed the concentration of CFC-12 higher than the sample from June, and more than the atmospheric level. In the natural case, the sample from the very late stage of the discharge recession represent the base flow from the very low flow system in the aquifer with the oldest resident groundwater, therefore the CFCs should be showing water from the older recharge event.
- Second; the sample lies off of the piston flow/mixed flow lines. So it does not have an interpretable age in terms of CFC-11vs. CFC-12 behaviours.

The most likely reason for this this sample to be outlier is uncertainty during the sample analysis.

7.6.2. Interpretation of the sample which contains CFC bigger than the Modern air/water equilibrium value:

Determination age from the contaminated water with CFCs is not possible unless there are local historical records of CFCs concentration in the air on the local scale. In the study area the local historical CFCs have not been recorded, therefore, the samples that show contamination do not give information about the age of the groundwater.

The Duggleby 1 spring is interpreted to contain two reservoirs of groundwater:

1) highly contaminated with CFC-11 from a local point source;
2) More weakly contaminated with CFC-11, similar to the Duggleby-1 springs.

The highly contaminated source predominates at high discharge giving very high CFC-11 concentrations (Figs 7-18, 7-22). The point source contamination has

“labelled” one reservoir with CFC-11; during recession the mixing ratio between the labelled reservoir and the “background” reservoir changes.

The Driffield spring shows a strong relation between degree of CFC contamination (both CFC-11 and CFC-12) and discharge (Figs 7-18, 7.20, 7-22), with higher concentrations at higher flows. This may also indicate two groundwater reservoirs one more highly contaminated and one less so.

There is no clear relation between CFC compositions and discharge in the Duggleby 2 spring. This might indicate a single reservoir; if multiple reservoirs exist they must have closely similar levels of CFC contamination.

From combining the result from CFCs vs. Q and result of analytical interpretation (Chapter 6) from same spring can be deduced that in the dual reservoir aquifer, the high flow stage of the recession curve represent the discharge from the high fractured zone in the aquifer, and low flow stage represents discharge from the low permeable zone (was explained in chapter 6 analytical interpretation of the recession curve). At the low flow stage of the recession period, the CFC-11, and CFC-12 in both Duggleby1 and Driffield were directly related, whereas the degree of contamination with CFC11 and CFC12 in Duggleby1 and Driffield respectively was greater during the high flow rate. This indicates that these elevated levels of CFC-11 and CFC-12 due to a quick propagation of a recent contamination event to the spring through the large fractures zone.

Analytical interpretation (chapter 6) concluded that the Kirby Grindalythe catchment behaves as a single reservoir aquifer, but Duggleby2 spring revealed that the part of the catchment which feeds this spring contains two flow systems.

7.7. Findings

The majority of the water samples showed that groundwater had been contaminated with the CFC as it been found the concentration of the CFC in the sample higher than the concentration of the CFC/in equilibrium with water in the modern air. Only one sample from Dugleby-2 contained a concentration of CFC-12 lower than modern air, and this sample estimated that recharge was returning to the year 1983. According the CFC-11 vs. CFC-12 this sample considered as an outlier as the sample lies off of the piston flow/mixed flow lines.

CFC-12 shows that the groundwater from the Kirby Grindalythe spring feed by a single reservoir, while two reservoir feeds the spring in the Driffield, high conductive and low conductive flow system.

The pattern of the CFC-11 vs. CFC-12 indicated that the catchment which feeds the Duggleby-2 consist of the single flow system, while the catchment which feeds Duggleby-1 and Driffield spring contain two flow systems.

The relation between the ratios of CFC-11: CFC-12 in the water samples and the historical ratio of the CFC-11: CFC-12, revealed that most likely the Duggleby-1 spring feeds by two sources of groundwater. While the springs Duggleby-2 and Driffield feeds by a single source.

Chapter 8. Numerical Modelling

8.1. Introduction:

Groundwater models are computer models used to simulate and predict aquifer conditions (Anderson and Wessner ,1992). Models are not reality but approximate reality based on some simplifying assumptions. The reliability of any model depends on how well the model represents the field situation (Wang and Anderson, 1995).

Numerical models are mathematical models which can produce approximate solutions to groundwater governing equations through the discretization of space and time. Through systematisation, the field parameters in numerical models can be used to translate the conceptual model and answer questions about the functioning of an aquifer. Since the 1960s, numerical modelling has been an indispensable technique for simulating groundwater. It is a tool which provides an opportunity to analyse many groundwater problems (Wang and Anderson, 1982; Anderson and Wessner, 1992;Wang and Anderson, 1995).

The finite difference method is one of the most popular methods for solving the groundwater flow governing equation (Stevens and Krauthammer, 1988; Magnus and NJ, 2011). In 1984, the United States Geological Survey (USGS) released the first version of a three-dimensional groundwater model, which is known as MODFLOW (McDonald and Harbaugh, 1984). MODFLOW, which is a finite-difference groundwater model built to simulate groundwater numerically, was developed using Fortran 66 code (Harbuagh, 2005). Whilst MODFLOW was originally designed to simulate groundwater flow, over time its applications have increased. Among these applications, MODFLOW modelling of equations for solving pollution transport problems is one of the most important.

Numerical modelling helps in understanding the physical behaviour of aquifer systems, groundwater flow in saturated and unsaturated zones, contaminate transport

through rocks, surface – subsurface water interaction, effect of artificial water bodies on groundwater, effect of pumping on groundwater depletion, etc. (Dagan et al., 1991; Tian et al., 2015).

Modelling is widely used in groundwater investigations, and is applied in groundwater management (Island, 2004), groundwater tracing (Simpson et al., 2011) and study of groundwater flow systems (Martin and Frind, 1998; Rani and Chen, 2010).

In general, the model for conceptualizing the fractured aquifer consists of low permeability matrix blocks separated by highly permeable fractures (Langevin, 2003). The equivalent continuum model, which is often referred to as an equivalent porous medium (EPM), is one of the most commonly used methods for simulating groundwater in the fractured aquifer (Lagevin, 2003). According to EPM, the heterogenetic fractured system can be conceptualized in a numerical model by dividing the system into a small number of regions of different hydraulic conductivity, with each region modelled as an equivalent porous medium. The assumption of this conceptual model is that flow through the fractures is similar to that through porous media that have equivalent hydraulic properties (NRC, 1996). Nyende et al. (2013) used EPM for numerical simulation of fractured aquifers in different catchments of Uganda. Gburek et al. (1999) applied groundwater modelling to determine watershed scale aquifer parameters in a layered system. They determined the parameters by calibration of the model to the observed data, e.g. they determined specific yield through calibration of the model against the recession curve of the stream base flow, and hydraulic conductivity from calibration of the model with groundwater levels from streams and boreholes. As the study catchments of this project consist of Chalk, which has a fractured aquifer system, the same EPM assumption will be applied for simulating the flow system.

One of the important tests during the calibration process of numerical modelling is sensitivity analysis. Sensitivity analysis is the assessment of model input parameters to see how much they affect model outputs. In a sensitivity analysis, comparisons are

made between outputs from the refined numerical model when the input parameters are changed (Rushton, 2005).

In the current study Groundwater Vistas (GV) was used for constructing the numerical models. GV is a software user-interface for groundwater flow and contaminant transport modelling, which supports MODFLOW and MODFLOW related codes. An overview of the groundwater numerical modelling process in this study is demonstrated in the schematic diagram, see figure (8.1).

8.1.1. Modelling objectives:

It is important to define the objectives of the numerical modelling at the beginning of the modelling process. It is essential that the modelling objectives meet the overall objectives of the study.

The main objectives of modelling in the current study can be summarised as follows:

- Simulating groundwater flow in the unconfined Chalk aquifer in East Yorkshire; the study will concentrate on examining Kirby Grindalythe and Driffield Chalk aquifers.
- Generating spring hydrograph recession curves during the period when recharge is absent.
- Calibration of the models' recession curves with those from the real aquifers. For achieving calibration, the model will be tested against several aquifer scenarios.
- Interpretation of the results in terms of aquifer structure, hydraulic properties, and boundary conditions.

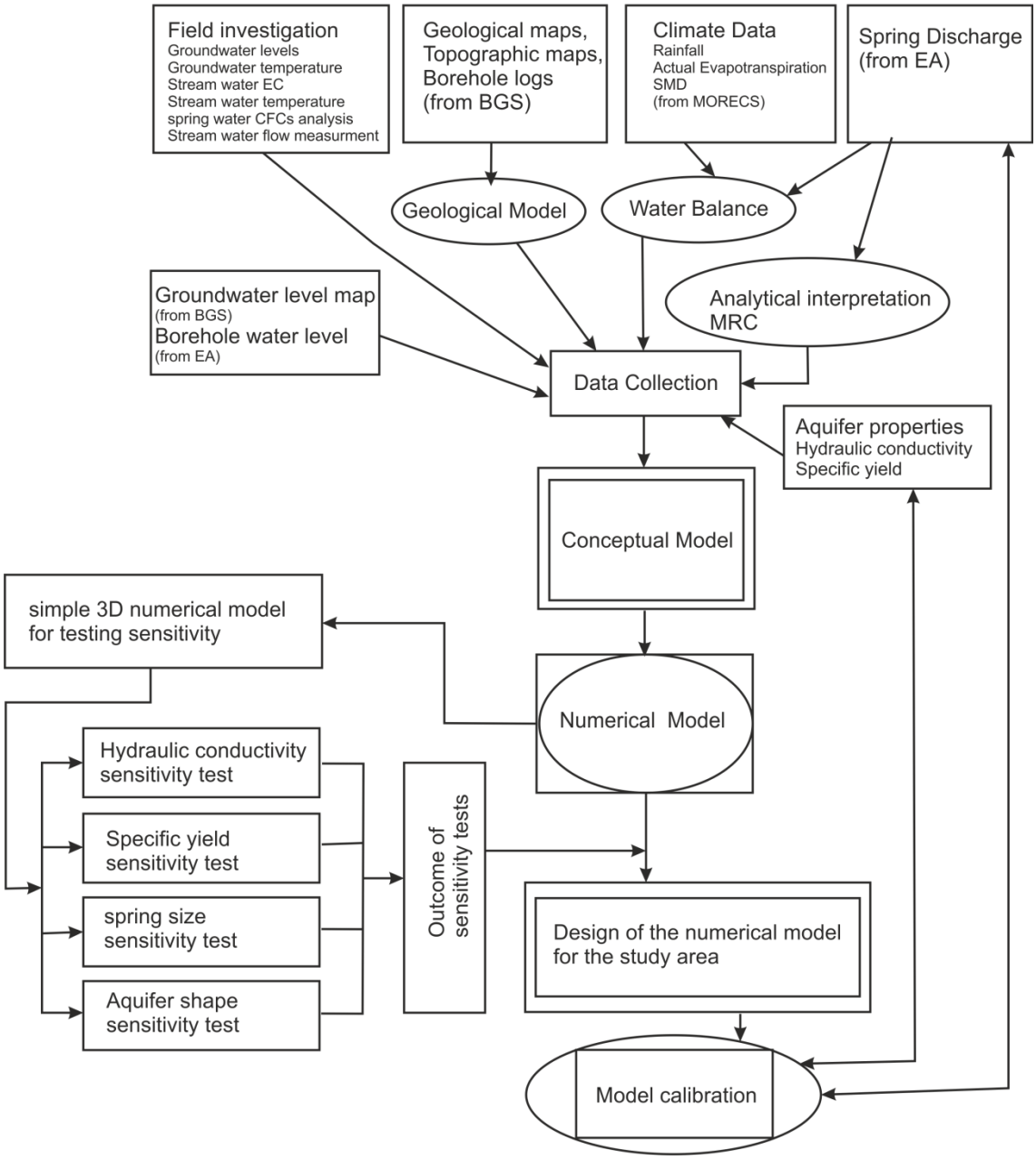

Figure 8-1 Schematic diagram of the models developing processes.

8.1.2. Factors that Contributed to development numerical model for study catchments:

Springs and drain cells:

Springs can be found in the Kirby Grindalythe and Driffield catchments. The discharge of groundwater from the aquifer to the surface through springs is a crucial factor in the models. For simulating the springs the study focused on the drain cells, using the MODFLOW drain package provided by McDonald and Harbaugh (1988). The drain cells remove water from the aquifer in proportion to the difference between the hydraulic head in the aquifer and the elevation of the drain cell (Batelaan and Smedt, 2004). Flow rate at the drain cells is thus proportional to the hydraulic gradient. Water will flow from drain cells whenever the water head is above the drain elevation, while the drain cells switch off when the water level in the model falls below the drain elevation.

The aquifers examined in this study are unconfined aquifers, from which the water discharges through a number of springs. Fundamentally the water that discharges from an unconfined aquifer through the springs is strongly related to the head in the aquifer (linear behaviour of the aquifer). The drain cell in the numerical model would behave in a similar manner to a spring from an unconfined aquifer and drain cells are thus capable of simulating springs. Consequently, drain cells were used in the numerical models constructed in this study to represent the springs.

Recharge:

Rainfall is the most important source of groundwater recharge in the area. However, in the constructed models, recharge was set at zero, because the models were intended to simulate flow from the aquifers during periods when recharge was absent, in other words, during the recession period. Therefore, rainfall and recharge were not included as factors in the numerical models constructed in this study.

Representation of springs:

Groundwater flow direction in the study catchments is mainly dominated by the topography as explained in section (3.2.1).

In the selected catchments, the gauging stations at the studied locations were expected to be the locations where all discharge water from the aquifer would congregate. Therefore the gauge station locations were assumed to represent the main springs in the catchments, and in the numerical models this was simulated by means of a single drain cell. Besides the use of this drain cell to simulate the spring, more drain cells were placed in the numerical model to simulate the subsurface discharge from the catchment.

Cell and layer size:

Selecting the appropriate cell size is a critical task in numerical modelling, in order to increase the probability that the model will adequately represent the real system (Faust and Mercer, 1980).

For both the Kirby Grindalythe and the Driffield numerical model a cell with surface dimensions of 100x100m and vertical thickness of 2 – 5 m was selected. This cell size was considered suitable for this area based on the availability of hydraulic data such as transmissivity and storage. The selected thickness provided the models with 5 to 10 layers, which was considered sufficient to represent heterogeneity in terms of vertical permeability and to represent zones of groundwater fluctuation in the aquifer at between 2 and 5 meters. Multi-layer models were needed for testing vertical hydraulic conductivity variations.

8.2. Parametrization:

Parameterization means representing the system in a form that expresses our understanding (Bear and Cheng, 2010). In terms of parameterizing an aquifer system, its behaviour will be dependent on the set of assumptions made.

8.3. Limitation and Reliability of model:

All numerical models are subject to limitations and errors because they simulate conceptual models which were subjected to a set of simplifying assumptions, e.g. regarding catchment shape and size, the hydrogeological relations between aquifer units, climatic conditions, and the aquifer's hydraulic properties. Perhaps more importantly, aquifer hydraulic parameters such as transmissivity, storage co-efficients, and distribution of the heads within the aquifer are seldom known accurately.

From this standpoint, the areas examined in this study can be considered simple sites. The aquifer stratigraphically consists of one geological unit which is Chalk, and is structurally very simple as no folds or big faults exist in the bedrock. The catchment areas are mainly covered with highly permeable soil. As the modelled catchments are small in area they are not subject to significant spatial variations in climatic and atmospheric factors. The amount of water which is abstracted artificially from the aquifers is small compared to the amount of recharge.

8.4. Identification of required information:

In the current project, the main aim of modelling is to determine the physical behaviour of spring discharge from the Chalk aquifer in East Yorkshire, i.e. to determine the extent to which spring recession curves can be used as a tool for interpretation of aquifer structure. The main information used was spring flow rate (recorded with a suitable time interval) and detailed information regarding the aquifer and catchment area, including geologic, hydrogeologic and topographic data.

Information on aquifer properties such as transmissivity and specific yield, the boundary condition of the aquifer, and feasible range of hydraulic head was also used to constrain the models. Table (8-1) lists the information and information sources used in model development and calibration.

8.5. Simple Models:

At the early stage of the modelling process, the models constructed to test the conceptual model were simple and regular in geometric shape. A very simple aquifer model was constructed to investigate the proposed boundary and initial conditions viable for producing model recession curves. The model consisted of 21 rows, 20 columns, with cell dimensions of 100 x 100 m to represent an aquifer of 4.2 km^2 surface area (catchment), and 20 layers to represent 100m thickness. Figure (8.2) is a schematic diagram illustrating the 3D model.

These simple 3D models were run in both steady and transient flow phases. A steady state phase was used for choosing an appropriate initial head for the aquifer (starting a transient simulation from a steady state head condition helps to reduce the running time during simulation). A transient phase was used to understand how the aquifer behaves over time, with the falling head representing a spring recession period. The model in the transient state was run for about 180 days to simulate the recession period of the spring discharge in the study area.

Table 8-1. Showing list of data which have been used during the modelling, also showing the source of the data.

Type of data	**Source which provided the data**	**Data interval**	**Data duration**
Flow discharge at Kirby Grindalythe gauging station	Environment Agency	Daily	2000-2015
Flow discharge at Driffield gauging station	Environment Agency	Daily	2000-2015
Actual evapotranspiration (daily average for grid square 94)	Met Office	Daily	2010-2015
Rainfall (daily average for grid square 94)	Met Office	Daily	2010-2015
Soil Moisture Deficit (daily average for grid square 94)	Met Office	Daily	2010-2015
Transmissivity	Parker (2009); Gale and Rutter; 2006 Boreholes (BGS)		
Water table	Gale and Rutter; 2006		
Borehole information	BGS http://www.bgs.ac.uk/data/boreholescans/home.html		
Borehole Water level fluctuation (Low Mowthorpe and Northend boreholes)	Measured in this study	15 minute	2013-2015

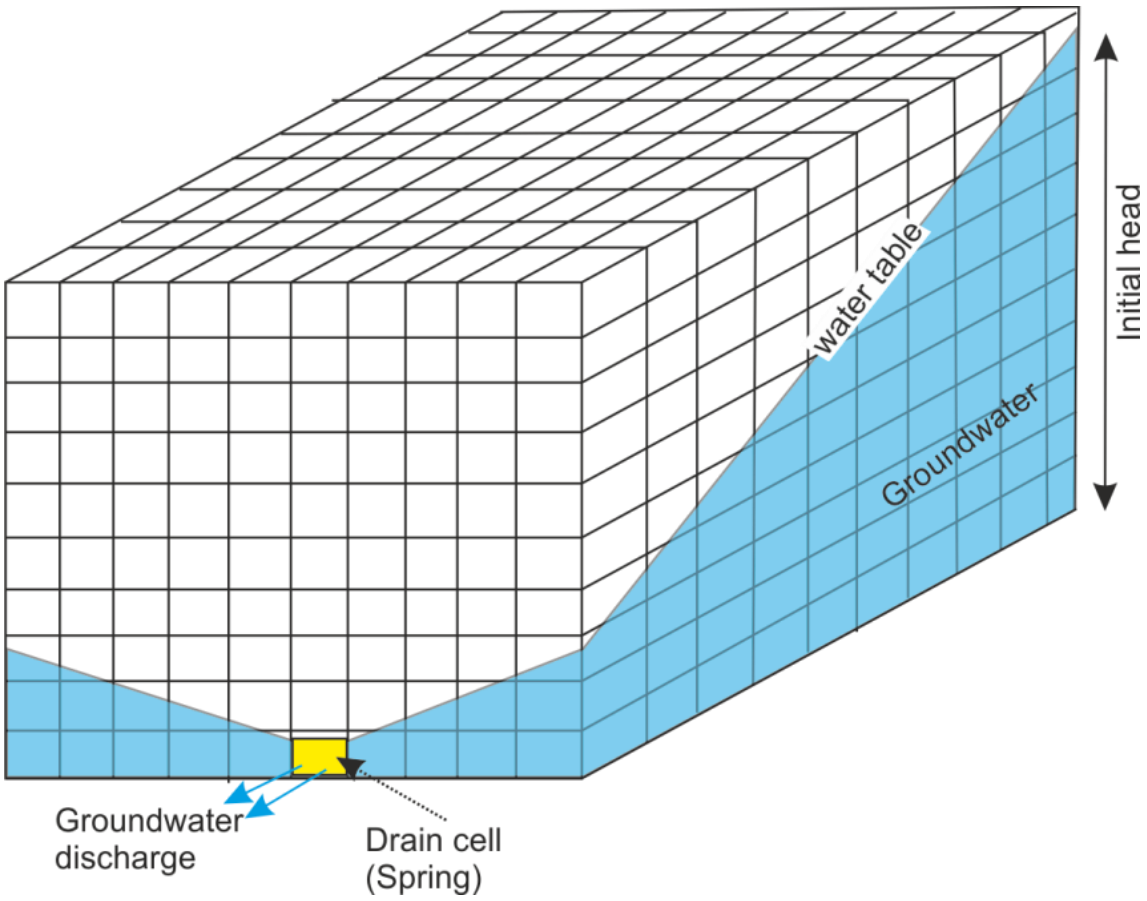

Figure 8-2. Schematic diagram, show geometry of 3D simple model and also demonstrate the boundary and initial condition of the simple model construed to simulate spring discharge from unconfined aquifer. Note: this diagram is a similar copy not an exact copy of the simple model constructed in this study. The number of the layers and rows reduced in this demonstrated diagram in order the cells appear in a bigger size (because the smaller size cells in the figure difficult to recognize).

The model was surrounded and underlain by no-flow zones. Water drains freely from the aquifer through the drain cell, under the influence of the earth's gravitational field (the aquifer is represented as unconfined). For this purpose a cell at the level of the base of the model was selected to be set up as a drain cell for draining water from the model. Hydraulic conductivity of the drain cell was set very

high in order not to mask the hydraulic properties of the model. Hence, drainage rate and hydraulic head variation in the aquifer would be controlled by the conductivity of the aquifer.

Below, section 8.7 describes further 3D models developed to represent the real aquifer catchments. These were used for evaluating the effect of aquifer hydraulic factors on spring discharge behaviour.

8.6. Sensitivity analysis:

Since various internal and external factors affect the pattern of the spring recession curve, to understand the intensity of each factor separately a sensitivity analysis of the simple model was undertaken. The main parameters of the simple model are the initial head, hydraulic conductivity, and specific yield, while hydraulic head and discharge versus time are the main outputs. In the simple model, it was assumed that the topography is horizontal, and during the recession period the recharge is zero; therefore, the sensitivity of ground surface topography and recharge variation was not tested.

8.6.1. Sensitivity to hydraulic parameters:

Hydraulic conductivity sensitivity test:

During sensitivity testing, the initial condition in the models was changed depending on the aim of the test. Where testing was to discover sensitivity of hydraulic parameters, the models were run with the same initial conditions during every test. These conditions included no recharge, model setup with initial condition of 100m initial head (above the base on the model), storage co-efficient of 0.01 (because the model represented an unconfined aquifer a value typical of specific yield was selected).

The results from analytical interpretation of MRC curves and CFC analysis for Kirby Grindalythe and Driffield catchment indicated the possibility of more than one flow system existing in the aquifer. Depending on this consequence, the sensitivity testing of the model was conducted under two case scenarios: in the first scenario the aquifer consisted of a single reservoir, and in the second scenario the aquifer consisted of two reservoirs with different hydraulic properties.

A. Single reservoir model: this model simulated the homogenous and isotropic aquifer. The model aquifer was of 100m thickness. The hydraulic conductivity of the system was changed between the repeated tests from 10 to 50 to 100 m/day.
B. Double reservoir model: this model was constructed to simulate a heterogeneous aquifer, consisting of two reservoirs, with different hydraulic properties. One reservoir represented a high permeability zone, corresponding to the fractures enhanced by dissolution activity, i.e. fractures where the maximum flow occurs. The second reservoir represented the cumulative effect of the matrix, small fractures with lower permeability, representing a zone that has been subjected to less water flow and fracture solution enhancement is therefore less well developed. This model was tested in three cases, with the value of K in the low flow zone being 1 m/day in each case, whereas the value of K in the high flow reservoir was changed between the repeated tests from 10 to 50 to 100 m/day.

    a. Parallel horizontal reservoir model: The high permeability lower zone corresponded to a zone just below the level of water table fluctuation. This zone is recognised to have very high hydraulic conductivity in chalk aquifers because of fracture enhancement due to calcite dissolution. The low permeability upper reservoir represented the cumulative effect of the matrix and small fractures. The thickness of the high permeability reservoir was 25 m and the thickness of the low flow reservoir was 75 m. In this model, the top reservoir represented the low permeable system and

the bottom reservoir the high permeable system. The highly permeable reservoir was placed at the bottom of the model, where the spring existed, because placing the lower permeable reservoir at the bottom would have masked the effect of higher permeability on the spring discharge.

b. Tunnel Model: this model was used to simulate a relatively low permeability aquifer containing a longitudinal tunnel-shaped high permeability zone at the drain cell level. This geometry represents a high permeability major fracture zone or solution conduit. The highly permeable zone works as the transporting medium and the less permeable surrounding rock as a storage reservoir.
c. Parallel vertical model: this model assumed that a zone of enhanced fracture network interconnected the full thickness of the aquifer with the spring outlet. Hence, a vertical transversal high K plane was cut through all the model layers in the direction of the spring outlet.

Specific yield sensitive test:

During sensitivity testing of the simple model for S_y, the K in the model was 100 m/day, while the S_y of the system was changed during the repeated tests from 0.01 to 0.03 and 0.5.

8.6.2. Sensitivity to a number of drain cells:

The catchments used in this study are of various shapes. Kirby Grindalythe is a fan-shaped catchment, while Driffield is leaf shaped. To investigate the effect of the shape of the catchment on the recession curve, the model was tested under different catchment shape conditions. For this test, a simple rectangular box shaped model was designed, which was then tested twice, transversely and longitudinally. In the first test, the drain cell was placed on the shorter side, whereas in the second test it was placed on the longer side.

The results and discussion of the sensitivity analysis conducted to explain the effect of aquifer type on MRC can be found in appendix 4.

8.6.3. Sensitivity to the shape of the catchment:

Shape of the catchments used in this study various. Kirby Grindalythe has a fan-shaped catchment while Driffield leaf shaped catchment. To investigate the effect of the shape of the catchment on the recession curve, the model tested under the different catchment shape conditions. For this test, a model was designed in a simple rectangular box shape, which was then been tested twice, transversely and longitudinally. In the first test, the drain cell placed on the shorter side whereas, in the second test, it was placed on the longer side.

The results and discussion of the sensitivity analysis for explaining the effect of aquifer type on MRC can be found in appendix 4.

8.7. Key learning points from the simple models regarding the effect of aquifer type on recession curve shape:

Simple 3D numerical models were constructed to simulate the recession stage of spring discharge from an unconfined aquifer. The models were tested in two cases: first, with the aquifer consisting of a homogenous single reservoir, and second, with the aquifer consisting of double reservoirs. The double reservoir model was tested in four case scenarios: double reservoir, horizontally parallel model; double reservoir aquifer, tunnel model; double reservoir parallel vertically; and vertical plane, high permeable zone, see figure (8.5).

The sensitivity tests accomplished included: hydraulic conductivity, specific yield, aquifer shape and number of the drain cells (to represent either the spring or subsurface discharges beneath the stream bed). In the double reservoir model the

effect of changing the size of the low and high flow reservoirs relative to each other was also investigated. The purpose of the sensitivity tests was to examine how changes in aquifer structure and properties influence the shape of the recession curve.

Hydraulic conductivity, single reservoir model: decreasing hydraulic conductivity decreased the slope of the recession curve. The maximum discharge at the start of the recession is directly related to the hydraulic conductivity, see appendix 3.1 Figure appx 3.1. This relation provided the opportunity during model calibration to select a suitable hydraulic conductivity for producing a specific starting discharge.

Hydraulic conductivity and reservoir sizes, double reservoir aquifer: the contrast in the relative hydraulic conductivity and size of the low and high reservoirs in the model would affect the shape of the recession curve. There is a correlation between the discharge rate and the contrast in K between the low and high flow reservoirs. The greater the contrast in the K, the steeper the recession. The higher permeability zone in the aquifer influences the early stage of the recession curve; the greater the size of the higher permeability zone, the greater the initial discharge rate. In addition, the size of the highly permeable zone in the double reservoir system affects the steepness of the early stage of the recession curve; with smaller high permeability zones the early stage of recession becomes steeper, see appendix 3.1 Figure appx 3.7. Also, the results indicated that where the size of the high permeability zone is very large relative to that of the low permeability zone, the aquifer behaves as a single reservoir with a K value equal to that of the higher K zone.

Specific yield: changing the specific yield does not affect the discharge value at the start of the recession curve, but it influences the recession rate. The smaller the specific yield, the greater the recession rate, see appendix 3.2 Figure appx 3.11.

Number of drain cells: the number of drain cells was increased in the same model while the flow rate from one particular drain cell (the drain cell representing the spring) was monitored. The purpose of this test was to examine how the subsurface

flows from the aquifer influence the discharge from the spring. The result showed that the there is an inverse relation between the number of drain cells and spring discharge rate from the spring during the recession, see appendix 3.3 Figure appx 3.12.

Shape of the catchment: two models with the same volume, same boundary condition and same initial conditions were tested, but while one was transversally shaped, the other was longitudinally shaped in relation to the drain cell location. The sensitivity test showed that the recession curve of the transversal shape starts when the discharge is 50% greater than that from the longitudinal aquifer, see appendix 3.4 Figure appx 3.13.

8.8. Numerical models of the study catchment:

8.8.1. Kirby Grindalythe numerical model:

Model design and boundary condition:

A transient three-dimensional numerical model was developed to simulate water drainage via springs (see figure 8.3). The aquifer was simulated with the finite difference block centred groundwater model MODFLOW2000 (Harbaugh et al., 2000), using Groundwater Vistas version 6 (GV 6). The model catchment was discretized into a uniform grid of finite-difference cells consisting of 70 rows of 45 columns of 100 m x 100m cells and 10 layers (15,750 cells in total). Each layer represented a 2m thickness of the aquifer. The model domain enclosed an area of 3.2 km x 5.2 km and 20m aquifer thickness. The model incorporated a drain cell simulating a spring. This model was built to simulate an unconfined chalk aquifer upstream of Kirby Grindalythe village. The model was developed based on the Kirby Grindalythe conceptual model constructed during this study (chapter 3, section 3.3).

The active domain (flow cells) of the model was limited to within each catchment area as defined in the conceptual model. All the cells outside the catchment were

non-flow cells. During the recession period, water depletes freely from the aquifer through a spring under the influence of gravity. One drain cell was placed in the model (in the bottom layer) to simulate discharge through the spring from the model. An extra drain cell was placed adjacent to the spring drainage cell to simulate subsurface water flow exiting the catchment. The initial head in the model was set up according to the maximum head in the aquifer estimated in the conceptual model, which was 20 m.

For the purpose of monitoring groundwater head and flow four targets (representing monitoring wells) were placed in the model. The targets were distributed along the mid-line extending upgradient from the drain cell. One of the targets was located at the drain cell that stimulated the spring on the aquifer for the purpose of recording the flow rate in the spring. Therefore, the data from this target only represented a recession curve from the drain cell that simulated the spring, rather than all the drain cells. The other three targets were located at different distances upstream from the drain cell (100 m, 500 m, and 2000 m upstream from drain cell) and represented wells for monitoring the hydraulic head.

Input parameters for Kirby Grindalythe numerical model:

Hydraulic properties obtained from the Low-Mowthorpe borehole, which is the only borehole in the area, provided pumping test information: transmissivity of 450 m^2/day and specific yield of 0.0016. In addition, information from previous studies suggested that the storage co-efficient and specific yield are 0.0001 and 0.01 respectively, and transmissivity is 100-300 m^2/day (Allen et al. 1997; Gale & Rutter 2006; ESI, 2010). The maximum saturated thickness of the aquifer was estimated as 20 m. As the head in the aquifer does not distribute similarly over the entire catchment, it is at its maximum height at the catchment boundary and reduces gradually toward the discharge location or spring. Therefore it was assumed that the average head in the aquifer would be 15 m. Taking 15m to represent the head in the aquifer, the K would be from 7 to 30 m/day.

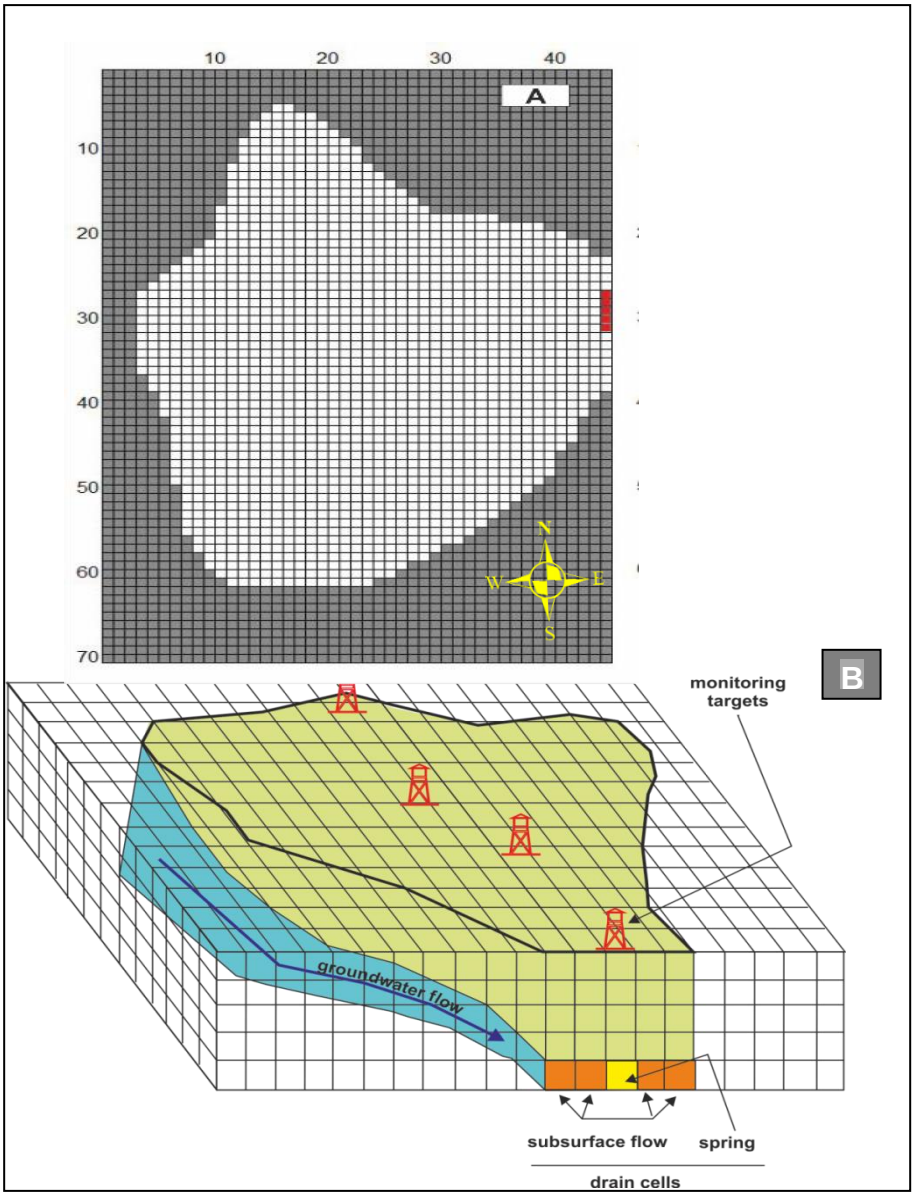

Figure 8-3. (A) top view of Kirby Grindalythe Numerical model from GV6. (B) Schematic diagram showing the 3D model design of the Kirby Grindalythe catchment.

8.8.2. Driffield numerical model:

Model design and boundary condition:

The model was discretized into a uniform grid of finite-difference cells (34090 cells) consisting of 113 rows by 60 columns of 100 m x 100m cells and 10 layers. The model active domain was developed based on the Driffield conceptual model, and describes a square area of 6 km x 11.3 km and rock aquifer of 40m in thickness (Figure 8.4).

The active domain in the model was limited to the Driffield catchment shape, and the permeable zone to the level of the spring. However, whilst permeability may develop at depths below spring level, as shown explicitly in Ch3, permeability is better developed towards the top of the aquifer, as explained in section 1.3.4. Therefore, permeability at depth was not represented in the corresponding numerical model. All cells outside the catchment border were switched to non-flow cells. Model thickness represented 50 m of unconfined Chalk rock. The initial groundwater head was 40m above the level of the spring. One drain cell was placed in the model to represent the spring. This drain cell was placed slightly towards the east side of the model's southern boundary, in the base layer of cells. An extra drain cell was activated in the model besides the spring cell to simulate the subsurface discharge. Because the model was constructed to simulate the aquifer during recession discharge in the absence of recharge, no recharge was added to the model. The head fall in the model was governed by the hydraulic properties (hydraulic conductivity and storage co-efficient) and the distribution of those properties in the model. Figure (8.4) shows the geometrical design of the Driffield numerical model.

Water flow and head in the model were monitored through four targets distributed at different distances from the drain cell. One of these targets was located at the drain cell that stimulated the spring on the aquifer for the purpose of recording the flow rate in the spring. The other three targets were located at different distances upstream

from the drain cell (100 m, 500 m, and 2000 m) and designed for monitoring hydraulic head.

The water balance investigation of the catchment identified subsurface flow from the catchment. In addition, the conceptual model indicated the possibility that this subsurface flow passes through the ground below the level of Driffield spring (see figure 3.13). In the numerical model, subsurface flow was simulated by the drain cells placed at the same level as the drain cell which simulated the spring. The reason for putting the subsurface flow beside the spring instead of under the spring was because of design considerations. If the drain cell representing subsurface flow had been placed below the spring drain cell, the majority of the water would have discharged through the lower level drain cell, in which case the model would not have been capable of simulating the spring.

Model input parameters:

Hydraulic properties of the aquifer were obtained from three boreholes (BGS). Driffield catchment has transmissivity of 1000 – 1500 m^2day^{-1}, except at the northeast border where it increases to over 2000 m^2day^{-1} and the specific yield ranges from 0.0004 to 0.0074, see table 3.1 chapter 3. The maximum saturated thickness of the aquifer was estimated as 40 m during development of the conceptual model. Assuming the average head in the aquifer to be 20 m, the K would be 50 to 100 m/day.

8.8.3. Calibration:

Model permeability scenarios for calibration test:

Five different scenarios to represent aquifer structure (see Figure 8.5) were tested in the study catchments. Whereas K was used to represent the hydraulic conductivity in the homogenous single reservoir aquifer model (Figure 8.5 A), K1 and K2

represented hydraulic conductivity of low permeability and high permeability reservoirs respectively in the double reservoir aquifer models (Figure 8.5 B-E).

During the calibration process, while the boundary conditions were kept the same, the input parameters and the size of the permeability zones in the double reservoir aquifer were changed. The process of model calibration was carried out by adjusting the input hydraulic parameters (K and S_y) in order to modify the outcome recession curve. This process continued until the model recession curve shown the best agreement with the MRC.

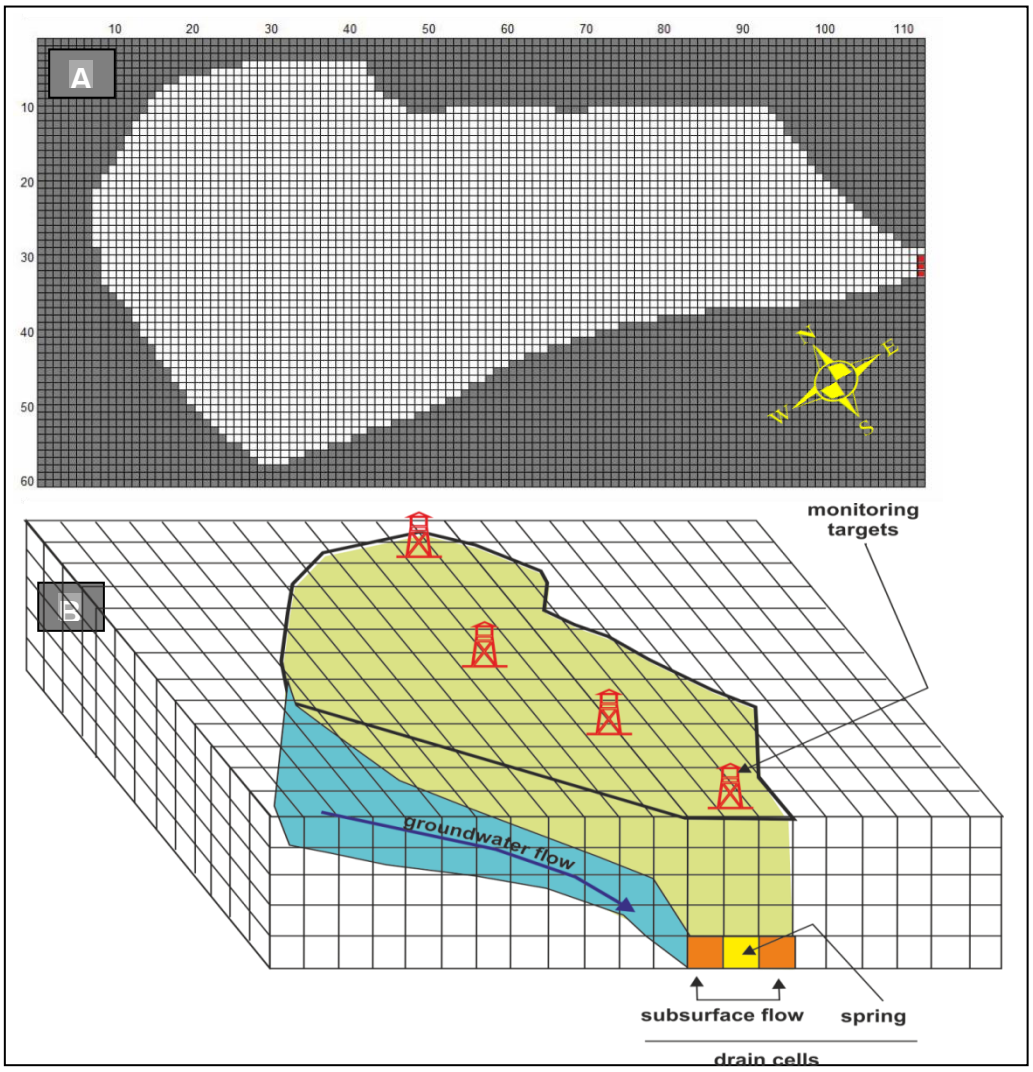

Figure 8-4. (A) top view of Driffield catchment Numerical model from GV 6. (B) Schematic diagram showing the 3D model design of Driffield catchment.

Table 8-2 summarises the input values used for testing sensitivity to hydraulic conductivity of the Kirby Grindalythe model. For this catchment, models (a, b and c), as shown in Figure (8.5), were tested. Note that hydraulic conductivity is represented by (K1) in the low permeability zones, and in high permeable zones by (K2).

In the parallel reservoirs model, the low permeability zone occupied 6 m and the high permeability zone 3.5 m of the total thickness of the model. In the tunnel model, the high permeability zone consisted of an elongated cuboid with dimensions of 2000 m x100 m, and thickness of 2 m (one cell thickness), located at the base of the model and at the level where the drain cell was placed. The model was drained by 5 drain cells, one of which represented the spring while the others represented the underground discharge.

Table 8-3 summarises the input values and the conditions used for testing the sensitivity of the Driffield model. The scenarios (a, c, d and e) from Figure (8.5) were tested under various assumptions for hydraulic properties.

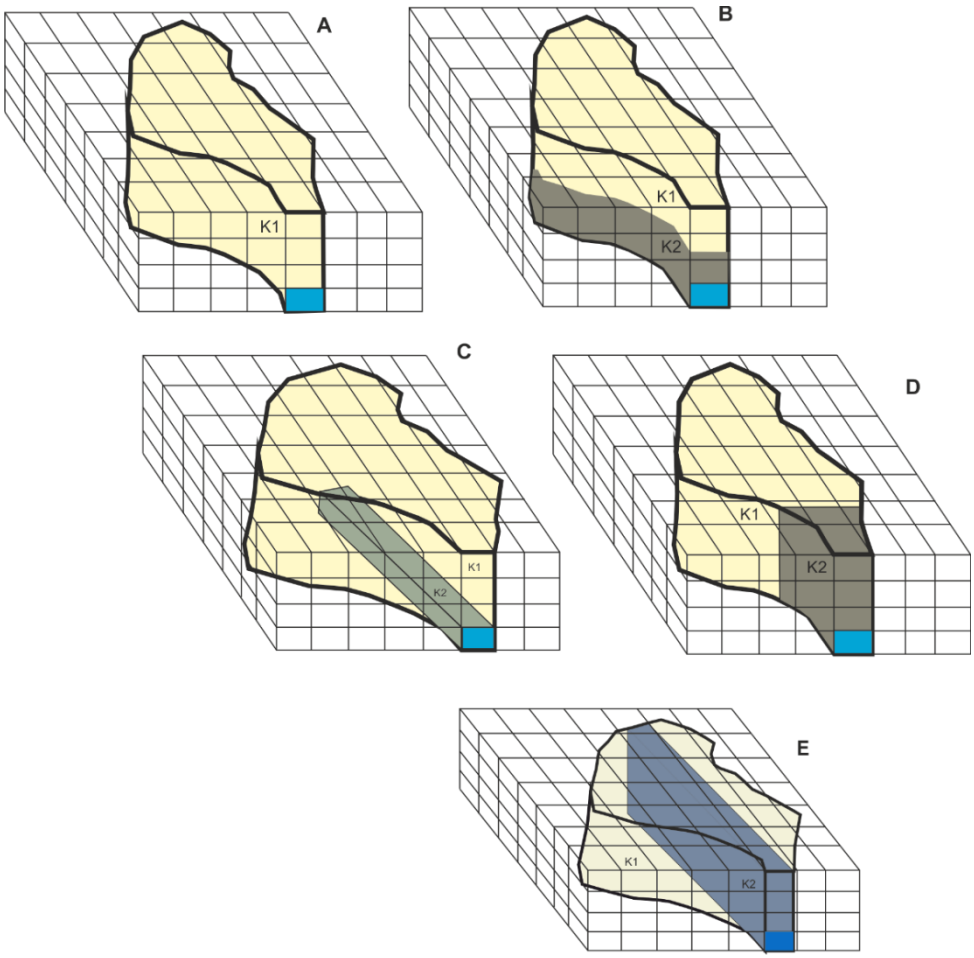

Figure 8-5. Suggested scenario for Driffield and Kirby Grindalythe aquifer systems . (A) Single reservoir aquifer; (B) Double reservoir, parallel horizontally model; (C) Double reservoir aquifer, tunnel model; (D) Double reservoir parallels vertically . (E) vertical high permeable zone. In the model, K1 represent hydraulic conductivity of low permeability system and K2 hydraulic conductivity of high permeability reservoir. (K1< K2).

Table 8-2. Values of hydraulic conductivity used for sensitivity test for Kirby Grindalythe model, K values are in m/day.

Test # Single reservoir	1	2	3	4	5	6	
K	10	125	200	400			
Test # parallel reservoirs and Tunnel model		1	2	3	4	5	
K1	400						500
K2	1	10	50	150	250		250

Table 8-3. Summary of tested characteristics in the suggested scenarios, Driffield catchment model.

	K (m/day)		K2 from			S_y	number of drain cell	model type
model #	K1	K2	column	row	layer			
1	40	\	\	\	\	0.01	1	homogenous
2	40	\	\	\	\	0.01	14	homogenous
3	40	\	\	\	\	0.007	14	homogenous
4	100	\	\	\	\	0.007	14	homogenous
5	100	\	\	\	\	0.007	7	homogenous
6	100	\	\	\	\	0.007	3	homogenous
7	150	\	\	\	\	0.007	3	homogenous
8	75	\	\	\	\	0.1	\	homogenous
9	5	150	71-113	\	1-10	0.007	3	two vertical reservoir
10	0.1	150	71-113	\	1-10	0.007	3	two vertical reservoir
11	0.1	200	71-113	\	1-10	0.007	3	two vertical reservoir
12	0.1	100	71-113	\	1-10	0.007	3	two vertical reservoir
13	1	100	71-113	\	1-10	0.007	3	two vertical reservoir
14	1	100	71-113	\	1-10	0.01	3	two vertical reservoir
15	1	200	71-113	\	1-10	0.05	3	two vertical reservoir
16	1	200	71-113	\	1-10	0.05	3	two vertical reservoir
17	0.1	200	81-113	\	1-10	0.05	3	two vertical reservoir
18	1	200	81-113	\	10	0.05	3	tunnel
19	1	200	\	30-32	8-10	0.05	3	tunnel
20	0.1	150	\	30-32	10	0.007	3	vertical plane
21	1	200	\	30-32	8-10	0.05	3	vertical plane

8.8.4. Results from Kirby Grindalythe and Driffield 3D models:

Results from calibration Kirby Grindalythe model:

The model was designed based on the boundary conditions and initial conditions estimated in the conceptual model and water balance. Calibration was then carried out depending on the outcome of the sensitivity tests. The model was tested under a wide range of hydraulic parameters, and the recession curve compared with the MRC from the Kirby Grindalythe station.

The results from the single reservoir model of the Kirby Grindalythe catchment are shown in figure (8.6). In the case of the single reservoir, the discharge reduced steadily during the recession. The rate of flow reduction showed a direct relation with the hydraulic conductivity of the aquifer; higher K values resulted in faster recession. To show how the flow changed in the model the recession curves from the tested model were analysed according to the Maillet model (the recession coefficient represents the gradient in the flow rate). The result of the analytical interpretation of the model recession curves is shown in table (8.4); it can be noticed that the single reservoir model curves were always represented by a single segment/recession coefficient.

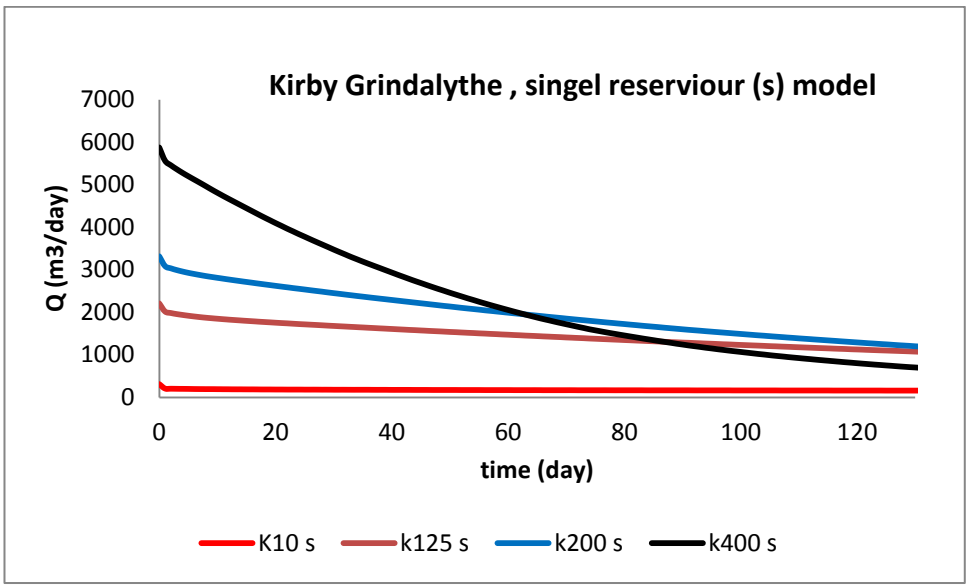

Figure 8-6 Recession curves from the single reserviour model (Kirby Grindalythe catchment) under different hydraulic conductivity (K). Graphs are showing flow from one drain cell. s symbolize to a single reservoir.

Table 8-4. Recession co-efficient from models and MRC recession curves (Kirby Grindalyte). s symbolize to a single reservoir, d to double reservoirs and t to tunnel model.

Model	recession co-efficient (days-1)			number of recession segment
	α 1	α 2	α 3	
MRC	0.017			1
k125 s	0.005			1
k200 s	0.007			1
k400 s	0.016			1
k400-10 d	0.046	0.012		2
k400-50 d	0.059	0.012		2
k400-150 d	0.014			1
k400-250 d	0.015			1
k500-250 d	0.018			1
K400-1 d	0.026	0.005		2
K400-10 t	0.047	0.010	0.003	3
K400-50 t	0.054	0.013	0.006	3
K400-150 t	0.022	0.012	0.009	3

The recession curves from the tunnel and double reservoir models are illustrated in Figure (8.7). The curves reveal that the flows from the double reservoir models did not decrease steadily, differing from the case with the single reservoir models. Generally, at the early stage of the recession period, the flow rate falls more rapidly, and then flattens off more quickly. This recession pattern was clearer when K1 was very small and the contrast between the hydraulic conductivity of the K1 and K2 was very large, e.g. when K1 was 1 m/day and K2 was 400 m/day. When the hydraulic conductivity value was high in both K1 and K2, the aquifer behaved similarly to a single reservoir, and the flow reduced steadily. The results from the analytical interpretation of the recession curve from the double and tunnel models according to the Maillet model clearly show a pattern of rapidly reducing flow during the recession, see table (8.4). Regarding the recession curve from the double reservoirs, where both K1 and K2 were large, this curve needed only a single recession co-efficient. Whereas, for the recession curve from double reservoir aquifers exhibiting very low K1 and very high K2, two recession co-efficients were required. The recession co-efficient was bigger at the early stage of the recession than at the late stage. The recession curves from the tunnel models required three recession co-efficients, with values in descending order. This indicates that the discharge reduced very rapidly during the early stage and at a very much slower rate toward the end of the recession period.

The pattern of the recession coefficients from the double and tunnel models showed that the steep recession curve at the early stage of the recession more probably arises from the rapid depletion of the hydraulic head within the high permeable zone. Meanwhile, the smaller recession coefficient reflects the late stage of recession drainage behaviour from the low permeability zone in the model.

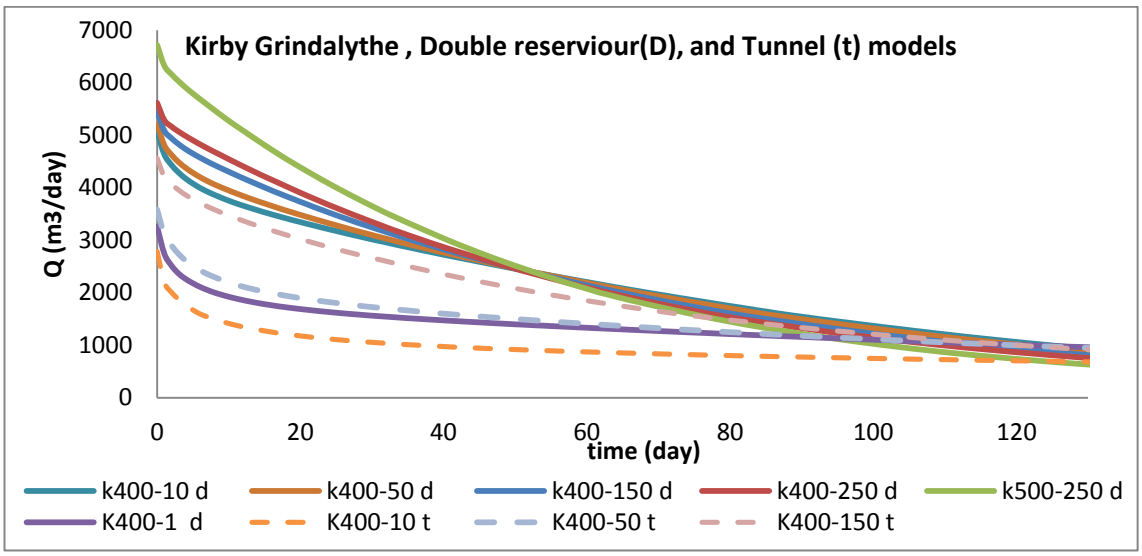

Figure 8-7 Recession curves from the tunnel and parallel reservoirs model of Kirby Grindalythe aquifer. K values are in m/day, t is tunnel and p parallel reservoir, the large value represents the hydraulic conductivity from the high permeable zone and small value from the low permeable zone (e.g. K400-10, K400 for high permeable and K10 for the low permeable zone). Graphs show flow from one drain cell which represents the spring; 4 more drain cells simulate subsurface discharge.

Recession curves from single and double reservoir models with various thicknesses of permeable layer are shown in figure (8.8). Both models behaved similarly where the thickness of the high permeability zone within the parallel horizontal reservoir model accounted for about 25% or more of the total aquifer thickness. In addition, when the high flow zone in the double reservoirs models had a high K value close to that of the single reservoir model, the recession curve from both models behaved similarly, Figure (8.9).

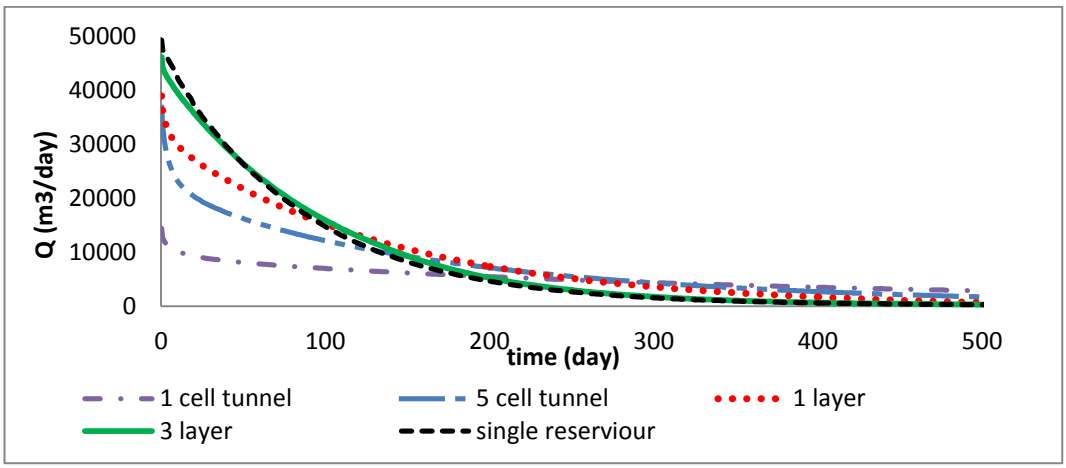

Figure 8-8. Effect of the size of high permeability zone on the shape of recession curve. Black dashed line is from single reservoir aquifer, with hydraulic conductivity =100m/day. The solid green line is from parallel reservoir model when the high permeability zone represents about 25% of total model volume. Red dotted line is from parallel reservoir model when high permeability zone represents about 10% of total model volume. The Blue dashed line is from tunnel model when high permeability zone represents about 1% of total model volume. The Orange dashed line is from tunnel model when high permeability zone represents about 0.3% of total aquifer volume. Note; in all double reservoirs models K1=1 m/day and K2= 100m/day.

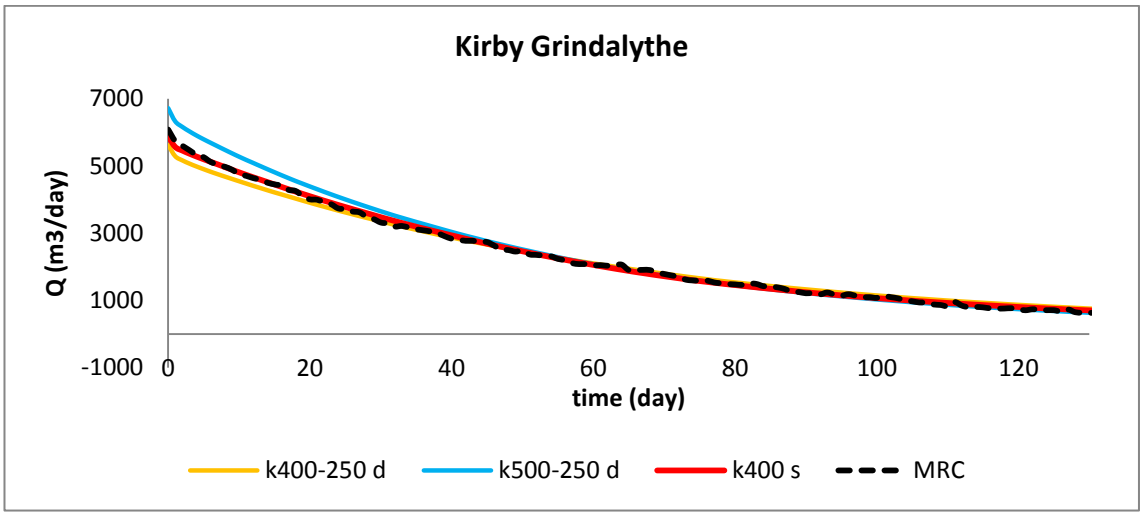

Figure 8-9 The result of calibration between MRC and recession curve deduced from the tested numerical models (s =single porosity model; d = double reservoir model. Graphs are show flow from one drain cell representing the spring.

Testing similarity between MRC of Kirby Grindalythe and best-fit recession curve from models:

The Maillet analytical interpretation approach was also used for identifying the most representative model recession curves. Both the model recession curves and MRC were analysed using the Maillet formula, and then the results were compared, see table (8-4). As was discussed in the analytical interpretation in Chapter 6 the MRC from Kirby Grindalythe was matched with a single co-efficient during the curve fitting process based on the Maillet model. The recession curve from the double reservoir numerical model (parallel reservoirs) required two segments during the curve fitting process when K1 was very small and K2 significantly large, but only one segment when both K1 and K2 were relatively large. Recession curves from tunnel models required three segments.

This result led the author to conclude that either the single reservoir model or double reservoir model (those with relatively high K1 and K2) can represent the real aquifer. The patterns of recession curves from some models from double reservoir aquifers show some similarity to the MRC, such as the recession curve from the model where K1=250 m/day and K2=400 m/day, and the model with K1=250 m/day and K2=500 m/day. However, although these two models showed a good fit to the MRC from the middle to the late stage of the MRC, they did not match the early stage of the MRC, see figure (8.9). The model recession curve that showed the best agreement to the MRC was from the model consisting of a single reservoir aquifer with K value of 400 m/day, see figure (8.9). This conclusion is also confirmed by comparing the recession co-efficients from the MRC and the models, see table (8.4). The results from calibration tests and analytical interpretation of the Kirby Grindalythe model suggest that the recession curve that was produced from the single reservoir model with a calibrated K value of 400 m/day and S_y 0.008 achieved the best agreement with the field recession curve. The recession co-efficient from the MRC was 0.017 day^{-1} and from the best-fitted model was 0.016 day^{-1}. The co-efficient of regression

(R-squared) between recession curves from the best fitting single reservoir model and the MRC was 0.99, see figure (8.10).

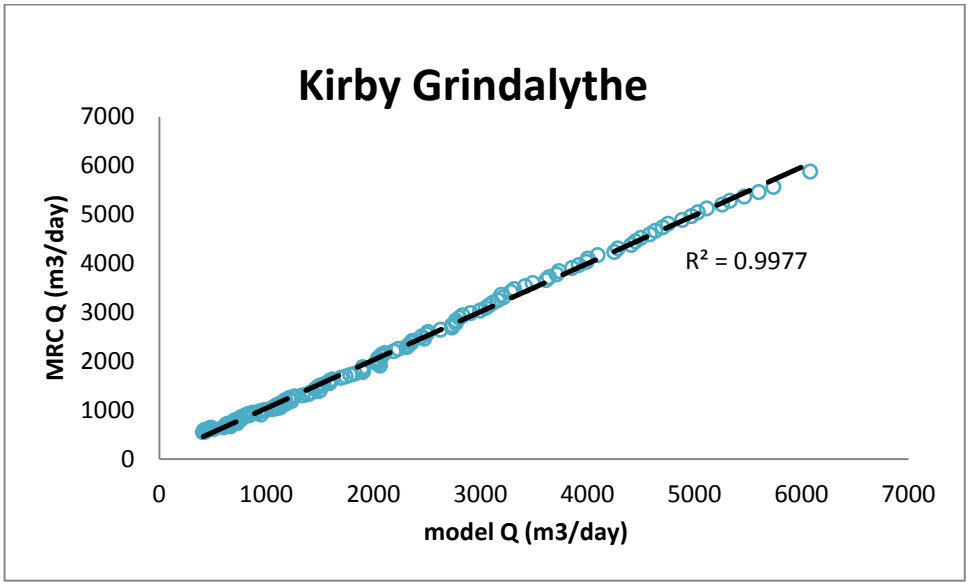

Figure 8-10 Match between the best fit-model recession curve and observed MRC (dashed line is 1:1).

Results from Driffield model and calibration:

Homogeneous model:

As a first step, the model was tested with the hydraulic test-measured parameters for the aquifer in the area, i.e. hydraulic conductivity of about 75-100 m/day and storage co-efficient of 0.01. Then, hydraulic properties in the model were changed both separately and simultaneously. Further tests were done where the number of drain cells was changed; large numbers of drain cells were used in the model in order to succeed in calibrating the recession curve.

Recession curves from the homogeneous permeability models are shown in Figure (8.11). The curves suggest that the homogeneous model failed to represent the real aquifer system using the range of feasible K values (50 – 100 m/day) based on the field-measured transmissivity and assuming the average saturated thickness to be 20m. During the calibration process, the recession curves from the model could not successfully be fitted to the recession curve of the real aquifer.

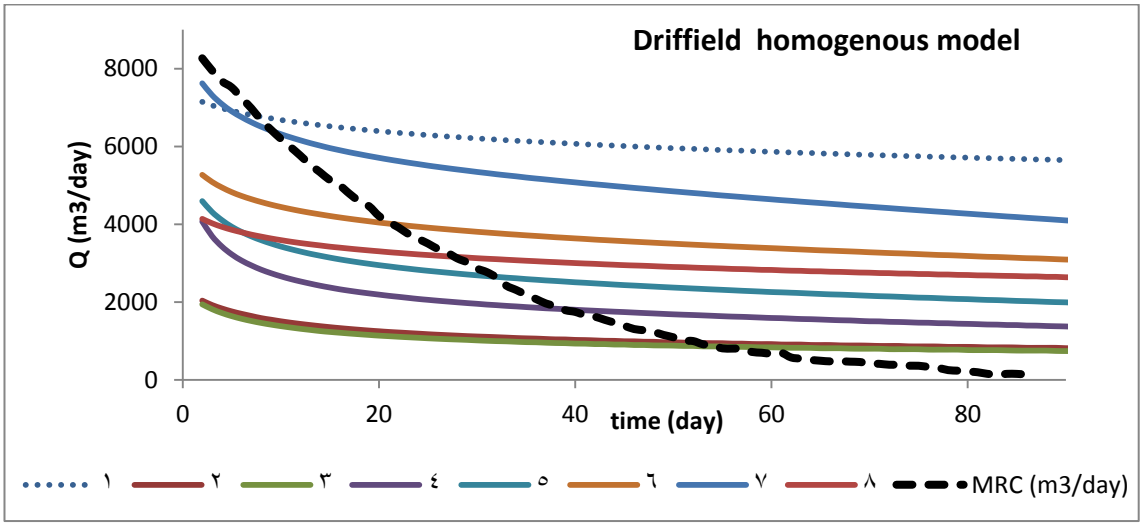

Figure 8-11. Recession curves from the Driffield homogeneous model (model a). Graphs are showing flow from one drain cell. Note: model parameters shown in table 8.3.

Tunnel model (C) and single vertical permeable zone (E) results:

See Figure 8.5 model C and E.

This scenario was tested several times. Between the successive tests, the model was subjected to changes in the volume of the tunnel-shaped highly permeable zone, the number of the drain cells, and the contrast in hydraulic properties between the low and high permeability zones. The aim was to obtain a recession curve from a model representative of the field data (MRC). In Figure (8.12) recession curves from four tested models are displayed (these four tests were selected as a sample). This figure

also includes a table showing the parameters which were used in the models. Curves 1 and 2 are from the model with a tunnel-shaped high permeability zone, whereas curves 3 and 4 are from models with a vertical high permeability zone extending from the bottom to the top of the model.

The results of calibration between the tunnel, high permeable vertical plane zone and observed data (Figure 8.12) show poor agreement with the recession curve from the real aquifer. This suggests that this model is not able to represent the real aquifer system.

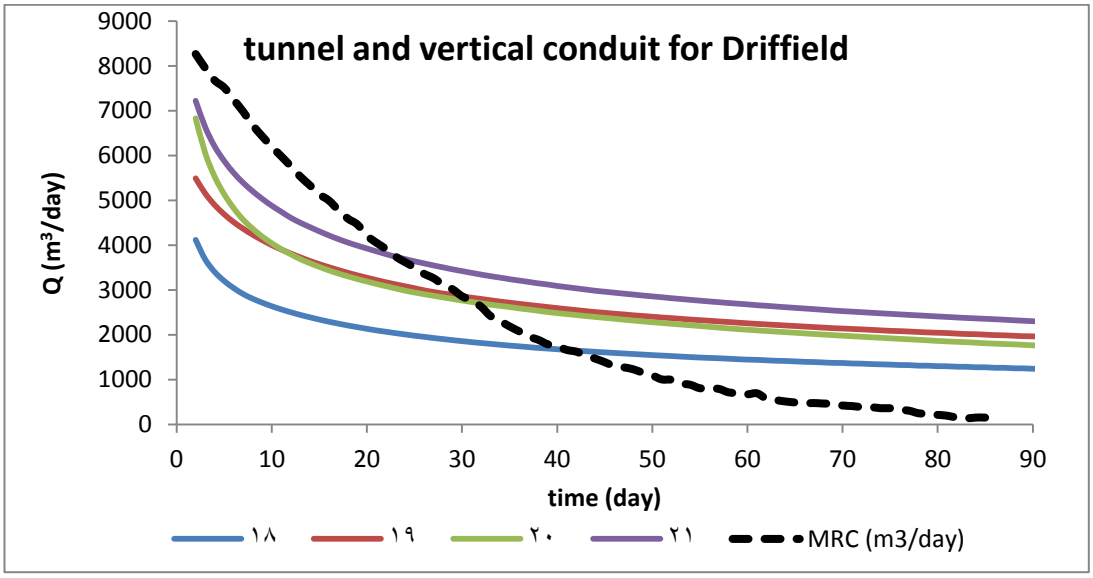

Figure 8-12. Recession curves from Driffield - tunnel and vertical permeable zone models, compared with MRC of real aquifer seen at Driffield gauging station. The graph show the discharge from one drain cell. Note: model parameters shown in table 8.3.

Vertically arranged double reservoir model (D) results:

See Figure 8.5 model D.

Some results from the vertically parallel double reservoir model are illustrated in Figure (8.13). This model is case scenario D in Figure (8.5).

For tests 1 to 7, the values of the hydraulic properties (hydraulic conductivity and storage co-efficient) of both the low and high permeability systems in the model were changed, while the size of the low and high permeability reservoirs remained the same. A big contrast was noticed between the recession curves; recession curve number 1 was derived from a model where hydraulic conductivity was 5 m/day and 150 m/day for the low permeability and high permeability reservoir respectively; the volume of the high permeability zone represented about 26% of total volume. This curve did not fit the real recession curve. At the early stage of the recession period (up to 10 days) the curve fell dramatically below the real recession curve; from 10 days until the end of recession period its slope became gentler and predicted flow rates higher than in the real recession curve. By reducing the hydraulic conductivity of the low permeability reservoir from 5 to 0.1m/day, and increasing that of the high permeability reservoir from 150 to 200 m/day, the model recession curve was made to mirror the real aquifer recession curve but with a higher discharge rate (curve number 3). In this model, the volume of high permeability remained at about 26% of the total. However, this curve showed rapid loss of flow rate at the start of the simulation, which suggests that the hydraulic head was depleting too quickly compared to the real case. To correct this, the specific yield of the high permeability zone was increased from 0.001 to 0.005, curve number 7. The recession curve from the model became closer to the shape of the observed recession curve, but the flow rate was still larger than that of the real aquifer. To correct this further, the volume of the high permeable reservoir was reduced from 26% to 18% of the total. The

recession curve from this model is displayed by curve number 9 in Figure (8.13), which shows good agreement to the real recession curve.

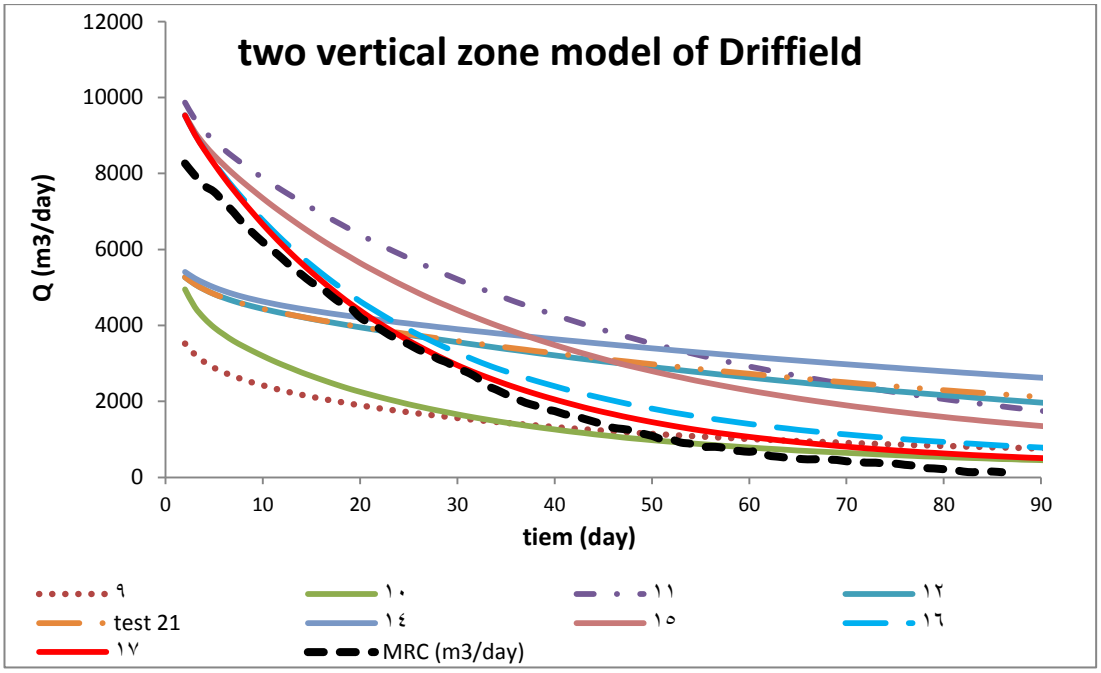

Figure 8-13. Recession curves from vertically arranged double reservoir model (scenario D in Fig. 8.5) representing the Driffield aquifer system, and MRC of the real aquifer. The graphs show discharge from singl drain cell. Note: model parameters in table 8.3.

Testing similarity between MRC of real aquifer and best-fit recession curve from models: (calibration result)

The results of calibration reveal that the recession curve from the dual reservoir model where the reservoirs were arranged vertically parallel showed good agreement with the real aquifer recession curve. The model with K of 0.1 m/day for the

upstream low permeability zone and 200 m/day for the downstream high permeability zone showed the best fit to the real recession curve, see Figure (8.13).

The co-efficient of regression (R-squared) between the recession curve from the vertical double reservoir model (which showed the best fit) and MRC of observed recession curves for the period between 2000 and 2014 was 0.98 (Fig, 8.14). A clear difference can be noticed between these two curves during the very last period of the recession. The recession curve from the real aquifer shows that the spring dried out, while at the same time point in the model recession curve there was discharge.

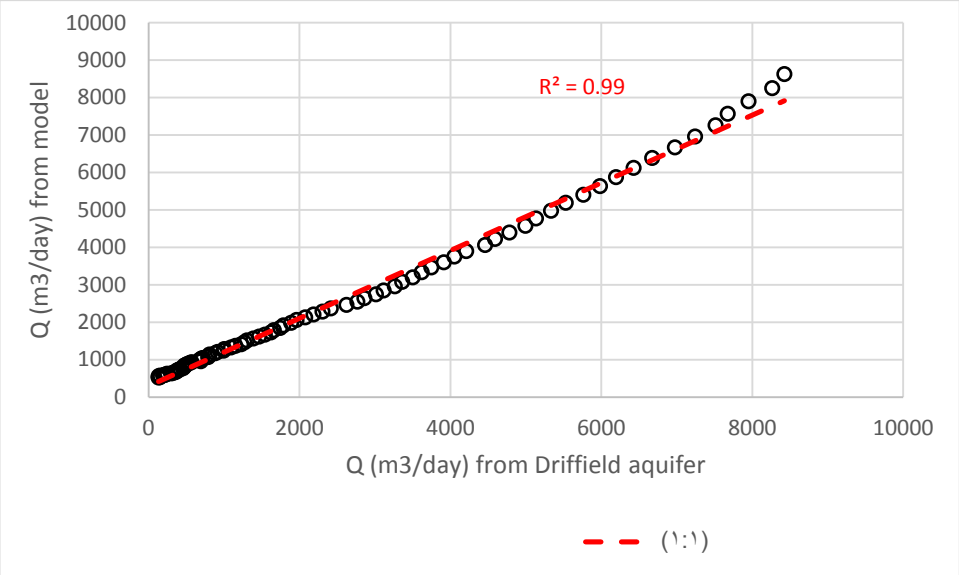

Figure 8-14. R-squared between Driffield model (vertical double reservoir model ; scenario D in Fig, 8.5) and MRC from the real aquifer.

Analytical interpretation of the recession curves from Driffield models:

The results from the analytical interpretation of the recession curves from different case models of the Driffield catchment, according to the Maillet model, are shown in table (8.5).

The results show that the recession curves were fitted either by two or three segments; recession co-efficients always sequentially decreased for all the models. Recession curves from the single reservoir (s), tunnel (t) and high permeable vertical plane (vP) models were fitted with three segments. Recession curves from double reservoir horizontally parallel (dH) and vertically parallel (dV) models were fitted with two segments.

Recession curves from the models clearly show that hydraulic conductivity and the recession coefficient are directly related; the higher conductivities generally gave larger recession coefficients.

Several model runs were aimed at constructing recession curves which would match the MRC of Driffield. The best fitting model curve – model 17, shown in Table 8-5 and Fig. 8.13, succeeded in fitting the high flow segment, but failed to match the low flow segment (as shown in Fig. 8.13 the flow in the model remained larger than the MRC at late stages). The mismatch is reflected by the recession co-efficients, with the recession coefficients for the first segment of the MRC and dv model being similar, while the recession coefficient of the second segment of the model curve is bigger than that for the MRC, which indicates that these segments are weakly matched.

The reason for the mismatch in the second segment is most likely due to the inability of the numerical model to simulate appropriately the spring and subsurface flow in the Driffield catchment. The water balance suggested that in the Driffield catchment a portion of the recharge water flow from the catchment is in the form of subsurface flow below the level of the gauging station. When the gauged stream reaches the minimum flow rate, or dries out at the very late stage of the recession, there is still water flow below the surface. The MRC only records the gauged stream flow, which at the late stage becomes very low or zero, while there is remaining flow from the catchment in the form of subsurface flow. In the numerical model, the drain cells which simulate the subsurface flow are all at the same level, i.e. the level of the drain

cell that represents the spring. This means that the discharge from the drain cell representing the spring and each drain cell representing subsurface flow will be equal. Thus at the time when the flow from the spring reaches zero in the real aquifer, some flow from the spring drain cell remains in the model.

To address this issue, attempts were made to arrange drain cells vertically in the model, i.e. to drain cells in the base layer to simulate subsurface flow, and one drain cell in the second layer from the base to simulate the spring. However, these models failed to simulate the system because the majority of the water in the model drained through the drain cells in the base layer, with very little draining via the drain cell in the second layer.

Table 8-5. Results from analytical interpretation of the recession curves from Driffield models according to Maillet model. Note: model # equivalent to table 8.3.

Model#	K m/day	Model type (in figure 8.5)	recession coefficient (days-1)			number of recession segment
			α 1	α 2	α 3	
	MRC Driffield		0.037	0.050		2
1	K40	s	0.007	0.003	0.001	3
5	K100	s	0.032	0.011	0.005	3
12	K2=100, K1=0.1	d_H	0.022	0.010		2
15	K2=200, K1=1	d_H	0.025	0.018		2
17	K2=200, K1=0.1	d_V	0.039	0.027		2
18	K2=200, K1=1	t	0.038	0.014	0.006	3
19	K2=150, K1=0.1	t	0.039	0.015	0.006	3
21	K2=200, K1=1	v_P	0.043	0.015	0.006	3

8.8.5. Comparison between the transmissivity from field measurements and model outcomes:

Kirby Grindalythe catchment: Regionally, the mean transmissivity value in the unconfined Yorkshire Chalk is about 1250 m2day-1 according to borehole measurements (Gale & Rutter, 2006). Locally, the pumping test in Low Mowthorpe borehole, which is located inside the catchment near the outlet border about 2km upstream from the gauging station, showed a transmissivity value of 450 m2day-1. The average saturated thickness of the aquifer according to the models was 15 m, and the best fit recession curve to the MRC from the model was with K of 400 m2day-1. Accordingly the modelling implies a transmissivity of the aquifer of 6000 m2/day.

Driffield catchment: The mean transmissivity value in the Chalk at the study area is about 1000- 2400 m2day-1, according to the contour map of transmissivity distribution constructed from data taken from borehole measurements (Parker, 2009). In addition, the corresponding figures are about 1000-1500 m2day-1according to data from the boreholes provided by the BGS (see table 3.1, section 3.1.3, chapter 3).

As explained earlier the average thickness of the aquifer at Driffield is about 20m, and the model with K of 0.1 m/day for the upstream low permeability zone, and 200 m/day for the downstream high permeability zone (model run 17) showed the best fit to the real recession curve. Consequently, the modelling implies a transmissivity in the high flow zone of about 4000 m2/day and about 2 m^2day^{-1} in the low flow zone.

It can be noticed that in both catchments the transmissivities obtained from the numerical simulation were bigger than those from the field observations. As previously explained in the introduction and geological chapters, the English Chalk is characterised by the existence of enlarged fissure networks, distributed irregularly. Generally, these fissures are more dominant in the aquifer near the water table

fluctuation zone, and spatially below streambeds. Therefore, the transmissivity will be smaller in any boreholes drilled in the low-intensity fractured zones than in boreholes in the areas of high-intensity fissures. Accordingly, this factor might explain the discrepancy between the transmissivity from the model and transmissivity estimations from the boreholes in the study catchments. Transmissivity from boreholes may represent the transmissivity of the area at and around the borehole, rather than the entire aquifer. Meanwhile, the estimation from the numerical simulation represents an effective transmissivity for the entire aquifer, which is dominated by the high transmissivity zones.

8.8.6. Other results

The modelling results indicate that the springs are not the only discharges from the aquifer. When only one drain cell was placed in the models, despite testing many scenarios, the models failed to fit the observed data. To calibrate the model curves with MRC from the study catchments the number of drain cells in the numerical models had to be increased (NB the volume of water from each drain cell in the model was similar, which means that each drain cell drains the same amount of water). The calibrated curve of Kirby Grindalythe matched the observed MRC best when 5 drain cells were inputted to the model. Similarly the Driffield model with 3 drain cells showed a better agreement with the observed MRC than that with a single cell.

The results from model calibration agree with the results from the water balance calculations. Water balance calculations indicate that both catchments lose water that does not pass through their respective gauging station. Therefore, besides the gauged springs, the aquifer catchments lose water through other routes. Water loss from aquifers can occur naturally through leakage of water below the ground under the gauging stations, or laterally through the (assumed impermeable) catchment divides to surrounding aquifers.

From the numerical models that simulated a single reservoir homogeneous aquifer, sensitivity tests were conducted to determine the effect of the aquifer characteristics (K and S_y) on the spring discharge recession co-efficient (depending on Maillet equation). The result showed that the recession co-efficient is directly related to K, while the relation between S_y and the recession co-efficient is non-linear. The relation between K and the recession co-efficient can be fitted by a straight line, while the relation between S_y and the recession co-efficient can be fitted by the inverse power regression line, see Figures 8.15 and 8.16.

The analytical interpretation of the recession curve from the models using the Maillet equation revealed that double reservoir systems are not always fitted with two recession co-efficients. In some cases, they can be fitted either by a single recession co-efficient, or require three segments, depending on the contrast in the hydraulic conductivity in the flow zones and the size of the reservoirs in the aquifer. When the conductivity in the low and high flow zones in the double reservoir system is high and relatively close they can be fitted by a single segment (i.e. one recession co-efficient). Whereas, if the contrast in the permeability is very high between the flow zones, and the size of the high flow zone is very small, the recession curve will require three segments, see table (8.4).

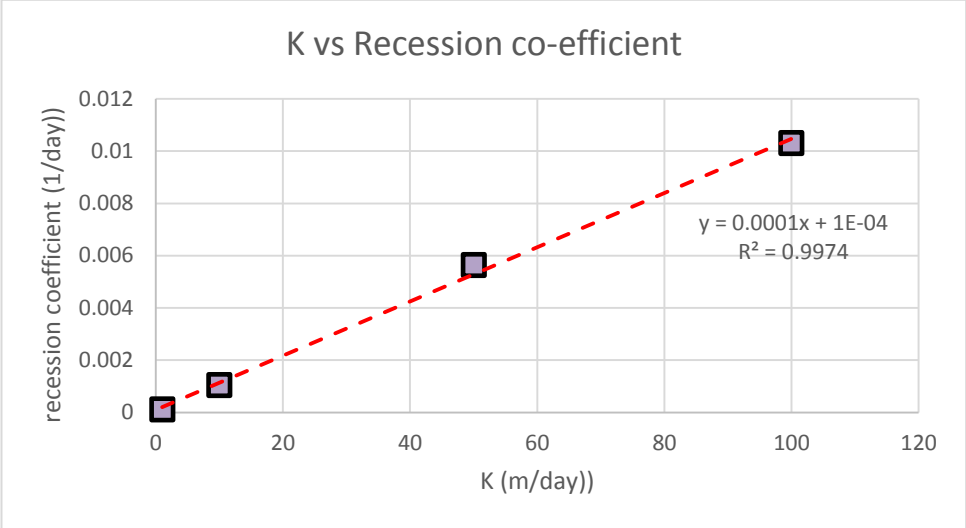

Figure 8-15. Relation between hydraulic conductivity (K) and spring discharge recession co-efficient from a sensitivity test of the single reservoir homogeneous aquifer.

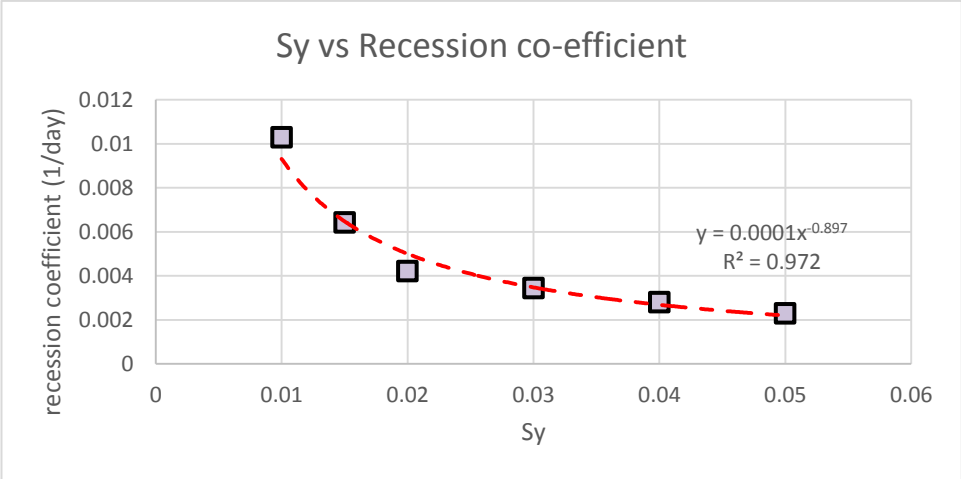

Figure 8-16. The relation between specific yield (S_y) and spring discharge recession co-efficient from sensitivity test of the single reservoir homogeneous aquifer.

8.9. Summary of chapter

A transient three-dimensional numerical model was developed to simulate Kirby Grindalythe and Driffield chalk aquifer. The aquifer was simulated with the finite difference block centred groundwater model MODFLOW2000 (Harbaugh et al., 2000), using Groundwater Vistas version 6 (GV 6). The models were designed to simulate the spring discharge from these two aquifers. A good agreement was achieved between the MRC for Kirby Grindalythe and Driffield spring discharge and the recession curves from the numerical models that simulated these two aquifers.

The Kirby Grindalythe catchment was discretized into a uniform grid of finite-difference cells consisting of 70 rows of 45 columns of 100 m x 100m cells and 5 layers. Each layer represented a 2 m thickness of the aquifer. The model domain enclosed an area of 3.2 km x 5.2 km and 10m aquifer thickness and was drained by a drain cell simulating a spring. The Driffield catchment was discretized into a uniform grid of finite-difference cells (34090 cells) consisting of 113 rows by 60 columns of 100 m x 100m cells and 10 layers. The model active domain was developed based on the Driffield conceptual model. It describes a square area of 6 km x 11.3 km and 40 m thickness of rock aquifer. The active domains in the numerical models were limited to within the boundaries of Kirby Grindalythe and Driffield as identified in their respective conceptual models.

The 3D numerical models were subjected to sensitivity tests for two scenarios. In the first scenario, the aquifer was homogeneous; in the second scenario, the aquifer contained two different flow systems (double reservoir aquifer: low permeability and high permeability). The homogeneous scenario was used to examine the influence of the hydraulic parameters on the discharge rate from the aquifer. The second scenario investigated how the contrasts in permeability and the size of the different permeability units in the aquifer influence the shape of the recession curve. The sensitivity and calibration tests show that the recession curve from the single reservoir model with hydraulic conductivity of 125 m/day and storativity of 0.01

from the model that contained three drain cells achieved a good fit to the MRC from Kirby Grindalythe[2]. Meanwhile, among all the models tested, the recession curve from the vertically parallel double reservoir model of K1 0.1 m/day and K2 200 m/day, with storativity of 0.01 and 5 drain cells showed the best fit with the MRC from Driffield catchment. However, the fit is not as good here as for Kirby Grindalythe. It might have been possible to get a better fit if more models had been tested.

These results indicate that the Kirby Grindalythe aquifer has a single flow system whereas the Driffield catchment consists of a double reservoir aquifer. The following may be reasons for the existence of a single reservoir in Kirby Grindalythe aquifer and double reservoirs in Driffield aquifer:

- The Driffield catchment is larger and will have a better developed conduit network towards its downstream end.
- Part of the Driffield aquifer near the downstream end actually occurs in chalk gravels rather than the Chalk itself.

In addition, the calibration results show that the recession curves from the Kirby Grindalythe model containing 5 drain cells and the Driffield model containing 3 drain cells matched with the MRC from the Kirby Grindalythe and Driffield aquifers respectively. These results agreed with the results from the water balance calculations for these aquifers (see section 4.3.1), as in Kirby Grindalythe the input/output value was 5 and for Driffield catchment it was 2.5; i.e. in Kirby Grindalythe 80% of the water exited via the subsurface rather than the gauging station, and in Driffield 60% did so.

[2] Meaning that water discharged from the model through three drain cells, one cell simulated spring discharge and two drain cells simulated a subsurface discharge. The recession curve from the model represented only the discharge from the drain cell that simulated the spring.

Chapter 9. Conclusion

9.1. Aim and objectives

The main aim of this study was to investigate the flow system in the unconfined chalk aquifers in East Yorkshire using physical (spring discharge recession curve, water balance, and stream water temperature analysis), chemical (spring water EC, CFCs analysis), and numerical simulation approaches. The project comprised six main investigative studies including constructing geological and hydrogeological models, groundwater and stream water monitoring, calculating catchment scale water balance, analytical interpretation of the spring discharge recession curves, analysis of CFC concentrations in spring water, and numerical simulation of groundwater flow and spring recession. The specific objectives and aims of each investigation are described below, also the project outcomes.

9.1.1. Geological and hydrogeological model outcomes

The main aim of the geological and hydrogeological model was to explain the influence of geological and hydrogeological factors on the groundwater flow system in the aquifer and to estimate the catchment boundaries and hydrological conditions.

Objectives:

- Using lithological and structural information to estimate the influence of geology on the hydrogeological characteristics of the aquifer, and the factors responsible for existence of the springs in the area.
- Combining the topographical map of the study catchments with the groundwater level map and location of the springs to identify the influence of the local topography on the groundwater flow direction, and catchment boundaries.

- Combining the hydrological information and the aquifer characteristics to identify the aquifer initial conditions at the start of spring recession.
- Combining geological, hydrological and topographical information to construct cross sections and conceptual models of the target aquifers.

The outcomes:

In the Kirby Grindalythe catchment the aquifer consists of Ferriby and Welton Chalk Formations, and in the Driffield catchment it consists of Welton, Burnham and Flamborough Chalk Formations. Folding and faulting are relatively minor in the study areas and unlikely to control the groundwater flow direction and lateral hydraulic properties significantly (in the Kilham catchment, which is located northeast of Driffield, the springs may be fault controlled, but there is no evidence of fault controls on the springs in the Kirby Grindalythe and Driffield catchments).

Groundwater depletes from the aquifers through several springs; all the springs in the study catchments consist of gravity overflow springs. Four springs were recognised in the Kirby Grindalythe catchment, including stratigraphical escarpment springs and dip slope springs that arise close to the contact surface between the chalk and underlying clay formations. The spring in the Driffield catchment is a dip slope spring arising due to the lateral variation in the lithology at the border between the Chalk outcrop and superficial deposits, where thick impermeable cover deposits restrict the groundwater discharge from the confined aquifer down-dip.

Elevation of the groundwater table and from boreholes revealed that the saturated thickness of the aquifer that feeds the springs in the Kirby Grindalythe catchment is around 20 m. Whereas, the corresponding figure for Driffield aquifer is probably around 40m at the start of the recession period. The main source of the groundwater recharge to the unconfined aquifer is rainfall as few natural or artificial surface water sources exist in the area. Combining the topographic map with the groundwater contour map showed that the groundwater flow direction is controlled by the topography.

Altitude of the unconformable contact surface between the Cretaceous Chalk and underlying Clay Formations:

- According to the altitude of the outcrop this surface slopes toward the north-northeast with an average slope angle of 0.4^{o} at Kirby Grindalythe catchment.
- Depending on the contour map of the base of the Chalk (from Galle and Rutt, 2006) it slopes towards southeast with an average angle about 0.8^{o} at Driffield catchment.

Altitude of the Chalk beds:

- According to the altitude of the outcropped contact surface between Ferriby Chalk and Welton Chalk Formation the Chalk beds dip toward the east with a dip angle of 0.5^{o}.
- Based on the altitude of the contact between the Burnham and Flamborough Chalk formations the Chalk beds dip toward the southeast with a dip angle of about 2.2^{o}

9.1.2. Groundwater and stream water monitoring:

Objectives:

- The water table was monitored in specific monitoring wells to obtain information regarding the regional groundwater flow direction.
- Groundwater temperature was monitored in monitoring wells to investigate seasonal groundwater temperature fluctuation.
- EC and T of the springwater was measured at the spring locations and in the streams downstream of the emergent spring locations to investigate the dominant components of streamflow. Relationships between the EC of the springs and effective rainfall and spring discharge were examined, to identify whether the water in the stream is supplied by the groundwater or from direct

rainfall, runoff or quick flow through the soil zone, or rapid bypass flow through the unsaturated zone.

The outcomes:

Five boreholes and three streams were used for monitoring ground and stream water. Borehole groundwater fluctuation and temperature were monitored using high-resolution probes. The temperature data showed that the temperature of the groundwater was almost steady during the year with a fluctuation not exceeding 1^{o}C and average value of 9.4 ^{o}C. CTD was used for monitoring stream water electrical conductivity and temperature, as a tracer for estimating sources of the water that feeds the stream.

Comparison of the EC at the spring locations and in the stream a few hundred meters downstream from the location of the springs showed a small contrast (at most a few tens of μS/cm); conductivities at the spring locations were generally slightly higher than those downstream. The small contrast in the EC between the springs and downstream water indicates that the springs are the predominant source feeding those streams. Carbon dioxide degassing between the spring and the downstream location, or contributions from other water sources to the downstream water may account for the small differences observed.

Little relation between EC of the springs and flow rate was observed; this indicates that the water that discharges at the springs is predominantly groundwater from the Chalk. However, in some cases quick-flow or bypass flow via the soil or unsaturated zone was evident in lower EC recorded after rainfall events. This is because rain water has a lower EC than groundwater (in the case of the Duggleby stream site, some higher EC values recorded after rainfall events may have occurred as a result of contaminated agricultural land runoff or piston effect).

9.1.3. Catchment water balance

Objectives:

- To estimate the annual recharge volume over the study catchments.
- To investigate if the springs in the study catchment are responsible for discharging all the recharged water to the aquifer or whether there is also underground flow from the catchment.
- To assess the reliability of the size of the catchment areas estimated from topographic divides.

The outcomes:

Depending on the rainfall and actual evapotranspiration, using data from MORECS for the years from 2010 to 2015, annual recharge for the study catchments was estimated. The data showed that the average annual recharge in the Kirby Grindalythe catchment was about 2,939,000 m3/year, while in the Driffield catchment it was about 5,286,000 m3/year. Water balance for the catchments was calculated from the annual recharge and gauged stream discharge. The results show that in both aquifers the amount of recharge to the catchment was bigger than the gauged outflow. The average recharge/gauged outflow ratio in the Kirby Grindalythe catchment was 5.6 for the water years 2010 to 2015. Recharge/gauged outflow ratio for the Driffield catchment was relatively constant for the study years 2010-2015, with an average of 3.5. The observable difference between recharge and gauged outflow is likely to have arisen from three possible factors: (a) uncertainty in climate information (because MORECS data from the 20*20 km grid square covers a much bigger area than the area of the study catchments), (b) Errors in estimating catchment size (because catchment boundaries were estimated from the topographic divide), (c) Underground flow from the catchments, in addition to the gauged flows in the streams. The difference between recharge and gauged outflow appears to be too large to be due only to uncertainty regarding the catchment size and climate data.

The most likely reason for the difference between inflow and gauged outflow is underground discharge from the catchments. This was supported by evidence from field investigations, e.g. observations and spot-measurements of streamflows up and downstream. Measuring the flow rate along the Gypsey Race stream in the Kirby Grindalythe catchment upstream of the gauging station showed that the stream lost water into the ground. In addition, the field investigation in the Driffield catchment showed flow downstream of the Driffield gauging station while the stream was dry at the gauging station. Both these situations indicate that part of the recharge water exits the catchments below the ground surface, therefore identifying this as the main reason for the difference between recharge and gauged outflow.

9.1.4. Analytical interpretation of spring discharge recession curve:

Objectives:

To investigate the aquifer flow system from the recession curve of the spring hydrograph using analytical approaches.

The outcomes:

Flow rate data used in this project consists of transformed discharge from stage measurements recorded at the gauging stations and transformed to discharge using rating curves supplied by the UK Environment Agency who operate the stations. During this project, using the flow meter and velocity-area method, the flow was measured at the gauging station together with the stage, during the low flow recession period in 2014. These measurements were used to assess the stage of zero flow of the rating curve, because changes in the stage of zero flow reveal whether the stage-discharge relation at the gauge station is subjected to change or not, for example due to accumulation of sediments in the station. The result showed that the stage of zero flow had not changed, which means that the rating curve did not require calibration.

The behaviour of the spring discharge during the recession period, in the absence of recharge, is controlled by the structure of the flow system in the aquifer. The start of the recession period at cessation of recharge was estimated using time series graphs of actual evapotranspiration (AE), as the point when the value of AE became greater than precipitation (P). Then, using the tabulation method, a master recession curve (MRC) for each study catchment was constructed to reduce the effect of spikes due to short recharge events, and remove the effect of difference in timing of the start of the recession period between successive years.

The analytical model indicated that Kirby Grindalythe aquifer most likely consists of a single reservoir, whereas Driffield aquifer consists of a double (or perhaps multiple) reservoir aquifer.

9.1.5. Analysis of CFC concentrations in spring water

Objectives:

To obtain information regarding the groundwater residence time in the aquifer.

The outcomes:

Water samples for CFC (CFC11 and CFC12) analysis were collected at 2 springs at Kirby Grindalythe (Duggleby 1 and 2) and the main spring in Driffield during the recession period of the water year 2015 at a sampling interval of 30 days. The results of the water samples showed evidence of local CFC contamination as all water samples (except one sample from Kirby Grindalythe spring Duggleby-1) contained CFC concentrations higher than the average global concentration of CFCs in recent air. This indicated that the samples could not be used for estimation of groundwater residence time (except the one from Duggleby1).

The relation between spring discharge and CFC concentration in the spring water indicated that the catchment which feeds Driffield spring contains two reservoirs. Regarding the Kirby Grindalythe catchment, two springs were monitored. The CFC-

flow relation indicated that the Duggleby1 spring is probably fed by two reservoirs, while a single reservoir aquifer feeds the Duggleby2 spring.

The relation between the ratios of CFC 11: CFC 12 in the water samples and the historical ratio of the CFC 11: CFC 12 revealed that most likely the groundwater discharged by Duggleby-1 spring consists of a mixture of water from two different sources (or ages). The Duggleby-2 and Driffield springs did not show signficant evidence of groundwater mixing.

9.1.6. Numerical simulation

Objectives:

To understand the effect of the hydraulic characteristics and structure of flow system in the aquifer on the pattern of the spring recession curve in Kirby Grindalythe and Driffield catchments.

The outcomes:

A transient three-dimensional numerical model was developed to simulate the chalk aquifers in the Kirby Grindalythe and Driffield catchments. The aquifers were simulated with the finite difference block centred groundwater model MODFLOW2000 using Groundwater Vistas version 6 (GV 6).

The Kirby Grindalythe catchment was discretized into a uniform grid of finite-difference cells consisting of 70 rows by 45 columns of 100 m x 100m cells and 5 layers. Each layer represented a 2 m thickness of the aquifer. The model domain enclosed an area of 3.2 km x 5.2 km and maximum 10 m aquifer saturated thickness, drained by a drain cell simulating a spring and four more representing subsurface drainage. The Driffield catchment was discretized into a uniform grid of finite-difference cells (34090 cells) consisting of 113 rows by 60 columns of 100 m x 100m cells and 10 layers. The model active domain was developed based on the Driffield conceptual model; it consisted of a square area of 6 km x 11.3 km and

maximum 40 m saturated thickness, and was drained by a drain cell simulating a spring and two more representing subsurface drainage. The studied aquifers were simulated in two scenarios representing possible situations within the real aquifers. The scenarios were single reservoir and double reservoirs aquifer, with the double reservoirs tested for three cases (vertically parallel reservoirs, horizontally parallel reservoirs and highly permeable tunnel shaped zone reservoirs).

The recession curve from the single reservoir model with hydraulic conductivity 400 m/day (equivalent to transmissivity of approximately 6400 m2/day) and specific yield 0.01 showed a good fit to the MRC on Kirby Grindalythe. Meanwhile, the recession curve from the vertically parallel double reservoir model of K1 0.1 m/day and K2 200 m/day, and the specific yield of 0.01, gave the best fit with the MRC from the Driffield catchment. The goodness of fit between the model and observed recession curves was calculated based on the r-squared method. The coefficients of regression (R-squared) between the recession curve from the best fitted calibrated models and the recession curve from Kirby Grindalythe and Driffield catchments were 0.99 and 0.98 respectively.

The outcome from numerical simulations showed that there was a difference between the transmissivity obtained from the calibrated models and the values from testing the boreholes located in the catchments. A pumping test in Low Mowthorpe borehole, which is located in the Kirby Grindalythe catchment near the outlet border about 1 km upstream from the gauging station, showed a transmissivity value of 450 m2/day. In comparison the recession curve best fitted to the MRC was from a model with transmissivity of the aquifer of 6000 m2/day. In the Driffield catchment the mean transmissivity value is about 930-1800 m2/day according to the data from testing boreholes (see table 3.1, section 3.1.3, chapter 3). The model best calibrated to the Driffield MRC showed that the aquifer consists of two main reservoirs with transmissivity of 4000 m2/day in the high flow reservoir and 2 m2/day in the low flow reservoir.

It can be noticed that in both catchments the transmissivities obtained from the numerical simulation were bigger than those from the field observations (except for the low flow reservoir in the Driffield case). In the introduction and geological chapters it was explained that the English Chalk is characterised by the existence of enlarged fissure networks, distributed irregularly in the aquifers. Generally, these fissures are more dominant inside the aquifer near the water table fluctuation zone, and spatially below streambeds. Therefore, the transmissivity in any boreholes drilled in the low-intensity fracture zones will be smaller than that in areas of high-intensity fracturing. Accordingly, this factor might be the reason for the discrepancy between the transmissivities from the models and those estimated from the boreholes in the study catchments. Transmissivity from boreholes may represent the transmissivity of the area at and around the borehole, rather than the entire aquifer. On the other hand, that estimated from numerical simulation represents an effective transmissivity across the entire aquifer, which is dominated by high transmissivity zones.

The results from calibrated models agreed with the results from water balance calculations for the study catchments. The recession curve from the Kirby Grindalythe model which contains 5 drain cells and Driffield model which contains 3 drain cells matched the respective MRCs from Kirby Grindalythe and Driffield aquifers. Each drain cell drained the same volume of water from the model, so the volume of water represented by the recession curve was 1/5 of the total water drained from the Kirby catchment model, and 1/3 of the Driffield catchment model. These results agree with the results from the water balance calculation of these aquifers, as in Kirby Grindalythe the recharge/outflow value was 5 (on average) and for Driffield catchment it was 2.5 for the hydrological years 2010-2014.

9.2. Main findings and overall implications:

9.2.1. EC of the groundwater:

The spring water from the Kirby Grindalythe catchment showed greater EC than that from the Little Driffield and Kilham catchments. This difference is believed to arise from differences in the average thickness of the unsaturated zone. The unsaturated zone is thinner in Kirby Grindalythe catchment (which is close to the escarpment) than in Driffield catchment (the dip slope catchments). Because in East Yorkshire Wolds the unsaturated zone is highly fractured, variation in its thickness is believed to have made a difference in the groundwater system with regard to the connection with the atmosphere. This means that the thinner the unsaturated zone the greater the connection between the groundwater in the aquifer and the atmosphere and vice versa.

9.2.2. Stream hydrology:

The streams in the East Yorkshire Wolds are dominated by Chalk derived groundwater with not much quick flow component. This is clearly confirmed by the fact that EC-Q relations of the streams do not show much variation. Chalk water dominates the EC signature of the springwaters both during the winter when the flow is high, and summer when the flow is smaller, in all three monitored catchments. Occasional deviations were seen at low flow, especially in the smallest catchment (Kirby Grindalythe), which may represent quickflow / runoff signatures.

9.2.3. Hydrogeology of the springs in the study area:

The hydrogeological models show that the springs in the Kirby Grindalythe catchment consist of both dip slope and escarpment slope springs. These springs arise at the locations where the contact surface between Cretaceous Chalk and underlying impermeable Jurassic Clay Formations intersects the ground surface. The spring at Driffield is a dip slope spring, located near the border between the

unconfined and confined Chalk Formations. It arises where thick impermeable or low permeability superficial deposits confine the aquifer, causing groundwater to exit to the surface.

9.2.4. Conceptual model of the flow system geometry in the Yorkshire Wolds in the light of the study findings

Analytical interpretation of the MRC and corresponding numerical simulation showed that Kirby Grindalythe catchment consists of a single reservoir aquifer. The CFC concentrations in two springs in Kirby Grindalythe catchment (Duggleby-1 and Duggleby-2) were monitored, and the CFC-Q relation suggested that the catchment which feeds the Duggleby-1 spring consists of two flow systems, while the catchment which feeds Duggleby-2 consists of a single reservoir. This indicates that the results from analytical interpretations of the MRC do not fully agree with the CFC results for spring Duggleby-1. However, it should be noted that the Kirby Grindalythe MRC curve represents the recession of all surface water (discharge via springs) flow from the Kirby Grindalythe catchment. Five visible springs were identified in the Kirby Grindalythe catchment, while the Duggleby-1 spring sub-catchment area comprises only about 20% of the total Kirby Grindalythe catchment, possibly explaining why any double reservoir response (inferred from the CFC data) here is not visible in the overall MRC, which reflects the accumulative effects of all spring flow from the catchment. However, it is also possible that the reservoirs identified from the CFC data do not correspond to those identified by recession analysis, i.e. 'compartments' with different CFC signatures do not necessarily reflect aquifer reservoirs of different permeability.

According to the analytical interpretation of the spring recession flow, numerical simulation and geochemical data (CFCs), the Driffield catchment consists of a double reservoir aquifer. Numerical modelling showed that the catchment consists of two flow zones: a high flow reservoir at the area downstream of the catchment, and low flow reservoir at the upstream end of the catchment. The following two factors

are considered most likely to have contributed to development of a more effective fracture system in the downstream part of the catchment:

- The shallower water table fluctuation zone, as the unsaturated zone is thin here (this may facilitate dissolution of more soil zone-derived CO_2 in the groundwater).
- Blocking of groundwater flow by impermeable superficial deposits leading to focused flow near the spring; flow focusing leads to greater permeability enhancement local to the spring.

Focusing of groundwater flow at the downstream area of the Driffield catchment near the contact between the Chalk and superficial deposits causes flow throughout the water year. This has created more opportunity for development of fractures due to the interaction between the groundwater and the Chalk. Eventually, the flow system in this part of the catchment became more developed compared to the other parts of the catchment (upstream area of the catchment).

Figure (9.1) shows a conceptual model of the flow system geometry in the East Yorkshire Wolds according to the analytical interpretation of the spring flow recession, numerical simulation and CFC concentrations in the spring water.

9.3. Recommendation and future works:

- ❖ In the current study, the EC of spring water was monitored through installation of CTD monitoring devices in the streams 1 to 3 km downstream of the springs. Checks showed that EC of stream water does broadly represent that of spring water, and this monitoring helped in determining the dominant source of the stream water. However, it is recommended that the CTD locations be placed closer to the spring site in future studies, to avoid complicating influences on the data from farm runoff and other waters.

- The analysis of CFC contamination showed that in the study catchments groundwater contamination with CFCs is due to a widespread airborne CFC source (maybe from a disposal/recycling station) with a low CFC-11:CFC-12 ratio. This source affects different catchments differently, and a more local source with a high CFC-11:CFC-12 ratio may be the result of a local point source. Therefore it is recommended that in the Yorkshire Wolds, without monitoring of local atmospheric CFC concentrations, CFCs are not appropriate for use as a tracer for estimating groundwater residence time, detecting patterns of groundwater mixing or evolution. SF6 may be a suitable alternative, as contamination of groundwater with SF6 is less likely since this gas is not commonly used in household appliances (Plummer and Busenberg, 2000).

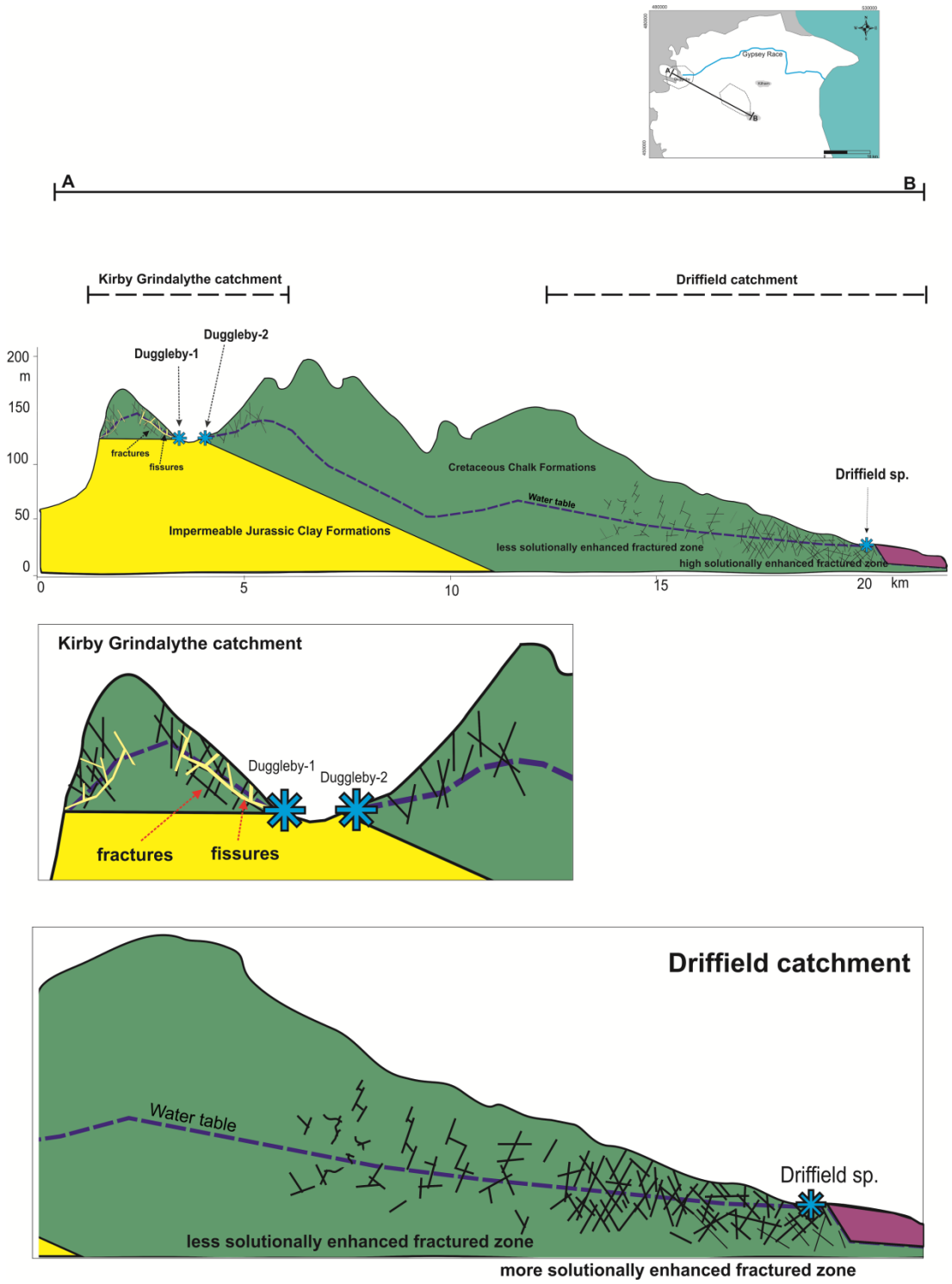

Figure 9-1Conceptual model showing the flow geometry in the Kirby Grindalythe and Driffield catchments.

- Because the calculation to estimate the total volume of recharge over the catchment depends on the size of the catchment area, it is important to define the catchment area. The water balance result for water years 2010- 2014 for the studied catchments showed that the total annual recharge was bigger than the total annual discharge (the gauged discharge). One of the reasons for the existence of this difference is uncertainty over the catchment size. The boundaries of the catchments in the study area were estimated according to the surface water divide (topographic water divides). Accordingly, this might indicate that the boundary of the surface water divide might not match the groundwater divide. This study recommends undertaking dye tracing tests for tracking groundwater flow over the topographical catchment and drilling monitoring boreholes at the sides of the topographic water divide (monitoring water table) to determine the groundwater divide.

- Comparison between the analytical interpretation of the MRC and recession curves for the Kirby Grindalythe and Driffield numerical models showed that the analytical method provided information on flow systems in the study catchments. However, numerical simulations showed that analytical interpretation of the flow recession does not always directly reflect the number of flow systems in the aquifer. For example, the numerical modelling showed that the recession from a single reservoir aquifer is not always matched by a single straight line during the analytical interpretation (according to Maillet method). Numerical modelling showed that correct identification of a number of reservoirs in a multi reservoir aquifer depends on the size of the reservoirs relative to each other and their contrasting hydraulic conductivity. In a dual-reservoir system, where the size of the high flow reservoir is too small compared to the low flow reservoir, the recession curve may decompose into three or more segments. The contrast in the hydraulic conductivity of the reservoir also affects the number of segments

that fit to the recession curve. For example, in a two reservoir system, when the contrast in K is small, the recession curve may fit with a single segment, while when there is a large contrast, the recession curve decomposes to two segments. Thus it is concluded that the Maillet model for estimating flow systems is better employed in a system where there is a small contrast in reservoir size, and a large contrast in hydraulic characteristics. It is important to combine the analytical method with other approaches to avoid misleading results.

- It is possible to deduce useful hydrogeological and hydrological information from the complex system through combining physical and chemical approaches. The technique of producing a relationship between flow rates from the aquifer with geochemical tracers such as CFCs, used during this study, revealed that it is possible to obtain information about the aquifer flow system. The spring samples showed that the groundwater CFCs cannot be used for groundwater age determination in the study areas, due to local contamination of the global signal. But, combining the CFC results with the spring discharge [CFC-Q and (CFC-11:CFC-12)-Q relation] suggested that it is possible to infer whether multiple groundwater reservoirs are present or not.

- Water balance indicated that the gauging stations in the study area do not pick up all the discharge from the catchment, while a portion of the recharge water leaves the catchment in the form of subsurface outflow. The subsurface outflow is one of the factors which affect the shape of the recession curve. If not enough information about the subsurface outflow is available, the recession curve may not suitable for characterising the aquifer flow system. This thesis suggests that analysis of the stream or spring recession discharge without combination of other approaches is not an adequate method for studying flow systems like those in the Chalk of East Yorkshire which have

subsurface outflows. Analysis of the recession discharge may work better in other catchments where the spring discharge is the main source of the outflow from the catchment.

- It is difficult to know whether the reservoirs identified by the CFC concentrations and ratios are the same as those derived from the analytical and numerical approaches. A clear inflection point was not observed on the CFC-Q relation, so it was difficult to determine if the change in CFC response coincided with the inflection point on the recession curve. For obtaining a clear result from comparison between the CFC-Q and recession curve analytical approach it is suggested that the CFC samples be taken at short sampling intervals, for instance weekly.

- The numerical models in this study were constructed to simulate spring flow recession from the Chalk aquifers in the East Yorkshire Wolds. The results showed that the Chalk of East Yorkshire consists of single and dual porosity systems that contain both high flow elements, due to large fissure networks, and large yield capacity, due to smaller fractures and matrix porosity. During the sensitivity testing process, several different reservoir scenarios and a wide range of permeability and storage were tested. In all the tested scenarios, the numerical models succeeded in producing spring recession curves. However, the approaches used here will not be suitable for systems of very high storage and very low storage. In the system of very high storage, there might not be very much recession as the spring flow might be essentially constant through the year. In the opposite case, a system might be so permeable that the response essentially represents the input signal (recharge signal) and gives little information on the aquifer.

Appendix

Appendix 1. OS map, showing some places of interest in the study area.

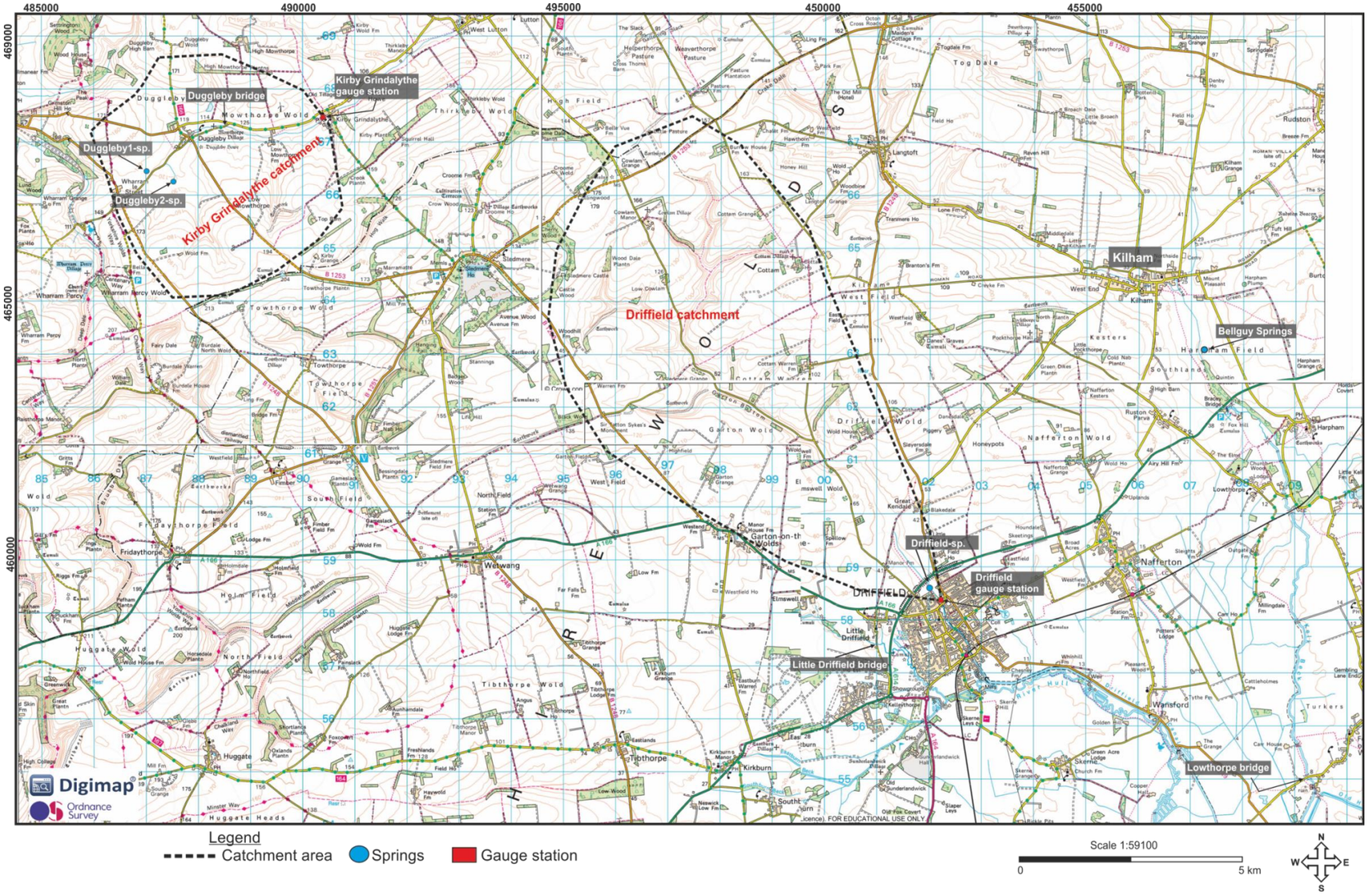

Appendix 1.

Appen. 1.1. Methods of measuring flow rate in open channel:

There are several approaches used for measuring flow discharge in open channels, the most commonly used methods are:

- Volumetrical method; this method is frequently used for measuring small stream discharges and it is considered a most accurate method for a small stream, through measuring the volume of water for a given moment. The material which is required for using this approach is volume measured containers and stopwatch (Richard and Gary, 2007)
- Area-velocity method; this method relies on the concept that flow discharge is the volume of water flowing through a given cross section of the channel per unit time. The flow rate can be determined using equation (Chanson, 2004; Das, 2008).
- Area slope method,
- Dilatation method; a tracer solution is injected into the flowing stream; the samples collect at cross sections downstream of the injection sites. The discharge is calculated from the rate of injection, the tracer concentration in the solution, and tracer concentration in the samples (Rantz et al., 1982; Kilpatrick and Ernest, 1985; Dutillet, 1993). This method is particularly useful for measuring discharge in the environment where it is hard to use current meters such as boulder-strewn and mountain flows (Kilpatrick and Ernest, 1985; Moore, 2004).

Hydraulic structures method; is one of the most common methods used for measuring discharge in open channels. There are two main artificial structures, which are used for measuring water discharge; Flume and Weir. Flume consist of the tapered box has a rectangular shape broad at both sides, commonly used flow measurement in a small channel and irrigation ditches. The discharge depends on

the depth of water and width of flume at the throat. This structure does not use widely in the hydrological study for continuous stream flow rate monitoring. Because there is not a linear relation between flume width, water depth, and stream discharge, there is not a simple equation to compute flow discharge and transform stage to discharge (Weight, 2008).

The area-velocity method and weir structure will be described in more detail because in this study area-velocity method have been used for observing discharge, and the gauging stations which provided the flow rate to this study are of weirs types.

Area-velocity method

This approach relies on the concept that flow discharge is the volume of water flowing through a given cross section of the channel per unit time. The flow rate can be determined using equation (equation 1).

$$Q = AV \qquad \text{Equation-1}$$

Where: Q is the discharge (m^3/s); A is the area of the cross section (m^2); V is the average flow velocity (m/s).

Usually, the discharge used by this method is the average discharge of many measurements spread across the channel cross-section.

The reason for measuring discharge at different points in channel cross section is because of water velocities not the same everywhere across a channel cross section. Many factors influence the velocity of water inside the canal for instance; the shape of the channel cross section, the roughness of the channel base and depth of water (Das, 2008). Typically, the velocity of water in the channel decreases with increasing depth because of the resistance to flow at the channel base due to the friction force between water and channel base, with increasing depth of water this force decreases and vice versa (Chanson, 2004). The maximum velocity is recorded just near the surface of the water, in contrast, the minimum velocity has been recorded at the

contact level with the channel base. Since the calculating discharge in this approach depends on both velocity of water and cross-section area of the channel (that occupied by flowing water), any changes in these two factors will cause a change in the discharge. Figure (appx 2.1) shows the estimated distribution of water velocity in the open channel. For the purpose of overcoming uncertainty due to the variation in the water velocity both vertically and horizontally across the channel, a reasonable solution has been suggested by USGS called Mid-Section method.

USGS proposed that the better way for measuring flow rate in a channel be by splitting the channel cross section into several vertical cells Figure (appx 2.2). Then at the middle of each of the cells, the velocity will be measured. If the depth of the channel (D) were less than 2.5 feet, the velocity would be measured at the depth 60% (0.6 D) of the channel depth at that point (by putting flow meter at that depth level). While if the depth of water in the channel at the centre of the cell (horizontal centre of the cell) was greater than 2.5 feet it will be better to measure the velocity at the depth 20% (0.2 D) and 80% (0.8 D) of the water depth. In this case, the average velocity of the measurements 20% and 80% will represent water velocity in that cell. Depending on USGS this method can obtain an acceptable result that can represent the total velocity of the water body passes across an area inside the river channel. The average of the calculated discharges at these points will represent the flow discharge at that gauge station at the time of measurement (Shrestha, and Simonovic, 2009).

Figure (appx 2.2) shows the schematic explanation of measuring discharge in the open channel using Mid-Section method.

The equation of calculating discharge depending on velocity-area method:

$$Q = VA$$

Discharge at specific cell (q_i) is $$q_i = V_i * D_i * \frac{W_{i+1} - W_{i-1}}{2}$$

e.g. discharge at cell one (q_1) is $q_2 = V_2 * D_2 * \frac{W_3 - W_1}{2}$

Where: Q is total is a charge, V is average water velocity in the channel, and A is a cross-section area of the channel where the water passes through.

Total discharge (Q):

$$Q = \sum_{i=1}^{n} \left(V_i * D_i * \frac{W_{i+1} - W_{i-1}}{2} \right)$$ Equation-2

Where: Q= discharge $(\frac{m^3}{s})$, $V_i = velocity\ at\ point\ i\ in\ m^3/s$, W = distance from initial point m and, D= depth(m), i is location number of the measurement.

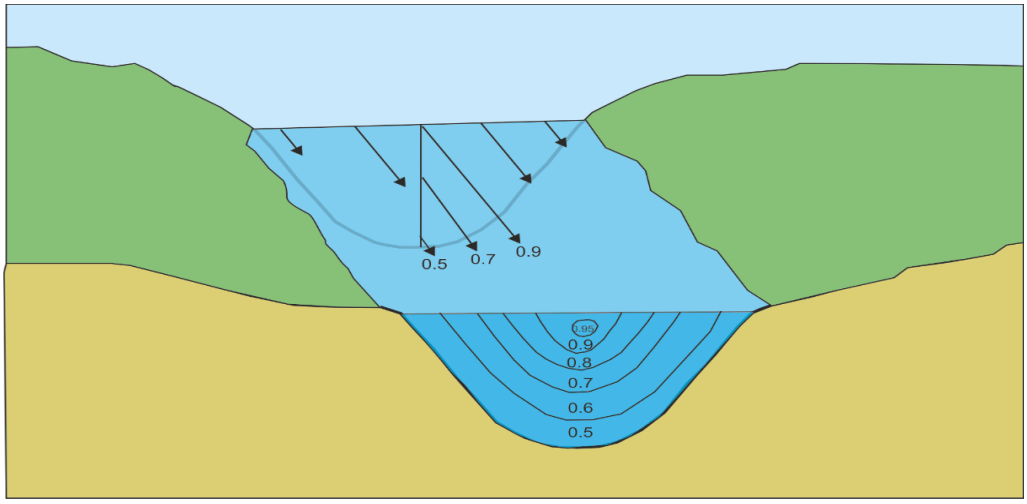

Figure appx 2.1 Illustrate distribution water velocity in open channel with depth.

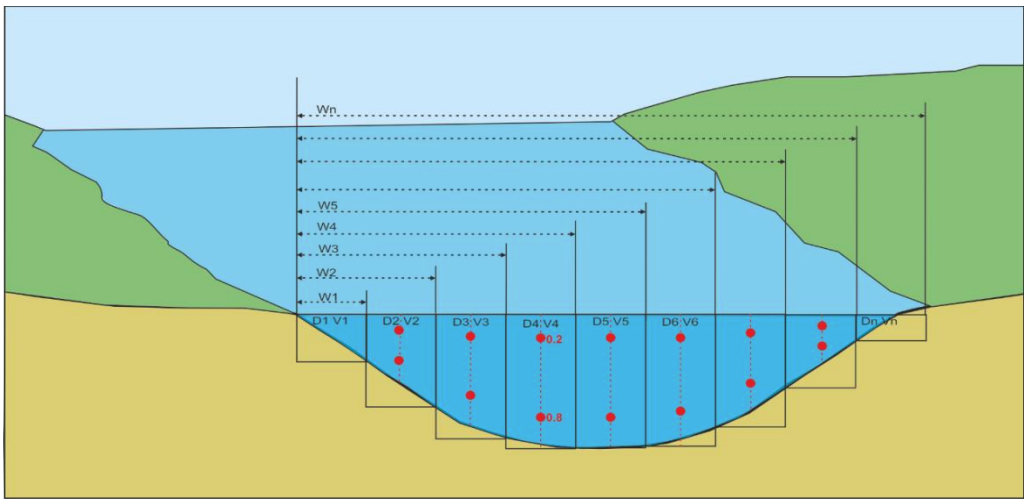

Figure appx 2.2 Sketch of midsection method of computing cross- section area for discharge measurement (after USGS midsection measurement 2013).

Weir

It is a hydraulic structure, which constructs across channels and is used for measuring water flow. It is an overflow structure which works on raising the water level in the stream on the upstream side and allowing the excess water to flow over its entire length into the downstream side. In general, weirs have a different geometrical shape, and they are classified depending on the form of opening and shape of the crest. Rectangular, triangular and trapezoidal are the three most important types of weirs depending on the shape of opening Figure (appx 2.3). Depending on the shape of the crest weirs also subdivided to sharp crest weir, narrow crest weir, broad crest weir and ogee-shaped weir (Singh, 2009). Essentially, the discharge of the water that flow over the weir is related to the head of water over the weir (Asawa,1999).

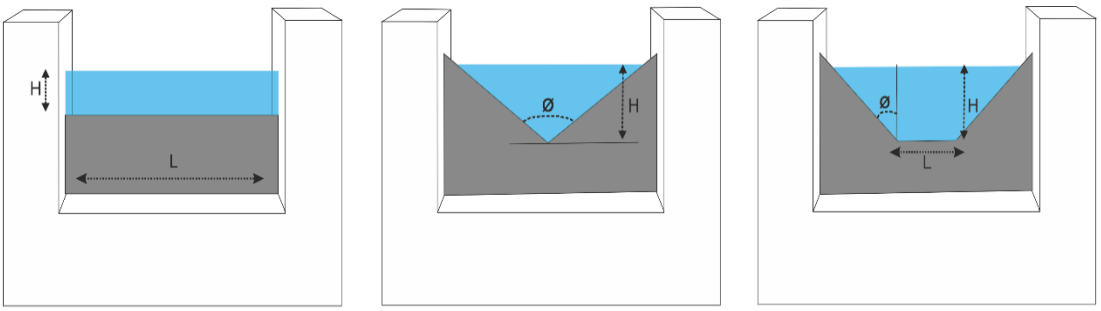

Figure appx 2.3 type of wire depending on the shape of the opening. (A) Rectangular weir, (B) Triangular weir, (C) trapezoidal weir. After ,(Madan, 2009).

Appen. 1.2. Analytical Models for interpretation of recession curve:

The analytical models in general classified into three groups; linear model, nonlinear model, and parallel aquifer.

Linear Aquifer:

A model, which is known as the Maillet exponential method, has been proposed by Maillet (1905). This approach considers that the aquifer consists of the single reservoir that behaves linearly (Kovac, 2003, 3005). Discharge is given by equation (3)

$$Q_t = Q_o e^{-\alpha t} \qquad \text{Equation-3}$$

Where Q_t is the discharge [L^3T^{-1}] at time t, and Q_0 is the initial discharge [L^3T^{-1}] at an earlier time, **α** is the recession coefficient [T^{-1}] usually expressed in $days^{-1}$.

Depending on the Maillet equation the recession curve represents a straight line with slope α when plotted on a semi-logarithmic graph (Atkinson 1977; Dewandel et al.,2003; Kovacs ,2003). Maillet illustrated his equation by an analog model that

expressed discharge of water from the fully saturated porous aquifer through an outlet point (Demuth and Schreiber 1994; Dewandel et al., 2003), see figure (appx 2.4).

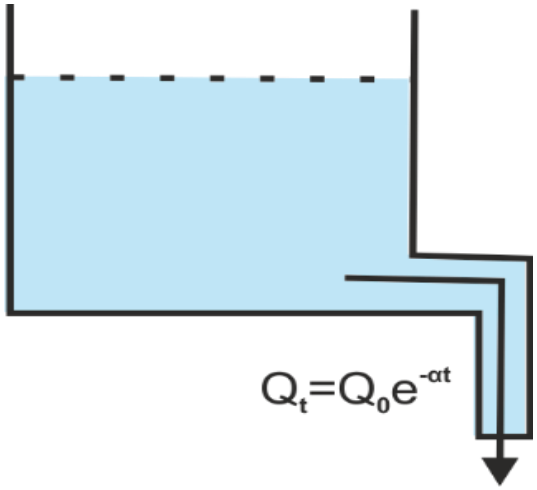

Figure appx 2.4 Simple exponential model for groundwater discharge.

Non-Linear Aquifers:

In nature depending on the behaviour of recession curves, it has been discovered that the relation between discharge and storage is rarely linear because of semi-logarithmic plotting of recession curve in most of the cases either not straight line or decomposed to more than one segment.

Several attempts have been carried out for describing nonlinearity behavior of the recession curve.

Mangin (1975) suggested that recession curve response to two different flow systems, first segment represent drainage from fast flow system which shows the nonlinear decay of the discharge, while the second segment reflects depletion from a low permeable system which shows the exponential decay of discharge.

In contrast, authors like Boussinesq (1904), Horton (1933), Coutagen (1948) claimed that non-linearity of recession curve is not an indication of superimposing of the different linear reservoir but it is a reflection of non-linearity of the storage-discharge relationship itself.

The following sub-section demonstrate the most popular non-linear models for analysis recession curve.

Boussinesq Model (1904):

Boussinesq (1904) offered a nonlinear analytical solution for diffusion equation for describing the water flow in the aquifer (equation 4). This model was constructed based on some assumptions (a) the aquifer is porous, homogeneous, and isotropic, (b) aquifers underlain by impermeable horizontal layer at same level of aquifer outlet (c) Water flows in the aquifer based on Dupuit assumption (assuming that there is not vertical flow in aquifer, water flow in aquifer only horizontally)(Dewandel et al., 2003, Farlin and Maloszewski, 2013) (Figure appx 2.5).

$$Q_t = \frac{Q_0}{(1+\alpha t)^2} \qquad \text{Equation-4}$$

Horton Model (1933):

Horton (1933) proposed a model (Figure appx 2.6) for discharge from the multi-reservoir aquifer. He believed that an aquifer with single reservoir would have a linear response and could represent by the simple exponential equation, but for the aquifer where more than one reservoir contributes the discharge will not response exponentially and would give a nonlinear recession curve. For the objective of coping with a nonlinear response, he suggested an improvement to a simple exponential and proposed a double exponential equation (equation 5) which generalizes the discharge from the aquifer (Toebes and Strang, 1964; Tallaksen, 1995).

$$\boldsymbol{Q_t = Q_0 e^{-\alpha t^m}}$$ Equation-5

Where α , m empirical value use for calibration line are constant, α also represent recession coefficient

$$\ln Q_t = \ln Q_0 - \alpha t^m$$

The data will plot as a straight line for t^m and $\ln Q_t$ on normal graph paper though selecting suitable m value (Toebes and Strang, 1964). And when $m = 1$ Horton equation will reduce to Maillet equation.

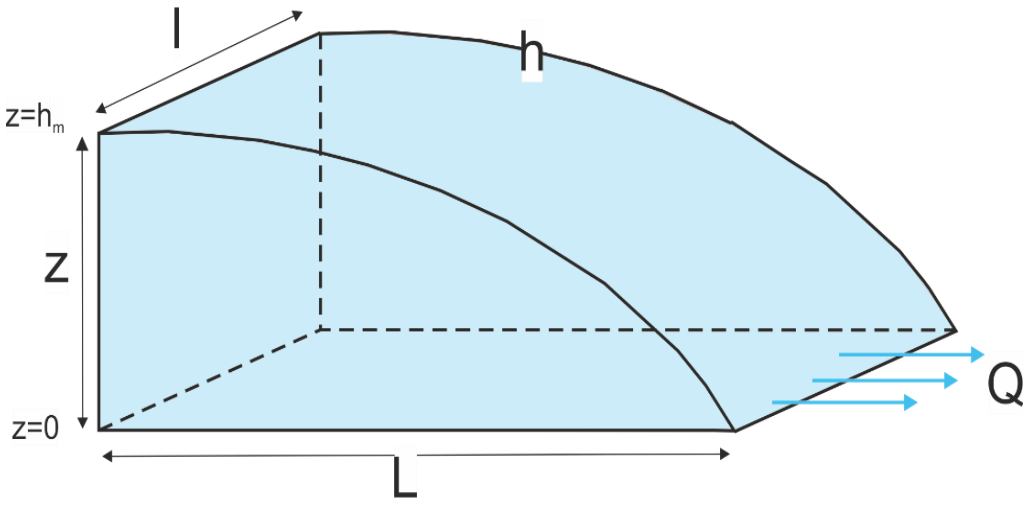

Figure appx 2.5 , Demonstrates design of aquifer which assumed by Boussinesq (1904) for analysing recession curve of the hydrograph. (h is head or water table drawdown , ***L*** is length of aquifer, ***l*** width of stream and Q is discharge).

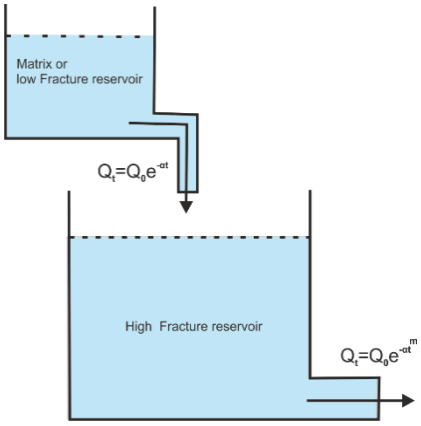

Figure appx 2.6 Groundwater depletion model depending on Horton (1933) , modified from (Dewandel et al., 2003)

Parallel reservoir model:

Different studies claimed that decomposition of the recession curve to several segments indicates the existence of parallel flow system (reservoir) in the aquifer (Barnes,1939; Forkasiewicz and Paloc,1967; Dewandel et al., 2003; Kovacs, 2003; Geyer et al., 2008). Schoeller (1967) in dealing with a karst aquifer, believed that different segments were related to the existence of different hydraulic system governing flow in the aquifer, considered that highest recession corresponds to high permeability and big fractures system and lowest to that of blocks and fissures. According to these authors, spring recession curve can be explained by the accumulation of multi-exponential segments.

A model for interpretation the entire recession curve (Figure appx 2.7), has been suggested by Barnes (1939; Schoeller,1948; Forkasiewicz and Paloc,1967; Eisenlohr et al., 1997; Dewandel et al.,2003). They considered that decomposition of the recession curve into components with different slope is represented discharge of the water from succession parallel reservoirs each reservoir has different hydraulic properties and behave linearly. They proposed a multi-exponential equation (equation 6):

$$Q_t = \sum_{i=1}^{N} Q_i e^{-\alpha_i t}$$ Equation-6

Where, N is number of the exponentials segments in the discharge curve. Depend on this method, the higher α value represents rapid flow system, intermediate α is return to the intermediate flow system in the aquifer and low α is due to the low flow system.

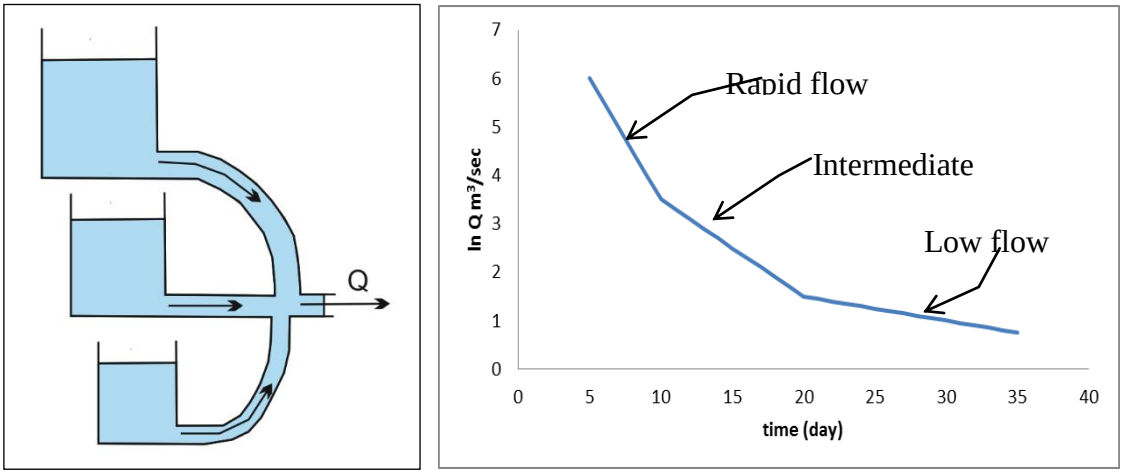

Figure appx 2.7 Model illustrates water discharge from the parallel reservoirs aquifer

Appen. 1.3. Stage-discharge data from Kirby Grindalythe and Driffield station by EA.

	Kirby Grindalythe				Driffield		
Date	Quality	SG [m]	Q [m3/s]	Date	Quality	SG [m]	Q [m3/s]
12/08/1999	G	0.018	0.003	10/05/2000	G	0.232	0.322
24/08/1999	G	0.019	0.003	08/06/2000	G	0.206	0.192
27/09/1999	G	0.021	0.004	11/07/2000	G	0.207	0.164
25/01/2000	G	0.022	0.01	10/08/2000	G	0.096	0.071
08/02/2000	G	0.023	0.005	08/02/2001	G	0.258	0.418
17/03/2000	G	0.024	0.007	08/03/2001	G	0.258	0.445
10/05/2000	G	0.024	0.026	11/02/2002	G	0.19	0.14
08/06/2000	G	0.025	0.006	14/05/2002	G	0.108	0.075
11/07/2000	G	0.025	0.006	31/05/2002	G	0.061	0.05
08/08/2000	G	0.027	0.006	17/02/2003	G	0.278	0.525
05/12/2000	G	0.028	0.009	13/07/2004	G	0.084	0.05
11/01/2001	G	0.029	0.008	10/08/2004	G	0.058	0.015
12/02/2001	G	0.032	0.008	23/08/2004	G	0.062	0.016
11/04/2001	G	0.032	0.006	07/09/2004	G	0.122	0.051
15/05/2001	G	0.042	0.013	10/11/2004	G	0.124	0.065
18/06/2001	G	0.044	0.014	03/02/2005	G	0.03	0.01
19/07/2001	G	0.047	0.016	24/02/2005	G	0.066	0.018
28/08/2001	G	0.048	0.015	30/03/2005	G	0.205	0.13
30/10/2001	G	0.05	0.013	19/08/2008	G	0.051	0.007
29/11/2001	G	0.058	0.02	09/09/2008	G	0.192	0.092
31/12/2001	G	0.063	0.022	14/07/2010	G	0.018	0.007
30/01/2002	G	0.063	0.021	13/01/2011	G	0.234	0.203
26/02/2002	G	0.07	0.024	08/02/2011	G	0.241	0.22
27/03/2002	G	0.071	0.029	17/05/2012	G	0.228	0.198
29/07/2002	G	0.072	0.032	25/05/2012	G	0.224	0.188
17/02/2003	G	0.073	0.031	13/11/2012	G	0.209	0.147
24/09/2003	G	0.073	0.033	13/12/2012	G	0.33	0.67
10/08/2004	G	0.075	0.034	09/01/2013	G	0.352	0.895
18/11/2004	G	0.083	0.03	05/02/2013	G	0.315	0.637
04/08/2005	G	0.09	0.04				
17/10/2007	G	0.096	0.037				
18/12/2007	G	0.102	0.051				
12/02/2008	G	0.12	0.07				
17/04/2008	G	0.12	0.061				
19/08/2008	G	0.126	0.078				
08/03/2010	G	0.136	0.073				
23/07/2010	G	0.138	0.072				
29/11/2010	G	0.14	0.091				
14/03/2011	G	0.14	0.085				
16/02/2012	G	0.14	0.074				
30/10/2012	G	0.17	0.12				
13/02/2013	G	0.175	0.116				

Note: based on EA quality code description G=Good

Appendix 2. Stratigraphic profile of some boreholes in Driffield catchment.

These data are available on Borehole record viewer- British Geological Survey web site, viewed10 November, 2016, http://www.bgs.ac.uk/data/boreholescans/home.html.

Appen. 2.1. Stratigraphic profile of borehole number 1 according to the map in Figure (2.13).

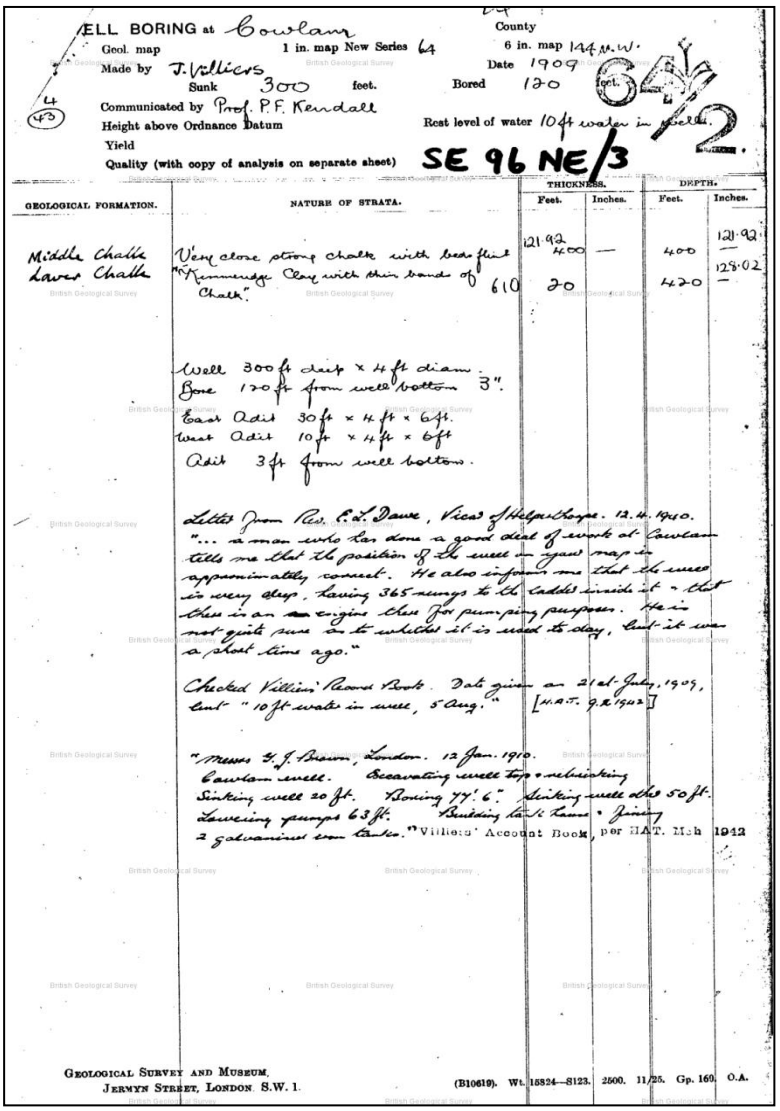

WELL BORING at Cowlam
Geol. map — 1 in. map New Series 64 — County
6 in. map 144 N.W.
Made by J. Villiers — Date 1909
Sunk 300 feet. — Bored 120 feet.
Communicated by Prof. P.F. Kendall
Height above Ordnance Datum — Rest level of water 10ft water in well.
Yield
Quality (with copy of analysis on separate sheet)
SE 96 NE/3

GEOLOGICAL FORMATION.	NATURE OF STRATA.	THICKNESS. Feet.	THICKNESS. Inches.	DEPTH. Feet.	DEPTH. Inches.
Middle Chalk	Very close stony chalk with bed of flint	121 92 400	—	400	121·92 —
Lower Chalk	"Kimmeridge Clay with thin bands of Chalk".	610	20	420	128·02 —

Well 300 ft deep × 4 ft diam.
Bore 120 ft from well bottom 3".
East Adit 30 ft × 4 ft × 6 ft.
West Adit 10 ft × 4 ft × 6 ft
Adit 3 ft from well bottom.

Letter from Rev. E. L. Dawe, Vicar of Helperthorpe. 12.4.1910.
"... a man who has done a good deal of work at Cowlam tells me that the position of the well in your map is approximately correct. He also informs me that the well is very deep, having 365 rungs to the ladder inside it - that there is an engine there for pumping purposes. He is not quite sure as to whether it is used to-day, but it was a short time ago."

Checked Villiers' Record Book. Date given as 21st July, 1909, sent "10 ft water in well, 5 Aug." [M.A.T. 9.2.1912]

"Messrs T. J. Braun, London. 12 Jan. 1910.
Cowlam well. Excavating well top + relining
Sinking well 20 ft. Boring 77' 6". Sinking well the 50 ft.
Lowering pumps 63 ft. Building in stone + joining
2 galvanised iron tanks." Villiers' Account Book, per MAT. Mch 1912

GEOLOGICAL SURVEY AND MUSEUM, JERMYN STREET, LONDON. S.W. 1.
(B10619). Wt. 18824—8123. 2500. 11/25. Gp. 160. O.A.

Appen. 2.2. Stratigraphic profile of borehole number 2 according to the map in Figure (2.13).

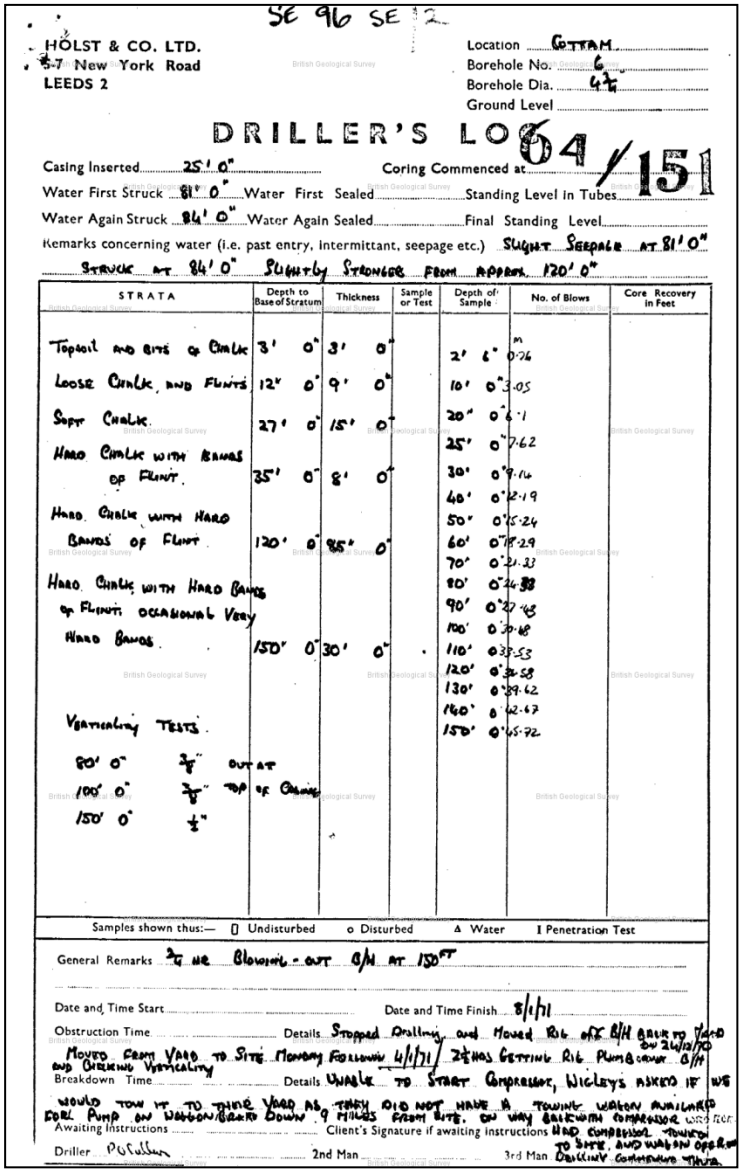

SE 96 SE 2

HOLST & CO. LTD.
57 New York Road
LEEDS 2

Location GOTHAM
Borehole No. 6
Borehole Dia. 4¼
Ground Level

DRILLER'S LOG 64/151

Casing Inserted 25' 0" Coring Commenced at
Water First Struck 81' 0" Water First Sealed Standing Level in Tubes
Water Again Struck 84' 0" Water Again Sealed Final Standing Level
Remarks concerning water (i.e. past entry, intermittant, seepage etc.) SLIGHT SEEPAGE AT 81' 0" STRUCK AT 84' 0" SLIGHTLY STRONGER FROM APPROX. 120' 0"

STRATA	Depth to Base of Stratum	Thickness	Sample or Test	Depth of Sample	No. of Blows	Core Recovery in Feet
Topsoil and bits of Chalk	3' 0"	3' 0"		2' 6"	m 0·76	
Loose Chalk and Flints	12' 0"	9' 0"		10' 0"	3·05	
Soft Chalk	27' 0"	15' 0"		20" 0"	6·1	
				25' 0"	7·62	
Hard Chalk with Bands of Flint	35' 0"	8' 0"		30' 0"	9·14	
				40' 0"	12·19	
Hard Chalk with Hard Bands of Flint	120' 0"	85" 0"		50" 0"	15·24	
				60' 0"	18·29	
				70' 0"	21·33	
Hard Chalk with Hard Bands of Flints occasional very				80' 0"	24·38	
				90' 0"	27·43	
Hard Bands.	150' 0"	30' 0"		100' 0"	30·48	
				110' 0"	33·53	
				120' 0"	36·58	
				130' 0"	39·62	
				140' 0"	42·67	
Verticality Tests.				150' 0"	45·72	
80' 0" ¾"						
100' 0" ¾"						
150' 0" ½"						

Samples shown thus:— ▯ Undisturbed o Disturbed ▵ Water I Penetration Test

General Remarks ¾ HR Blowing - OUT C/H AT 150FT

Date and Time Start Date and Time Finish 8/1/71

Obstruction Time Details STOPPED DRILLING AND MOVED RIG OFF B/H BACK TO YARD ON 24/12/70 MOVED FROM YARD TO SITE MONDAY FOLLOWING 4/1/71 2½ HRS GETTING RIG PLUMB & CHECK C/H AND CHEKING VERTICALITY

Breakdown Time Details UNABLE TO START COMPRESSOR, WICLEYS ASKED IF WE WOULD TOW IT TO THEIR YARD AS THEY DID NOT HAVE A TOWING VEHICLE AVAILABLE FOR PUMP ON WOBURN/BEARD DOWN 9 MILES FROM SITE. ON WAY BACK WITH COMPRESSOR WICLEYS TOWED TO SITE, AND WAS ON OPERATIVE DRILLING COMMENCED THERE.

Awaiting Instructions Client's Signature if awaiting instructions

Driller P. Pullen 2nd Man 3rd Man

Appen. 2.3. Stratigraphic profile of borehole number 3 according to the map in Figure (2.13).

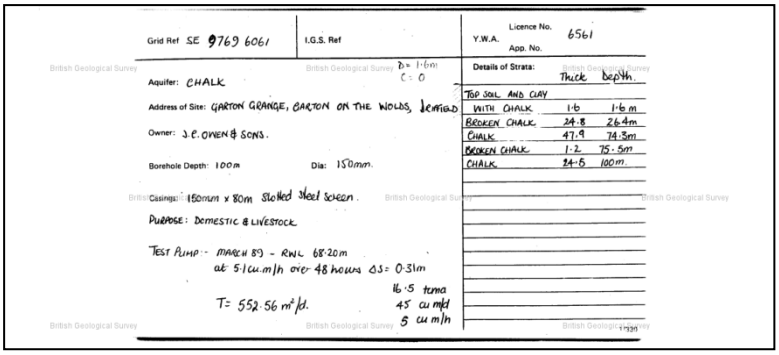

Grid Ref SE 9769 6061 | I.G.S. Ref | Y.W.A. Licence No. 6561 App. No.

Aquifer: CHALK

Address of Site: GARTON GRANGE, GARTON ON THE WOLDS, DRIFFIELD

Owner: J.C. OWEN & SONS.

Borehole Depth: 100m Dia: 150mm.

Casings: 150mm x 80m Slotted steel screen.

PURPOSE: DOMESTIC & LIVESTOCK

TEST PUMP:- MARCH 80 - RWL 68.20m
at 5.1 cu.m/h over 48 hours ΔS = 0.31m
T = 552.56 m²/d.

D = 1.60
C = 0

16.5 tema
45 cu m/d
5 cu m/h

Details of Strata:

	Thick	Depth
TOP SOIL AND CLAY		
WITH CHALK	1.6	1.6 m
BROKEN CHALK	24.8	26.4m
CHALK	47.9	74.3m
BROKEN CHALK	1.2	75.5m
CHALK	24.5	100m.

Appen. 2.4. Stratigraphic profile of borehole number 4 according to the map in Figure (2.13).

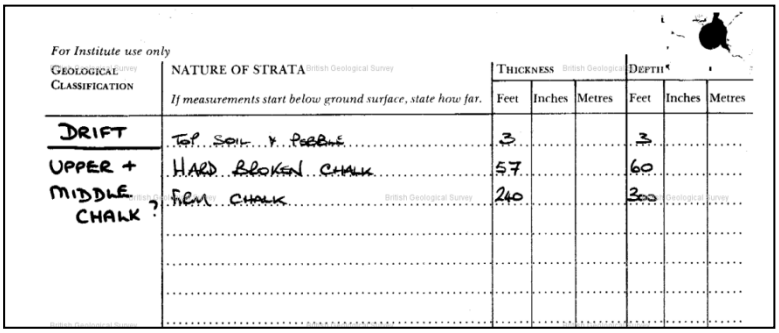

For Institute use only

GEOLOGICAL CLASSIFICATION	NATURE OF STRATA *If measurements start below ground surface, state how far.*	THICKNESS Feet	Inches	Metres	DEPTH Feet	Inches	Metres
DRIFT	~~TOP SOIL & PEBBLE~~	~~3~~			~~3~~		
UPPER + MIDDLE CHALK ?	~~HARD BROKEN CHALK~~	~~57~~			60		
	~~FIRM CHALK~~	240			~~300~~		

Appen. 2.5. Stratigraphic profile of borehole number 5 according to the map in Figure (2.13).

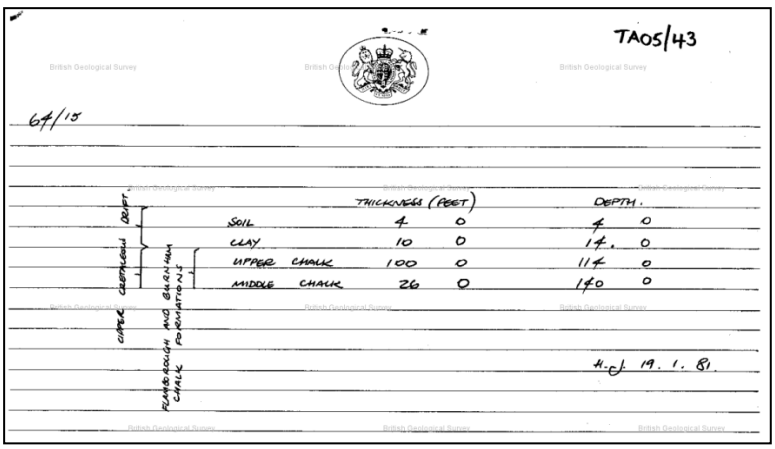

TA05/43

64/15

		THICKNESS (FEET)		DEPTH	
SOIL		4	0	4	0
CLAY		10	0	14	0
UPPER	CHALK	100	0	114	0
MIDDLE	CHALK	26	0	140	0

UPPER CRETACEOUS DRIFT

FLAMBOROUGH AND BURNHAM CHALK FORMATION

H.C.J. 19.1.81.

Appen. 2.6. Stratigraphic profile of borehole number 6 according to the map in Figure (2.13).

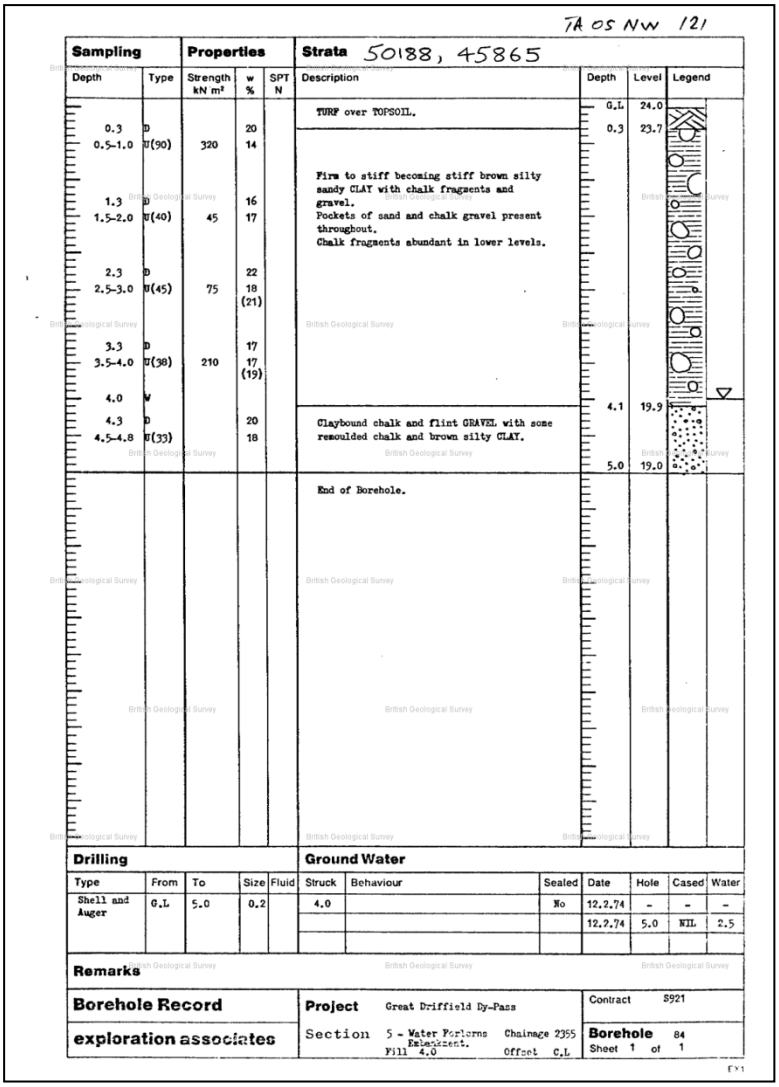

TA 05 NW 121

Sampling | **Properties** | **Strata** 50188, 45865

Depth	Type	Strength kN m²	w %	SPT N	Description	Depth	Level
					TURF over TOPSOIL.	0.L	24.0
0.3	D		20			0.3	23.7
0.5-1.0	U(90)	320	14		Firm to stiff becoming stiff brown silty sandy CLAY with chalk fragments and gravel. Pockets of sand and chalk gravel present throughout. Chalk fragments abundant in lower levels.		
1.3	D		16				
1.5-2.0	U(40)	45	17				
2.3	D		22				
2.5-3.0	U(45)	75	18 (21)				
3.3	D		17				
3.5-4.0	U(38)	210	17 (19)				
4.0	W						
4.3	D		20		Claybound chalk and flint GRAVEL with some remoulded chalk and brown silty CLAY.	4.1	19.9
4.5-4.8	U(33)		18			5.0	19.0
					End of Borehole.		

Drilling

Type	From	To	Size	Fluid
Shell and Auger	0.L	5.0	0.2	

Ground Water

Struck	Behaviour	Sealed	Date	Hole	Cased	Water
4.0		No	12.2.74	-	-	-
			12.2.74	5.0	NIL	2.5

Remarks

Borehole Record

exploration associates

Project Great Driffield By-Pass

Section 5 - Water Forlorns Embankment.

Chainage 2355

Fill 4.0

Offset C.L

Contract S921

Borehole 84

Sheet 1 of 1

Appen. 2.7. Stratigraphic profile of borehole number 7 according to the map in Figure (2.13).

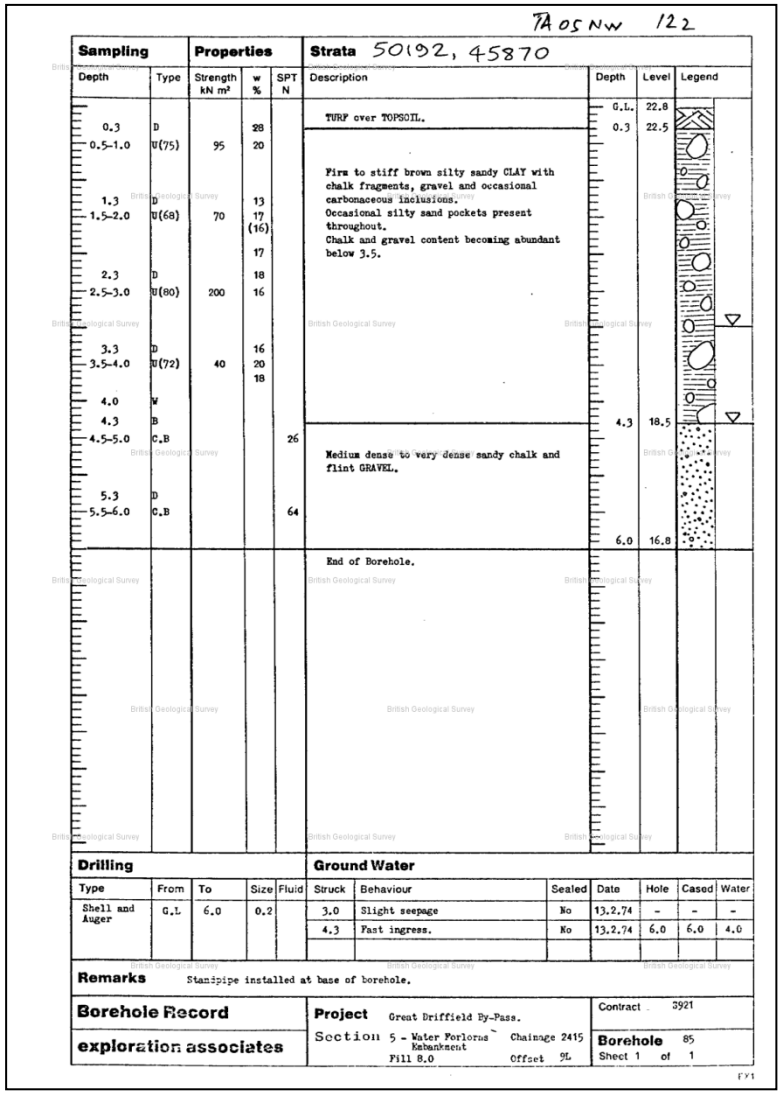

TA 05 NW 122

Sampling | **Properties** | **Strata** 50192, 45870

Depth	Type	Strength kN m²	w %	SPT N	Description	Depth	Level
						G.L.	22.8
0.3	D		28		TURF over TOPSOIL.	0.3	22.5
0.5-1.0	U(75)	95	20		Firm to stiff brown silty sandy CLAY with chalk fragments, gravel and occasional carbonaceous inclusions. Occasional silty sand pockets present throughout. Chalk and gravel content becoming abundant below 3.5.		
1.3	D		13				
1.5-2.0	U(68)	70	17				
			(16)				
			17				
2.3	D		18				
2.5-3.0	U(80)	200	16				
3.3	D		16				
3.5-4.0	U(72)	40	20				
			18				
4.0	W						
4.3	B					4.3	18.5
4.5-5.0	C.B			26	Medium dense to very dense sandy chalk and flint GRAVEL.		
5.3	D						
5.5-6.0	C.B			64			
						6.0	16.8
					End of Borehole.		

Drilling

Type	From	To	Size	Fluid
Shell and Auger	G.L	6.0	0.2	

Ground Water

Struck	Behaviour	Sealed	Date	Hole	Cased	Water
3.0	Slight seepage	No	13.2.74	-	-	-
4.3	Fast ingress.	No	13.2.74	6.0	6.0	4.0

Remarks Standpipe installed at base of borehole.

Borehole Record

exploration associates

Project Great Driffield By-Pass.

Section 5 - Water Forlorns Embankment Chainage 2415

Fill 8.0 Offset 9L

Contract 3921

Borehole 85

Sheet 1 of 1

FY1

Appen. 2.8. Stratigraphic profile of borehole number 8 according to the map in Figure (2.13).

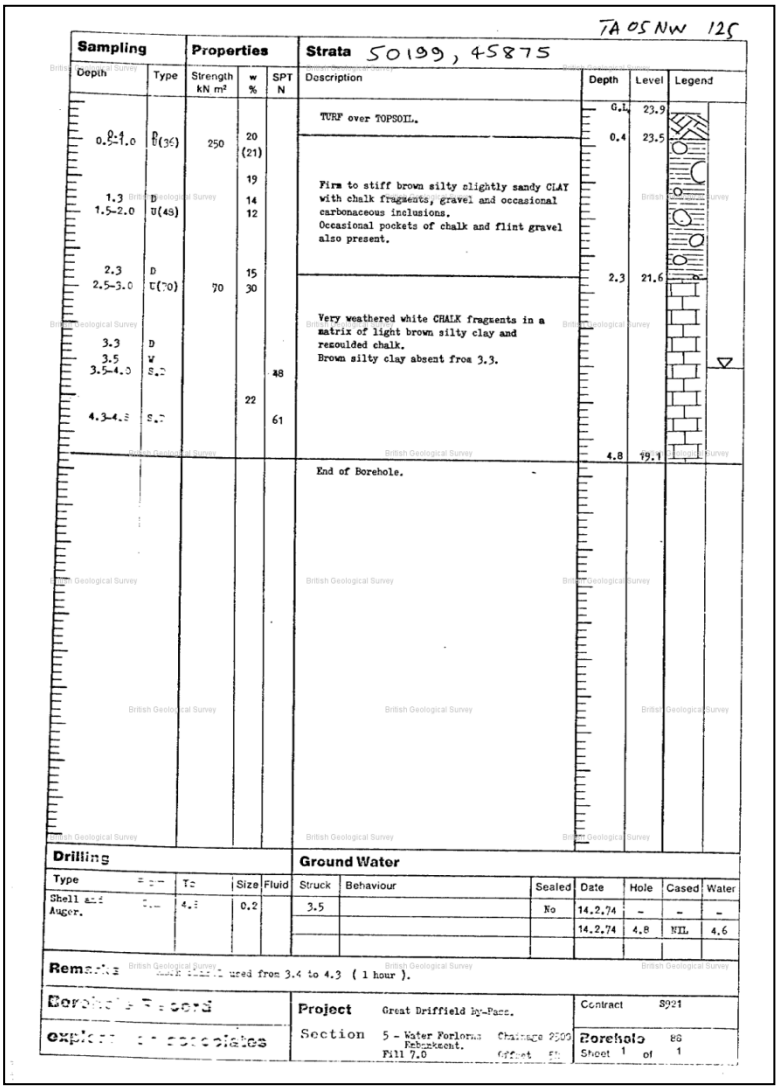

TA 05 NW 125

Sampling | **Properties** | **Strata** 50199, 45875

Depth	Type	Strength kN m²	w %	SPT N	Description	Depth	Level
					TURF over TOPSOIL.	G.L.	23.9
0.5-1.0	D U(36)	250	20 (21)			0.4	23.5
			19		Firm to stiff brown silty slightly sandy CLAY with chalk fragments, gravel and occasional carbonaceous inclusions. Occasional pockets of chalk and flint gravel also present.		
1.3	D		14				
1.5-2.0	U(48)		12				
2.3	D		15				
2.5-3.0	U(70)	70	30			2.3	21.6
					Very weathered white CHALK fragments in a matrix of light brown silty clay and recoulded chalk. Brown silty clay absent from 3.3.		
3.3	D						
3.5	W						
3.5-4.0	S.P			48			
			22				
4.3-4.8	S.P			61		4.8	19.1
					End of Borehole.		

Drilling

Type	Top	To	Size	Fluid
Shell and Auger.	G.L.	4.8	0.2	

Ground Water

Struck	Behaviour	Sealed	Date	Hole	Cased	Water
3.5		No	14.2.74	-	-	-
			14.2.74	4.8	NIL	4.6

Remarks Core barrel used from 3.4 to 4.3 (1 hour).

Borehole Record

explanation of symbols

Project Great Driffield by-Pass.

Section 5 - Water Forlorn Embankment. Chainage 2500 Fill 7.0 Offset 5m

Contract 8921

Borehole 8G

Sheet 1 of 1

Appen. 2.9. Stratigraphic profile of borehole number 9 according to the map in Figure (2.13).

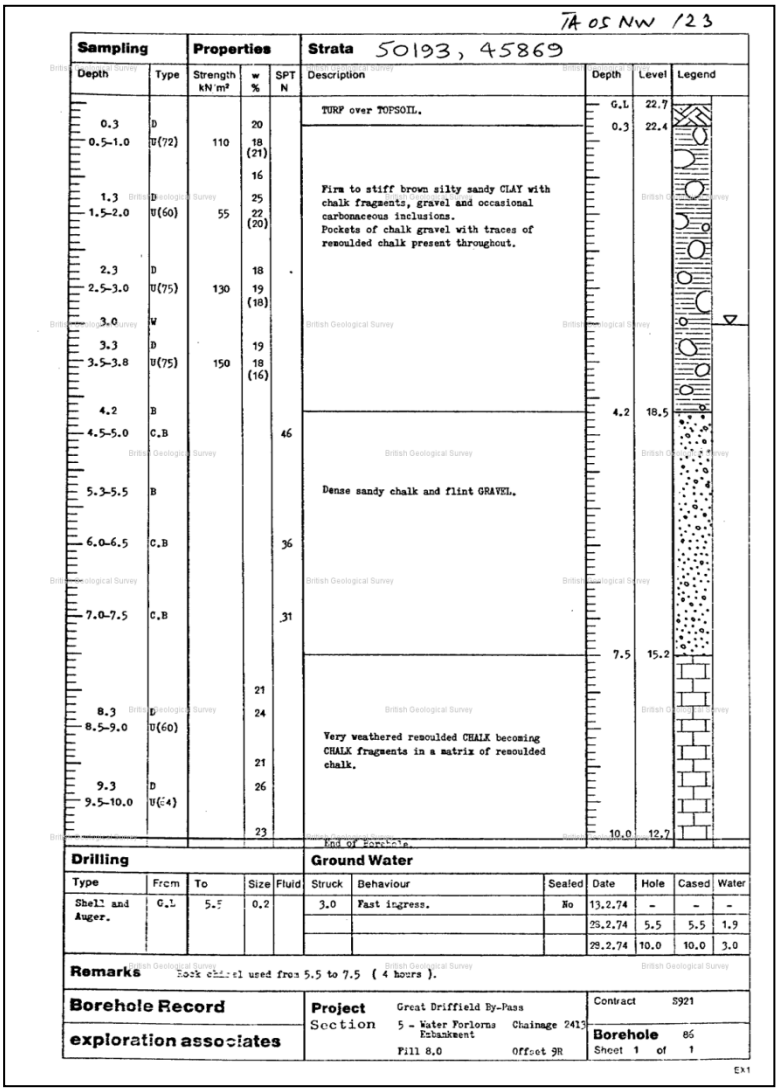

TA 05 NW 123

Sampling | **Properties** | **Strata** 50193, 45869

Depth	Type	Strength kN/m²	w %	SPT N	Description	Depth	Level
					TURF over TOPSOIL.	G.L	22.7
0.3	D		20			0.3	22.4
0.5–1.0	U(72)	110	18 (21)				
			16				
1.3	D		25		Firm to stiff brown silty sandy CLAY with chalk fragments, gravel and occasional carbonaceous inclusions. Pockets of chalk gravel with traces of remoulded chalk present throughout.		
1.5–2.0	U(60)	55	22 (20)				
2.3	D		18				
2.5–3.0	U(75)	130	19 (18)				
3.0	W						
3.3	D		19				
3.5–3.8	U(75)	150	18 (16)				
4.2	B					4.2	18.5
4.5–5.0	C,B			46			
5.3–5.5	B				Dense sandy chalk and flint GRAVEL.		
6.0–6.5	C,B			36			
7.0–7.5	C,B			31			
						7.5	15.2
			21				
8.3	D		24		Very weathered remoulded CHALK becoming CHALK fragments in a matrix of remoulded chalk.		
8.5–9.0	U(60)						
			21				
9.3	D		26				
9.5–10.0	U(54)						
			23		End of Borehole.	10.0	12.7

Drilling

Type	From	To	Size	Fluid
Shell and Auger.	G.L	5.5	0.2	

Ground Water

Struck	Behaviour	Sealed	Date	Hole	Cased	Water
3.0	Fast ingress.	No	13.2.74	-	-	-
			28.2.74	5.5	5.5	1.9
			28.2.74	10.0	10.0	3.0

Remarks Rock chisel used from 5.5 to 7.5 (4 hours).

Borehole Record

exploration associates

Project Great Driffield By-Pass

Section 5 - Water Forlorns Embankment Chainage 2413

Fill 8.0 Offset 9R

Contract S921

Borehole 86

Sheet 1 of 1

EX1

Appen. 2.10. Stratigraphic profile of borehole number 10 according to the map in Figure (2.13).

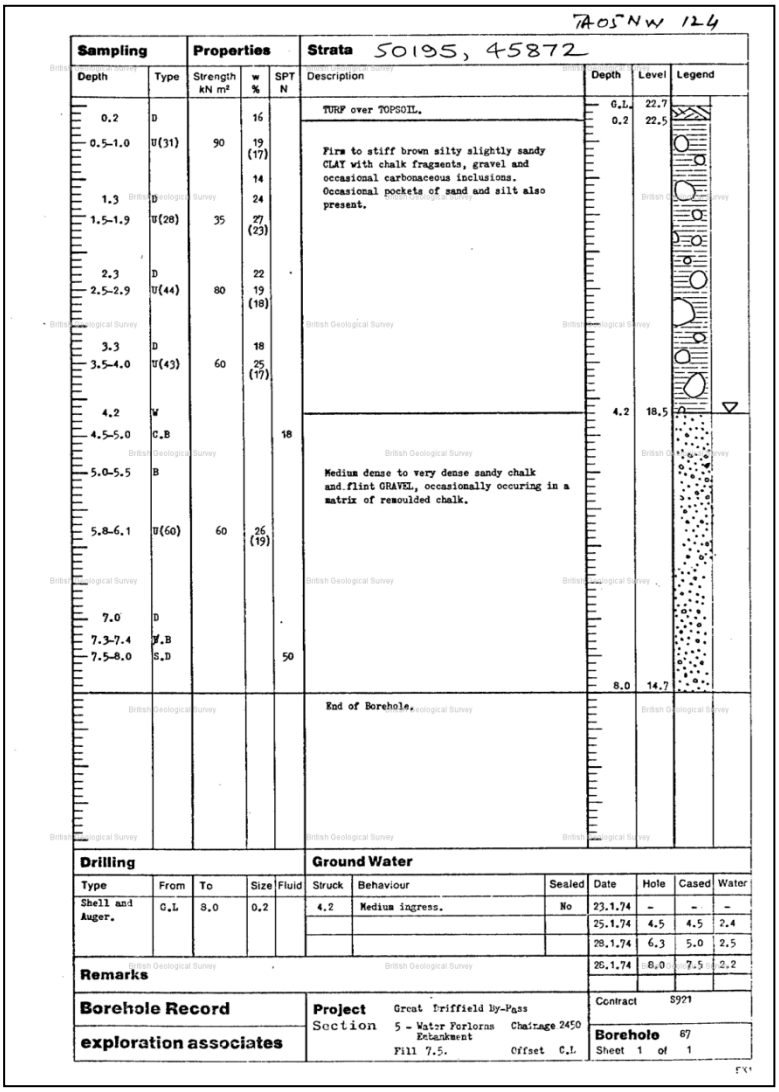

TA05NW 124

Sampling

Depth	Type	Strength kN m²	w %	SPT N
0.2	D		16	
0.5-1.0	U(31)	90	19 (17)	
			14	
1.3	D		24	
1.5-1.9	U(28)	35	27 (23)	
2.3	D		22	
2.5-2.9	U(44)	80	19 (18)	
3.3	D		18	
3.5-4.0	U(43)	60	25 (17)	
4.2	W			
4.5-5.0	C.B			18
5.0-5.5	B			
5.8-6.1	U(60)	60	26 (19)	
7.0	D			
7.3-7.4	W.B			
7.5-8.0	S.D			50

Strata 50195, 45872

Description	Depth	Level
TURF over TOPSOIL.	G.L.	22.7
	0.2	22.5
Firm to stiff brown silty slightly sandy CLAY with chalk fragments, gravel and occasional carbonaceous inclusions. Occasional pockets of sand and silt also present.		
	4.2	18.5
Medium dense to very dense sandy chalk and flint GRAVEL, occasionally occuring in a matrix of remoulded chalk.		
	8.0	14.7
End of Borehole.		

Legend

Drilling

Type	From	To	Size	Fluid
Shell and Auger.	G.L	8.0	0.2	

Ground Water

Struck	Behaviour	Sealed
4.2	Medium ingress.	No

Date	Hole	Cased	Water
23.1.74	-	-	-
25.1.74	4.5	4.5	2.4
28.1.74	6.3	5.0	2.5
26.1.74	8.0	7.5	2.2

Remarks

Borehole Record

exploration associates

Project Great Driffield By-Pass

Section 5 - Water Forlorns Chainage 2450 Embankment

Fill 7.5. Offset C.L

Contract S921

Borehole 67

Sheet 1 of 1

Appendix 3. Result and Discussion from numerical model sensitivity test:

Appen. 3.1. The results from hydraulic conductivity sensitivity:

Figure appx 3.1 demonstrates the discharge recession curve from the single reservoir aquifer under the various hydraulic conductivity situations. With decreasing hydraulic conductivity the slope of the recession curve decreased remarkably. The flow rate in the aquifers with lower hydraulic conductivity reduced more gently and smoothly. In contrast, the high hydraulic conductivity aquifer flow rate decreased dramatically during the first stage of the recession period. The model, which contains a low hydraulic conductivity, also required a long period to drain, while the high conductive model drained fully in 600 days.

Moreover, the recession curves from this sensitivity test showed that the maximum discharge during recession period (represent discharge at the start of the recession period) is directly related to the hydraulic conductivity in the model, see Figure appx 3.2. This type of relation allows selection of a suitable hydraulic conductivity value for producing specific starting discharge during model calibration, for the more realistic catchment models described below.

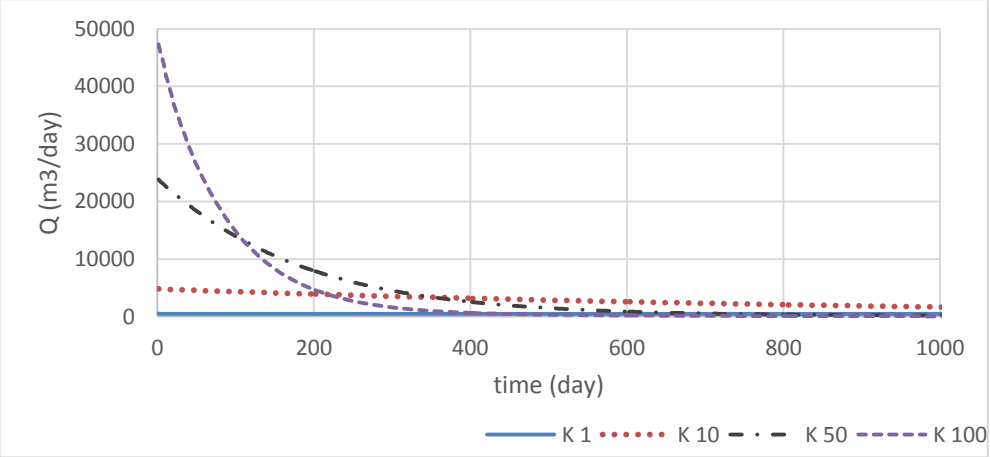

Figure appx 3.1 Hydrograph recession curve from single reservoir aquifer after K sensitivity test (K values are in m/day)

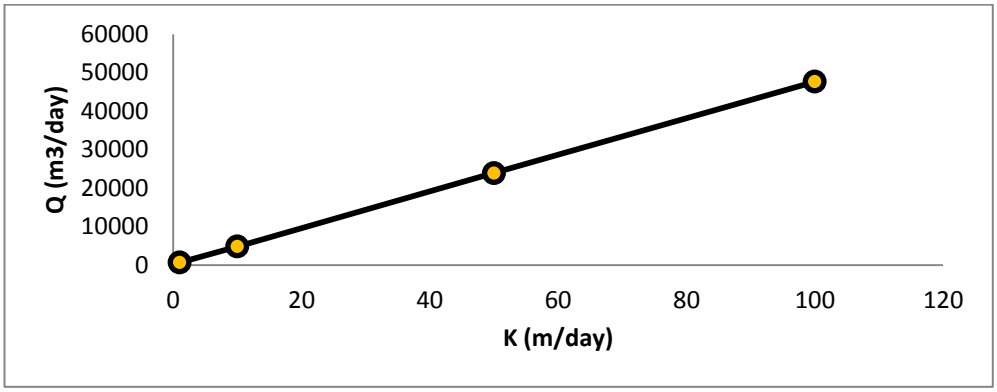

Figure appx 3.2 Relation between discharge at the beginning of the recession and K (single reservoir model).

Figure (appx 3.3) demonstrates the behaviour of the discharge recession curve from the double reservoir model under the various hydraulic conductivity conditions. In general recession curves from this model showed a pattern similar to that of the single reservoir aquifer. For this purpose, it has been compared with the result from the single reservoir model in order to identify the difference, see Figure (appx 3.4). The figure shows that the recession curve of hydraulic conductivity 100 m/day from single reservoir model have the same pattern as recession curve from 1-100 m/day from double reservoirs model with little difference. The recession curves from single reservoir starts with slightly higher flow rate compared to the double reservoir , but its value fall below the level of flow discharge of the double reservoir during the middle and late stage of the recession period.

The hydrograph recession curve from the tunnel model is illustrated in Figure (appx 3.5). Output recession curves reveal that at the early stage of the recession period the flow rate fell rapidly, then it becomes gentle toward the end of recession . This pattern in recession curve appeared more clearly when the contrast between the hydraulic conductivity of the block and tunnel zone became bigger.

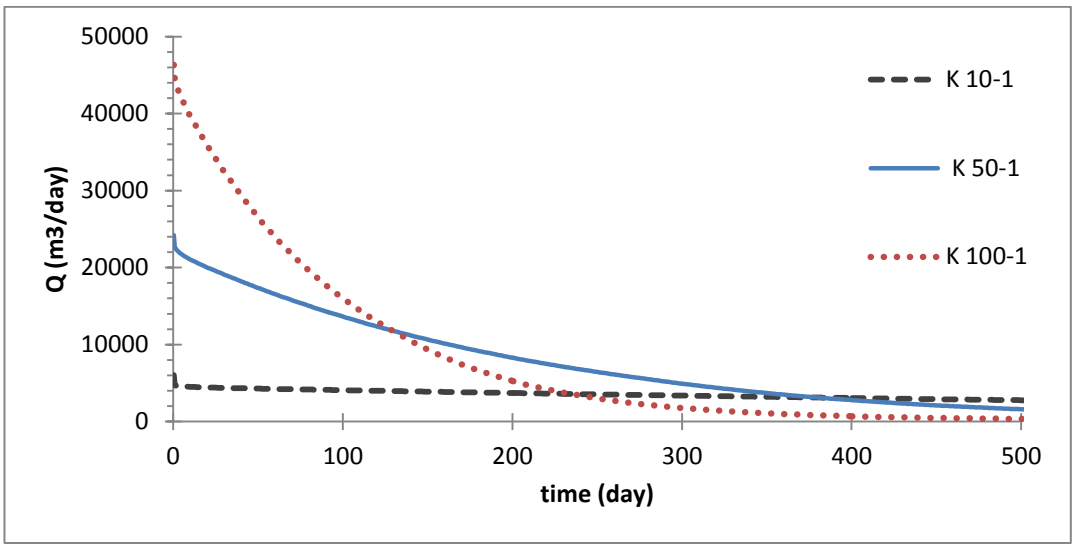

Figure appx 3.3. Double reservoir aquifer, recession curve after K sensitivity test. K values are in m/day –the first number represents the K value of the more permeable, lower reservoir. This from horizontally parallel duble reservoir aquifer , model (B.a section 8.6.1).

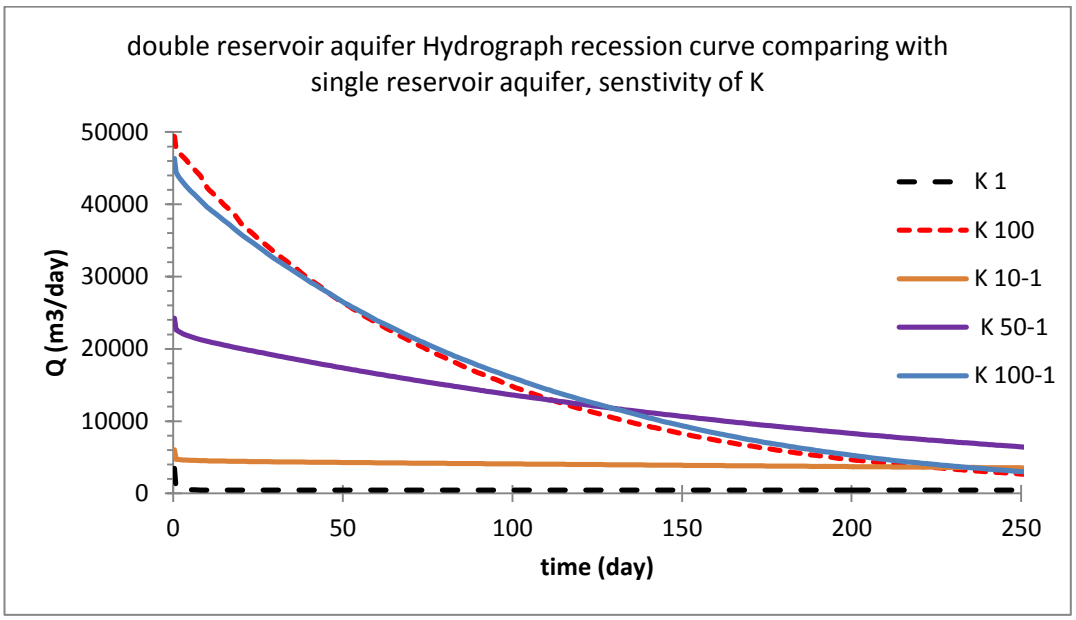

Figure appx 3.4 Single (dash line) and double reservoir (solid line) aquifer recession curve after K sensitivity. K values are in m/day – for the double reservoir model (horizontally parallel model)the first number represents the K value of the more permeable, lower reservoir.

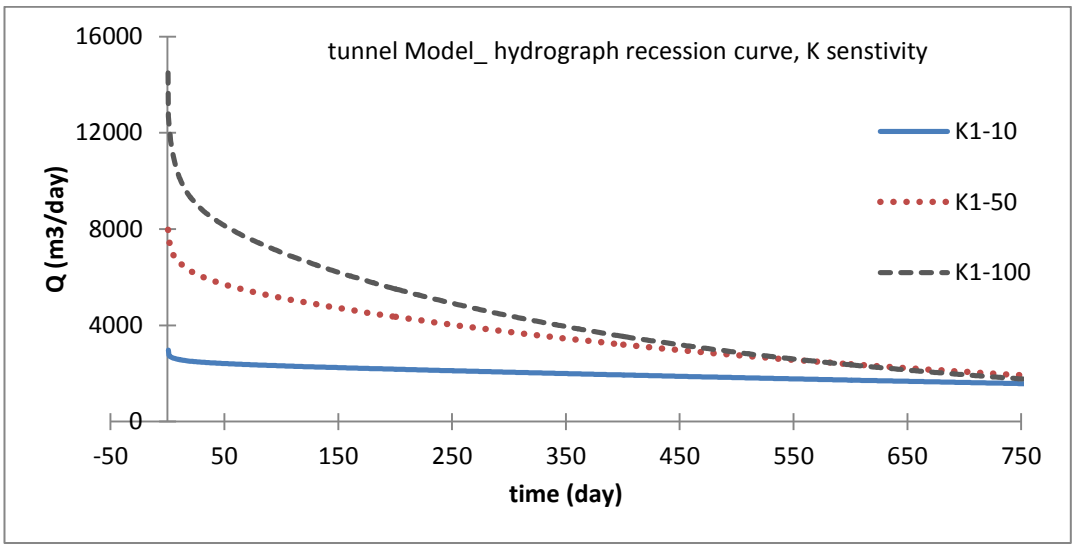

Figure appx 3.5 Demonstrating the pattern of recession curve from tunnel aquifer model under variable K value, K values are in m/day.

The double reservoir and tunnel shaped models are used for simulating the double reservoir aquifer. The result from sensitivity test of hydraulic conductivity from parallel in tunnel model showed that although the parameters in both models were same (low and high K was same in both models) but the recession curves differed, see Figure (appx 3.6).

This result explained that the size of the reservoirs relative to each other. In order to understand the effect of the size of the reservoir in the aquifer on the recession curve an extra sensitivity test has been done, to investigate the influence of the size of the high permeability zone.

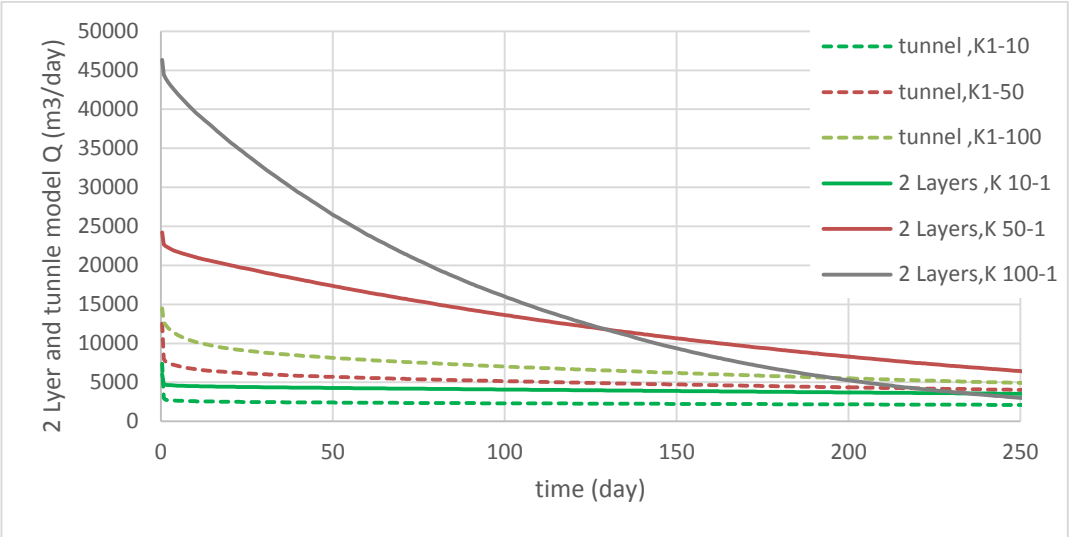

Figure appx 3.6 Recession curves from double and tunnel reservoir model, after K sensitivity. K values are in m/day.

Another sensitivity test was done to test the effect of the size of the reservoirs in the double reservoir model relative to each other on the pattern of the recession curve. The model consists of 100 m aquifer thickness, the aquifer consists of two reservoirs; low flow and high flow reservoirs. Hydraulic conductivity of the low flow zone is 1 m/day while the hydraulic conductivity of high flow zone 100 m/day. The size of the high flow reservoir changed between repeated tests, the size were 18.75%, 6.25%, 1.5 % and 0.02% of the total size of the aquifer. The results from this model illustrated in the Figure appx 3.7). It can be noticed that the bigger size of the high flow reservoir, the larger the initial flow rate, which then falls rapidly during the recession period. . In contest when the size of high hydraulic conductivity zone is small compared to the low conductivity reservoirs in the aquifer, the recession curve starts with lower flow rate and the flow reduces more gently during the recession period.

It appears that the rate of recession at the early stage in tunnel model much faster than in the equivalent double reservoir model. This reveals that the volume of the highly permeable zone is affecting the early stage of the recession curve, and

confirms that the effect of the highly permeable zone appears mainly on the early stage of the recession period.

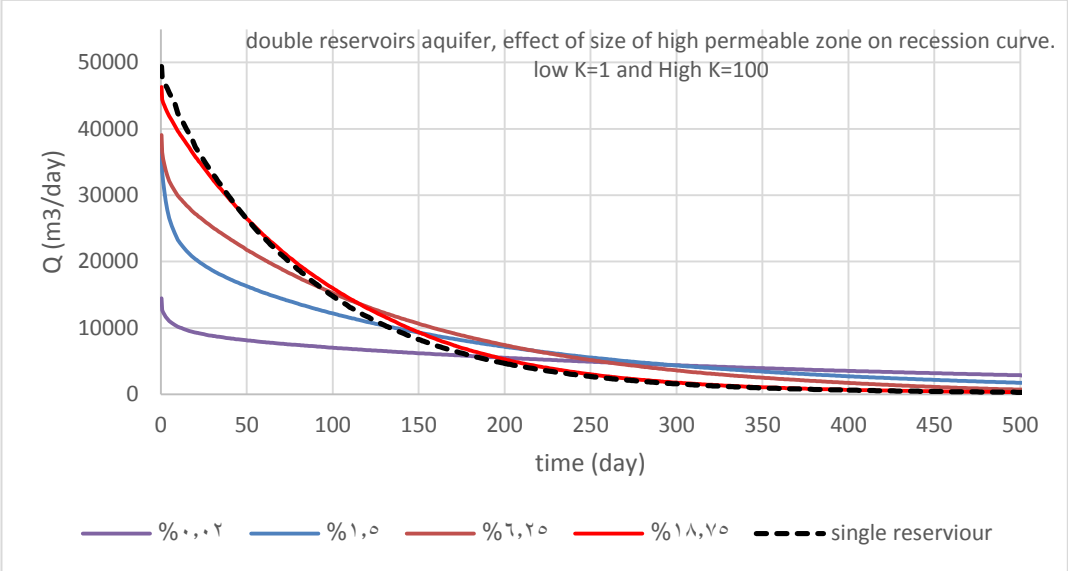

Figure appx 3.7 show the effect of the size of high flow reservoir on the recession curve from double reservoir aquifer. The percentage is of the total aquifer volume.It can be noticed that when the aquifer is homogenous (black dash line) with K=100 m/d almost has same recession curve as of the aquifer consist of double reservoir with low K=1 and high K=100 m/d, when size of the high K layer is about 20% of total aquifer size (red curve).

The size of the highly permeable zone in the double reservoir model is 2100*2000*15 m (4.2 km2 surface by 15 m thickness, total volume was 0.063 km3), whereas the size of the highly permeable zone in tunnel model is 2100*100*5 m (with a surface area of 0.21 Km2 and thickness 5 m, the volume w 0.00105 km3).

The result from the size of high K zone indicates that the greater the size of the high permeability zone, the more the aquifer behaves as a single reservoir with a K value equal to that of the higher K zone (see figure appx 3.7). In contrast, the smaller the sizes of the high permeability zone the faster the early stage of the recession.

A further model was constructed to represent a double reservoir aquifer containing a vertical high permeable zone intersecting the drain cell (this is intended to represent

a permeable fault zone). The hydrograph recession curves from this model have been expressed in Figure (appx 3.8).

Figure (appx 3.9) show the comparison between the recessions curves from the vertically paralleled double reservoir model and tunnel model, in the models the size of the high and low permeable reservoirs were similar. The result showed that the recession curve from the tunnel model started with high discharge rate and it reduces dramatically and became nearly horizontal during the middle and late of the recession period. Meanwhile, the recession curve from the vertical permeable reservoir model started with lower discharge rate, the discharge reduced more gradually toward the end of the recession period with a value higher than discharge at the late stage of the recession in the tunnel model. Head changes in the both models were observed from the boreholes placed at the aquifer border opposite the location of the spring. It appeared that the head falls similarly in both models, but the rate of fall in the vertical model is bigger than in the tunnel model, see Figure (appx 3.10).

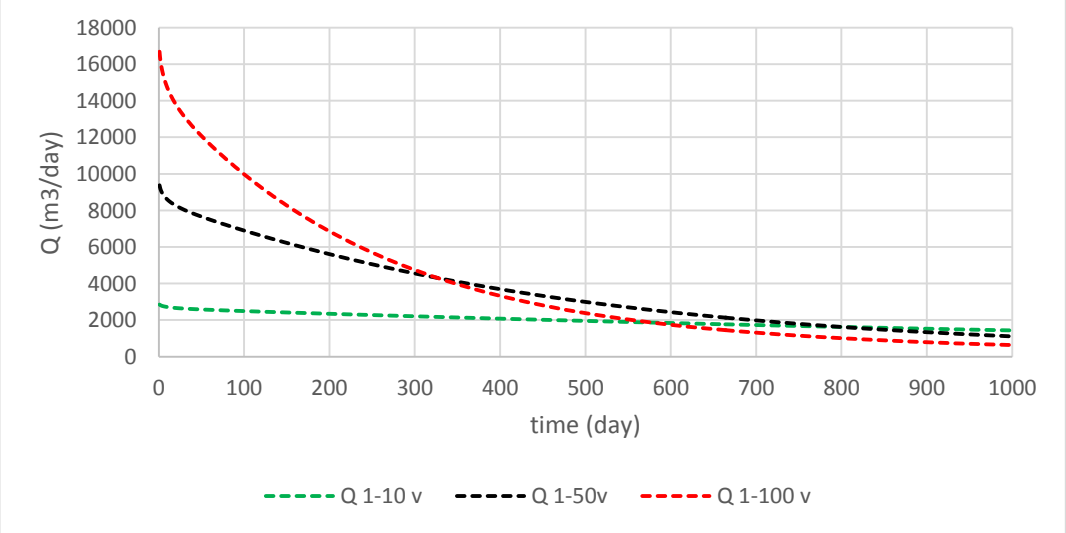

Figure appx 3.8 Hydrograph recession curve from Vertical zone model. K values are in m/day.

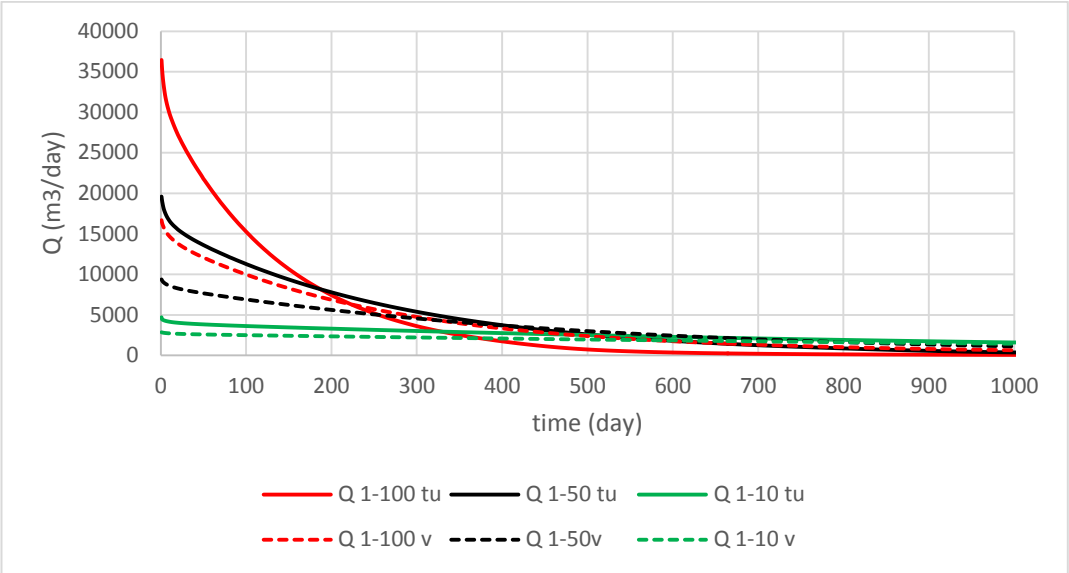

Figure appx 3.9 comparing the recession curves from tunnel (tu) model and duble reserviours vertically parralle (v) zone model.

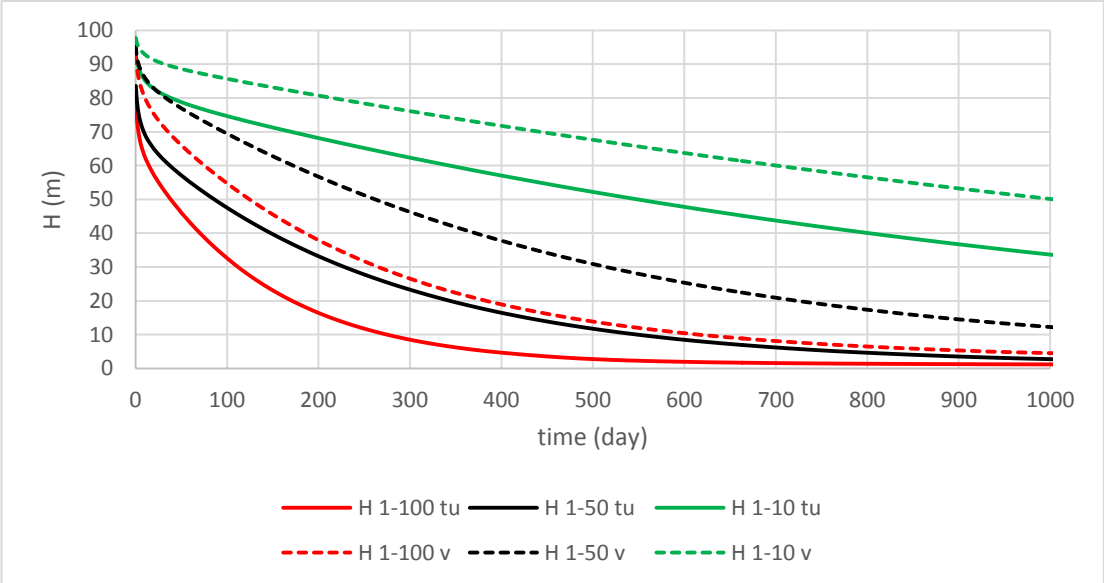

Figure appx 3.10 Difference between the pattern of groundwater head change during the recession period in both tunnel (tu) model and double reservior vertically parallel (v) zone model.

Appen. 3.2. Testing sensitivity to the Specific Yield:

A sensitivity test was done for the specific yield to investigate how variation in the specific yield affects the recession curve. A testing was done on a homogenous model by running the model several times, each time the Sy value has been changed while other parameters' value remained constant. The result of sensitivity test been presented in Figure (appx 3.11) which shows significant changes in the recession rate responding to variation in Sy . The sensitivity test of Sy shows Sy has a significant impact on the discharge rate, with larger Sy values leading to slower recession.

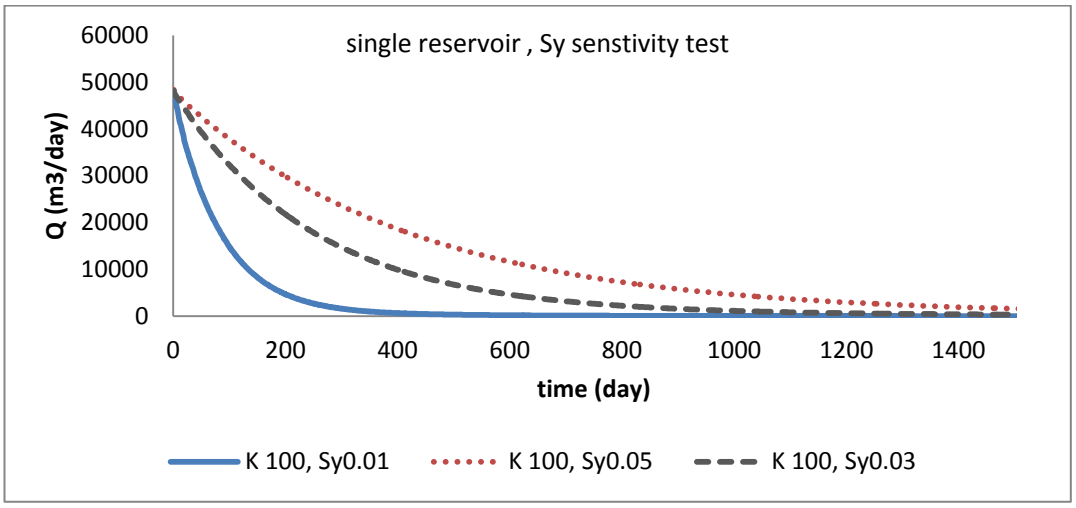

Figure appx 3.11 Single reservoir aquifer, Sy sensitivity test. K values in m/day.

Appen. 3.3. Sensitivity of drain cell

An increasing number of drain cells in the model were tested to investigate how it will affect the shape and pattern of the recession curve. The number of the drain cells has been increased in the same model while the flow rate from one drain cell (drain cell which simulates spring) was monitored. The result showed that with increasing the number of the drain cell in the model the discharge from the monitored-drain cell

has decreased, Figure (appx 3.12). Also it been noticed that the amount of flow from each drain cells nearly similar. The reason for doing this test was to simulate subsurface discharge via drain cell. During the water balance chapter in this thesis it has been noticed that the part of the recharge water flows from the aquifer via subsurface discharge.

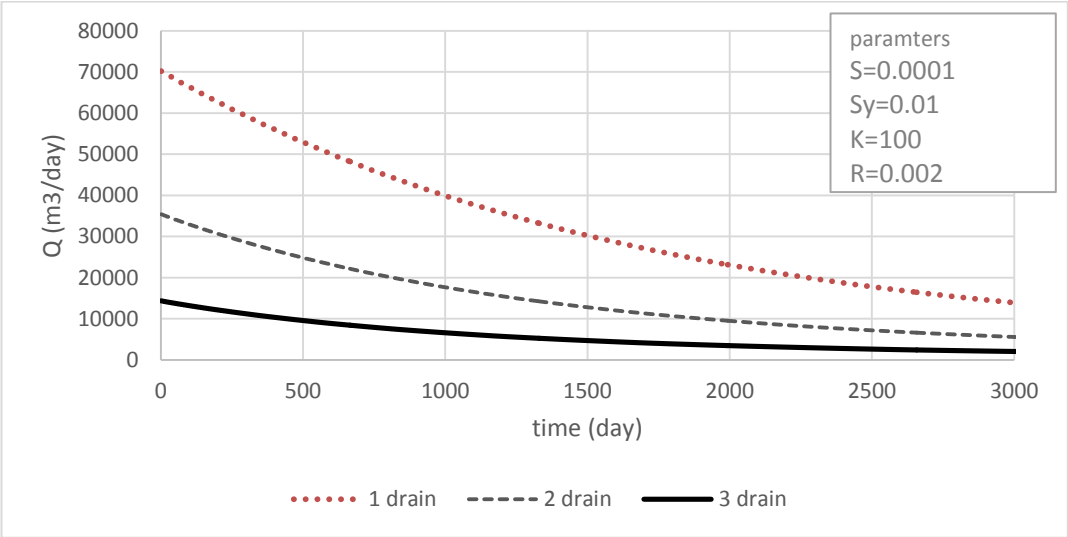

Figure appx 3.12 This graph showing the effect of a number of drain cells in the model on the shape of recession curve. K value in m/day.

Appen. 3.4. Shape of aquifer:

Another sensitivity test which has been done was testing effective shape of the catchment on recession curve pattern. A cuboid-shaped model was tested twice; under the same initial conditions, boundary conditions and hydraulic properties except for the location of drain cell. Figure (appx 3.13 A) shows a schematic diagram of the models which were tested for understanding the influence of the shape of the aquifer on the discharge during the recession period.

The recession curve from each model are plotted on same time series graph. Figure (appx 3.13 B), shows a significant different between the recession curves from the models. This test revealed that the location of the spring relative to the catchment

shape will affect the recession curve even if the other model parameters are the same.

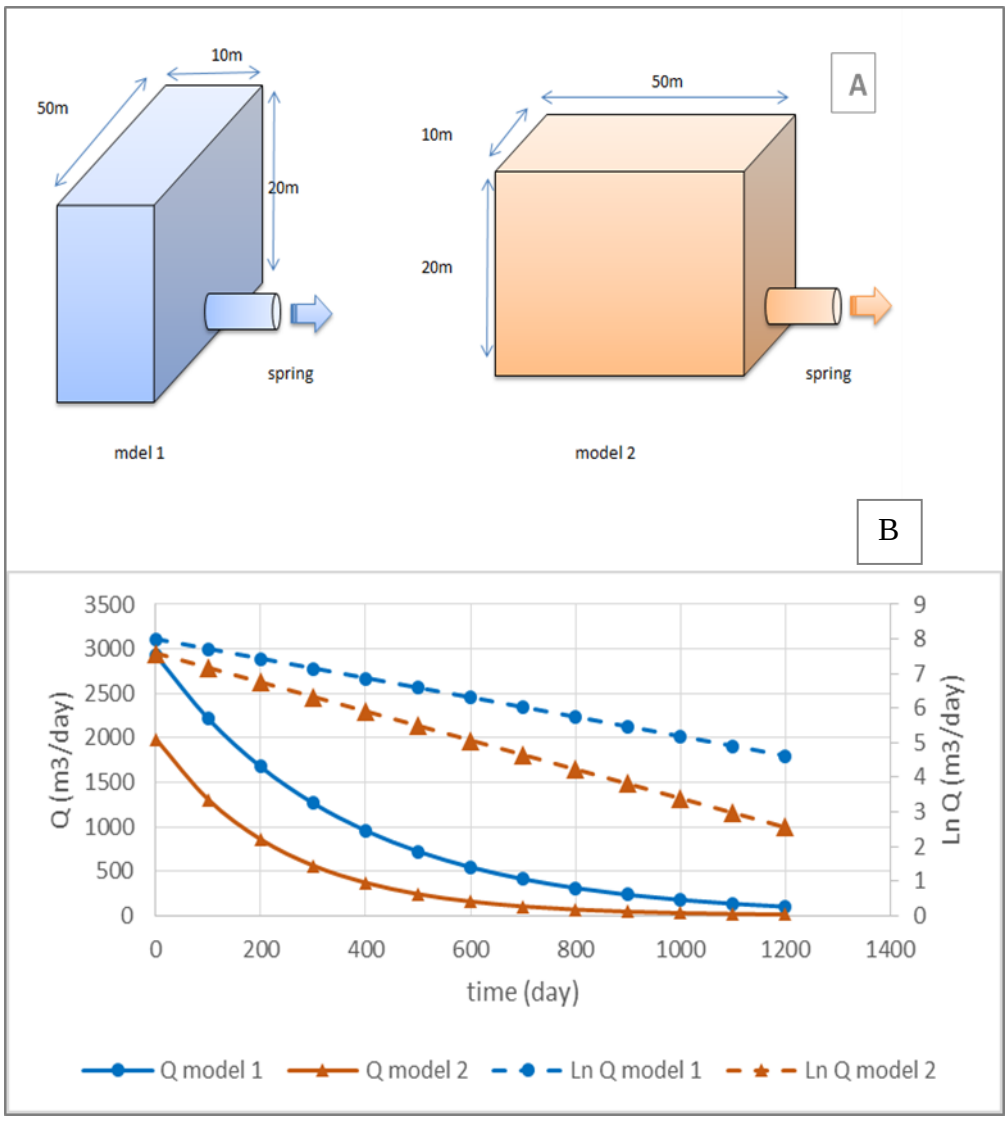

Figure appx 3.13. 3D model demonstrating the effect of the aquifer shape on the recession curve a) model shapes B) solid line represents recession curve from the models, and dash line represents logarthmic plot of the recesson curve.

References

Allen, D.J., Brewerton, L., Bloomfield, J., Coleby, L.M., Gibbs, B.R., Lewis, M.A., MacDonald, A.M., Wagstaff, S.J., Williams, A.T.P. and Robinson, V.K., 1997. The Physical Properties of Major Aquifers in England and Wales. British Geological Survey. Technical Report WD/97/24. Environment Agency R&D Publication 834.

Allen, R.G., Pereira, L.S., Raes, D. and Smith, M., 1998. FAO Irrigation and Drainage Paper No. 56, Crop Evapotranspiration (Guidelines for Computing Crop Water Requirements). FAO. Water Resources, Development and Management Service, Rome, Italy.

American Society of Civel Engineers (ASCE), 1996. Hydrology handbook. 2nd Ed., New York. Prepared by the Task Committee on Hydrology

Amit, H., Lyakhovsky, V., Katz, A., Starinsky, A. and Burg, A., 2002. Interpretation of spring recession curves. Ground Water, 40(5), pp.543-551.

Anderson M, Woessner WW. 1992. Applied groundwater modeling; simulation of flow and advective transport. San Diego (CA): Academic Press.

Anderson, M.P., 2005. Heat as a ground water tracer. Ground water, 43(6), pp.951-968.

Artimo, A., Mäkinen, J., Berg, R.C., Abert, C.C. and Salonen, V.P., 2003. Three-dimensional geologic modeling and visualization of the Virttaankangas aquifer, southwestern Finland. Hydrogeology Journal, 11(3), pp.378-386.

Asawa L. 1999, Elementary Irrigation Engineering, New Delhi, DEL , India.

Atkinson, T.C. and Smith, D.I., 1974. Rapid groundwater flow in fissures in the chalk: an example from south Hampshire. Quarterly Journal of Engineering Geology and Hydrogeology, 7(2), pp.197-205.

Atkinson, T.C., 1977, Diffuse flow in limestone terrain in the Mendip Hills, Somerset (Great Britain): Journal of Hydrology, v. 35, p. 93–100

Atkinson, T.C., and Smart, P.L., 1981. Artificial tracers in hydrogeology. In A survey of British Hydrogeology 1980: London, Royal Society. 173-190

Bailly V., Jonathan B. , Jourdea H. , Elizabeth J. , Pistrea S. And Langstonb A. (2010), Water exchange and pressure transfer between conduits and matrix and their influence on hydrodynamics of two karst aquifers with sinking streams, Journal of Hydrology 386 (2010) 55–66.

Bakalowicz M. 2005. Karst groundwater: a challenge for new resources. Hydrogeology Journal 13(1): 148-160.

Baker, D.N., Bame, S.J., Belian, R.D., Feldman, W.C., Gosling, J.T., Higbie, P.R., Hones, E.W., McComas, D.J. and Zwickl, R.D. (1984). Correlated dynamical changes in the near-earth and distant magnetotail regions: ISEE 3. Journal of Geophysical Research 89: doi: 10.1029/JA089iA06p03855. issn: 0148-0227.

Banks, D., Davies, C., and Davies,W., 1995. The Chalk as a karstic aquifer: evidence from a tracer test at Stanford Dingley, Berkshire, UK. Quarterly Journal of Engineering Geology 28, S31-S38

Barfield, B. J., Felton, G. K., Stevens, E. W. & Mccann, M. 2004. A simple model of karst spring flow using modified NRCS procedures. Journal of Hydrology, 287, 34-48.

Barker, J. A. 1991. Transport in fractured rock. In: Downing, R. A. & Wilkinson, W. B. (eds) Applied Groundwater Hydrology, Clarendon Press, Oxford. 199-216

Barnes, B.S., 1939. The structure of discharge-recession curves. Eos, Transactions American Geophysical Union, 20(4), pp.721-725.

Barron, J.J. and Ashton, C., 2005. The effect of temperature on conductivity measurement. TSP, 7(3).

Baskaran, S., Brodie, R.S., Ransley, T. and Baker, P., 2009. Time-series measurements of stream and sediment temperature for understanding river–groundwater interactions: Border Rivers and Lower Richmond catchments, Australia. Australian Journal of Earth Sciences, 56(1), pp.21-30.

Batelaan, O. and Smedt, F.D., 2004. SEEPAGE, a new MODFLOW DRAIN package. Ground Water, 42(4), pp.576-588

Bear, J. and Cheng, A.H.D., 2010. Modeling groundwater flow and contaminant transport (Vol. 23). Springer Science & Business Media.

Bell, F.G., Culshaw, M.G. and Cripps, J.C., 1999. A review of selected engineering geological characteristics of English Chalk. Engineering geology, 54(3), pp.237-269.

Berridge, N G and Pattison, J. 1994. Geology of the country around Grimsby and Patrington. Memoir of the British Geological Survey, Sheets 90, 91, 81 and 82 (England and Wales).

Birgand, F et al 2012, Uncertainties on flow calculated from stage-discharge rating curve in small streams, available from: http://www.bae.ncsu.edu/people/faculty/birgand/Downloads/Dallas_2012/Birgand_Q_uncertainties_poster_ASABE.pdf : [8 August 2013]

Blaskova, S., K. Beven, P. Tachecci, and A. Kulasova. 2002. Testing the distributed water table predictions of TOPMODEL (allowing for uncertainty in model calibration): The death of TOPMODEL? Water Resources Research 38, no. 11: 1257–1268.

Bloomfield, J.P., 1996. Characterisation of hydrogeologically significant fracture distributions in the Chalk: An example from the Upper Chalk of Southern England. Journal of Hydrology 184 (3-4), 355-379"

Bloomfield, J.P., 1997. The role of diagenesis in the hydrogeological stratification of carbonate aquifers: An example from the Chalk at Fair Cross, Berkshire, UK. Hydrology and Earth System Science 1, 19-33"

Bloomfield, J.P., Brewerton, L.J., and Allen, D.J., 1995. Regional trends in matrix porosity and dry density of the Chalk of England. Quarterly Journal of Engineering Geology 28, S131-S142"

Boggs, S., 2009. Petrology of sedimentary rocks. Cambridge University Press.

Bonacci, O. and Magdalenić, A., 1993. The catchment area of the Sv. Ivan Karst spring in Istria (Croatia). Ground water, 31(5), pp.767-773.

Bonacci, O., 1993. Karst springs hydrographs as indicators of karst aquifers. Hydrological Sciences Journal, 38(1), pp.51-62.

Bourke, S.A., Cook, P.G., Shanafield, M., Dogramaci, S. and Clark, J.F., 2014. Characterisation of hyporheic exchange in a losing stream using radon-222. Journal of Hydrology, 519, pp.94-105.

Boussinesq, J., 1904. theoretical research on the flow sheets of water infiltrated into the soil and the flow of springs. Pure Mathematics and Applied Journal , pp.5-78.

Braca G., 2008. Stage-discharge relationships in open channels: Practices and problems. FORALPS Technical Report, 11. Università degli Studi di Trento, Dipartimento di Ingegneria Civile e Ambientale, Trento, Italy.

Brownlee KA. 1960. Statistical theory and methodology in science and engineering. New York (NY): John Wiley and Sons.

Brutsaert W,Nieber JL. 1977. Regionalized drought flow hydrographs froma mature glaciated plateau. Water Resources Research 13: 637–643.

Bu, X. and Warner, M.J., 1995. Solubility of chlorofluorocarbon 113 in water and seawater. Deep Sea Research Part I: Oceanographic Research Papers, 42(7), pp.1151-1161.

Buczyński, S. and Rzonca, B., 2011. Effects of crystalline massif tectonics on groundwater origin and catchment size of a large spring area in Zieleniec, Sudety Mountains, southwestern Poland. Hydrogeology Journal, 19(5), pp.1085-1101.

Bullister, J.L. and Weiss, R.F., 1988. Determination of CCl 3 F and CCl 2 F 2 in seawater and air. Deep Sea Research Part A. Oceanographic Research Papers, 35(5), pp.839-853.

Busenberg, E. and Plummer, L.N., 1992. Use of chlorofluorocarbons (CCl3F and CCl2F2) as hydrologic tracers and age-dating tools: The alluvium and terrace system of central Oklahoma. Water Resources Research, 28(9), pp.2257-2283.

Busenberg, E. and Plummer, L.N., 1993. Use of trichlorofluorocarbon-113 (CFC113) as a hydrologic tracer and age-dating tool for young groundwater. In Geological Society of America, 1997 Annual Meeting, Salt Lake City-US, Abstracts with Programs (Vol. 29, No. 6).

Carlisle, S.C., 2005. Soil survey of St. Lawrence County, New York. Natural Resources Conservation Service.

Chafetz, H. S. and R. L. Folk, 1984, Travertines: Depositional morphology and the acterially constructed constituents: J. Sediment. Petrol., 54, 289–316.

Chang, Y., Wu, J. and Liu, L., 2015. Effects of the conduit network on the spring hydrograph of the karst aquifer. Journal of Hydrology, 527, pp.517-530.

Chanson, H. 2004. The hydraulics of open channel flow: An introduction, Butterworth-Heinemann, Oxford, UK. P 27-29

Civita, M.V., 2008. An improved method for delineating source protection zones for karst springs based on analysis of recession curve data. Hydrogeology Journal, 16(5), pp.855-869.

Clarke, R.T., Mendiondo, E.M. and Brusa, L.C., 2000. Uncertainties in mean discharges from two large South American rivers due to rating curve variability. Hydrological Sciences Journal, 45(2), pp.221-236.

Clarke, RT 1999. Uncertainty in the estimation of mean annual flood due to rating-curve indefinition. Journal of Hydrology, 222(1-4):185–190, 1999. 11, 15

Cook, P.G. and Böhlke, J.K., 2000. Determining timescales for groundwater flow and solute transport. In Environmental tracers in subsurface hydrology (pp. 1-30). Springer US.

Cook, P.G. and Solomon, D.K., 1997. Recent advances in dating young groundwater: chlorofluorocarbons, 3H3He and 85 Kr. Journal of hydrology, 191(1), pp.245-265.

Cook, P.G., and Herczeg, A.L., eds., 2000, Environmental tracers in subsurface hydrology: Kluwer Academic Publishers, Boston, 529 p.

Cook, P.G., Solomon, D.K., Plummer, L.N., Busenberg, E. and Schiff, S.L., 1995. Chlorofluorocarbons as tracers of groundwater transport processes in a shallow, silty sand aquifer. Water Resources Research, 31(3), pp.425-434.

Coto, B., Martos, C., Peña, J.L., Rodríguez, R. and Pastor, G., 2012. Effects in the solubility of CaCO 3: experimental study and model description. Fluid Phase Equilibria, 324, pp.1-7.

Coutagne, A., 1948. Les variations de de´bit en pe´riode non influence´e par les pre´cipitations. La Houille Blanche 3, 416–436

Covington, M.D., Banwell, A.F., Gulley, J., Saar, M.O., Willis, I. and Wicks, C.M., 2012. Quantifying the effects of glacier conduit geometry and recharge on proglacial hydrograph form. Journal of Hydrology, 414, pp.59-71.

Covington, M.D., Wicks, C.M. and Saar, M.O., 2009. A dimensionless number describing the effects of recharge and geometry on discharge from simple karstic aquifers. Water resources research, 45(11).

Cozma, A.I., Baciu, C., Moldovan, M. and Pop, I.C., 2016. Using Natural Tracers to Track the Groundwater Flow in a Mining Area. Procedia Environmental Sciences, 32, pp.211-220.

Cunningham, W.L. and Schalk, C.W., 2011. Groundwater technical procedures of the US Geological Survey. US Geological Survey Techniques and Methods, pp.1-A1.

Dagan, G., 1991. Dispersion of a passive solute in non-ergodic transport by steady velocity fields in heterogeneous formations. Journal of Fluid Mechanics, 233, pp.197-210.

Darling, W.G., Gooddy, D.C., MacDonald, A.M. and Morris, B.L., 2012. The practicalities of using CFCs and SF 6 for groundwater dating and tracing.Applied Geochemistry, 27(9), pp.1688-1697.

Darling, W.G., Morris, B.L., Stuart, M.E., Gooddy, D.C., 2005. Groundwater age indicators from public supplies tapping the Chalk aquifer of Southern England. Water and Environment Journal 19, 30–40.

Darling, W.G.; Gooddy, D.C.; Morris, B.L.; MacDonald, A.M.. 2010 Using CFCs and SF6 for groundwater dating: a SWOT analysis. In: Birkle, Peter; Torres-Alvarado, Ignacio, (eds.) Water-rock interaction XIII. CRC Press, 15-22.

Das, M. M 2008. Open channel flow. New Delhi, II: Prentice-Hall India ,p 9-11

Delleur, J. ,2007. The handbook of groundwater engineering. Boca Raton: CRC Press.

Demuth, S. and Schreiber, P., 1994. Studying storage behaviour using an operational recession method. IAHS Publications-Series of Proceedings and Reports-Intern Assoc Hydrological Sciences, 221, pp.51-60.

Desbarats, A.J., Logan, C.E., Hinton, M.J. and Sharpe, D.R., 2002. On the kriging of water table elevations using collateral information from a digital elevation model. Journal of Hydrology, 255(1), pp.25-38.

Dewandel, B., Lachassagne, P., Bakalowicz, M., Weng, P.H. and Al-Malki, A., 2003. Evaluation of aquifer thickness by analysing recession hydrographs.

Application to the Oman ophiolite hard-rock aquifer. Journal of hydrology, 274(1), pp.248-269.

Di Baldassarre, G., Laio, F. and Montanari, A., 2012. Effect of observation errors on the uncertainty of design floods. Physics and Chemistry of the Earth, Parts A/B/C, 42, pp.85-90.

Dingman, S.L., 2002. Physical Hydrology. Macmillan Publishing Company, New York.

Divya, J. and Belagali, S.L., 2012. Impact of chemical fertilizers on water quality in selected agricultural areas of Mysore district, Karnataka, India. International journal of environmental sciences, 2(3), p.1449.

Docherty, J., 1971. Chalk karst. A synthesis of C.C. Fagg's theories of chalkland morphology in the light of recent hydrological research. Proceedings of the Croydon Natural History Society 15 (2), 21-34"

Dodge, R., 2001. Water measurement manual: A guide to effective water measurement practices for better water management. Government Printing Office.

Dottori, F., Martina, M.L.V. and Todini, E., 2009. A dynamic rating curve approach to indirect discharge measurement. Hydrology and Earth System Sciences, 13(6), pp.847-863.

Downing RA, Price M, Jones GP. 2005. The Hydrogeology of the Chalk of North-West Europe. Oxford (UK): Clarendon Press.

Downing, R.A., Price, M. and Jones, G.P., 1993. The hydrogeology of the Chalk of north-west Europe. Clarendon Press.

Dreiss SJ. 1982. Linear kernels for karst aquifers. Water Resources Research 18 (4): 865-876.

Dutillet, J.L., 1993. Flow measurement: the dilution method. Flow Measurement and Instrumentation, 4(1), pp.51-52.

Dymond, J.R. and Christian, R., 1982. Accuracy of discharge determined from a rating curve. Hydrological Sciences Journal, 27(4), pp.493-504.

Edmonds, C N. 1983. Towards the prediction of subsidence risk upon the Chalk outcrop. Quarterly Journal of Engineering Geology, 16, 261–266."

Eisenlohr, L., Király, L., Bouzelboudjen, M. and Rossier, Y., 1997. Numerical simulation as a tool for checking the interpretation of karst spring hydrographs. Journal of Hydrology, 193(1), pp.306-315.

Ernst, W.G. ed., 2000. Earth systems: processes and issues. Cambridge University Press.

ESI, 2010. East Yorkshire Chalk aquifer :Conceptual Mosel. Report by ESI environmental Specialists.

ESI, 2015. East Yorkshire Chalk aquifer investigation: Numerical Model update and recalibration. Report by ESI environmental Specialists.

Fagg, C C. 1958. Swallow holes in the Mole gap. South East Naturalist and Antiquary, 62, 1–13.

Farlin, J. and Maloszewski, P., 2013. On the use of spring baseflow recession for a more accurate parameterization of aquifer transit time distribution functions. Hydrology and Earth System Sciences, 17(5), pp.1825-1831.

Faust, C.R. and Mercer, J.W., 1980. Ground-water modelling: numerical models. Ground Water, 18(4), pp.395-409.

Feinstein, D.T., Eaton, T.T., Hart, D.J., Krohelski, J.T. and Bradbury, K.R., 2005. A regional aquifer simulation model for southeastern Wisconsin. Southeastern Wisconsin Regional Planning Commission Technical Report Number, 41, p.63.

Fenton, J.D. and Keller, R.J., 2001. The calculation of streamflow from measurements of stage. CRC for Catchment Hydrology.

Fetter C W 2000 Applied Hydrogeology 4th edn (Englewood Cliffs, NJ: Prentice-Hall)

Fiorillo, F. and Guadagno, F.M., 2010. Karst spring discharges analysis in relation to drought periods, using the SPI. Water resources management,24(9), pp.1867-1884.

Fiorillo, F., 2009, Spring hydrographs as indicators of droughts in a karst environment: Journal of Hydrology, v. 373, p. 290–301. doi:10.1016/ j.jhydrol.2009.04.034

Fiorillo, F., 2014. The recession of spring hydrographs, focused on karst aquifers. Water resources management, 28(7), pp.1781-1805.

Florea, L.J. and Vacher, H.L., 2006. Springflow hydrographs: eogenetic vs. telogenetic karst. Ground Water, 44(3), pp.352-361.

Fogg, T. 1984. Surprise find in Irish Chalk. Caves and Caving, 26, 26"

Ford, D.C., P. williams, 2007: Karst hydrogeology and geomorphology. Academic Division of Unwin Hyman Ltd, p.601.

Forkasiewicz, J., Paloc, H., 1967. Le re´gime de tarissement de la Foux-de-la-Vis. Etude pre´liminaire. Chronique d'Hydroge´ologie, BRGM 3 (10), 61–73.

Foster, S.S.D. and Crease, R.I., 1974. Nitrate pollution of chalk ground water in east Yorkshire- a hydrogeological appraisal. J Inst Wat Engrs, 28(3), pp.178-194.

Foster, S.S.D. and Milton, V.A, 1976. Hydrogeological basis for large-scale development of groundwater storage capacity in the East Yorkshire Chalk. IGS Technical Report 76/3.

Freeze, R.A., and Cherry, J.A., 1979, Groundwater: Englewood Cliffs, NJ, Prentice-Hall, 604 p.

Fronczyk, J., Lech, M., Radziemska, M., Sieczka, A. and Lechowicz, Z.,. 2016. Monitoring of Groundwater Chemical Composition in Areas of Crop Production. 5th International Conference on Biological, Chemical and Environmental Sciences (BCES-2016) March 24-25, 2016 London (UK).

Fu, T., Chen, H. and Wang, K., 2016. Structure and water storage capacity of a small karst aquifer based on stream discharge in southwest China. Journal of Hydrology, 534, pp.50-62.

Gale I, Rutter H. 2006. The Chalk aquifer of Yorkshire. British Geological Survey Report RR/06/004.

Gan, R. and Luo, Y., 2013. Using the nonlinear aquifer storage–discharge relationship to simulate the base flow of glacier-and snowmelt-dominated basins in northwest China. Hydrology and Earth System Sciences, 17(9), pp.3577-3586.

Gannett MW, Lite KE Jr. 2004. Simulation of regional ground-waterflow in the Upper Deschutes Basin, Oregon. Water-Resources Investigations Report 2003-4195, 95 p

Garrels R.M., Mackenzie F.T., 1971. Evolution of sedimentary rocks. 1st ed. ed. Norton, New York, xvi, 397.

Garrels, R.M. and Christ, C.L., 1965. Solutions, minerals, and equilibria.

Gburek, W.J., Folmar, G.J. and Urban, J.B., 1999. Field data and ground water modeling in a layered fractured aquifer. Ground Water, 37(2), pp.175-184.

Gebreyohannes. T., et al. 2013. Application of a spatially distributed water balance model for assessing surface water and groundwater resources in the Geba basin, Tigray, Ethiopia. Journal of Hydrology, 499: 110–123.

Geyer, T et al 2008. Quantification of temporal distribution of recharge in karst systems from spring hydrographs. Journal of Hydrology, 348, 452-463.

Glass, R.L., 2002. Ground-water age and its water-management implications, Cook Inlet Basin, Alaska (No. 022-02).

Goldscheider, N. and Drew, D., 2007. Methods in karst hydrogeology. International contribution to hydrogeology, IAH.

Gooddy, D.C., Darling, W.G., Abesser, C. and Lapworth, D.J., 2006. Using chlorofluorocarbons (CFCs) and sulphur hexafluoride (SF 6) to characterise groundwater movement and residence time in a lowland Chalk catchment. Journal of hydrology, 330(1), pp.44-52.

Gordon, N. et al, 2004. Steam hydrology: an introduction from ecologists. 2nd edition. Sussex , UK. pp 100-101

Grannemann, N.G., Hunt, R.J., Nicholas, J.R., Reilly, T.E. and Winter, T.C., 2000. The Importance of Ground Water in the Great Lakes. USGS Water Resources Investigations.

Gregory, H.E., others, 1918, Military geology and topography: a presentation of certain phases of geology, geography, and topography for military purposes.

Grindley, J., 1969, The calculation of evaporation and soil moisture deficit over specified catchment area, Hydrological Memorandum 28, Meteorological Office, Bracknell, UK, pp 10

Harbaugh, A.W., E.R. Banta, M.C. Hill, and M.G. McDonald. 2000. MODFLOW-2000, the U.S. Geological Survey modular ground-water model—User guide to

Harold C., 1937. The flow and bacteriology of underground water in the Lee Valley. Metropolitan Water Board 32nd Annual Report, 89-99."

Harter, T. and Rollins, L., 2008. Watersheds, Groundwater and Drinking Water: A Practical Guide (Vol. 3497). UCANR Publications.

Hauer, F.R. and Lamberti, G.A. eds., 2011. Methods in stream ecology. Academic Press.

Hauser, V.L., 2009. Evapotranspiration covers for landfills and waste sites. Resource Magazine, 16(3), pp.14-16.

Hayashi, M., 2004. Temperature-electrical conductivity relation of water for environmental monitoring and geophysical data inversion. Environmental monitoring and assessment, 96(1-3), pp.119-128.

Hayes, J.M. and Thompson, G.M., 1976. Trichlorofluoromethane In Groundwater--A Possible Indicator Of Groundwater Age.

Hem, J.D., 1985. Study and Interpretation of the Chemical Characteristics of Natural Water. US Geological Survey, Water Supply Paper 2254, third ed.

Herschy, R., 1994. The analysis of uncertainties in the stage-discharge relation. Flow Measurement and Instrumentation, 5(3), pp.188-190.

Herschy, R. 2009. Streamflow measurement. 3rd edition. London, UK. p page 168-169

Herschy, R.W., 2002. The uncertainty in a current meter measurement. Flow Measurement and Instrumentation, 13(5), pp.281-284.

Herschy, R.W., 1985. Streamflow Measurement–Elsevier Applied Science Publishers.

Hinsby K, and Abatzis I.2004. Petroleum geology modelling tools of relevance to groundwater investigations. – Geologisk Tidsskrift 2004 2: 10–11 (in Danish)

Ho, D.T., Schlosser, P., Smethie, W.M. and Simpson, H.J., 1998. Variability in atmospheric chlorofluorocarbons (CCl3F and CCl2F2) near a large urban area: Implications for groundwater dating. Environmental science & technology, 32(16), pp.2377-2382.

Holmes Jr, R.R., Terrio, P.J., Harris, M.A. and Mills, P.C., 2001. Introduction to field methods for hydrologic and environmental studies (No. 2001-50).

Hopson, P., 2005. A stratigraphical framework for the Upper Cretaceous Chalk of England and Scotland with statements on the Chalk of Northern Ireland and the UK Offshore Sector. British Geological Survey.

Horton, R.E., 1933. The role of infiltration in the hydrologic cycle. Eos, Transactions American Geophysical Union, 14(1), pp.446-460.

Horton, R.E., 1935. Surface runoff phenomena. Part 1. Analysis of the hydrograph. Horton Hydrological Laboratory, Publication 101. Edward Bros.Ann Arbor, Michigan.

Horton, R.E., 1937. Natural stream channel-storage (second paper). Eos, Transactions American Geophysical Union, 18(2), pp.440-456.

Hudak, P. F., 2001. "Groundwater and the Hydrologic Cycle" Principles of Hydrogeology.Ed. Paul F. Hudak, Ph.D.Boca Raton: CRC Press LLC.

Humphries, R., Venditti, J.G., Sklar, L.S. and Wooster, J.K., 2012. Experimental evidence for the effect of hydrographs on sediment pulse dynamics in gravel-bedded rivers. Water Resources Research, 48(1).

IAEA, 2006. Use of Chlorofluorocarbons in hydrology, A Guidebook. International Atomic Energy Agency (IAEA). Vienna,2006.

Ineson, J., 1962. A hydrogeological study of the permeability of the Chalk. Journal of the Institute of Water Engineers 16, 449-463"

Island, P.E., 2004. Application of numerical modeling to groundwater assessment and management in Prince Edward Island.

Jackson, D. & Rushton, K.R., 1987. A S S E S S M E N T OF RECHARGE COMPONENTS FOR A CHALK. Journal of Hydrology,, 92, pp.1–15.

Jackson, R.E., Lesage, S. and Priddle, M.W., 1992. Estimating the fate and mobility of CFC-113 in groundwater: results from the Gloucester Landfill project. Groundwater Contamination and Analysis at Hazardous Waste Sites, pp.511-526.

Jarraud, M., 2008. Guide to meteorological instruments and methods of observation (wmo-no. 8). World Meteorological Organisation: Geneva, Switzerland.

Jukes-Brown, A.J. and Hill, W., 1904. The Cretaceous Rocks of Britain: The Upper Chalk of England (Vol. 3). HM Stationery Office.

Jukes-Brown, A.J. 1880. On the subdivisions of the Chalk. Geological Magazine, Vol. 17, 248–257.

Jukes-Browne, A.J., 1903. The Lower and Middle Chalk of England. HM Stationery Office.

Kafri, U., 1970. Factors controlling the location of the groundwater divide in northern Israel. Journal of Hydrology, 11(1), pp.22-29.

Karanjac, J. and Altug, A., 1980. Karstic spring recession hydrograph and water temperature analysis: Oymapinar Dam Project, Turkey. Journal of Hydrology, 45(3-4), pp.203-217.

Kassenaar D, Holysh S and Gerber R,.2003. An integrated 3D Hydrostratigraphic Interpretation Methodology for Complex Aquifer Systems. – In: Poeter, Zheng, Hill and Doherty (eds.): Proceedings, MODFLOW and More, understanding through modelling, Colorado School of Mines, Golden CO, September 16–19, 2003, p. 661–665.

Kilpatrick, F and Ernest, C, 1985, Measurement of discharge using tracers: USGS Techniques of Water Resources Investigations Report, Book 3, chapter A16,52p.

Kiraly, L. and Perr0chet, P., 1995. Effect of the epikarst on the hydrograph of the karst springs. Bulletin d'hydrogéologie, 14, pp.199-220.

Kirby, J.A. and Swallow P.W. 1987. Tectonism and sedimentation in the Flamborough Head region of north-east England. Proceedings of the Yorkshire Geological Society, 46, 301-9.

Kova´cs, A.,(2003). Geometry and hydraulic parameters of karst aquifers: a hydrodynamic modeling approach. Doctoral Thesis, University of Neuchaˆtel, Switzerland.

Kovács, A. and Perrochet, P., 2008. A quantitative approach to spring hydrograph decomposition. Journal of hydrology, 352(1), pp.16-29.

Kovács, A., Perrochet, P., Király, L. and Jeannin, P.Y., 2005. A quantitative method for the characterisation of karst aquifers based on spring hydrograph analysis. Journal of Hydrology, 303(1), pp.152-164.

Kresic, N. ,2006. Hydrogeology and Groundwater Modeling, Second Edition. Hoboken: CRC Press.

Kresic, N. and Stevanovic, Z. eds., 2009. Groundwater hydrology of springs: Engineering, theory, management and sustainability. Butterworth-Heinemann.

Kreye, R., Wei, M. and Reksten, D., 1996. Defining the source area of water supply springs. Hydrology Branch, Ministry of Environment, Lands and Parks.

Lamont-Black J., 1995. The engineering classification of chalk with special reference to the origins of fracturing and dissolution. PhD Thesis, University of Brighton.

Langbein, W.B., 1938. Some channel-storage studies and their application to the determination of infiltration. Eos, Transactions American Geophysical Union, 19(1), pp.435-447.

Langevin, C.D., 2003. Stochastic ground water flow simulation with a fracture zone continuum model. Ground Water, 41(5), pp.587-601.

Lee, J.Y., Lim, H.S., Yoon, H.I. and Park, Y., 2013. Stream water and groundwater interaction revealed by temperature monitoring in agricultural areas. Water, 5(4), pp.1677-1698.

Lee, L.J.E., Lawrence, D.S.L. & Price, M., 2006. Analysis of water-level response to rainfall and implications for recharge pathways in the Chalk aquifer, SE England. Journal of Hydrology, 330(3-4), pp.604–620. Available at: http://linkinghub.elsevier.com/retrieve/pii/S002216940600237X [Accessed September 11, 2014].

Liu L, Li X. 2012. A Laboratory Study of Spring Hydrograph in Karst Triple Void Media, South-western China. International Conference On Civil Engineering And Urban Planning. Yantai, China.

Lloyd., J.W., 1993. United Kingdom. In The hydrogeology of the Chalk of North-West Europe. Edited by Downing, R.A., Price, M., and Jones, G.P. 220-250"

Lowe, D.J., 1992. Chalk caves revisited. Cave Science, Transactions of the BritishCave Research Association 19, 55-58"

MacDonald A, Allen D. 2001. Aquifer properties of the chalk of England. Journal of Engineering Geology and Hydrogeology. 34: 371-384.

Mackay, E., 2003. Predicting in situ sulphate scale deposition and the impact on produced ion concentrations. Chemical Engineering Research and Design, 81(3), pp.326-332

Madan, D 2009 . Fluid mechanics and turbomachines. New Delhi , India.

Magnus U, I. and NJ, A., 2011. Finite difference method of modelling groundwater flow. Journal of Water Resource and Protection, 2011.

Mangin, A., 1975. Contribution à l'étude hydrodynamique des aquifères karstiques (Doctoral dissertation, Laboratoire souterrain du Centre national de la recherche scientifique).

Mäntynen, M., 2001. Temperature correction coefficients of electrical conductivity and density measurements for saline groundwater. POSIVA Oy, Eurajoki, Finland. Working report, 15.

Martin, P.J. and Frind, E.G., 1998. Modeling a Complex Multi-Aquifer System: The Waterloo Moraine. Ground Water, 36(4), pp.679-690.

Mathias SA, Butler AP, Mcintyre N. Wheater HS. 2005. The significance of flow in the matrix of the chalk unsaturated zone. Journal of Hydrology 310: 62-77.

Maurice, L., 2009. Investigations of rapid groundwater flow and karst in the Chalk (Doctoral dissertation, UCL (University College London)).

Maurice, L.D., Atkinson, T.C., Barker, J.A., Bloomfield, J.P., Farrant, A.R. and Williams, A.T., 2006. Karstic behaviour of groundwater in the English Chalk. Journal of Hydrology, 330(1), pp.63-70.Maurice, L.D., Atkinson, T.C., Barker, J.A., Bloomfield, J.P., Farrant, A.R. and Williams, A.T., 2006. Karstic behaviour of groundwater in the English Chalk. Journal of Hydrology, 330(1), pp.63-70.

Maurice, L.D., Atkinson, T.C., Barker, J.A., Williams, A.T. and Gallagher, A.J., 2012. The nature and distribution of flowing features in a weakly karstified porous limestone aquifer. Journal of Hydrology, 438, pp.3-15.

MBCHS, 2009. Manual of British Columbia Hydrometric Standards. The Province of British Columbia Published by the Resources Information Standards Committee.

McDonald, M.G. and Harbaugh, A.W., 1988. A modular three-dimensional finite-difference ground-water flow model.

McDonald, M.G., and Harbaugh, A.W., 1984, A modular three-dimensional finite-difference ground-water flow model: U.S. Geological Survey Open-File Report 83-875, 528 p.

Metcalfe, D.B., Meir, P., Aragao, L.E.O.C., Malhi, Y., Da Costa, A.C.L., Braga, A., Gonçalves, P.H.L., De Athaydes, J., De Almeida, S.S. and Williams, M., 2007. Factors controlling spatio-temporal variation in carbon dioxide efflux from surface litter, roots, and soil organic matter at four rain forest sites in the eastern Amazon. Journal of Geophysical Research: Biogeosciences, 112(G4).

Michalski, A., 1989. Application of Temperature and Electrical-Conductivity Logging in Ground Water Monitoring. Groundwater Monitoring & Remediation, 9(3), pp.112-118.

Millero, F.J., 2001. The physical chemistry of natural waters/by Frank J. Millero. Wiley-Interscience series in geochemistry.

Milsom J, 1996. Field Geophysics, 2nd Edition. John Wiley & Sons, 131-141.

Mohammadi, Z., Salimi, M. and Faghih, A., 2014. Assessment of groundwater recharge in a semi-arid groundwater system using water balance equation, southern Iran. Journal of African Earth Sciences, 95, pp.1-8.

Moore RD. 2004, Introduction to salt dilution gauging for stream flow measurements: Part 1. Streamline Watershed Management Bulletin , volume 7, Number 4: 20–24 p.

Moore, R.D., and J.C. Thompson. 1996. Are water table variations in a shallow forest soil consistent with the TOPMODEL concept? Water Resources Research 32, no. 3: 663–669.

Mortimore, R.N., Wood, C.J. and Gallois, R.W., 2001. British upper Cretaceous stratigraphy. (Peterborough: Joint Nature Conservation Committee). Geological Conservation Review Series, No. 23.

Morris, B.L., Darling, W.G., Gooddy, D.C., Litvak, R.G., Neumann, I., Nemaltseva, E.J. and Poddubnaia, I., 2006. Assessing the extent of induced leakage to an urban aquifer using environmental tracers: an example from Bishkek, capital of Kyrgyzstan, Central Asia. Hydrogeology Journal, 14(1-2), pp.225-243.

National Research Council (NRC). 1996. Committee on Fracture Characterization and Fluid Flow,. Rock fractures and fluid flow: contemporary understanding and applications. National Academies Press.

Nyende, J., Van, T.G. and Vermeulen, D., 2013. Conceptual and Numerical Model Development for Groundwater Resources Management in a Regolith-Fractured-Basement Aquifer System. Journal of Earth Science & Climatic Change, 2013.

Oberlander P. L., and Russell Ch. E., 2005. Borehole flow and horizontal hydraulic conductivity with depth at well ER-12-3. Report to Naveda site office NNSA, U.S. Department of Energy Las Vegas, Nevada.

Okafor, P. and Mamah, L., 2012. Integration of Geophysical Techniques for Groundwater Potential Investigation in Katsina-Ala, Benue State, Nigeria.

Oster, H., Sonntag, C. and Münnich, K.O., 1996. Groundwater age dating with chlorofluorocarbons. Water Resources Research, 32(10), pp.2989-3001.

Parker AH. 2009. The distribution of permeability in the Chalk aquifer of East Yorkshire. [PhD dissertation]. Leeds (UK): University of Leeds.

Patsoules MG & Cripps JC (1982) The application of resin impregnation to the three-dimensional study of chalk pore geometry. Engineering Geology, 19(1), 15-27.

Penman, H.L., 1948, April. Natural evaporation from open water, bare soil and grass. In Proceedings of the Royal Society of London A: Mathematical, Physical and Engineering Sciences (Vol. 193, No. 1032, pp. 120-145). The Royal Society.

Penning, W H, Jukes-Brown, A J.1881. The geology of the neighbourhood of Cambridge. Memoir of the Geological Survey of Great Britain

Peters, N.E., 1984. Evaluation of environmental factors affecting yields of major dissolved ions of streams in the United States (No. 2228). USGPO,.

Petersen-Øverleir, A. 2004. Accounting for heteroscedasticity in rating curve estimates. Journal of Hydrology, 292, 173-181.

Plummer, L. N., and E. Busenberg (2000), Chlorofluorocarbons. Environmental Tracers in Subsurface Hydrology, edited by P. Cook and A. Herczeg, chap. 15, pp. 441 – 478, Kluwer Acad., Boston

Plummer, L.N. and Friedman, L.C., 1999, Tracing and dating young ground water: U.S. Geological Survey Fact Sheet 134- 99, 4 p.

Price, M., 1987. Fluid flow in the Chalk of England. Geological Society, London, Special Publications, 34(1), pp.141-156.

Price, M., Bird, M.J. and Foster, S.S.D., 1976. Chalk pore-size measurements and their significance. Water Services, 80(968), pp.596-600.

Price, M., Downing, R.A., and Edmonds, W.M., 1993. The Chalk as an aquifer. In The hydrogeology of the Chalk of North-West Europe. Edited by Downing, R.A., Price, M., and Jones, G.P. 35-59

RA, 2004. Conductivity Theory and Practice. France: Radiometer Analytical SAS.

Radtke, D.B., W.G. Kepner, and R.J. Effertz. 1988. Reconnaissance investigation of water quality, bottom sediment, and biota associated with irrigation drainage in the Lower Colorado River Valley, Arizona, California, and Nevada. U.S. Geological Survey, Water-Resources Investigations Report 88-4002, Tucson, Arizona. 77 pp.

Raeisi, E . 2008. Ground-water storage calculation in karst aquifers with alluvium or no-flow boundaries. J Cave Karst Stud 70(1):62–70

Raghunath, H.M., 2006. Hydrology: principles, analysis and design. New Age International.

Rahman A, Goonetilleke A. 2001. Effects of non-linearity in storagedischarge relationships on design flood estimates. Proceedings of the Conference: MODSIM 2001, International Congress on Modelling and Simulation; 113–117.

Randall, J., Schultz, T. and Davis, S., 1977. Suitability of fluorocarbons as tracers in ground water resources evaluation.. Technical report to Office of Water Research and Technology, U.S. Department of the Interior, NTIS PB 277 488, 37pp

Randall, J.H. and Schultz, T.R., 1976, May. Chlorofluorocarbons as hydrologic tracers, a new technology. In Hydrology and Water Resources in Arizona and the Southwest. Arizona-Nevada Academy of Science.

Rani, F.M. and Chen, Z.H., 2010. Numerical modeling of groundwater flow in karst aquifer, Makeng mining area. American Journal of Environmental Sciences, 6(1), pp.78-82.

Rantz, E., et al 1982, Measurement and computation of stream flow ,volume 1, measurement stage and discharge : USGS, Paper 2175, 211-256 p.

Rau, G.C., Andersen, M.S., McCallum, A.M. and Acworth, R.I., 2010. Analytical methods that use natural heat as a tracer to quantify surface water–groundwater exchange, evaluated using field temperature records.Hydrogeology Journal, 18(5), pp.1093-1110.

Rawson, P F, Allen, P M, and Gale, A S. 2001. The Chalk Group – a revised lithostratigraphy. Geoscientist, Vol. 11, p.21.

Reeve, T.J., 1981. Beachy Head Cave. Caves and Caving 12, 2-4

Reeve, T.J., 1982. Flamborough Head Cave. Caves and Caving 17, 23

Richard, H and Gary , L 2007,Methods in stream ecology, 2nd edition, MA, USA and London,UK.

Reynolds, R. C., and Johnson, N. M., 1972, Chemical weathering in the temperate glacial environment of the northern Cascade Mountains: Geochemica et Cosmochemica Acta, v. 36, p. 537-554.

Ritter, J.A., 2010. Water Quality, Principles and practices of water supply operations. 4th ed.,

Robert, H., Jr, Paul, T. , Mitchell , H. , and Patrick, M. 2001, Introduction to field methods for hydrologic and environmental studies, USGS open-file report 01-50.

Rorabaugh, M.I., 1964. Estimating changes in bank storage and ground-water contribution to streamflow. International Association of Scientific Hydrology, 63, pp.432-441.

Roy, R.N., Gibbons, J.J., Williams, R., Godwin, L., Baker, G., Simonson, J.M. and Pitzer, K.S., 1984. The thermodynamics of aqueous carbonate solutions II. Mixtures of potassium carbonate, bicarbonate, and chloride. The Journal of Chemical Thermodynamics, 16(4), pp.303-315.

Rushton, 2003. Groundwater Hydrology: Conceptual and Computational Models.

Rushton, K.R., 2003. Groundwater Hydrology, Chichester, UK: John Wiley & Sons, Ltd. Available at: http://doi.wiley.com/10.1002/0470871660.

Salkind, N 2010. (Ed.). Encyclopedia of research design. Thousand Oaks, CA: SAGE Publications, Inc. doi: 10.4135/9781412961288

Schlumberger Water Services, 2014. Diver Manual.

Schoeller, H., 1948. Le re´gime hydroge´ologique des calcairese´oce`nes du Synclinal du Dyr el Kef (Tunisie). Bull. Soc. Ge´ol.Fr. 5 (18), 167– 180

Schoeller, H., 1967. Hydrodynamique dans le karst. Chronique d'Hydrogéologie, 10, pp.7-21.

Schultz, T.R., 1979. Trichlorofluoromethane as a ground-water tracer for finite-state models.

Schultz, T.R., Randall, J.H., Wilson, L.G. and Davis, S.N., 1976. Tracing Sewage Effluent Recharge Tucson, Arizona. Ground Water, 14(6), pp.463-471.

Schwartz, F.W. and Zhang, H., 2003. Fundamentals of ground water. Wiley.

Sefe, F.T.K., 1996. A study of the stage-discharge relationship of the Okavaiigo River at Mohembo, Botswana. Hydrological sciences journal,41(1), pp.97-116.

Shabalala, A.N., Combrinck, L. and McCrindle, R., 2013. Effect of farming activities on seasonal variation of water quality of Bonsma Dam, KwaZulu-Natal. South African Journal of Science, 109(7-8), pp.01-07.

Shaman, J., M. Stieglitz, V. Engel, R. Koster, and C. Stark. 2002. Representation of subsurface storm flow and a more responsive water table in a TOPMODEL-based hydrology model. Water Resources Research 38, no. 8: 1156–1172.

Shapiro, S.D., Plummer, L.N., Busenberg, E., Widman, P.K., Casile, G.C., Wayland, J.E., and Runkle, D.L., 2012, Estimates of tracer-based piston-flow ages of groundwater from selected sites—National Water-Quality Assessment Program, 2006–10: U.S. Geological Survey Scientific Investigations Report 2012–5141, 100 p.

Shrestha, R. & Simonovic, S. 2009. Fuzzy Nonlinear Regression Approach to Stage-Discharge Analyses: Case Study. Journal of Hydrologic Engineering, 15, 49-56

Shrestha, R. and Simonovic, S. (2010). Fuzzy Nonlinear Regression Approach to Stage-Discharge Analyses: Case Study. Journal of Hydrologic Engineering, 15(1), pp.49-56.

Silliman, S.E. and Booth, D.F., 1993. Analysis of time-series measurements of sediment temperature for identification of gaining vs. losing portions of Juday Creek, Indiana. Journal of Hydrology, 146, pp.131-148. 6. Anderson, M.P. Heat as a ground water tracer. Ground Water 2005, 43, 951–968.

Simpson, T.B., Holman, I.P. and Rushton, K.R., 2011. Understanding and modelling spatial drain–aquifer interactions in a low-lying coastal aquifer—the Thurne catchment, Norfolk, UK. Hydrological Processes, 25(4), pp.580-592.

Singh, H. 2009, Expriment in fluid mechanics, New Delhi, Inida.

Singhal, B.B.S. and Gupta, R.P., 2010. Applied hydrogeology of fractured rocks. Springer Science & Business Media.

Smedley, P.L., Gibbs, B.R. and Trafford, J.M. 1996. Hydrogeochemistry and water quality of the Chalk aquifer of North Humberside and Yorkshire. British Geological Survey Technical Report, WD/96/80C, 67pp.

Smedley, P.L., Neumann, I. and Farrell, R., 2004. Baseline report series 10: The Chalk aquifer of Yorkshire and North Humberside. British Geological Survey commissioned report no. CR/04/128.

Sorensen, J.A. and Glass, G.E., 1987. Ion and temperature dependence of electrical conductance for natural waters. Analytical Chemistry, 59(13), pp.1594-1597.

Southern Science. 1992. A historical review of the Warningcamp borehole and recommendations for future work. Report No. 92/6/451, Southern Science, Worthing."

Southern Science. 1994. The effect of pumping from Tortington and Madehurst in 1993 on water levels in the vicinity of Swanbourne lake. Report No 94/7/800. Southern Science, Worthing."

Sperling, C.H. B., Goudie, A.S., Stoddart, D.R., and Poole, G.G., 1977. Dolines of the Dorset chalklands and other areas in southern Britain. Transactions of the Institute of British Geographers 2, 205-223"

Stallman, R.W., 1965. Steady one-dimensional fluid flow in a semi-infinite porous medium with sinusoidal surface temperature. Journal of geophysical Research, 70(12), pp.2821-2827.

Starmer, I.C. 2008. The concentration of folding and faulting in the Chalk at Staple Newk (Scale Nab), near Flamborough, East Yorkshire. Proceedings of the Yorkshire Geological Society, 57, 95-106.

Starmer, I.C., 1995. Contortions in the Chalk at Staple Nook, Flamborough Head. Proceedings of the Yorkshire Geological Society, 50, 271-275.

Stevens, D.J. and Krauthammer, T., 1988. A finite difference/finite element approach to dynamic soil-structure interaction modelling. Computers & structures, 29(2), pp.199-205.

Stonestrom, D.A. and Constantz, J. eds., 2003. Heat as a tool for studying the movement of ground water near streams (No. 1260). US Dept. of the Interior, US Geological Survey.

Stumm, W. and Morgan, J.J., 1996. Aquatic chemistry New York. NY: John Wiley and Sons.

Sugiyama H. 1996. Analysis and extraction of low flow recession characteristics. Journal of the American Water Resources Association. 32 (3): 491-497.

Sullivan, T.J., 2000. Aquatic effects of acidic deposition. CRC Press.

Sumbler, M.G., 1999. The stratigraphy of the Chalk Group in Yorkshire and Lincolnshire. British Geological Survey Technical Report, WA/99/02

Sweeting, M. M., 1966, The weathering of limestones, in Essays in Geomorphology, Dury, G. E., ed.: New York, American Elsevier Publishing Co., p. 177-210.

Tallaksen, L.M., 1995. A review of baseflow recession analysis. Journal of hydrology, 165(1), pp.349-370.

Taylor, C.J. and Alley, W.M., 2001. Ground-water-level monitoring and the importance of long-term water-level data (Vol. 1217). Geological Survey (USGS).

Thompson, G.M. and Hayes, J.M., 1979. Trichlorofluoromethane in groundwater—a possible tracer and indicator of groundwater age. Water Resources Research, 15(3), pp.546-554.

Thompson, G.M., 1976. Trichlorofluoromethane, a new hydrologic tool for tracing and dating ground water.

Thompson, G.M., Hayes, J.M. and Davis, S.N., 1974. Fluorocarbon tracers in hydrology. Geophysical research letters, 1(4), pp.177-180.

Tian, H., Kempka, T., Yu, S. and Ziegler, M., 2016. Mechanical Properties of Sandstones Exposed to High Temperature. Rock Mechanics and Rock Engineering, 49(1), pp.321-327.

Toebes C, Strang DD. 1994. On recession curves, 1. Recession equations. J. Hydrol. N.Z., p. 2–15.

Toebes C. 1969. Base-flow-recession curveseWellington (NZ): Water and Soil Division, Ministry of Works for the National Water and Soil Conservation Organization.

Toth, J., 1963. A theoretical analysis of groundwater flow in small drainage basins. Journal of geophysical research, 68(16), pp.4795-4812

Troch PA, De Troch FP, Brutsaert W. 1993. Effective water table depth to describe initial conditions prior to storm rainfall in humid regions. Water Resources Research 29: 427–434.

Turnipseed, D.P. and Sauer, V.B., 2010. Discharge measurements at gaging stations (No. 3-A8). US Geological Survey.

Versey, H.C., 1949. The hydrology of the East Riding of Yorkshire. Proceedings of the Yorkshire Geological Society, 27, 231-246.

Vogel M, Kroll N. 1992. Regional geohydrologic-geomorphic relationships for the estimation of low-flow statistics. Water Resources Research 28(9): 2451–2458.

Walsh, P T, and Ockenden, A C. 1982. Hydrogeological observations at the Water End swallow hole complex, North Mimms, Hertfordshire. Cave Science, 9, 184–194."

Wang, H. and Anderson, M. ,1982. Introduction to groundwater modeling. San Francisco: W.H. Freeman.

Wang, H.F. and Anderson, M.P., 1995. Introduction to groundwater modeling: finite difference and finite element methods. Academic Press.

WARD, R S, AND WILLIAMS, A T, and CHADHA, D S. 1997. The use of groundwater tracers for assessment of protection zones around water supply boreholes — a case study. Proceedings of the 7th International Symposium in

water tracing, Portoroz, Slovenia, May 1997, 369–375 (Rotterdam: Balkema.)"

Ward, R S, and Williams, A T. 1995. A tracer test in the chalk near Kilham, North Yorkshire. British Geological Survey Technical Report, WD/95/7."

Ward, R.S., 1989. Artificial tracer and natural 222Rn studies of the East Anglian Chalk aquifer. Unpublished PhD thesis, School of Environmental Sciences, University of East Anglia."

Ward, S., 1990. Geotechnical and environmental geophysics, in Geotechnical and Environmental Geophysics Environmental groundwater, S.E.G. Investigations in Geophysics.5.

Warner, M.J. and Weiss, R.F., 1985. Solubilities of chlorofluorocarbons 11 and 12 in water and seawater. Deep Sea Research Part A. Oceanographic Research Papers, 32(12), pp.1485-1497.

Weeks, E.P., Earp, D.E. and Thompson, G.M., 1982. Use of atmospheric fluorocarbons F-11 and F-12 to determine the diffusion parameters of the unsaturated zone in the Southern High Plains of Texas. Water Resources Research, 18(5), pp.1365-1378.

Weight, W 2008. Hydrogeology field manual, 2nd edition. McGraw-Hill, USA.

Wellings, S.R., Bell, J.P., 1980. Movement of water and nitrate in the unsaturated zone of the Upper Chalk near Winchester, Hants., England. Journal of Hydrology 48, 119–136

Weight, W 2008. Hydrogeology field manual, 2nd edition. McGraw-Hill, USA.

Wittenberg H, Sivapalan M. 1999. Watershed groundwater balance estimation using streamflow recession analysis and baseflow separation. Journal of Hydrology 219: 20–33.

Wittenberg, H. 1999 . Baseflow recession and recharge as nonlinear storage processes, Hydrol. Process., 13, 715–726, 1999

WMO 2008. Guide to meteorological instruments and methods of observation, WOM.8 . 7th edition. Geneva , Switzerland

Wood, C.J. and Smith, E.G., 1978, September. Lithostratigraphical classification of the chalk in North Yorkshire, Humberside and Lincolnshire. InProceedings

of the Yorkshire Geological and Polytechnic Society (Vol. 42, No. 2, pp. 263-287). Geological Society of London.

Woods, Mark A.; Mortimore, Rory N.; Wood, Christopher J.. 2012 The Chalk of Suffolk. In: Dixon, Roger, (ed.) A celebration of Suffolk geology : GeoSuffolk 10th

Woodland, A.W., 1946. Water Supply from Underground Sources of Cambridge-Ipswich District-Quarter-inch Geological Sheet 16. Part X. General Discussion... With a Contribution on Rainfall Supplied by the Director, Meteorological Office, Air Ministry.

Younger, P.L., 2009. Groundwater in the environment: an introduction. John Wiley & Sons.

Zuber, A., 1986, Mathematical models for the interpretation of environmental radioisotopes in groundwater systems., in Fritz, P., and Fontes, J. C., eds., Handbook of Environmental Geochemistry, Volume 2, The Terrestrial Environment B: Elsevier, p. 1-59.